

PHYSICAL OCEANOGRAPHIC INFLUENCES ON Queensland reef fish and scallops



Final Report FRDC 2013/020
December 2015

A. J. Courtney, C. M. Spillman, R. T. Lemos, J. Thomas, G. M. Leigh and A. B. Campbell



© 2015 Fisheries Research and Development Corporation.
All rights reserved.
ISBN: 9780734504500

Physical oceanographic influences on Queensland reef fish and scallops FRDC 2013/020 2015

Ownership of Intellectual property rights

Unless otherwise noted, copyright in this publication is owned by the Fisheries Research and Development Corporation and the Department of Agriculture and Fisheries, Queensland.

This publication (and any information sourced from it) should be attributed to A. J. Courtney, C. M. Spillman¹, R. Lemos², J. Thomas², G. M. Leigh and A. B. Campbell. Department of Agriculture and Fisheries, Queensland, ¹Centre of Australian Weather and Climate Research, Australian Government Bureau of Meteorology, ²Centre for Applications in Natural Resource Mathematics, School of Mathematics and Physics, University of Queensland

Creative Commons licence

All material in this publication is licenced under a Creative Commons Attribution 3.0 Australia Licence, save for content supplied by third parties, logos and the Commonwealth Coat of Arms.



Creative Commons Attribution 3.0 Australia Licence is a standard form licence agreement that allows you to copy, distribute, transmit and adapt this publication provided you attribute the work. A summary of the licence terms is available from creativecommons.org/licenses/by/3.0/au/deed.en. The full licence terms are available from creativecommons.org/licenses/by/3.0/au/legalcode. Inquiries regarding the licence and any use of this document should be sent to: frdc@frdc.gov.au

Front cover image credits are as follows:

1. Satellite image of Queensland coast and Capricorn Eddy (source: IMOS OceanCurrent, <http://oceancurrent.imos.org.au/>)
2. *Plectropomus leopardus* on the Great Barrier Reef (source: Graham Edgar, www.reeflifesurvey.com, Creative Commons by Attribution licence for non-commercial use).
3. Severe Tropical Cyclone Yasi off the Queensland east coast on 1 February 2011 (source: University of Wisconsin—CIMSS, Creative Commons by Attribution licence).

Disclaimer

The authors do not warrant that the information in this document is free from errors or omissions. The authors do not accept any form of liability, be it contractual, tortious, or otherwise, for the contents of this document or for any consequences arising from its use or any reliance placed upon it. The information, opinions and advice contained in this document may not relate, or be relevant, to a reader's particular circumstances. Opinions expressed by the authors are the individual opinions expressed by those persons and are not necessarily those of the publisher, research provider or the FRDC. The Fisheries Research and Development Corporation plans, invests in and manages fisheries research and development throughout Australia. It is a statutory authority within the portfolio of the federal Minister for Agriculture, Fisheries and Forestry, jointly funded by the Australian Government and the fishing industry.

Researcher Contact Details

Name: Dr. Tony Courtney
Address: Level 1, Ecosciences Precinct, 41 Boggo Road,
Dutton Park QLD 4102
Phone: 07 3255 4227
Fax: 07 3846 1207
Email: Tony.Courtney@daf.qld.gov.au

FRDC Contact Details

Address: 25 Geils Court
Deakin ACT 2600
Phone: 02 6285 0400
Fax: 02 6285 0499
Email: frdc@frdc.com.au
Web: www.frdc.com.au

In submitting this report, the researcher has agreed to FRDC publishing this material in its edited form.

Contents

1	Acknowledgements	1
2	Abbreviations/Acronyms.....	1
3	Executive Summary	2
3.1	Objectives	2
3.2	Background	2
3.3	Results and Recommendations.....	3
3.3.1	Cyclones and reef fish	3
3.3.2	Saucer scallops and coastal and oceanographic influences	3
4	Introduction.....	5
4.1	Background	5
4.2	Need.....	6
5	Objectives	6
6	Methods.....	7
6.1	Coastal and oceanographic influences on the Queensland saucer scallop fishery.....	7
6.2	Saucer scallop larval advection	8
6.3	Influence of tropical cyclones and other low-pressure systems on reef fish.....	9
7	Results	9
7.1	Influences on saucer scallop catch rates	9
7.2	Does inclusion of oceanographic covariates improve scallop stock assessment?	11
7.3	Simulating larval advection	13
7.4	Influence of low-pressure systems on the reef fin-fish fishery	16
8	Discussion	18
8.1	Coastal and oceanographic influences on scallop catch rates.....	18
8.2	Scallop larval advection	19
8.3	Effects of cyclones and other low-pressure systems on reef fish	19
9	Conclusion	20
10	Implications	22
11	Recommendations.....	23
12	Further development	23
13	Extension and Adoption	25
14	Project materials developed.....	25
15	Appendix 1. Staff.....	25
16	Appendix 2. Intellectual property	25
17	Appendix 3. References	26
18	Appendix 4. Review of relevant literature, data and physical oceanographic features.....	36
18.1	Physical oceanographic features of the Queensland east coast.....	36
18.1.1	Geology	36
18.1.2	East Australian Current	37

18.1.3	The Capricorn Eddy	38
18.2	Examples of coastal and oceanographic influences on fisheries.....	38
18.2.1	Coral bleaching	39
18.2.2	Oceanography and aquaculture	39
18.3	Ocean modelling.....	40
18.3.1	A synopsis of data, numerical, and assimilation modelling	40
18.3.2	Sharing data and knowledge	41
18.3.3	Dominant patterns of ocean variability	41
19	Appendix 5. Coastal and oceanographic influences on the Queensland (Australia) east coast saucer scallop (<i>Amusium balloti</i>) fishery.....	42
19.1	Abstract	42
19.2	Introduction.....	43
19.3	Methods	43
19.3.1	Scallop catch rates.....	44
19.3.2	SOI and freshwater flow	45
19.3.3	Statistical analysis	46
19.4	Results.....	47
19.4.1	Scallop catch rates.....	47
19.4.2	Freshwater flow.....	47
19.4.3	Sea water temperature	50
19.4.4	Sea level	54
19.4.5	Eddy kinetic energy.....	57
19.4.6	Chlorophyll-a	60
19.4.7	SOI	63
19.5	Discussion	64
19.5.1	Suitability of BRAN.....	64
19.5.2	Influential coastal and oceanographic properties	64
19.5.3	Spatial comparison of coastal and oceanographic influences.....	66
19.5.4	Management implications	67
19.6	Conclusions.....	67
19.7	Acknowledgements	68
20	Appendix 6. Larval Advection Patterns in the Queensland Scallop Fishery.....	69
20.1	Abstract	69
20.2	Introduction.....	69
20.3	Chapter 1 Literature Review	71
20.3.1	Scallop Recruitment Modelling.....	71
20.3.2	Oceanography in the Queensland Fishery	71
20.3.3	Larval Transport.....	73
20.4	Chapter 2 Numerical Modelling.....	76
20.4.1	Introduction	76
20.4.2	Materials and resources.....	76
20.4.3	Results and discussion.....	79
20.4.4	Conclusion	83
20.5	Chapter 3 Climatology Performance Assessment.....	85
20.5.1	Introduction	85
20.5.2	Methods.....	85
20.5.3	Results.....	87
20.5.4	Conclusions	88
20.6	Chapter 4 Statistical Modelling of Recruitment	89
20.6.1	Introduction	89

20.6.2	Methods.....	89
20.6.3	Results for Model 1	93
20.6.4	Results for Model 2.....	99
20.6.5	Conclusion	108
20.7	Final Summary.....	109
21	Appendix 7. Impacts of low-pressure systems on the Great Barrier Reef: Confirmation of a causal mechanism using catch rates of the coral trout fishery	111
21.1	Abstract	111
21.2	Introduction.....	112
21.3	Observations from previous analysis	115
21.4	The causal mechanism.....	118
21.4.1	Description	118
21.4.2	Explanation	118
21.4.3	Predictions.....	119
21.5	Analysis of wave height data from an oceanographic model.....	119
21.5.1	Methods.....	119
21.5.2	Results	120
21.6	Direct measurements of wave height	142
21.7	Subjective standardisation of catch rates for weather systems	143
21.7.1	Methods.....	143
21.7.2	Results	144
21.8	Discussion and recommendations.....	147
22	Appendix 8. Local averaging optimisation and sea surface temperatures	148
22.1	Abstract	148
22.2	Introduction.....	148
22.3	Methods	148
22.4	Results.....	149
22.5	Conclusion	152
22.6	References.....	153

List of Tables

Table 7-1. Scallop fishery population model likelihood components under different stock-recruitment anomaly scenarios.....	12
Table 20-1. Types of connectivity.....	90
Table 21-1. Cyclones with winds of gale force (17 ms^{-1}) or above to affect the GBR since 1988. Location is roughly classified as North (Cape York to Cairns Subregions), Central (Townsville Subregion and Whitsunday Islands) or South (Mackay Region south of the Whitsundays, to Swains or Capricorn–Bunker); P_{\min} = minimum central pressure (hPa); V_{\max} = maximum wind speed (ms^{-1}). Note that P_{\min} and V_{\max} are taken over the life of a cyclone, including times when it is not impacting the Great Barrier Reef. Cyclones with high numbers of four-metre wave locations in Table 21-2 below are listed in boldface. Source: Leigh et al. (2014), original data from Australian Bureau of Meteorology (BoM) and Joint Typhoon Warning Center (JTWC) Best Tracks databases.	117
Table 21-2. Some tropical cyclones to hit the GBR between 1985 and 2014, with their measurements based on wave-height. The month is that in which the cyclone formed, not necessarily when its impact	

was greatest. Measurements listed are the maximum number of hours of large enough waves at any location, total number of hours summed over all locations ($k = 1000$), and number of locations subject to large enough waves for one hour or more. Numbers in parentheses are ranks in the collection of all cyclones to hit the GBR in the period, and are shown when one or more cyclones not listed in the table have a higher rank..... 121

Table 21-3. Highest recorded significant wave heights (H_{sig}) for low-pressure systems that affected the GBR. The list includes all tropical cyclones of Australian Tropical Cyclone Category (“Cat”) 3 or above, and all other low pressure systems that produced large wave heights and for which records were available. Locations are (left to right) Cairns, Townsville, Abbot Point, Mackay, Hay Point, Emu Park, Gladstone, Brisbane and Gold Coast. Non-cyclonic weather system abbreviations are East Coast Low (ECL, single centre formed outside the tropics), East Coast Hybrid Low (ECHL, multiple centres formed outside the tropics), Tropical Hybrid Low (THL, multiple centres formed in the tropics), Tropical Low (TL, single centre formed in the tropics). Sources: Queensland Government wave station data, cyclones records from the Australian Bureau of Meteorology (BoM); cyclone track summaries from www.australiasevereweather.com; case studies from www.hardenup.org (a project of Green Cross Australia); other reports where available, including many by J. Callaghan (BoM, retired). 142

Table 22-1. ENSO cycle timeline from 1991 to 2006 including strength of ENSO [5]..... 151

List of Figures

Figure 6-1. Map of the study domain showing the location of the major rivers, the distribution of saucer scallop catches, logbook grids T30 Bustard Head, V32 Hervey Bay and W34 Fraser Island, the Capricorn Eddy and the Whole fishery (thick black dots)..... 7

Figure 6-2. The three regions of highest scallop fishing effort, from Campbell *et al.* (2012)..... 9

Figure 7-1. The correlation between adjusted mean November catch rates and Chl-a concentration in T30 Bustard Head five months earlier in June. The upper graph shows logged catch rates from the REML while the lower graph shows the back-transformed catch rates. Straight lines are simple linear regressions of best fit. Catch rates for selected years are labelled for clarity. 10

Figure 7-2. a) The mean number of connections made by each cell, and b) variance in connectedness, for the QLD Scallop fishery. Zero is represented by white, and black represents 339 connections..... 13

Figure 7-3. a) The mean number of larvae wasted by each cell, and b) variance in wastage, for the Queensland scallop fishery. No wastage is represented by white, and black represents 100% wastage. 14

Figure 7-4. a) The level of self-seeding on a relative scale, b) the variance in that self-seeding behaviour. 14

Figure 7-5. a) All potential source cells for Region 1, and b) the relative contribution by these source cells to Region 1. 15

Figure 7-6. a) All potential source cells for Region 2, and b) the relative contribution by these source cells to Region 2. 15

Figure 7-7. a) All potential source cells for Region 3, and b) the relative contribution by these source cells to Region 3. 16

Figure 7-8. a) All potential destination cells for larvae from Region 3, and b) the proportion of larvae from Region 1 that end up in each cell. Note: it is evident that the majority of larvae are washed against the coast. 16

Figure 18-1. Distribution of the Queensland scallop fishery and the Capricorn Eddy. The blue, green and red are zones in the Great Barrier Reef Marine Park. 36

Figure 19-1. Map of the study domain showing the location of the major rivers, the distribution of saucer scallop catches, logbook grids T30 Bustard Head, V32 Hervey Bay and W34 Fraser Island, the Capricorn Eddy and the Whole fishery (thick black dots).....	44
Figure 19-2. The adjusted mean monthly catch rates of scallops based on the mandatory CFISH logbook database, in baskets boat-day ⁻¹ . The means were derived from the REML model. November catch rates (black stars) were used in the correlation analyses.	47
Figure 19-3. Mean daily flow in the major coastal river systems adjacent to the Queensland saucer scallop fishery from January 1986 to December 2013.	48
Figure 19-4. Correlations between adjusted mean catch rates of scallops in November (log number of baskets boat-day ⁻¹) and freshwater flow from four adjacent coastal river systems. Logbook data are from 1988 to 2013, inclusive.	49
Figure 19-5. Monthly surface and bottom water temperature anomalies at T30 Bustard Head, V32 Hervey Bay, W34 Fraser Island, the Capricorn Eddy area and the Whole fishery area.....	51
Figure 19-6. Correlations between adjusted mean catch rates of scallops in November and water temperature anomalies at five locations. The similarity between surface and bottom correlations at T30 Bustard Head, V32 Hervey Bay and W34 Fraser Island is due to the mixing of water at different depth layers in these relatively shallow coastal areas.....	53
Figure 19-7. The correlation between adjusted mean catch rates of scallops in November and bottom water temperature anomalies at the Capricorn Eddy three months earlier in August (from BRAN 3.5). The upper graph shows logged catch rates from the REML while the lower graph shows the back-transformed catch rates. Straight lines are simple linear regressions of best fit. Catch rates for selected years are labelled for clarity.	54
Figure 19-8. Monthly mean sea level at T30 Bustard Head, V32 Hervey Bay, W34 Fraser Island, the Capricorn Eddy area and the Whole fishery area, from BRAN 3.5.	55
Figure 19-9. Correlations between adjusted mean catch rates of scallops in November and monthly sea level anomalies at the five locations.	56
Figure 19-10. The correlation between adjusted mean catch rate of scallops in November and monthly sea level anomalies at the Capricorn Eddy area three months earlier in August (from BRAN 3.5). The upper graph shows logged catch rates from the REML while the lower graph shows the back-transformed catch rates. Straight lines are simple linear regressions of best fit. Catch rates for selected years are labelled for clarity.	57
Figure 19-11. Monthly EKE at the surface and bottom at T30 Bustard Head, V32 Hervey Bay, W34 Fraser Island, the Capricorn Eddy area and the Whole fishery area, from BRAN 3.5. Note the y-axis scale is not fixed.	58
Figure 19-12. Correlations between adjusted mean catch rates of scallops in November and monthly EKE at the surface and bottom at the five locations.....	59
Figure 19-13. The correlation between adjusted mean catch rate of scallops in November and bottom EKE at the Capricorn Eddy area 22 months earlier in January (from BRAN 3.5). The upper graph shows logged catch rates from the REML while the lower graph shows the back-transformed catch rates. Straight lines are simple linear regressions of best fit. Catch rates for selected years are labelled for clarity.	60
Figure 19-14. Time series of mean monthly Chl-a concentrations from T30 Bustard Head, V32 Hervey Bay, W34 Fraser Island, the Capricorn Eddy area and the Whole fishery. The data were acquired by the MODIS Aqua satellite and provided by the Australian Government Bureau of Meteorology.....	61
Figure 19-15. Correlations between adjusted mean catch rate of scallops in November and monthly mean Chl-a concentrations from the five locations.	62

Figure 19-16. The correlation between adjusted mean catch rate of scallops in November and Chl-a concentration in T30 Bustard Head five months earlier in June. The upper graph shows logged catch rates from the REML while the lower graph shows the back-transformed catch rates. Straight lines are simple linear regressions of best fit. Catch rates for selected years are labelled for clarity. The MODIS Aqua satellite dataset for Chl-a does not extend back to 1996 when the fishery crashed.63

Figure 19-17. The Southern Oscillation Index (upper graph) and correlations between the SOI and adjusted mean catch rates of scallops in November (lower graph). Lags ranging from 0 (no lag) to 24 months have been applied to the SOI.64

Figure 20-1. Each row of images in the figure represents a different spawning location, which is indicated by the black grid. Each column corresponds to a different depth; 1 m, 5 m, 13 m, 24 m and 40 m respectively. The blue grid indicates the location of larvae after advection.....78

Figure 20-2. The three regions of highest fishing effort, from Campbell *et al.* (2012).79

Figure 20-3. a) Mean number of connections made by each cell, and b) the variance in connectedness, for the Queensland scallop fishery. Zero is represented by white, and black represents 339 connections.80

Figure 20-4. a) Mean number of larvae wasted by each cell, and b) the variance in wastage, for the Queensland scallop fishery. No wastage is represented by white, and black represents 339 connections.80

Figure 20-5. a) The level of self-seeding on a relative scale, and b) variance in that self-seeding behaviour.81

Figure 20-6. a) All potential source cells for Region 1, and b) the relative contribution by these source cells to Region 1.81

Figure 20-7. a) All potential source cells for Region 2, and b) the relative contribution by these source cells to Region 2.82

Figure 20-8. a) All potential source cells for Region 3, and b) the relative contribution by these source cells to Region 3.82

Figure 20-9. a) All potential destination cells for larvae from Region 3, and b) the proportion of larvae from Region 1 that end up in each cell. It is quite clear that the majority of larvae are washed against the coast.83

Figure 20-10. Histogram of the number of cells below the threshold in each of the 1000 average connectivity matrices. The numbers 1 through 5 represent where the counts for the variance matrix of each month June through October sit in the histogram.....87

Figure 20-11. Histogram of the number of cells below the threshold in each of the 1000 average connectivity matrices. The numbers 1 through 5 represent where the counts for the variance matrix of each month June through October sit in the histogram.....88

Figure 20-12. The DIC achieved by Model 1 fitted to each type of connectivity. They are plotted from left to right in the same order they appear in Table 20-1.....93

Figure 20-13. Density plots for the weights and deviance fitted using Model 1 using type 8 connectivity. It is clear for $w[6]$, $w[7]$, that the chains did not mix and convergence failed.....93

Figure 20-14. Estimates for the weights. The x axis numbers the weights from 1-5 corresponding to the months June through October. The y axis displays the estimated scalar quantity assigned to each weight. It is clear that the latter months have been weighted highly compared to the preceding three.94

Figure 20-15. Fit plots and quantile-quantile plots. Each row of plots corresponds to a different year fitted, and rows 1-3 are the years 1997, 1998 and 2000 respectively. The fit plots on the left indicate the probability of making a prediction less than or equal to the LTMP observation. Green indicates that the probability of making a prediction less than the LTMP observation is greater than 97.5%,

while red indicates the probability is less than 2.5%. Thus they represent cells where we are under predicting, and over predicting respectively.....95

Figure 20-16. The estimates for the weights. The x axis numbers the weights from 1-20 corresponding weeks 1-20 of the spawning season. The y axis displays the estimated scalar quantity assigned to each weight. It is clear that the latter months have been weighted highly compared to the preceding three.96

Figure 20-17. Fit plots and quantile-quantile plots. Each row of plots corresponds to a different year fitted, and rows 1-3 are the years 1997, 1998 and 2000 respectively. The fit plots on the left size of the figure indicate the probability of making a prediction less than or equal to the LTMP observation. Green indicates that the probability of making a prediction less than the LTMP observation is greater than 97.5%, while red indicates the probability is less than 2.5%. Thus they represent cells where we are under predicting, and over predicting respectively.....97

Figure 20-18. The DIC achieved by Model 1 fitted to each type of connectivity. They are plotted from left to right in the same order they appear in Table 1.99

Figure 20-19. The estimates for the weights. The x axis numbers the weights from 1-15 corresponding to the months June through October for the years 1997, 1998 and 2000. The y axis displays the estimated scalar quantity assigned to each weight. It is clear that the latter months have been weighted highly compared to the preceding three..... 100

Figure 20-20. Fit plots and quantile-quantile plots. Each row of plots corresponds to a different year fitted, and rows 1-3 are the years 1997, 1998 and 2000 respectively. The fit plots on the left size of the figure indicate the probability of making a prediction less than or equal to the LTMP observation. Green indicates that the probability of making a prediction less than the LTMP observation is greater than 97.5%, while red indicates the probability is less than 2.5%. Thus they represent cells where we are under predicting, and over predicting respectively..... 101

Figure 20-21. The estimates for the weights. The x axis numbers the weights from 1-60 corresponding to weeks 1-20 of the spawning season for the years 1997, 1998 and 2000. The y axis displays the estimated scalar quantity assigned to each weight. It is clear that the latter months have been weighted highly compared to the preceding three..... 102

Figure 20-22. Fit plots and quantile-quantile plots. Each row of plots corresponds to a different year fitted, and rows 1-3 are the years 1997, 1998 and 2000 respectively. The fit plots on the left size of the figure indicate the probability of making a prediction less than or equal to the LTMP observation. Green indicates that the probability of making a prediction less than the LTMP observation is greater than 97.5%, while red indicates the probability is less than 2.5%. Thus they represent cells where we are under predicting, and over predicting respectively..... 103

Figure 20-23. The estimates for the weights. The x axis numbers the weights from 1-60 corresponding to weeks 1-20 of the spawning season for the years 1997, 1998 and 2000. The y axis displays the estimated scalar quantity assigned to each weight. It is clear that the latter months have been weighted highly compared to the preceding three..... 104

Figure 20-24. Density plots for parameters fitted for Model 2 using type 9 connectivity (excluding the 60 weights). 104

Figure 20-25. Fit plots and quantile-quantile plots. Each row of plots corresponds to a different year fitted, and rows 1-3 are the years 1997, 1998 and 2000 respectively. The fit plots on the left size of the figure indicate the probability of making a prediction less than or equal to the LTMP observation. Green indicates that the probability of making a prediction less than the LTMP observation is greater than 97.5%, while red indicates the probability is less than 2.5%. Thus they represent cells where we are under predicting, and over predicting respectively..... 105

Figure 20-26. The estimates for the weights. The x axis numbers the weights from 1-15 corresponding to June through October for the years 1997, 1998 and 2000. The y axis displays the estimated scalar quantity assigned to each weight. It is clear that the latter months have been weighted highly compared to the preceding three..... 106

Figure 20-27. Fit plots and quantile-quantile plots. Each row of plots corresponds to a different year fitted, and rows 1-3 are the years 1997, 1998 and 2000 respectively. The fit plots on the left size of the figure indicate the probability of making a prediction less than or equal to the LTMP observation. Green indicates that the probability of making a prediction less than the LTMP observation is greater than 97.5%, while red indicates the probability is less than 2.5%. Thus they represent cells where we are under predicting, and over predicting respectively..... 107

Figure 21-1. Reef Bioregions defined by GBRMPA expert committees as part of the preparation for the Representative Areas Program implemented in 2004. Source: GBRMPA (2009). 114

Figure 21-2. Map showing the Regions and Subregions of the GBR used by Leigh *et al.* (2014), which were used to divide the northern Reef Bioregions from Figure 21-1 into Sub-bioregions. Regions are based on the Reef Bioregions, and two of the northern Regions are split into Subregions by latitude to account for increases in fishing intensity from north to south: the Far Northern Region is divided into three Subregions, and the Cairns–Townsville Region is divided into two Subregions. The small squares on the map are six-nautical-mile fishery logbook grid squares. Colours are chosen only to distinguish the Regions and Subregions, and have no other meaning. Source: Leigh *et al.* (2014). 115

Figure 21-3. Monthly time series (green dots) of standardised catch rates of coral trout in the commercial fishery on the GBR, for each Sub-bioregion. The grey bars show standard errors. The yellow diamonds show the proportions of Sub-bioregion area affected by 4 m or 2 m waves: the lower horizontal red dotted line represents zero area, and the upper one represents 100% of the Sub-bioregion area. (Continued next 19 pages) 122

Figure 21-4. Subjective standardised catch rates (bold black lines) of coral trout to account for effects of weather systems in the major Sub-bioregions of the reef line fishery. Catch rates that don't account for weather systems are also shown (red lines). The green dots are the same as in Figure 21-3 and are monthly standardised catch rates from a model that does not include any effects of weather systems. (Continued next page)..... 145

Figure 22-1. Sea surface temperatures (°C) varying with time (weeks after the 07/06/2006) taken from a depth of 15 m at a latitude and longitude of -22.95 and 155.95 respectively were used to forecast the next 5 temperatures (through to the 25/10/2006). The black points represent the original data used in the forecasting function, the red points the forecast values for the next 5 time steps and corresponding original data values are in blue. The optimum forecasting parameters were determined to be $k_{opt} = 9$ and $\lambda_{opt} = (0.896281607, 0.317031591, 0.088095156, -0.010149950, -0.017388793, -0.008844277, -0.009258766, -0.006303262, -0.006683757, -0.003470069, -0.009484341, -0.010851779, -0.008957675, -0.013793656, -0.015319032)$ using the input values; 150

Figure 22-2. Sea surface temperatures (°C) varying with time (weeks after the 02/03/2005) taken from a depth of 15 m at a latitude and longitude of -22.95 and 155.95 respectively were used to forecast the next 5 temperatures (through to the 05/07/2006). The black points represent the original data used in the forecasting function, the red points the forecast values for the next 5 time steps and corresponding original data values are in blue. The optimum forecasting parameters were determined to be $k_{opt} = 10$ and $\lambda_{opt} = (0.78096113, 0.21079572, -0.08029546, -0.15665996, -0.15551428, -0.13221321, -0.11339021, -0.10469518, -0.10193321, -0.10076513, -0.10014239, -0.09989629, -0.09983056, -0.09979750, -0.099781140)$ using the input values; 151

Figure 22-3. Lorenz time series from $t = 800$ to $t = 1010$. The black dots represent the data used to forecast the future values (red), which have been overlayed with the original data (blue). The forecast values were obtained using $n_d = 20, n_c = 10, n_s = 10, k_{max} = 15, \lambda_{opt} = (2e^{-x}, 2e^{-2x}, \dots, 2e^{-x*n_d})$ and $k_{opt} = 4$ 152

Figure 22-4. Sea surface temperatures (°C) varying with time (weeks from 02/12/1992 to 13/09/2006) taken from a depth of 15 m at a latitude and longitude of -22.95 and 155.95 respectively..... 152

1 Acknowledgements

The project was largely funded by FRDC (Project number 2013/020). We thank the GBRMPA and Rachel Pears (GBRMPA) for the additional cash contribution which supported Jesse Thomas' postgraduate research on scallop larval advection. We appreciate the support provided by FRDC staff Carolyn Stewardson, Crispian Ashby, Julie Haldane, Jo-Anne Ruscoe and Kylie Giles.

Nadia Engstrom and Anna Garland (DAF) provided CFISH logbook data and advice. David Mayer (DAF) provided statistical support. We also thank DAF staff Ben Bassingthwaighe, Tara Patel, Donna Buckley, Carrie Wright, Debra Davis, Carmel Barrie, Paul Hickey and Stephen Nottingham for administrative and financial support and advice.

We thank Andreas Schiller, Russ Fiedler and Griffith Young (CSIRO & Bureau of Meteorology, BOM, Australia) for advice and access to the BRAN dataset. Craig Steinberg (Australian Institute of Marine Science) provided advice and assisted with accessing the Integrated Marine Observing System (IMOS) data. Matt Campbell (DAF) assisted with the scallop logbook catch data and REML. Julie Robins (DAF) provided advice on flow data and the Capricorn Eddy. Paul Sandery and Eric Schulz (BOM), Brad Zeller, Warwick Nash and Carmel Barrie (DAF), and Anthony Richardson (CSIRO, University of Queensland), provided constructive comments on the report.

We greatly appreciate the following project steering committee members who provided their time and advice; Chris Neill (Queensland reef line fisher), Nick Schultz (Urangan Fisheries, fisher/processor), Nick Caputi (Western Australian Department of Fisheries), Bradley Congdon (James Cook University), Rachel Pears (GBRMPA), Craig Steinberg and DAF Fisheries Queensland staff Darren Roy, John Kung and Eddie Jebreen.

2 Abbreviations/Acronyms

AMSA	Australian Marine Sciences Association
BOM	Australian Bureau of Meteorology
BRAN 3.5	19-year numerical hindcast dataset, based on the Bluelink ocean model (Oke <i>et al.</i> 2013)
CFISH	Queensland commercial fishery logbook database
DAF	Department of Agriculture and Fisheries, Queensland
DIC	Deviance Information Criterion
EAC	East Australian Current
EKE	eddy kinetic energy
ENSO	El Niño Southern Oscillation
GBR	Great Barrier Reef
GBRMPA	Great Barrier Reef Marine Park Authority
IMOS	Integrated Marine Observing System
LTMP	Long-Term Monitoring Program
MSY	maximum sustainable yield
QEC	Queensland east coast
QECOTF	Queensland east coast otter trawl fishery
REML	restricted maximum likelihood model
SH	shell height
SOI	Southern Oscillation Index
SRA	scallop replenishment area
SST	sea surface temperature
WA	Western Australia

3 Executive Summary

The project examined coastal and physical oceanographic influences on the catch rates of coral trout (*Plectropomus leopardus*) and saucer scallops (*Amusium balloti*) in Queensland. The research was undertaken to explain variation observed in the catches, and to improve quantitative assessment of the stocks and management advice.

3.1 OBJECTIVES

1. Review recent advances in the study of physical oceanographic influences on fisheries catch data, and describe the major physical oceanographic features that are likely to influence Queensland reef fish and saucer scallops.
2. Collate Queensland's physical oceanographic data and fisheries (i.e. reef fish and saucer scallops) data.
3. Develop stochastic population models for reef fish and saucer scallops, which can link physical oceanographic features (e.g. sea surface temperature anomalies) to catch rates, biological parameters (e.g. growth, reproduction, natural mortality) and ecological aspects (e.g. spatial distribution).

3.2 BACKGROUND

Previous research has established a link between tropical cyclones and catch rates of reef fish. Catch rates of coral trout (*P. leopardus*) fall after a major cyclone, while those of red throat emperor (RTE, *Lethrinus miniatus*) rise. These changes endure for some years after the cyclone. The causal mechanism underlying the effects is not known, but a number of hypotheses pertaining to factors affecting catchability of reef fish have been put forward.

Like many scallop fisheries, catch rates and annual landings from the Queensland saucer scallop (*A. balloti*) fishery display considerable variation. Recruitment failure in the fishery occurred in 1996 causing considerable hardship and forcing management to implement spawning stock closures. Research shows such variation in scallop fisheries can often be explained by environmental drivers, particularly oceanographic properties such as water temperature anomalies, changes in current vectors and Chlorophyll-a (Chl-a) levels. Often these properties are related to the El Niño Southern Oscillation (ENSO).

In recent years the Integrated Marine Observing System (IMOS) has expanded, greatly enhancing its coverage of Australia's coasts. This has resulted in increased observational and modelled data on coastal and oceanic properties, and importantly, improved availability of these data for fisheries research and management.

A significant physical oceanographic feature of the southeast Queensland coast is the Capricorn Eddy, which forms adjacent to the scallop fishing grounds. The eddy is produced by the East Australian Current (EAC) and brings cool nutrient-rich water up from great depths onto the continental shelf. Despite the eddy's close proximity, its influence on the scallop fishery has not been investigated.

It is noteworthy that a severe marine heat wave event on the Western Australian (WA) coast in the summer of 2010/11 has had a sustained detrimental impact on the WA saucer scallop (the same species as in Queensland *A. balloti*) fishery in Shark Bay and the Abrolhos Islands.

We propose to examine how physical oceanographic conditions along the Queensland coast, including the Capricorn Eddy, variations in SST and tropical cyclones, affect stocks of reef fish and scallops. We expect that this will lead to improved modelling, assessment and advice on these important stocks.

3.3 RESULTS AND RECOMMENDATIONS

3.3.1 Cyclones and reef fish

Cyclones and other low pressure systems that create large swells and wave heights offshore do not necessarily result in reduced coral trout catch rates. This is because the outer barrier reef efficiently dissipates offshore swells and protects coral reef habitats. However, systems that create large southeasterly swells in waters between the GBR and the coast can cause significant habitat damage. GBR waters between Rockhampton and Townsville act as a long southeast–northwest fetch over which such a swell can build. Also Townsville has its own fetch which runs nearly east–west. These swells bypass the GBR’s natural protection from its barrier reefs. It is the inshore fetches that are most important for explaining the decline in coral trout catch rates after a cyclone. Declines in coral trout catch rates are believed to stem mainly from reduced catchability rather than reduced abundance. From Cairns north, due to the lack of suitable fetches, cyclones have almost no discernible effect on catch rates.

- We recommend recognition of the importance of inshore wave-height measurements, and the collation of available historical measurements. These data could then be used in new fishery catch rate standardisations that can properly take account of the effects of tropical cyclones.
- We also suggest that new oceanographic models for the GBR be developed to take account of the prime importance of the inshore-fetch mechanism in generating damaging swells.

New catch rate standardisations should prove very valuable in fishery management as they may finally separate the effects of tropical cyclones from the effects of fishing, which to date has been impossible. The process of setting quota in the fishery could then be based on the effects of fishing alone and made largely independent of cyclones.

3.3.2 Saucer scallops and coastal and oceanographic influences

The project examined larval advection patterns for Queensland saucer scallops and relationships between commercial catch rates of scallops and coastal and oceanographic variables.

Current strength and direction vectors from a 19-year hindcast dataset (i.e. BRAN 3.5) were used to model scallop larvae advection trajectories in the scallop fishing grounds. Larvae were generally found to move in a northwest direction towards the coast. Although larval connectivity between areas was highly variable, the three scallop replenishment areas (SRAs, Yeppoon, Bustard Head and Hervey Bay), which are opened and closed to trawling on a rotational basis, each showed relatively high rates of self-seeding. This may explain why adult scallop densities in the areas are relatively high, and why the areas receive high levels of fishing effort. No one single area is responsible for supplying larvae in the fishery and larval advection patterns differed significantly between years, over the 19-year time series.

- Future larval advection modelling of the fishery should use oceanographic models that include tidal vectors. This was not captured in the BRAN 3.5 hindcast dataset.
- Studies that provide some understanding of scallop larval vertical migration behaviour, especially diel and tidal variation, would also improve the modelling.

The study examined a large number of correlations between commercial catch rates in November (when the fishery has traditionally opened each year) and coastal and physical oceanographic variables, over 26 years (1988-2013). The strongest correlation found was 0.85 for Chl-a concentration five months earlier in June. Chl-a appears to have a significant influence on scallop catch rates, probably as an important food source to scallops and other fauna, although the relationship may not be a simple one.

Physical oceanographic properties of the area where the Capricorn Eddy forms, adjacent to and east of the fishery, produced twice as many strong, statistically significant correlations with scallop catch rates

than any other area, suggesting that the eddy has a significant effect on the fishery. November catch rates are negatively correlated with bottom water temperature anomalies (correlation = -0.74) and sea level (-0.60) at the eddy area three months earlier in August.

November catch rates declined when surface water temperature anomalies were elevated 16-18 months prior (May-July, winter previous year) when the scallops were spawned. Saucer scallop larvae have a relatively narrow range of water temperature tolerance and we speculate that elevated SST during the winter spawning reduces reproductive output and/or lowers survival of larvae. This negative correlation was common to all five areas examined and is consistent with research from Western Australia's Shark Bay and Abrolhos Is. saucer scallop fisheries where elevated SST during spawning results in reduced recruitment.

Chl-a, freshwater flow from rivers adjacent to the scallop fishery, and temperature anomalies had the most statistically significant correlations with scallop catch rates. Sea level and eddy kinetic energy generally had relatively few significant correlations with catch rates, while the SOI had no significant correlations. This ranking helps identify the most influential environmental drivers in the scallop fishery and future areas for research.

- We recommend that key environmental variables be monitored in conjunction with scallop catch rates, including Chl-a, SST and freshwater flows. Key correlations suggest catch rates in November (when the fishery commences each year) may be predicted using environmental data.
- Key relationships should be incorporated in the quantitative models used to assess the scallop fishery. We examined how three such relationships, for water temperature anomalies, eddy kinetic energy and Chl-a, affected performance of the age-structured model used to assess the fishery. Two of the relationships improved the model fit and the estimate of maximum sustainable yield (MSY). Further work is required to determine which relationships result in the most improvement to the models.
- Catch rates and annual landings in the Queensland saucer scallop fishery are highly variable. In 1996 the fishery experienced recruitment failure, resulting in the lowest catch rates on record, severe hardship to industry and emergency management measures which included spatial closures (SRAs). These rotational closures remain today. Given that the project identified a number of strong correlations with environmental variables (although no causal mechanisms were demonstrated), particularly relationships with Chl-a and water temperature, we recommend reviewing the need and function of the SRAs.

KEYWORDS: coral trout, *Plectropomus leopardus*, saucer scallop, *Amusium balloti*, ocean data reanalysis, BRAN, tropical cyclones, wave height, Chlorophyll-a, eddy kinetic energy, Capricorn Eddy

4 Introduction

4.1 BACKGROUND

There is evidence to suggest that some of Queensland's major commercial and recreational fisheries are affected by physical oceanographic conditions and that in order to improve our ability to assess, forecast and manage stocks, some understanding of these influences is required.

In the past, emphasis has been placed on determining inshore and riverine influences, such as freshwater flow, on fish stocks. In contrast, we have relatively little understanding of potentially important offshore influences, such as current systems and eddies, cyclone-induced mixing, sea surface temperature (SST) and Chl-a. In recent years, the amount of data being collected on Australia's physical oceanography has greatly increased, mainly due to the Australian Integrated Marine Observing Systems (IMOS), but also improved international satellite-based measures.

Previous research has established a link between tropical cyclones and catch rates of reef fish (Leigh *et al.* 2006; Tobin *et al.* 2010). Catch rates of coral trout (*Plectropomus leopardus*) fall after a major cyclone, while those of red throat emperor (RTE, *Lethrinus miniatus*) rise. These changes endure for some years after the cyclone. The exact causal mechanism is not known.

Leigh *et al.* (2006) found that a cyclone appears to bring forward the recruitment of RTE to the fishery, and hypothesised that this takes place by transporting young fish upwards from deeper, colder water. The actual whereabouts of young RTE prior to recruitment are unknown.

Tobin *et al.* (2010) point out that the effect of a cyclone on the fishery is much longer-lasting than the associated cool-water anomaly in sea surface temperature. They state that the metabolism of coral trout may slow down in cooler water, thereby affecting feeding behaviour and catchability, but that it remains unexplained why the reduced catchability persists beyond the duration of the temperature anomaly. Tobin *et al.* (2010) also examined warm water anomalies, which are believed to be unrelated to cyclones. There was some evidence that these anomalies produced higher catch rates of coral trout, but it was not conclusive.

Previous research has shown that SST affects foraging success of sea birds on the Great Barrier Reef (GBR) (Peck *et al.* 2004; Erwin and Congdon 2007). This is thought to be related to availability of prey (squid and bait fish), which can also be expected to affect reef fish.

Recent modelling of SST allows accurate forecasts of SST on the GBR to be made several months in advance (Spillman and Alves 2009). Such forecasts can also predict the spatial distribution of pelagic fish for use in fishery management (Hobday *et al.* 2011). Reef fish on the GBR are thought to be relatively sedentary, and SST forecasts, instead of indicating spatial distribution of fish, may predict their behaviour, prey availability and willingness to take bait.

Research undertaken by Weeks *et al.* (2010) used satellite and IMOS data to identify and describe the Capricorn Eddy, which forms seasonally in the Capricorn-Bunker region off the southeast Queensland coast. This mesoscale cyclonic lee eddy forms by breaking off from the East Australian Current and moves westward, bringing cold nutrient-rich water up onto the continental shelf. The Queensland saucer scallop (*Amusium balloti*) trawl fishery is located adjacent to, and west of, where the eddy typically forms. Relationships between physical features of the eddy and the scallop fishery have not previously been investigated.

It is noteworthy that a severe marine heat wave event on the Western Australian (WA) coast in 2011 appears to have had a detrimental impact on the WA saucer scallop fishery in Shark Bay and the Abrolhos Islands (Pearce and Feng 2013; Caputi *et al.* 2015).

We propose to examine how physical oceanographic conditions along the Queensland coast, including properties of the Capricorn Eddy and tropical cyclones, affect stocks of reef fish and scallops. We expect that this will lead to improved modelling and assessment of stocks, and improved forecasting.

4.2 NEED

There is a strong need for Queensland fishery stakeholders, managers and scientists to better-understand key physical oceanographic influences on target species of commercial and recreational fisheries.

Tropical cyclones have been associated with reef fish catch rates. Coral trout (*P. leopardus*) catch rates typically fall after a major cyclone, while those of red throat emperor (*L. miniatus*) rise (see 'Background' above). The effects on catchability can last several years. While the exact causal mechanism is not known, it is thought to be related to water temperature.

A meso-scale nutrient-rich cold water eddy, which breaks from the East Australian Current and moves westward onto the Queensland continental shelf is likely to affect the spat settlement, growth, abundance and catch rates of saucer scallop (*A. balloti*). Understanding these relationships may lead to improved management, assessment and forecasting of catch in these fisheries, and it may also lead to improved acceptance of quantitative stock assessment results by industry.

This study differs from previous abiotic studies because it focuses more on offshore, oceanic influences, rather than coastal rainfall and flow data.

5 Objectives

1. Review recent advances in the study of physical oceanographic influences on fisheries catch data, and describe the major physical oceanographic features that are likely to influence Queensland reef fish and saucer scallops.
2. Collate Queensland's physical oceanographic data and fisheries (i.e. reef fish and saucer scallops) data.
3. Develop stochastic population models for reef fish and saucer scallops, which can link physical oceanographic features (e.g. sea surface temperature anomalies) to catch rates, biological parameters (e.g. growth, reproduction, natural mortality) and ecological aspects (e.g. spatial distribution).

6 Methods

The methods were applied in discrete steps associated with each of the project's objectives. The following are brief descriptions of the general methodologies. More detailed descriptions associated with each objective can be found in the relevant Appendices.

6.1 COASTAL AND OCEANOGRAPHIC INFLUENCES ON THE QUEENSLAND SAUCER SCALLOP FISHERY

Full details of the methods can be found in section 19 Appendix 5. Coastal and oceanographic influences on the Queensland (Australia) east coast saucer scallop (*Amusium balloti*) fishery.

Scallop fisheries are often associated with large annual variation in catch and effort. To help explain this variation, this part of the report examined relationships between environmental variables and catch rates in the Queensland saucer scallop fishery. Coastal and oceanographic variables were examined from five areas associated with the fishery; three logbook grids where significant catches of scallops are reported annually (T30 Bustard Head, V32 Hervey Bay and W34 Fraser Island), an area where the Capricorn Eddy typically forms, and an area encompassing the Whole scallop fishery (Figure 6-1).

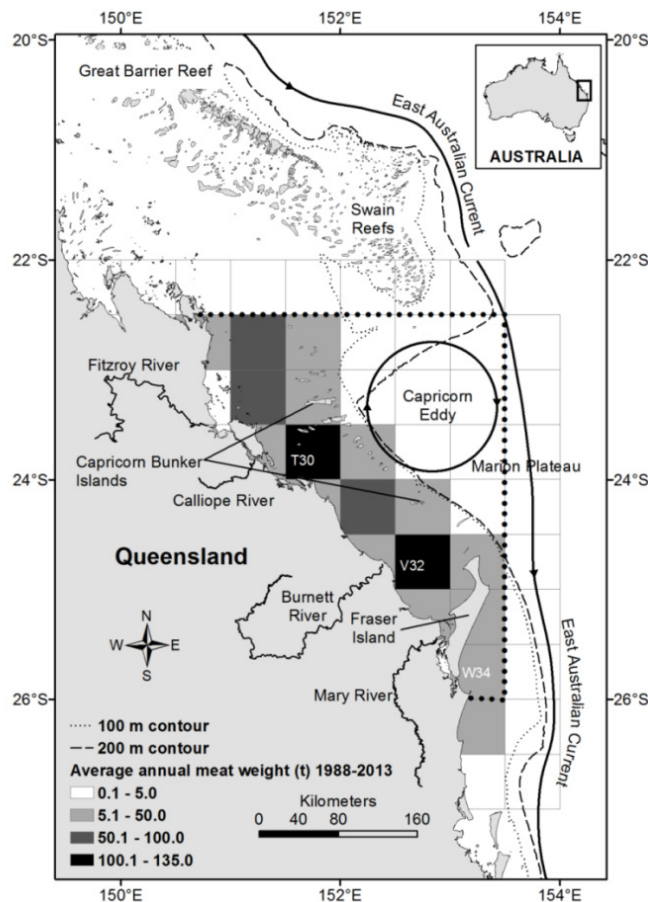


Figure 6-1. Map of the study domain showing the location of the major rivers, the distribution of saucer scallop catches, logbook grids T30 Bustard Head, V32 Hervey Bay and W34 Fraser Island, the Capricorn Eddy and the Whole fishery (thick black dots).

The environmental variables were monthly mean measures of:

- i. freshwater flow from each of four coastal river systems (Fitzroy, Calliope, Burnett and Mary Rivers) adjacent to the scallop fishery

- ii. surface and bottom sea water temperature anomalies
- iii. sea level and sea level anomalies
- iv. surface and bottom eddy kinetic energy (EKE)
- v. Chlorophyll-a (Chl-a) in surface waters, and
- vi. The Southern Oscillation Index (SOI).

Catch rates were adjusted using a restricted maximum likelihood (REML) approach, mainly to standardise monthly catch rates for changes in fishing power over the decades. Physical oceanographic parameters were derived from a 19-year numerical hindcast Bluelink ReAnalysis (BRAN 3.5) dataset which is based on the Bluelink ocean model (Oke *et al.* 2013). Lags were applied to the environmental data so that the influence of conditions 0-24 months prior to the November catches could be examined.

Relationships between the environmental variables and scallop catch rates were examined using simple correlation. In each case the response variable was the adjusted mean catch rate of scallops from the whole fishery in November. November was chosen as it is considered to be the start of the fishing year and is likely to be when the scallop biomass is at its annual peak. As the scallops have a minimum legal size of 90 mm shell height (SH), the commercial catches are largely composed of individuals that are at least one year old (i.e. 1+ age class) that were spawned during winter of the previous year (i.e. May-August 15-18 months prior).

Most of the correlation analyses were based on 26 years (1988-2013) of environmental and catch rate data. However, as some datasets are only available for shorter time series, such as the satellite-measured Chl-a data that only commenced in 2002, fewer observations were available. It is important to note that as the methods were based on correlation, no causal mechanism was demonstrated in the study.

6.2 SAUCER SCALLOP LARVAL ADVECTION

Full details of the methods used to model and analyse saucer scallop larval advection are provided in section 20 Appendix 6. Larval Advection Patterns in the Queensland Scallop Fishery.

In order to uncover patterns in scallop larval dispersal off the Queensland East Coast (QEC), we generated a 19-cell grid of 0.5° resolution, as in Campbell *et al.* (2012), covering the QEC from 22.5°S to 27°S. These large grid cells were then each subdivided into 25 smaller cells (0.1° resolution). Cells with a significant portion of their area covered by the mainland or islands were excluded, leaving a total of 411 cells. Utilising current velocity data for this region from the BRAN 3.5 global ocean model, we were able to simulate the advection of virtual larvae for 19 annual spawning seasons, from 1993 to 2011. Grid cells were seeded with larvae at random, at a rate of nine per week. Their trajectories were simulated for three weeks corresponding to scallop planktonic larval duration. This was done for twenty-four weeks, from June till October each year, corresponding to the Queensland scallop spawning season (Dredge 1981). Seeding was performed at midnight of the first day of each week and the final locations of all particles were recorded. In total, we modelled the fate of $9_{\text{Larvae}} \times 411_{\text{Cells}} = 3699$ tracer larvae seeded per week across the QEC, over a total of $19_{\text{years}} \times 24_{\text{weeks}} = 456$ weeks. This was done for the surface depth layer of 1-5 metres, and also for the 15m depth layer, in accordance with where the Connie simulation suggested distinct current strata may exist. For both depths, both a purely deterministic simulation and a simulation with a random walk were performed. The random walk component was implemented such that at each 15-minute time step in the simulation, the larvae receive an impulse in a random direction at 5% of the magnitude of the local instantaneous current velocity.

From each weekly simulation of larval dispersion, a connectivity matrix was formed, recording the number of larvae from each origin cell that ended up in each destination cell, or was lost off the grid. An average connectivity matrix was then calculated by taking the element-wise average across all connectivity matrices recorded, allowing us to explore which zones lose the most larvae to the ocean,

which cells have had the widest spatial seeding range, which cells self-seed, and for the regions with the highest fishing effort (Figure 6-2), where their source larvae come from, and where they send their larvae to. A matrix of element-wise variance over time was also calculated to capture variability in the dynamics of each site.

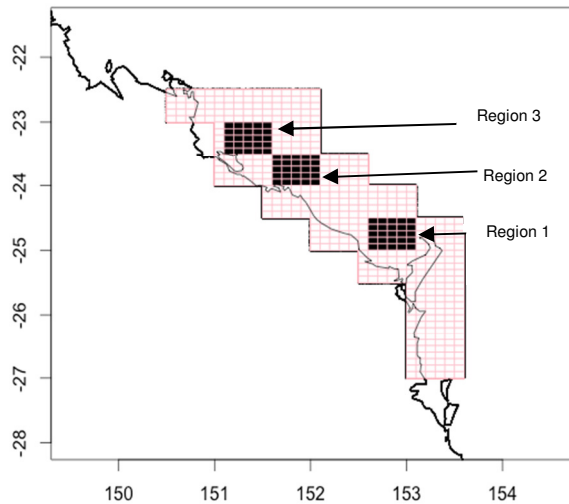


Figure 6-2. The three regions of highest scallop fishing effort, from Campbell *et al.* (2012).

6.3 INFLUENCE OF TROPICAL CYCLONES AND OTHER LOW-PRESSURE SYSTEMS ON REEF FISH

Full details of the methods used to investigate the effects of cyclones on the Queensland coral reef fin fish fishery are provided in section 21 Appendix 7. Impacts of low-pressure systems on the Great Barrier Reef: Confirmation of a causal mechanism using catch rates of the coral trout fishery. The methods used comprised:

- appreciation of a hitherto-overlooked mechanism for generating damaging swells, the inshore-fetch mechanism of Callaghan (2011a)
- correlation of data from an existing offshore-fetch model of cyclone-induced wave height (M. L. Puotinen, unpublished data) with catch rates from the coral trout fishery.

7 Results

7.1 INFLUENCES ON SAUCER SCALLOP CATCH RATES

A complete presentation of these results can be found in section 19 Appendix 5. Coastal and oceanographic influences on the Queensland (Australia) east coast saucer scallop (*Amusium balloti*) fishery.

A total of 900 correlations were examined between adjusted mean November catch rates and coastal and oceanographic parameters (freshwater flows, sea water temperatures anomalies, sea level, EKE, Chl-a and SOI), including lagged relationships. Because the number of correlations is quite large, it is important to be aware that about 5% (45 correlations) may be statistically significant simply by chance. Several strong, statistically significant correlations were found, as summarised below. Adjusted mean November catches were:

1. Almost always positively correlated with freshwater flow from river systems adjacent to the fishery, regardless of the lag.
2. Positively correlated (r ranged from 0.32 to 0.53) with flow for all rivers four months prior (July).

3. Negatively correlated (r ranged from -0.14 to -0.55) with flow from all rivers 12 months prior (November previous year).
4. Negatively correlated ($r=-0.74$) with bottom water temperature anomalies at the Capricorn Eddy area three months prior (August).
5. Negatively correlated (r ranged from -0.34 to -0.74) with bottom water temperature anomalies at the Eddy area 0-7 months prior. This indicates that elevated bottom water temperatures anytime from April to November in the Eddy area are associated with reduced November catch rates.
6. Negatively correlated (r ranged from -0.28 to -0.51) with surface water temperature anomalies 16-18 months prior (May-July, winter spawning period previous year) at all locations.
7. Positively correlated (r ranged from 0.47 to 0.65) with bottom temperature anomalies at the Whole fishery area 21-24 months prior.
8. Negatively correlated ($r=-0.60$) with sea level for the Eddy area three months prior (in August).
9. Negatively correlated ($r=-0.64$) with the Eddy area surface EKE one month earlier (in October).
10. Positively correlated ($r=0.71$) with bottom EKE 22 months prior (January previous year) in the Eddy area.
11. Positively correlated ($r=0.85$) with Chl-a in T30 Bustard Head five month prior (June).
12. Negatively correlated ($r=-0.80$) with Chl-a in T30 Bustard Head 12 months prior (November previous year).

The strongest correlation found during the study was 0.85 for Chl-a five months prior in June at T30 Bustard Head (Figure 7-1). Although we have not demonstrated any cause or effect, we suspect that increased Chl-a in June increases the survival rates of 1+ scallops over the following months from June to when the scallops were caught in November.

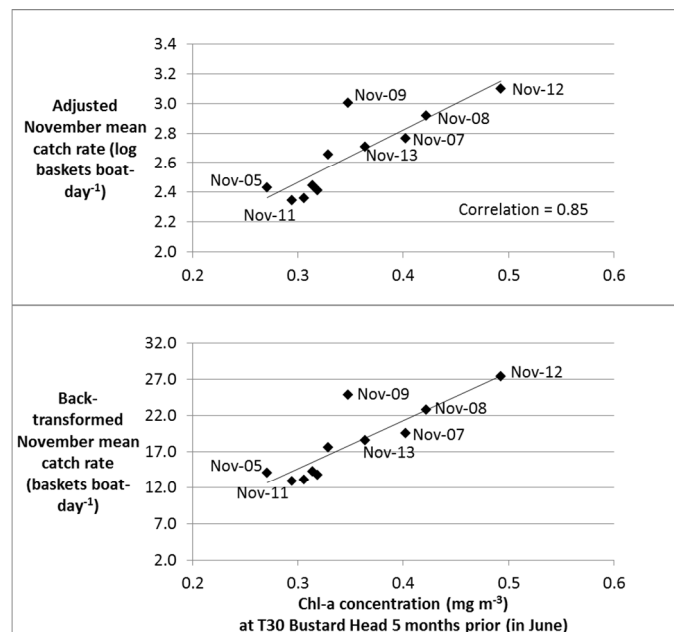


Figure 7-1. The correlation between adjusted mean November catch rates and Chl-a concentration in T30 Bustard Head five months earlier in June. The upper graph shows logged catch rates from the REML while the lower graph shows the back-transformed catch rates. Straight lines are simple linear regressions of best fit. Catch rates for selected years are labelled for clarity.

A total of 125 correlations, based on physical oceanographic properties derived from BRAN 3.5 (water temperature anomalies, sea level and EKE) were examined for each of the five areas (T30 Bustard Head, V32 Hervey Bay, W34 Fraser Island, Capricorn Eddy and Whole fishery, Figure 6-1). We found that the Capricorn Eddy area had the highest number of strong correlations (i.e. correlations \geq an absolute value of 0.5) with November catch rates. The Eddy area had 12 strong correlations, followed

by the Whole fishery area with five. T30 Bustard Head had four strong correlations, while V32 Hervey Bay and W34 Fraser Island each had two. This suggests that the physical oceanographic conditions in the area where the Eddy forms have a relatively strong influence on the scallop's population dynamics and fishery.

The Queensland saucer scallop fishery has displayed significant interannual variation in catch rates and landings over the past four decades. In 1996, the fishery is generally considered to have experienced recruitment failure. This resulted in the lowest catch rates on record and caused significant hardship among fishers and processors. At the time, there was no quantitative evidence to suggest that the collapse was due to environmental conditions and the response by the fishery managers was to implement three permanently closed areas, referred to as the scallop replenishment areas, as a means of reducing the risk of recruitment overfishing. Although the closures have been modified over the past two decades and are now rotationally opened and closed to trawling, they are still used to manage the scallop fishery. Results from the present study suggest that the 1996 collapse may not have been entirely attributed to fishing mortality. Several correlations show that low catch rates, including that of November 1996, were associated with environmental conditions in the previous months.

7.2 DOES INCLUSION OF OCEANOGRAPHIC COVARIATES IMPROVE SCALLOP STOCK ASSESSMENT?

Three abiotic variables were selected for incorporation into the scallop fishery population model:

1. 'Whole fishery' bottom (95 m) temperature in December, 23 months prior to the November catch rates ('WFBT').
2. Capricorn Eddy area bottom (95 m) EKE, 22 months prior in January of the previous year ('CEBEKE').
3. Chl-a concentration at T30 Bustard Head, 12 months prior in November of the previous year ('Chl-a').

These variables were chosen based on a high correlation (or in the case of Chl-a, negative correlation), with standardised fishery catch rates in November the following 'fish year', defined to be November through to October. Thus, WFBT is operating at a 23-month lag, CEBEKE is operating at a 22-month lag, and Chl-a is operating at a 12-month lag.

The fishery population model is described in detail in Campbell *et al.* (2012), wherein Equation 2 specifies the stock recruitment relationship,

$$\log\left(\frac{R_{y,k}}{A_k/A_*}\right) = \log\left(\alpha P_{y-1}(1 - \beta\delta P_{y-1})^{1/\delta}\right) + \xi_y + \psi_k$$

where $R_{y,k}$ is recruitment (in numbers of scallop) into spatial cell k in year y , A_k is the area of cell k (in km²), A_* is the total area of the fishery, α , β , and δ are the productivity, optimality and limitation parameters of the Deriso-Schnute stock-recruitment function (Schnute 1985), P_y is the egg production of the fishery in year y , ξ_y is the temporal recruitment anomaly in year y and ψ_k is the spatial recruitment anomaly in cell k . These anomaly terms are modelled as 'random effects': they are estimated parameters that are unconstrained other than that they sum to unity, and are integrated out of the final results via Markov-chain Monte Carlo.

To gauge the impact of an abiotic covariate on the model, we replaced the temporal anomaly with the abiotic covariate, and estimated the magnitude of this relationship. Call the abiotic covariate in year y ϕ_y , and the magnitude parameter τ . The abiotic covariate is standardised so that it sums to zero and has a standard deviation of unity. The stock recruitment relationship becomes

$$\log\left(\frac{R_{y,k}}{A_k/A_*}\right) = \log\left(\alpha P_{y-1}(1 - \beta\delta P_{y-1})^{1/\delta}\right) + \tau\phi_y + \psi_k.$$

If τ is estimated to be non-zero, the impact of the covariate is assessed through a comparison of the model fit (overall and to specific data sets) with a model run when τ is forced to zero (no abiotic

covariate). If τ is estimated to be zero, this indicates the covariate does not improve the model fit, and is not in agreement with the fishery model.

Chl-a produced an insignificant τ ($< 1e-9$), however both WFBT and CEBEKE produced non-zero values: 0.1056 and 0.1475.

To give these values some meaningful reference point (and to verify that no error had been made in coding this modification) the following procedure was implemented:

1. Parameters were estimated as in the original model, with a full 32 recruitment anomalies estimated.
2. The last 13 years of these anomalies (i.e. fish year 1997-2009) were captured, and then standardised as above (zero sum, unity standard deviation).
3. The full model parameters are re-estimated with the first 19 years of recruitment anomalies estimated freely (as in the original model), and the last 13 years fixed at the captured recruitment series multiplied by the estimated magnitude parameter.

This produced a τ value of 0.414. An analogy can be made here with ‘explained variation’ (i.e. WFBT and CEBEKE ‘explain’ 25% and 36% of the variation in the data respectively); however, given the complexity of the data, the model, and the estimation process, this lacks theoretical justification and should not be taken literally. The overall model likelihood has eight components, corresponding to six (weighted) data sets and two penalty components, one for the spatial random effects and one for the temporal random effects. It is instructive to compare each of these across four model runs: one where the last 13 years have no temporal anomaly (τ is fixed at zero), one where the last 13 years are the WFBT series (τ is estimated), one where the last 13 years are the CEBEKE series (τ is estimated), and finally one where the temporal anomaly is allowed to float freely (as in the original model). The results of this analysis are presented in Table 7-1.

Table 7-1. Scallop fishery population model likelihood components under different stock-recruitment anomaly scenarios.

Anomaly scenario	Lu_1	Lu_2	LC	$L\xi$	$L\psi$	LEsCFISH	LEvms	LCsCFISH
No anomalies ($\tau = 0$)	-352.93	-344.73	-47.03	-44.87	5.88	208.10	77.34	72.07
WFBT ($\tau = 0.1056$)	-359.36	-362.35	-49.21	-40.75	6.69	209.09	77.06	71.49
CEBEKE ($\tau = 0.1475$)	-365.95	-384.88	-50.48	-37.35	6.59	209.91	78.11	71.46
Anomalies estimated	-409.4	-487.99	-55.38	-21.18	0.60	211.10	73.36	70.40

where Lu_1 is the likelihood component (calculated as twice the negative log-likelihood) for the ‘long-term’ catch per unit effort series, Lu_2 is the likelihood component for the ‘CFISH’ catch per unit effort series (CFISH is the mandatory commercial fishery logbook database managed by Fisheries Queensland), LC is the likelihood for the total annual catch series between 1978 and 1996, $L\xi$ is the penalty on the free floating temporal anomalies, $L\psi$ is the penalty on the free floating spatial anomalies, LEsCFISH is the likelihood for the CFISH monthly-six minute grid effort, LEvms is the likelihood for the fit to the fishing effort calculated from Vessel Monitoring System data, and LCsCFISH is the likelihood for the CFISH monthly-six minute grid catch. For more details on these data sets and the likelihood equations see Campbell *et al.* (2012). In the above table, row one (τ fixed at zero) leads to a total (twice negative log) likelihood of -426, row two (WFBT) gives a likelihood of -447, row three (CEBEKE) produces -472, and row four (all anomalies estimated) produces -618.

A more direct way to gauge the impact of including one or more abiotic relationships on the model is to evaluate various equilibrium quantities (such as maximum sustainable yield, MSY), with and without the data. The following procedure was followed:

1. Model parameters were estimated with τ at zero (row one of the above table).
2. An MSY estimation procedure was run [see Campbell *et al.* (2012) for details].
3. Model parameters were estimated using CEBEKE (row three of the above table).

4. An MSY estimation procedure was run.

The results of this analysis were: 526 tonnes ($\tau=0$) and 468 tonnes (CEBEKE). (These values are not to be interpreted as actual MSY values for the stock – for that see SAFS 2014).

It is clear from these analyses that i) CEBEKE and, to a lesser extent, WFBT, improve the fit of the model, and that ii) this impact is significant with respect to management-relevant quantities. More research is needed to explore the causal mechanisms behind these effects.

7.3 SIMULATING LARVAL ADVECTION

At the level of a global average, the surface (1-5 m) and deep (15 m) layers did not produce widely different results, and so only the surface layer plots are presented in the discussion that follows. The issue of which kind of connectivity best captures the most likely advection path of the larvae is explored in the section on fitting a statistical model. Figure 7-2a plots the mean connectedness of each cell, where connectedness is defined simply as the number of other cells a particular cell sent larvae to over the 19 years. Figure 7-2b plots the variance in the connectedness of each site. It is clear from the plots that the mean and the variance in connectedness are strongly correlated. This implies that the mean connectivity alone is an inadequate predictor of the connections a particular site will make in a particular spawning.

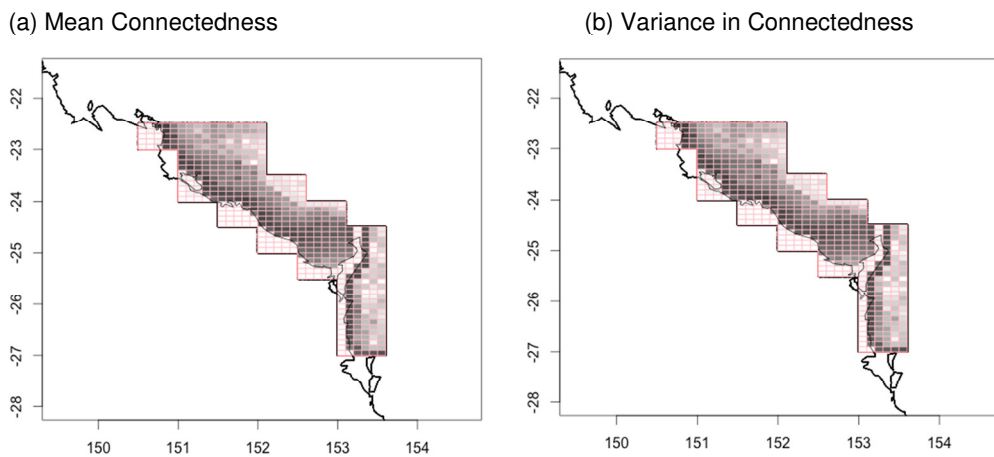


Figure 7-2. a) The mean number of connections made by each cell, and b) variance in connectedness, for the QLD Scallop fishery. Zero is represented by white, and black represents 339 connections.

Next, in Figure 7-3 we considered which sites waste the most larvae, losing larvae to outside the general scallop fishery area. Given the dominant current in the region is to the northwest, it is unsurprising that cells near to the top end of the region experience the highest wastage. It is clear from the variance plot that the wastage dynamic is as variable as it is pronounced, however, and in a given season it is quite possible for these cells to both experience a completely wasted spawning, and a spawning with adequate retention.

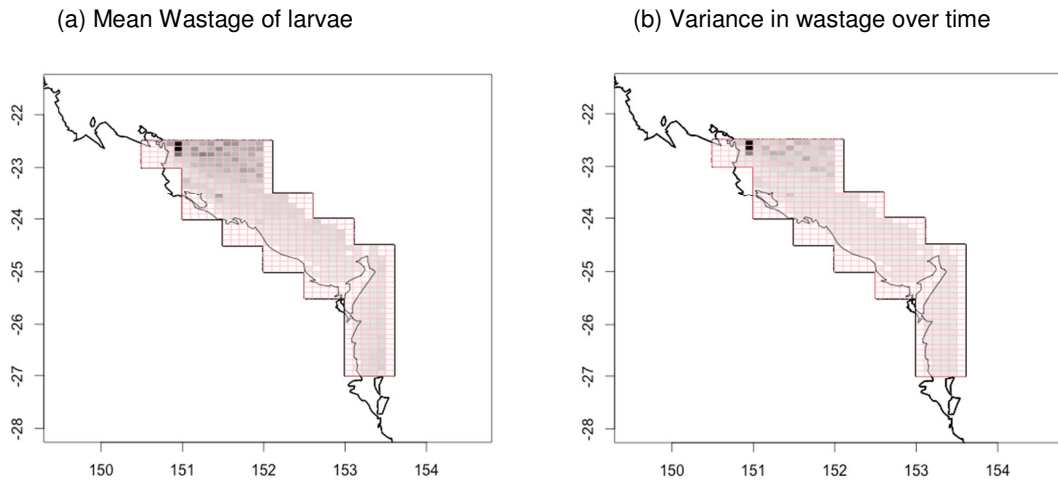


Figure 7-3. a) The mean number of larvae wasted by each cell, and b) variance in wastage, for the Queensland scallop fishery. No wastage is represented by white, and black represents 100% wastage.

The level of self-seeding by sites was also considered, as measured by the total number of larvae that settle in their initial spawning location. Significantly, High Fishing Effort Regions 1, 2 and 3 (Figure 6-2) experience reasonably high levels of self-seeding (Figure 7-4a) and a low variance over time in this pattern (Figure 7-4b). This is a more significant result than the high self-seeding indicated along the coast because of its consistency, and because the coastal region’s apparent high self-seeding is in part an artefact of the simulation setup. When the larvae encounter the coast they ‘stick’ there artificially as if they settled. Some may indeed settle there in reality, but a significant portion would also become beached and die, or get flushed back out to sea by the tides.

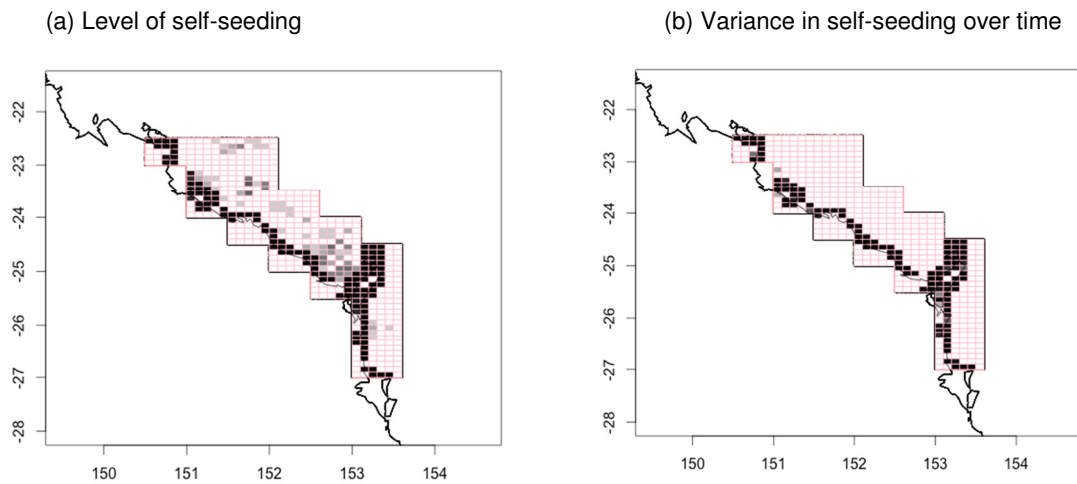


Figure 7-4. a) The level of self-seeding on a relative scale, b) the variance in that self-seeding behaviour.

Turning our attention specifically to the three regions of high fishing effort indicated in Figure 6-2 we are interested in determining 1) the sites whose larvae are responsible for seeding these three regions, and 2) where larvae from the three regions end up. Figure 7-5 shows where the larvae that settle in Region 1 come from using a binary scale (a) and a relative grey-scale (b). Region 1 is the region of highest fishing effort in the fishery. It is quite apparent that self-seeding is very important for this region’s maintenance. Moreover, we already know from Figure 7-4 that self-seeding here is relatively stable over time.

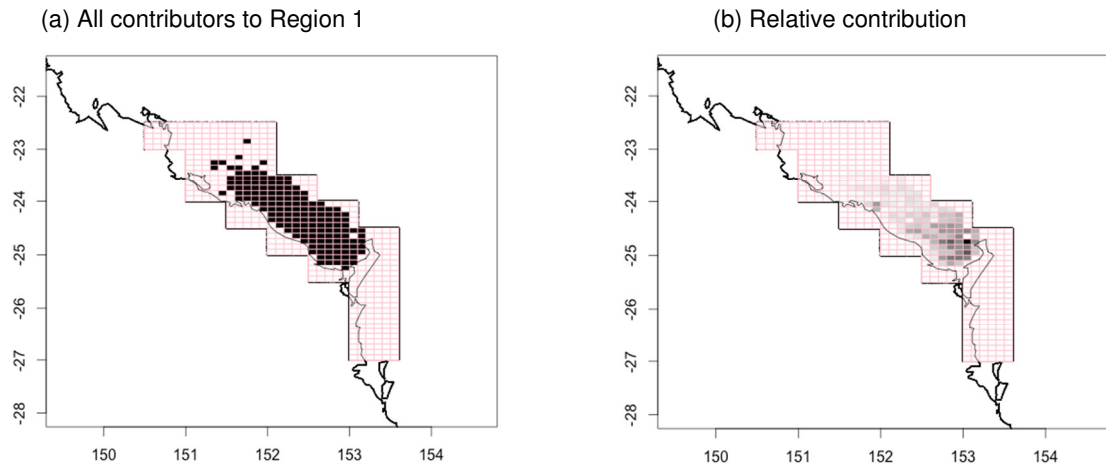


Figure 7-5. a) All potential source cells for Region 1, and b) the relative contribution by these source cells to Region 1.

Next we considered Regions 2 and 3. Figure 7-6a and Figure 7-7a display all sites that contribute to Regions 2 and 3 respectively, while Figure 7-6b and Figure 7-7b show the relative contribution of those sites. It is clear that almost any site north of Fraser Island can contribute to Regions 2 and 3 in a given spawning season. However, the dominant sources are clustered in a horizontal band that begins in each region, and stretches eastward.

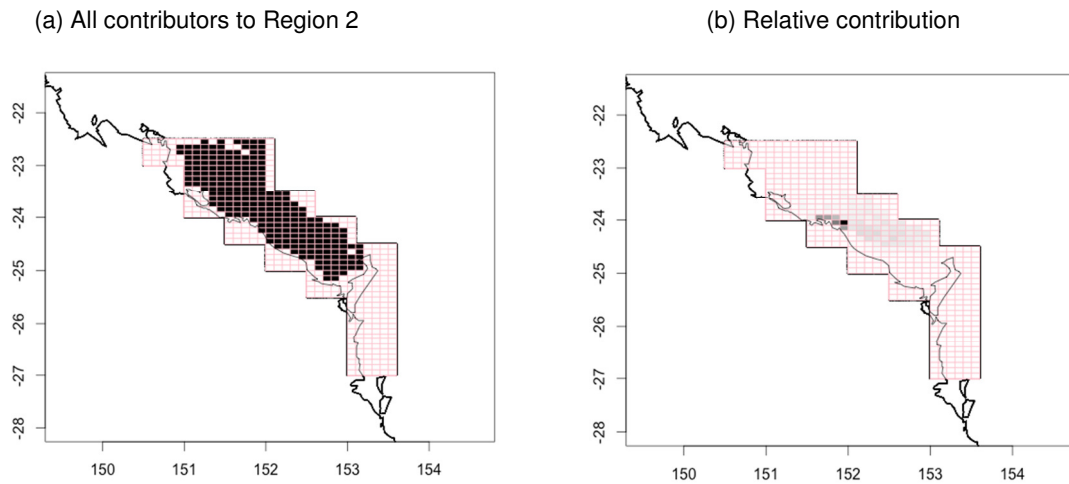


Figure 7-6. a) All potential source cells for Region 2, and b) the relative contribution by these source cells to Region 2.

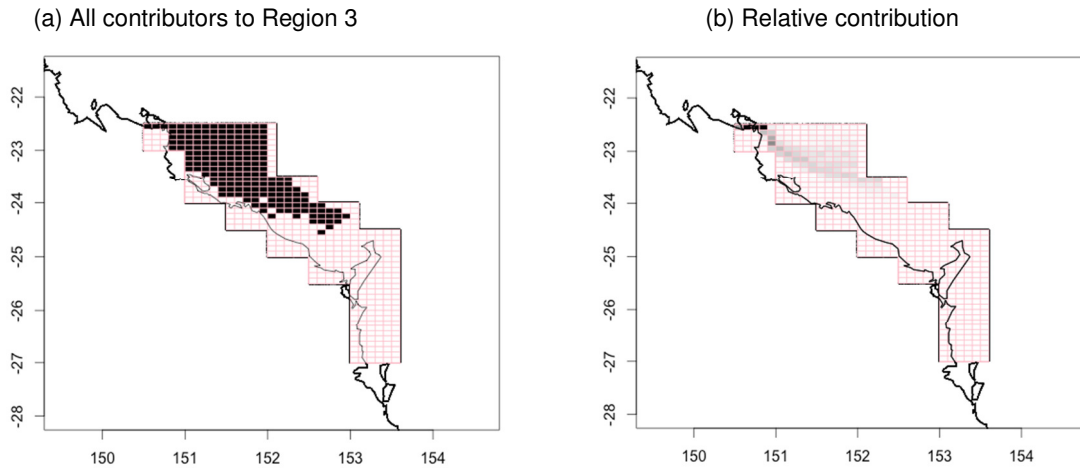


Figure 7-7. a) All potential source cells for Region 3, and b) the relative contribution by these source cells to Region 3.

In the final step of the analysis we also investigated the destinations of larvae spawned from each of the three regions of high fishing effort. Results from Region 1 are plotted below (Figure 7-8). It is not surprising that the destination cells differ from the source cells, but it does come as a surprise that Region 1 appears to send the majority of its larvae to the coast, potentially resulting in beaching of the larvae and subsequent loss. This indicates that the self-seeding dynamic driving the productivity of this region is in fact not very common. Instead it is more common for larvae to be swept coastward in a given spawning event. Results for Regions 2 and 3 reflected a similar pattern, but for these regions, the larvae were not swept coastward, but out of the fishery to the north.

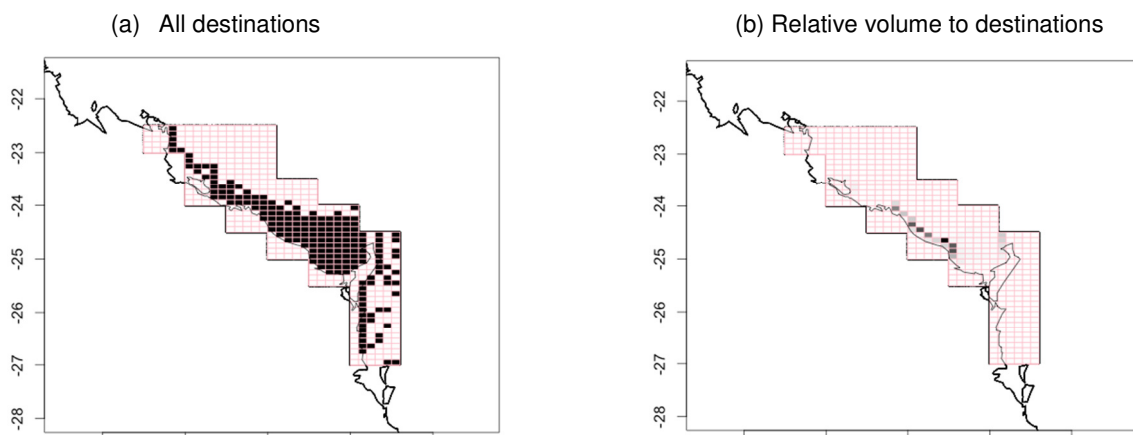


Figure 7-8. a) All potential destination cells for larvae from Region 3, and b) the proportion of larvae from Region 1 that end up in each cell. Note: it is evident that the majority of larvae are washed against the coast.

7.4 INFLUENCE OF LOW-PRESSURE SYSTEMS ON THE REEF FIN-FISH FISHERY

In the inshore-fetch mechanism, a tropical cyclone or other low-pressure system with a particular size and position can generate a large southeasterly swell in the waters between the GBR and the coast. The waters between Rockhampton and Townsville act as a long fetch over which such a swell can build. At Townsville another, somewhat shorter, fetch runs east–west over which easterly swells can build. These swells bypass the GBR’s natural protection from its barrier reefs which efficiently dissipate offshore swells but are much less effective at dealing with swells from inshore.

The results bear out the inshore-fetch mechanism, in that the correlation of coral trout catch rates with data from the offshore-fetch model is poor, as was the correlation with cyclone energy in the analysis conducted by Leigh *et al.* (2014). A few systems have big impacts across very large areas of the GBR, while most tropical cyclones, even very powerful ones, have no noticeable effect on the fishery. The offshore-fetch model cannot explain these observations, whereas the inshore-fetch theory does. The few cyclones that have big impacts affect a bigger area than the offshore-fetch model can explain. Conversely, the majority of cyclones with large wave-height contributions in the offshore-fetch model have no discernible effect on the fishery. Moreover, the inshore-fetch theory also explains why catch rates from Cairns north are hardly ever noticeably affected by tropical cyclones whereas the Townsville and Mackay regions are the most affected.

In addition to tropical cyclones, the fishery can be strongly affected by a monsoonal weather pattern whereby low pressure cells form from a trough over the Coral Sea while a high pressure cell remains fairly stationary over the Tasman Sea, causing a strong pressure gradient. In extreme cases, such a system can generate easterly or southeasterly gales over the majority of the GBR for a week or more, as happened in April–May 2000.

We recommend recognition of the importance of inshore wave-height measurements, and the collation of available historical measurements. These data could then be used in new fishery catch rate standardisations that can properly take account of the effects of tropical cyclones. We also suggest that new oceanographic models for the GBR should be developed to take account of the prime importance of the inshore-fetch mechanism in generating damaging swells.

New catch rate standardisations should prove very valuable in fishery management as they may finally separate the effects of weather systems from the effects of fishing, which to date has been impossible. The process of setting quota in the fishery could then be based on the effects of fishing alone and made largely independent of cyclones.

8 Discussion

8.1 COASTAL AND OCEANOGRAPHIC INFLUENCES ON SCALLOP CATCH RATES

The study examined correlations between adjusted mean November catch rates and coastal and oceanographic variables (freshwater flow, surface and bottom sea water temperature anomalies, sea level, surface and bottom EKE, Chl-a and SOI). Several strong correlations were identified. In terms of ranking variables that are likely to have significant effects, Chl-a and water temperature anomalies had the strongest correlations with scallop catch rates. Sea level and EKE could be deemed as intermediate in terms of the number and strength of their correlations, while surprisingly, no significant correlations were obtained for SOI. Freshwater flows were generally positively correlated with catch rates, and may be correlated with Chl-a.

Of the five areas where physical oceanographic properties were examined, the area associated with the Capricorn Eddy produced the highest number of strong correlations with November catch rates. This suggests that the dynamics of the Eddy have a relatively strong influence on the scallop population dynamics. As the Eddy area is located further offshore, in greater depths and further from the scallop fishing grounds compared to the other areas considered, the mechanisms underlying its influence may be indirect and more challenging to describe.

Significant short-term (i.e. small lags of 3-6 months) and long-term (i.e. 12-24 month lags) correlations were identified, with the largest absolute correlation value of 0.85 obtained for Chl-a five months earlier in June at T30 Bustard Head. As saucer scallops are filter feeders, we speculate that elevated June Chl-a levels increase the survival, and possibly growth rate, of adult scallops (i.e. 1+ year old scallops) from June to when they were caught in November, probably as a result of increased food supply in the coastal ecosystem. This appears to be a short-term effect and unrelated to recruitment (i.e. it does not have a direct effect on reproductive output).

Significant long-term influences, such as the negative correlations with SST anomalies 16-18 months prior to the November catch rates (Figure 19-6), are likely to be associated with reduced recruitment. These lag periods coincide with the previous year winter spawning which produced the 1+ year old individuals that make up the November catches. This negative correlation with SST is similar to the negative effect of elevated water temperatures associated with strong *La Niña* conditions during the saucer scallop winter spawning in Shark Bay, Western Australia (Joll and Caputi 1995; Lenanton *et al.* 2009; Caputi *et al.* 2015). In brief, elevated SST during the winter spawning period (May-August) is associated with reduced catch rates in November the following year.

Three high-correlation relationships were separately incorporated in the quantitative age-structured scallop fishery model developed by Campbell *et al.* (2012), to test whether they improve model performance and estimation of key management measures. Two of these relationships, CEBEKE (bottom EKE at the Eddy area in January 22 months prior) and WFBT (bottom temperature anomalies in the Whole fishing area 23 months prior) improved model fit and estimation of MSY. As the age-structured model estimates recruitment from adult abundance from the previous year, it is the relationships with large lags (i.e. 12-24 months) that result in the model improvement.

Incorporating the 12-month lagged Chl-a correlation did not improve the model. This is probably because a 12-month lag is not long enough for the model to include in its estimate of recruitment, which is based on the previous year's spawning stock. If this Chl-a correlation is due to an increase in scallop catchability, then it could be incorporated by allowing the catchability parameter to vary. This highlights that not all strong correlations are likely to improve the fitting of the population model.

While the results are promising and show that assessment of the fishery can be improved, further research is required to understand the mechanisms underlying how key coastal and oceanographic variables affect the scallop's population dynamics.

8.2 SCALLOP LARVAL ADVECTION

A number of interesting dynamics of the Queensland Scallop Fishery's connectivity were explored, including site connectedness, site wastage, and site self-seeding. The sources of larvae responsible for seeding the main fishing areas, and destinations of larvae from those same regions were also explored. Connectedness was measured as the number of other sites a given site has sent larvae to at any point over the 19-season time period from 1993 to 2011. It is clear from the plots that connectedness is strongest close to the coast within Hervey Bay. Significantly however, connectedness was very variable over time, and no region could be identified which seeds many other regions with any reliable consistency.

Wastage of larvae from each cell was defined as the number of larvae that exited the fishery within the three-week advection period. Given the dominant regional current is north-westward, the results are somewhat intuitive; with the cells in the northern part of the fishery being most likely to have their larvae lost across the northern 'border'. The variance plots show that these cells are not guaranteed to lose larvae, however, as high variability indicates that it is possible for these cells to have a good spawning sometimes, and we thus cannot ignore their potential influence on the productivity of the fishery entirely.

Next, self-seeding throughout the region was analysed and some very interesting results were observed. The three regions of highest fishing effort were found to experience moderately high self-seeding, and the variance plots indicated that this pattern was consistent. We do not see this as a coincidence and instead propose that it is likely self-seeding is a driver of the high productivity of these high-effort areas. Notably, there is also a region south of Fraser Island that experiences high self-seeding with low variance (see Figure 7-4). This region is not regarded as a high fishing effort region, but is of interest due to its intermittent productivity.

Focus was then directed specifically to the dynamics of the three regions of highest fishing effort. It was found that each is potentially seeded by a very wide area, but a significantly smaller number of cells are responsible for the majority of seeding. This subset of contributing regions is typically within, or adjacent to the high fishing effort region itself, reinforcing our conclusion that self-seeding plays an important role in the productivity of these regions. When we looked at where larvae spawned in these three regions end up, however, it was found that Region 1 (Figure 6-2) sends a very large proportion of its larvae directly to the coast, potentially resulting in the beaching and loss of those larvae. Regions 2 and 3 are also highly likely to lose the majority of larvae due to the dominant northward current carrying them off the grid. This might suggest that while key to productivity, self-seeding in these regions does not occur in the majority of spawning events, but rather, is the result of a less-frequent current pattern.

Overall, this simulation has shown that the dynamics of regional connectivity are highly variable over time. The implication of this is that a single average connectivity matrix cannot provide a sufficient description of all connective patterns and is a significant finding, as dominant literature to date has tended to rely on average connectivity to describe the regional dispersion patterns. Crucially, we also found that self-seeding seems to be important to sustaining the scallop population in the regions of highest fishing effort. This has implications for the management of the fishery as it suggests that rotational closure of portions of the region is more likely to sustain the scallop population than protecting a single sub-region, whose larvae are expected to seed the rest of the region.

8.3 EFFECTS OF CYCLONES AND OTHER LOW-PRESSURE SYSTEMS ON REEF FISH

The time series of fishery catch rates support the theory that the major impacts of low-pressure systems to the GBR come from the few systems that are able to use the waters inshore of the GBR as a fetch and generate large southeasterly swells behind the outer barrier of the GBR. The correlations of catch rates with the wave-height model using offshore fetch are poor, as were the correlations of Leigh *et al.*

(2014) using cyclone wind energy. The inshore-fetch mechanism is the only available hypothesis that can explain the observations.

Apart from explaining why only a few systems have significant effects on the GBR fishery, while many powerful tropical cyclones do not, the inshore-fetch mechanism also explains

- why the effects of the important systems cover such huge areas of the GBR which cannot be explained by other means, and
- why tropical cyclones have little if any effect north of Cairns.

The inferred large impact of Cyclones Dylan and Ita in 2014 is a new result from this project. Previously, it was known that coral trout catch rates fell in 2014, resulting in a decrease in quota allocations in 2015, but even the fishers as far as we know did not suggest that Dylan and Ita were responsible.

This project has taken substantial steps towards finding a useful correlation between cyclone measurements and coral trout catch rates. The cyclone measurements that are needed appear to be easy to collect and are already being collected as part of Queensland's beach protection program. Models based on offshore fetch and northeasterly swells are not likely to be useful because the outer reefs of the GBR are very well adapted to dissipating swells from offshore of the GBR. Models based on the SST effects of cyclones, the original aim of this project, will be even less useful.

9 Conclusion

All of the project objectives have been achieved. The key findings are that stakeholders (i.e. fishers, fishery managers, the science community and others) will have a greater understanding of the influence of coastal and oceanographic conditions, including cyclone effects, on the Queensland fisheries for reef fish and saucer scallops. These findings are now being incorporated in the stock assessment procedures for these important resources. For scallops, the outcomes include improved management advice for the sustainability of the stocks, based on better understanding of their population dynamics and susceptibility, and better forecasting of catches to help fishers prepare for fishing seasons. For reef fish, the major outcome is better estimation of abundance of coral trout due to the ability to standardise catch rates for the effects of weather systems; this may also increase the acceptance of quantitative stock assessment results by industry.

Objective 1. Review recent advances in the study of physical oceanographic influences on fisheries catch data, and describe the major physical oceanographic features that are likely to influence Queensland reef fish and saucer scallops.

This objective has been achieved. Literature reviewed includes a description of the physical oceanographic conditions on the Queensland coast, examples of physical oceanographic influences on fisheries and reef systems, ocean modelling and larval advection. The coastal and physical oceanographic variables considered include freshwater flow, Chl-a, sea level and wave height data, EKE, sea water temperature and temperature anomalies at the surface and bottom, current strength and direction, SOI and tropical cyclones.

Objective 2. Collate Queensland's physical oceanographic data and fisheries (i.e. reef fish and saucer scallops) data.

This objective has been achieved. The project collated physical oceanographic and fisheries data from several sources. We used both raw observational data and model-derived predictions. Freshwater flows were obtained from the Queensland Department of Natural Resources and Mines. SOI data were obtained from the BOM. Monthly Chl-a were downloaded from the BOM eReefs Data Access - Thredds data server (http://ereefstds.bom.gov.au/ereefs/tds/catalogs/ereefs_data.html). Physical oceanographic data on temperature anomalies, sea level and EKE were obtained using the BRAN 3.5 hindcast dataset with assistance from BOM and CSIRO. Data on wave heights were obtained from the

Queensland Government's environmental monitoring program (<http://www.qld.gov.au/environment/coasts-waterways/beach/monitoring/>) and from models of tropical cyclones by Marjietta L. Puotinen. Fisheries catch rate data were obtained from the Queensland DAF CFISH logbook system and survey data, and standardised to take account of changes in fleet fishing power over the ~ 26 year time series (i.e. catch rates were adjusted for fishing effort creep).

Objective 3. Develop stochastic population models for reef fish and saucer scallops, which can link physical oceanographic features (e.g. sea surface temperature anomalies) to catch rates, biological parameters (e.g. growth, reproduction, natural mortality) and ecological aspects (e.g. spatial distribution).

For saucer scallops this objective has been achieved. Several high-correlation relationships between scallop catch rates and coastal and oceanographic variables were demonstrated. These provide an improved understanding of the likely biotic (i.e. Chl-a) and abiotic (i.e. the Capricorn Eddy) drivers affecting the scallop stock and the fishery. Some of the relationships may at least partially explain why the fishery crashed in 1996. The influence of three of these relationships was investigated using the age-structured model that is used to assess the fishery. Two of the three were found to improve the model fit, and the estimate of MSY.

For reef fish the objective was achieved by subjective analysis of weather systems, due to lack of predictive capability of available oceanographic models for the GBR. The effect of a given weather system on catch rates was found to be highly dependent on the exact position and size of the weather system, which makes oceanographic modelling exceptionally difficult. Objectivity of the analysis was improved, however, by the availability of physical measurements of wave height which were collated by the project.

It was established that wave height, not sea surface temperature, was the important quantity in gauging the effect of tropical cyclones on catch rates, and moreover that the important fetches for generating waves on the Great Barrier Reef run between Yeppoon in the southeast and Townsville in the northwest, and between Darley Reef in the east and Townsville in the west. Current oceanographic models derived from cyclone wind fields are not able to adequately predict wave height, due to the difficulty of modelling the wave-dissipation capability of coral reefs. Also many low-pressure systems that markedly affect the GBR are not, in fact, tropical cyclones. The oceanographic model that was used was, however, beneficial in indicating that the important variable was the presence or absence of exposure to large waves, and that the duration of exposure was much less important. This supports the hypothesis that it is physical damage to coral reefs that affects fishery catch rates.

For oceanographic models to be able to predict the effects of low-pressure systems on catch rates, new features are needed that emphasise inshore fetches and also consider systems that are not tropical cyclones. The project has shown that the use of direct wave-height measurements is essential, even though these may be primarily shore-based.

10 Implications

The commercial catch rate correlation analyses (Appendix 5. Coastal and oceanographic influences on the Queensland (Australia) east coast saucer scallop (*Amusium balloti*) fishery) provide insight and direction for further research into likely coastal and oceanographic influences on the scallop stock. While no causal mechanisms were demonstrated, it is likely that some of the strong correlations, such as the relationship between November catch rates and Chl-a concentration five months prior in June, do reflect cause and effect based on primary productivity and scallop food supply. Hence, it is likely that at least some of the correlations can be used to explain variation in the Queensland saucer scallop's population dynamics, catch rates and annual landings.

This is important because the fishery's landings are highly variable and recruitment has previously failed (e.g. 1996) resulting in the fishery's collapse and subsequent emergency management intervention (i.e. scallop replenishment areas implemented since 1997 that persist today). Prior to this project there has been no research to explain the collapse and other significant annual variation in landings. Therefore, a significant outcome of the project is the ability to explain variation in the scallop fishery catch rates and landings. This variation applies to both past catches, such as the 1996 collapse, and forecasts.

An outcome of the project is the knowledge that when the fishery opens annually in November, catch rates can be expected to be reduced if SST was elevated 16-18 months prior during the previous year winter spawning period (Figure 19-6). Similarly, the correlation between Chl-a in June and catch rates the following November (Figure 19-16) can be used to help forecast the upcoming season. Fishers and managers can readily access Chl-a data from the BOM eReefs Data Access - Thredds data server to help predict catch rates when the scallop fishing year commences in November.

Another outcome of the project is improved quantitative assessment of the scallop stock (section 7.2 Does inclusion of oceanographic covariates improve scallop stock assessment?). The age-structured model fit and estimates of key management measures, including MSY, have been improved as a result of including key environmental relationships in the model.

Outcomes of the larval advection modelling (Appendix 6. Larval Advection Patterns in the Queensland Scallop Fishery) include improved understanding of the likely advection of scallop larvae in the region. The findings are relevant to the design and management of closures, including the currently-deployed scallop replenishment areas (SRAs), which were implemented in 1997 following the collapse of the fishery in 1996. The SRAs are now used both as reproductive refugia to reduce recruitment overfishing, and as rotationally targeted fished areas of high scallop density. The larval advection modelling shows that the dominant movement of larvae in the region, based on prevailing currents, is north-westerly towards the coast. It also indicates that the three scallop replenishment areas have relatively high rates of self-seeding, which may explain their relatively high densities and why they were chosen for closure.

The project has taken substantial steps towards finding correlation between weather-system effects and coral trout catch rates (Appendix 7. Impacts of low-pressure systems on the Great Barrier Reef: Confirmation of a causal mechanism using catch rates of the coral trout fishery). Many of the measurements that are needed are already being collected as part of Queensland's beach protection program. Models based on offshore fetch and northeasterly swells are not likely to be useful because the outer reefs of the GBR are very well adapted to dissipating swells from offshore of the GBR. Incorporating inshore wave height measurements in the standardisation of the coral trout catch rates should improve stock assessment advice, including the derivation of TAC estimates.

11 Recommendations

For the scallop fishery we put forward the following recommendations:

1. Key environmental variables, particularly Chl-a, SST and freshwater flows, should be routinely monitored in conjunction with scallop catch rates to help interpret catch rate trends and provide forecasts.
2. Three SRAs are used to regulate much of the effort in the scallop fishery. These closures were implemented in 1997 in high scallop density areas following what was considered to be recruitment failure in 1996. Initially the areas were permanently closed, but were later rotationally opened for nine months and closed for 15 months (i.e. two-year cycle). This rotational management regime continues to present day. Given that the project identified several strong environmental drivers in the fishery, including variables that largely explain the record low catch rates of 1996, we recommend a review of the need and function of the SRAs, particularly in regard to their role in reducing the risk of recruitment overfishing.
3. The influence of three environmental relationships was considered in the age-structured model used to assess the fishery. Two of the three relationships improved model fit. The influence of the other relationships (listed in 7.1 Influences on saucer scallop catch rates) should also be examined and where suitable, incorporated in the stock assessment process. Influential relationships could be incorporated as: a) a modified stock-recruitment-environment relationship to improve recruitment prediction, or as b) additional explanatory term/s in the catch rate standardisation.
4. Future larval advection modelling should use oceanographic models that include tidal vectors. Studies that provide some understanding of scallop larval vertical migration behaviour, especially diel and tidal variation, might also improve the larval modelling.

For the coral trout reef fishery we recommend that:

5. Inshore wave height measurements should be recognised for their importance in gauging the effects of east-coast weather systems on the GBR.
6. New oceanographic models for the GBR should be developed which take account of the prime importance of the inshore-fetch mechanism in generating damaging swells.
7. Historical inshore wave height measurements should be used in new fishery catch-rate standardisations that can properly take account of the effects of east-coast weather systems.

New catch rate standardisations should prove very valuable in fishery management as they may finally separate the effects of low-pressure systems from the effects of fishing, which to date has been impossible. The process of setting quota in the fishery could then be based on the effects of fishing alone and made largely independent of weather systems.

12 Further development

Although several strong correlations between catch rates and environmental variables were derived for the scallop fishery, no causal mechanism was demonstrated. In fact, for most of the correlations, the mechanism underlying how scallop catch rates are affected is unclear. For example, we don't know whether the strong correlation with June Chl-a (Figure 19-16) is a result of scallop abundance increasing, or scallop catchability increasing with Chl-a. The relatively short period between June and November (five months) could suggest the relationship is more likely attributed to increased catchability. Depletion experiments on scallop fishing grounds in areas of high and low Chl-a could provide information on how catchability varies with Chl-a.

Better understanding of the diet of scallops, and the role of Chl-a would be useful. Although June Chl-a has a strong positive correlation with November catch rates (i.e. five month lag, Figure 19-16), we also note that Chl-a has a strong negative correlation at a lag of 12-13 months (Figure 19-15). By studying bycatch in the scallop fishery, we know that sponges dominate the benthic faunal biomass on

the fishing grounds (Courtney *et al.* 2008). Sponges are also filter feeders and probably compete with scallops for planktonic food, including Chl-a.

We speculate that the strong negative correlations with Chl-a at 12-13 month lags are due to sponges outcompeting scallops for Chl-a, resulting in a decline in scallop catch rates. In brief, the effect of Chl-a on scallop catch rates appears complex and may be summarised as follows: elevated June Chl-a (short lag of five months) increases November catches, while elevated Chl-a 12-13 months prior results in significant sponge population growth (i.e. explosion), which outcompetes the scallops, resulting in reduced November scallop catch rates 12-13 months later. This hypothesis would explain the apparent anomaly of finding both strongly positive and strongly negative Chl-a correlations (Figure 19-15).

Reduced food availability is one of the possible causes that Caputi *et al.* (2015) put forward to explain the decline of 1+ age classes (i.e. residual stock) in the Shark Bay scallop fishery following strong *La Niña* conditions in 2011. Better understanding of such a possibly-antagonistic relationship between scallops and sponges could be obtained via annual fishery-independent monitoring of both species groups, in conjunction with Chl-a and fishing effort.

The Capricorn Eddy area was associated with the highest number of strong correlations with physical oceanographic variables (sea level, EKE and water temperature anomalies), suggesting that it has a significant influence on the scallop population and fishery. However, the mechanisms underlying how these features of the Eddy affect catch rates are unknown. We don't know why elevated August bottom temperature (Figure 19-7) and sea level (Figure 19-10) in the Eddy area are associated with decreased catch rates in November. Further research on the Eddy properties might help explain the mechanisms.

Ready access to updated time series of the coastal and oceanographic variables would be helpful. For the physical oceanographic variables of sea water temperature anomalies, EKE and sea level, the project was dependent on the BRAN 3.5 hindcast dataset, which ended in September 2012. An updated times series of these data is currently unavailable, although an updated version of the BRAN dataset is planned (Peter Oke CSIRO pers. comm).

Stock assessment of saucer scallops in Queensland is largely based upon commercial catch data, which are limited to 1+ scallops, due to the minimum legal size limit. This contrasts with the WA assessment that is primarily based on a November survey catch rate of 0+ scallops which enables an assessment of spawning stock and environmental conditions in the previous year which may affect the recruitment, as well as providing a reliable predictor of catch in the following year which facilitates the management of the stock, which is very important for fishers. The possibility of obtaining an index of 0+ abundance for the Queensland scallop fishery should be explored. This could be obtained in collaboration with industry e.g. from observers on board the trawl fleet at different locations when the fishery opens in each November.

Following recruitment failure in 1996, an annual fishery-independent survey of the Queensland scallop fishery was funded by the state government from 1997 to 2006 (Dichmont *et al.* 2000). This survey provided valuable information on the relative abundance of 0+ and 1+ scallops from several hundred sites annually. However, after 2006 support for the survey waned and it has not been undertaken since.

The BRAN 3.5 hindcast dataset does not include tidal vectors and therefore is probably limited in regard to modelling scallop larval trajectories, especially in shallow water fisheries close to the coast. Coastal oceanographic models that incorporate tidal vectors could improve the modelling, although it may be unlikely that such a model encompasses the 19-year time series of BRAN 3.5. Information on scallop larval vertical migration behaviour, especially information on diel and tidal patterns would be useful. As this type of information was unknown, two behavioural scenarios were modelled, with similar results - larvae were assumed to remain at the surface (1-5 m) or at 15 m, before settling.

Long-term time series on wave height data within the GBR that reflect events associated with low-pressure systems should be collated and used in the coral trout catch rate standardisation. They would also be useful to development of new oceanographic models for the southern GBR which could emphasise inshore fetches and predict damaging swells which affect coral trout catch rates.

13 Extension and Adoption

- Results were presented and discussed three times during the project at dedicated project steering committee meetings (see section 1 Acknowledgements for list of committee members) on 13 December 2013, 15 August 2014 and 18 September 2015. Copies of the presentations and minutes of the meetings have been forwarded to FRDC with Milestone reports.
- An article about the project was published in the IMOS newsletter *Marine Matters* issue 16 December 2013.
- Findings were presented at the AMSA 2015 conference. Courtney, A. J. and C. M. Spillman (2015). Coastal and oceanographic influences on the Queensland (Australia) east coast saucer scallop (*Amusium balloti*) fishery. Australian Marine Sciences Association Conference, Deakin University, Geelong, Australia July 5-9, 2015.
- Project findings are now being incorporated in the stock assessment for Queensland coral trout and scallops. High-correlation relationships are being incorporated in the age-structured model used to assess the scallop fishery and derive reference points (i.e. MSY). The project has made significant progress understanding how tropical cyclones affect coral trout catch rates. It was established that wave height, not sea surface temperature, was the important quantity in gauging the effect of tropical cyclones on catch rates, and moreover that the important fetches for generating waves on the Great Barrier Reef run between Yeppoon in the southeast and Townsville in the northwest, and between Darley Reef in the east and Townsville in the west. As a result of the project, the coral trout catch rate standardisation has improved, resulting in improved stock assessment advice on this high-value iconic species.

14 Project materials developed

The contents of section 19 “Appendix 5. Coastal and oceanographic influences on the Queensland (Australia) east coast saucer scallop (*Amusium balloti*) fishery” by A. J. Courtney and C. M. Spillman are intended to be published as a scientific paper in *Fisheries Oceanography*.

15 Appendix 1. Staff

Dr Alex Campbell, Fishery Resource Assessment Scientist (DAF)

Dr Tony Courtney, Principal Fisheries Biologist (DAF)

Dr George Leigh, Fishery Resource Assessment Scientist (DAF)

Dr Ricardo Lemos, Lecturer, Centre for Applications in Natural Resource Mathematics (CARM), University of Queensland

Dr Claire Spillman, Australian Weather and Climate Research (CAWCR), Australian Bureau of Meteorology (BOM)

Mr Jesse Thomas, Master’s degree student, Centre for Applications in Natural Resource Mathematics (CARM), University of Queensland

16 Appendix 2. Intellectual property

No intellectual property has been generated by the project.

17 Appendix 3. References

- Bank of New South Wales. (1979) Offshore resources: Australia's continental shelf and beyond.
- Bureau of Meteorology. (2012) Record-breaking La Nina events. (Ed. Bureau of Meteorology).
- Baker, A.C., Glynn, P.W. and Riegl, B. (2008) Climate change and coral reef bleaching: An ecological assessment of long-term impacts, recovery trends and future outlook. *Estuarine Coastal and Shelf Science* **80**, 435-71.
- Bakun, A. (2006) Fronts and eddies as key structures in the habitat of marine fish larvae: opportunity, adaptive response and competitive advantage. *Scientia Marina*(70), 105-122.
- Banerjee, S., Gelfand, A.E. and Carlin, B.P. (2004) 'Hierarchical Modeling and Analysis for Spatial Data.' (Taylor & Francis)
- Battaglione, S., Carter, C., Hobday, A.J., Lyne, V. and Nowak, B. (2008) Scoping Study into Adaptation of the Tasmanian Salmonid Aquaculture Industry to Potential Impacts of Climate Change. National Agriculture & Climate Change Action Plan: Implementation Programme Report.
- Beggs, H., Zhong, A.H., Warren, G., Alves, O., Brassington, G. and Pugh, T. (2011) RAMSSA - An operational, high-resolution, Regional Australian Multi-Sensor Sea surface temperature Analysis over the Australian region. *Australian Meteorological and Oceanographic Journal* **61**(1), 1-22.
- Bennett, A.F. (1992) 'Inverse Methods in Physical Oceanography.' First edn. (Cambridge University Press: New York)
- Berliner, L.M., Wikle, C.K. and Cressie, N. (2000) Long-lead prediction of Pacific SSTs via Bayesian dynamic modeling. *Journal of Climate* **13**(22), 3953-3968.
- Bograd, S.J., Thomson, R.E., Rabinovich, A.B. and LeBlond, P.H. (1999) Near-surface circulation of the northeast Pacific Ocean derived from WOCE-SVP satellite-tracked drifters. *Deep-Sea Research Part II-Topical Studies in Oceanography* **46**(11-12), 2371-2403.
- Boland, F.M. (1973) A monitoring section across the east Australian current.
- Boland, F.M. and Church, J.A. (1981) The East Australian Current 1978. *Deep Sea Research (Part II, Topical Studies in Oceanography)* **28A**, 937-957.
- Boland, F.M. and Hamon, B.V. (1970) The East Australian Current, 1965-1968. *Deep Sea Research (Part II, Topical Studies in Oceanography)* **17A**, 777-794.
- Brando, V.E., Dekker, A.G., Park, Y.J. and Schroeder, T. (2012) An adaptive semianalytical inversion of ocean colour radiometry in optically complex waters. *Applied Optics* **51**(15), 2808-2833.
- Brasseur, P., Beckers, J.M., Brankart, J.M. and Schoenauen, R. (1996) Seasonal temperature and salinity fields in the Mediterranean Sea: Climatological analyses of a historical data set. *Deep-Sea Research Part I-Oceanographic Research Papers* **43**(2), 159-192.
- Brown, P.J., Le, N.D. and Zidek, J.V. (1994) Multivariate spatial interpolation and exposure to air-pollutants. *Canadian Journal of Statistics-Revue Canadienne De Statistique* **22**(4), 489-509.
- Bryan, K. and Cox, M.D. (1967) A numerical investigation of the oceanic general circulation. *Tellus* **19**(1), 54-80.

- Bryan, K. and Cox, M.D. (1968) A nonlinear model of an ocean driven by wind and differential heating .I. Description of 3-dimensional velocity and density fields. *Journal of the Atmospheric Sciences* **25**(6), 945-&.
- Burston, J.M., Nose, T. and Tomlinson, R. Options for real-time forecasting of storm tide inundation for emergency management in Queensland, Australia. In 'Oceans 2013', 23–27 September 2013 2013, San Diego, CA,
- Callaghan, J. (2011a) Case Study: Tropical Cyclone Justin, March 1997. (Green Cross Australia)
- Callaghan, J. (2011b) Tropical Cyclone Larry, 2006. (Green Cross Australia)
- Campbell, A.B., O'Neill, M.F., Leigh, G.M., Wang, Y.-G. and J., J.E. (2012) Reference points for the Queensland scallop fishery.
- Campbell, M.J., Campbell, A.B., Officer, R.A., O'Neill, M.F., Mayer, D.G., Thwaites, A., Jebreen, E.J., Courtney, A.J., Gribble, N., Lawrence, M.L., Prosser, A.J. and Drabsch, S.L. (2010a) Harvest strategy evaluation to optimise the sustainability and value of the Queensland scallop fishery - FRDC Final Report Number 2006/024. Department of Employment, Economic Development and Innovation, Brisbane, Queensland.
- Campbell, M.J., Officer, R.A., Prosser, A.J., Lawrence, M.L., Drabsch, S.L. and Courtney, A.J. (2010b) Survival of Graded Scallops *Amusium balloti* in Queensland's (Australia) Trawl Fishery. *Journal of Shellfish Research* **29**(2), 373-380.
- Caputi, N., Feng, M., Pearce, A., Benthuyesen, J., Denham, A., Hetzel, Y., Matear, R.J., Jackson, G., Molony, B.W., Joll, L. and Chandrapavan, A. (2015) Management implications of climate change effect on fisheries in Western Australia: Part 1 Environmental change and risk assessment. FRDC Project 2010/535. Fisheries Research Report 260, Department of Fisheries, Western Australia.
- Caputi, N., Fletcher, W.J., Pearce, A. and Chubb, C.F. (1996) Effect of the Leeuwin Current on the recruitment of fish and invertebrates along the Western Australian coast. *Marine & Freshwater Research* **47**(2), 147-55.
- Caputi, N., Melville-Smith, R., Lestang, S.d., Pearce, A. and Feng, M. (2010) The effect of climate change on the western rock lobster (*Panulirus cygnus*) fishery of Western Australia. *Canadian Journal of Fisheries and Aquatic Sciences* **67**(1), 85-96.
- Carton, J.A. and Giese, B.S. (2008) A reanalysis of ocean climate using Simple Ocean Data Assimilation (SODA). *Monthly Weather Review* **136**(8), 2999-3017.
- Chang, C.W.J. and Chao, Y. (2000) A comparison between the World Ocean Atlas and Hydrobase Climatology. *Geophysical Research Letters* **27**(8), 1191-1194.
- Chassignet, E.P., Hurlburt, H.E., Smedstad, O.M., Halliwell, G.R., Hogan, P.J., Wallcraft, A.J., Baraille, R. and Bleck, R. (2007) The HYCOM (HYbrid Coordinate Ocean Model) data assimilative system. *Journal of Marine Systems* **65**(1-4), 60-83.
- Chiswell, S.M. and Rickard, G.J. (2014) Evaluation of Bluelink hindcast BRAN 3.5 at surface and 1000m. *Ocean Modelling* **83**(0), 63-81.
- Church, J.A. (1987) East Australian Current Adjacent to the Great Barrier Reef. *Australian Journal of Marine and Freshwater Research* **38**, 671-83.

- Condie, S.A., Mansbridge, J.V. and Cahill, M.L. (2011) Contrasting local retention and cross-shore transports of the East Australian Current and the Leeuwin Current and their relative influences on the life histories of small pelagic fishes. *Deep Sea Research (Part II, Topical Studies in Oceanography)* **58**(5), 606-615.
- Cornillon, P., Adams, J., Blumenthal, M.B., Chassignet, E., Davis, E., Hankin, S., Kinter, J., Mendelssohn, R., Potemra, J.T., Srinivasan, A. and Sirott, J. (2009) NVOODS and the development of OPeNDAP. *Oceanography* **22**(2), 116-127.
- Courtney, A.J., Campbell, M.J., Roy, D.P., Tonks, M.L., Chilcott, K.E. and Kyne, P.M. (2008) Round scallops and square-meshes: a comparison of four codend types on the catch rates of target species and bycatch in the Queensland (Australia) saucer scallop (*Amusium balloti*) trawl fishery. *Marine and Freshwater Research* **59**, 849–864.
- Cressie, N.A.C. (1993) 'Statistics for spatial data.' (J. Wiley)
- Dichmont, C.M., Dredge, M.C.L. and Yeomans, K. (2000) The first large-scale fishery-independent survey of the saucer scallop, *Amusium japonicum balloti* in Queensland, Australia. *Journal of Shellfish Research* **19**(2), 731-739.
- Doney, S.C., Lindsay, K., Caldeira, K., Campin, J.M., Drange, H., Dutay, J.C., Follows, M., Gao, Y., Gnanadesikan, A., Gruber, N., Ishida, A., Joos, F., Madec, G., Maier-Reimer, E., Marshall, J.C., Matear, R.J., Monfray, P., Mouchet, A., Najjar, R., Orr, J.C., Plattner, G.K., Sarmiento, J., Schlitzer, R., Slater, R., Totterdell, I.J., Weirig, M.F., Yamanaka, Y. and Yool, A. (2004) Evaluating global ocean carbon models: The importance of realistic physics. *Global Biogeochemical Cycles* **18**(3).
- Dredge, M.C.L. (1981) Reproductive biology of the Saucer Scallop *Amusium japonicum balloti* (Bernardi) in Central Queensland Waters. *Australian Journal of Marine and Freshwater Research* **32**(5), 775-787.
- Dredge, M.C.L. (1985) Estimates of natural mortality and yield-per-recruit for *Amusium japonicum balloti* Bernardi (*Pectinidae*) based on tag recoveries. *Journal of Shellfish Research* **5**(2), 103-109.
- Dunn, K. and Smyth, G. (1996) Randomized quantile residuals. *J. Comput. Graph. Statist.* **5**, 236-244.
- Edwards, P.N., Mayernik, M.S., Batcheller, A.L., Bowker, G.C. and Borgman, C.L. (2011) Science friction: Data, metadata, and collaboration. *Social Studies of Science* **41**(5), 667-690.
- England, M. and Oke, P. (2002) Ocean Modelling and Prediction. In *Environmental Modelling and Prediction*. (Eds. G Peng, L Leslie and Y Shao) pp. 125-171. (Springer Berlin Heidelberg)
- Erwin, C.A. and Congdon, B.C. (2007) Day-to-day variation in sea-surface temperature reduces sooty tern (*Sterna fuscata*) foraging success on the Great Barrier Reef, Australia. *Marine Ecology Progress Series* **331**, 255-266.
- Fernandes, L., Day, J., Lewis, A., Slegers, S., Kerrigan, B., Breen, D., Cameron, D., Jago, B., Hall, J., Lowe, D., Innes, J., Tanzer, J., Chadwick, V., Thompson, L., Gorman, K., Simmons, M., Barnett, B., Sampson, K., De'ath, G., Mapstone, B., Marsh, H., Possingham, H., Ball, I., Ward, T., Dobbs, K., Aumend, J., Slater, D. and Stapleton, K. (2005) Establishing representative no-take areas in the Great Barrier Reef: large-scale implementation of theory on marine protected areas. *Conservation biology* **19**(6), 1733-1744.
- Fletcher, W.J., Kearney, R.E., Wise, B.S. and Nash, W.J. (2015) Large-scale expansion of no-take closures within the Great Barrier Reef has not enhanced fishery production. *Ecological Applications*.

Appendices – References

- Ganachaud, A. (2003) Large-scale mass transports, water mass formation, and diffusivities estimated from World Ocean Circulation Experiment (WOCE) hydrographic data. *Journal of Geophysical Research-Oceans* **108**(C7).
- GBRMPA (2009) Great Barrier Reef Outlook Report 2009. Great Barrier Reef Marine Park Authority, Townsville.
- Gelman, A., Carlin, J.B., Stern, H.S., Dunson, D.B., Vehtari, A. and Rubin, D.B. (2013) 'Bayesian Data Analysis, Third Edition (Chapman & Hall/CRC Texts in Statistical Science).' (Chapman & Hall/CRC)
- GenStat (2011) 'GenStat Fourteenth Edition.' (Laws Agricultural Trust)
- Gordon, H.R. (1997) Atmospheric correction of ocean color imagery in the Earth Observing System era. *Journal of Geophysical Research-Atmospheres* **102**(D14), 17081-17106.
- Gregg, W.W. and Casey, N.W. (2004) Global and regional evaluation of the SeaWiFS chlorophyll data set. *Remote Sensing of Environment* **93**(4), 463-479.
- Griffies, S.M., Boning, C., Bryan, F.O., Chassignet, E.P., Gerdes, R., Hasumi, H., Hirst, A., Treguier, A.M. and Webb, D. (2000) Developments in ocean climate modelling. *Ocean Modelling* **2**(3-4), 123-192.
- Griffin, D.A. and Middleton, J.H. (1986) Coastal-trapped waves behind a large continental shelf island, Southern Great Barrier Reef. *Journal of Physical Oceanography* **16**, 1651-1664.
- Griffin, D.A., Middleton, J.H. and Bode, L. (1987) The tidal and longer-period circulation of capricornia, southern great barrier reef. *Australian Journal of Marine and Freshwater Research* **38**(4), 461-474.
- Guttorp, P., Meiring, W. and Sampson, P.D. (1994) A space-time analysis of ground-level ozone data. *Environmetrics* **5**(3), 241-254.
- Hamon, B.V. (1965) The east Australian current. *Deep Sea Research* **12**, 899-921.
- Handcock, M.S. and Wallis, J.R. (1994) An approach to statistical spatial-temporal modeling of meteorological fields. *Journal of the American Statistical Association* **89**(426), 368-378.
- Harris, P.T. (1993a) Near Bed current measurements from the continental shelf off Fraser Island Queensland during June-July 1993. *Ocean Sciences Institute Technical Report* **30**, 1-53.
- Harris, P.T. (1993b) Near bed current measurements from the continental shelf off Fraser Island, Queensland during November-December 1992. *Ocean Sciences Institute Technical Report* **28**, 1-66.
- Hekel, H., Ward, W.T., Jones, M. and Searle, D.E. Geological development of northern Moreton Bay. In 'Northern Moreton Bay Symposium. The proceedings of a symposium held at , September 23-24, 1978'. (Eds. A. Bailey and N. C.Stevens.) pp.7-18. (Royal Society of Queensland: Brisbane, Queensland.)', 1979, Abel Smith Lecture Theatre, University of Queensland. (Ed. ABaN C.Stevens),
- Hobday, A.J., Flint, N., Stone, T. and Gunn, J.S. (2009) 'Electronic tagging data supporting flexible spatial management in an Australian longline fishery.' (Springer, Dordrecht, Netherlands)
- Hobday, A.J. and Hartmann, K. (2006) Near real-time spatial management based on habitat predictions for a longline bycatch species. *Fisheries Management and Ecology* **13**(6), 365-380.

Appendices – References

- Hobday, A.J., Hartog, J.R., Spillman, C.M. and Alves, O. (2011) Seasonal forecasting of tuna habitat for dynamic spatial management. *Canadian Journal of Fisheries and Aquatic Sciences* **68**, 898-911.
- Hobday, A.J. and Lough, J. (2011) Projected climate change in Australian marine and freshwater environments. *Marine and Freshwater Research* **62**, 1000-1014.
- Hoegh-Guldberg, O. (1999) Coral bleaching, climate change and the future of the world's coral reefs. Review. *Marine and Freshwater Research* **50**, 839–866.
- Holbrook, N.J., Goodwin, I.D., McGregor, S., Molina, E. and Power, S.B. (2010) ENSO to multi-decadal time scale changes in East Australian Current transports and Fort Denison sea level: Oceanic Rossby waves as the connecting mechanism. *Deep-Sea Research II* **58**, 547-558.
- Huang, B.Y., Xue, Y. and Behringer, D.W. (2008) Impacts of argo salinity in NCEP global ocean data assimilation system: The tropical Indian ocean. *Journal of Geophysical Research-Oceans* **113**(C8).
- Huyer, A., Smith, R.L., Stabeno, P.J., Church, J.A. and White, N.J. (1988) Currents off south-eastern Australia: results from the Australian coastal experiment. *Australian Journal of Marine and Freshwater Research* **39**, 245-88.
- Joll, L.M. and Caputi, N. (1995) Environmental influences on recruitment in the saucer scallop (*Amusium balloti*) fishery of Shark Bay, Western Australia. *International Council for the Exploration of the Sea Journal of Marine Science* **199**, 47-53.
- Kangas, M.I., Chandrapavan, A., Hetzel, Y.L. and Sporer, E. (2012) Minimising gear conflict and resource sharing issues in the Shark Bay trawl fisheries and promotion of scallop recruitment. FRDC Project 2007/051.
- Kaplan, A., Cane, M.A., Kushnir, Y., Clement, A.C., Blumenthal, M.B. and Rajagopalan, B. (1998) Analyses of global sea surface temperature 1856-1991. *Journal of Geophysical Research-Oceans* **103**(C9), 18567-18589.
- King, E., Schroeder, T., Brando, V. and Suber, K. (2014) A Pre-operational System for Satellite Monitoring of Great Barrier Reef Marine Water Quality. Wealth from Oceans Flagship report.
- Kininmonth, S.J., De'ath, G. and Possingham, H.P. (2010) Graph theoretic topology of the Great but small Barrier Reef world. *Theoretical Ecology* **3**, 75-88.
- Knorr-Held, L. and Besag, J. (1998) Modelling risk from a disease in time and space. *Statistics in Medicine* **17**(18), 2045-2060.
- Kolman, B. and Hill, D.R. (2004) 'Introductory Linear Algebra: An Applied First Course (8th Edition).' (Pearson)
- Kroese, D. and Chan, J. (2012) 'Statistical Modeling and Computation. Springer. New York.'
- Lacroix, G., Maes, G.E., Bolle, L.J. and Volckaert, F.A.M. (2013) Modelling dispersal dynamics of early life stages of a marine flatfish. *Journal of Sea Research* **84**, 13 - 25.
- Large, W.G., Danabasoglu, G., Doney, S.C. and McWilliams, J.C. (1997) Sensitivity to surface forcing and boundary layer mixing in a global ocean model: Annual-mean climatology. *Journal of Physical Oceanography* **27**(11), 2418-2447.

Appendices – References

- Leigh, G.M., Campbell, A.B., Lunow, C.P. and O'Neill, M.F. (2014) Stock assessment of the Queensland east coast common coral trout (*Plectropomus leopardus*) fishery. Department of Agriculture, Fisheries and Forestry, Brisbane.
- Leigh, G.M., Williams, A.J., Begg, G.A., Gribble, N.A. and Whybird, O.J. (2006) Stock assessment of the Queensland east coast red throat emperor (*Lethrinus miniatus*) fishery. Department of Primary Industries and Fisheries, No. QI06068, Brisbane, Queensland, Australia.
- Lemos, R.T. and Sanso, B. (2009) A Spatio-Temporal Model for Mean, Anomaly, and Trend Fields of North Atlantic Sea Surface Temperature. *Journal of the American Statistical Association* **104**(485), 5-18.
- Lenanton, R.C., Caputi, N., Kangas, M. and Craine, M. (2009) The ongoing influence of the Leeuwin Current on economically important fish and invertebrates off temperate Western Australia - has it changed? *Journal of the Royal Society of Western Australia* **92**, 111-127.
- Mao, Y. and Luick, J.L. (2014) Circulation in the southern Great Barrier Reef studied through an integration of multiple remote sensing and in situ measurements. *Journal of Geophysical Research: Oceans* **119**(3), 1621-1643.
- Marsland, S.J., Haak, H., Jungclaus, J.H., Latif, M. and Roske, F. (2003) The Max-Planck-Institute global ocean/sea ice model with orthogonal curvilinear coordinates. *Ocean Modelling* **5**(2), 91-127.
- Mauna, A.C., Acha, E.M., Lasta, M.L. and Iribarne, O.O. (2011) The influence of a large SW Atlantic shelf-break frontal system on epibenthic community composition, trophic guilds, and diversity. *Journal of Sea Research* **66**(1), 39-46.
- Mauna, A.C., Franco, B.C., Baldoni, A., Acha, E.M., Lasta, M.L. and Iribarne, O.O. (2008) Cross-front variations in adult abundance and recruitment of Patagonian scallop (*Zygochlamys patagonica*) at the SW Atlantic Shelf Break Front. *ICES Journal of Marine Science* **65**(7), 1184-1190.
- Maxwell, W.G.H. (1970) The sedimentary framework of Moreton Bay, Queensland. *Australian Journal Marine Freshwater Research* **21**, 70-88.
- Maynard, J.A., Johnson, J.E., Marshall, P.A., Eakin, C.M., Goby, G., Schuttenberg, H. and Spillman, C.M. (2009) A Strategic Framework for Responding to Coral Bleaching Events in a Changing Climate. *Environmental Management* **44**, 1-11.
- McClain, E.P., Pichel, W.G. and Walton, C.C. (1985) Comparative performance of avhrr-based multichannel sea-surface temperatures. *Journal of Geophysical Research-Oceans* **90**(NC6), 1587-1601.
- McWilliams, J.C. (1996) Modeling the oceanic general circulation. *Annual Review of Fluid Mechanics* **28**, 215-248.
- Middleton, J.H., Coutis, P., Griffin, A., Macks, A., McTaggart, A., Merrifield, M.A. and Nippard, G.J. (1994) Circulation and water mass characteristics of the southern Great Barrier Reef. *Australian Journal of Marine and Freshwater Research* **45**(1), 1-18.
- Moore, A.M., Arango, H.G., Di Lorenzo, E., Cornuelle, B.D., Miller, A.J. and Neilson, D.J. (2004) A comprehensive ocean prediction and analysis system based on the tangent linear and adjoint of a regional ocean model. *Ocean Modelling* **7**(1-2), 227-258.
- Nilsson, C.S. and Cresswell, G.R. (1981) The formation and evolution of East Australian Current warm-core eddies. *Progress in Oceanography* **9**, 133-183.

Appendices – References

- O'Neill, M.F. and Leigh, G.M. (2007) Fishing power increases continue in Queensland's east coast trawl fishery, Australia. *Fisheries Research* **85**(1-2), 84-92.
- Oke, P.R., Allen, J.S., Miller, R.N., Egbert, G.D. and Kosro, P.M. (2002) Assimilation of surface velocity data into a primitive equation coastal ocean model. *Journal of Geophysical Research-Oceans* **107**(C9).
- Oke, P.R., Brassington, G.B., Griffin, D.A. and Schiller, A. (2008) The Bluelink ocean data assimilation system (BODAS). *Ocean Modelling* **21**(1-2), 46-70.
- Oke, P.R., Sakov, P., Cahill, M.L., Dunn, J.R., Fiedler, R., Griffin, D.A., Mansbridge, J.V., Ridgway, K.R. and Schiller, A. (2013) Towards a dynamically balanced eddy-resolving ocean reanalysis: BRAN3. *Ocean Modelling* **67**, 52-70.
- Paduan, J.D. and Shulman, I. (2004) HF radar data assimilation in the Monterey Bay area. *Journal of Geophysical Research-Oceans* **109**(C7).
- Pearce, A.F. and Feng, M. (2013) The rise and fall of the “marine heat wave” off Western Australia during the summer of 2010/2011. *Journal of Marine Systems* **111–112**(0), 139-156.
- Peck, D.R., Smithers, B.V., Krockenberger, A.K. and Congdon, B.C. (2004) Sea-surface temperature constrains wedge-tailed shearwater foraging success within breeding seasons. *Marine Ecology Progress Series* **281**, 259–266.
- Philander, G.S. (1989) 'El Nino, La Nina, and the Southern Oscillation.' (Academic Press)
- Porkess, R. (1988) 'Dictionary of Statistics.' (Collins, London and Glasgow)
- Potter, M. (1975) Sea-bed currents in south-east Queensland. Preliminary Findings. February 1975.
- Qin, Y., Brando, V.E., Dekker, A.G. and Blondeau-Patissier, D. (2007) Validity of SeaDAS water constituents retrieval algorithms in Australian tropical coastal waters. *Geophysical Research Letters* **34**(21), L21603.
- Ray, S. and Giese, B.S. (2012) Historical changes in El Niño and La Niña characteristics in an ocean reanalysis. *Journal of Geophysical Research: Oceans* **117**(C11), C11007.
- Ridgway, K.R. and Dunn, J.R. (2003) Mesoscale structure of the mean East AUstralian Current System and its relationship with topography. *Progress in Oceanography* **56**, 189-222.
- Ridgway, K.R., Dunn, J.R. and Wilkin, J.L. (2002) Ocean interpolation by four-dimensional weighted least squares - application to the waters around Australasia. *Journal of Atmospheric and Oceanic Technology* **19**(9), 1357-1375.
- Ridgway, K.R. and Godfrey, J.S. (1997) Seasonal cycle of the East Australian Current. *Journal of Geophysical Research* **102**, 22921-22936.
- Ridgway, K.R. and Hill, K. (2009) The East Australian Current. In "A marine climate change impacts and adaptation report card for Australia 2009" Poloczanska, E.S., Hobday, A.J., Richardson, A.J. (eds). NCCARF Publication 05/09 No. 978-1-921609-03-9.
- Roemmich, D. and Gilson, J. (2009) The 2004-2008 mean and annual cycle of temperature, salinity, and steric height in the global ocean from the Argo Program. *Progress in Oceanography* **82**(2), 81-100.

- Roemmich, D. and Sutton, P. (1998) The mean and variability of ocean circulation past northern New Zealand: Determining the representativeness of hydrographic climatologies. *Journal of Geophysical Research-Oceans* **103**(C6), 13041-13054.
- Roughan, M., Macdonald, H.S., Baird, M.E. and Glasby, T.M. (2011) Modelling coastal connectivity in a Western Boundary Current: Seasonal and inter-annual variability. *Deep Sea Res Part II* **58**(5), 628– 644.
- Schabenberger, O. and Gotway, C.A. (2004) 'Statistical Methods for Spatial Data Analysis.' (Taylor & Francis)
- Schnute, J. (1985) A general theory for analysis of catch and effort data. *Canadian Journal of Fisheries and Aquatic Sciences* **42**(3), 414-429.
- Shchepetkin, A.F. and McWilliams, J.C. (2005) The regional oceanic modeling system (ROMS): a split-explicit, free-surface, topography-following-coordinate oceanic model. *Ocean Modelling* **9**(4), 347-404.
- Siegel, D.A., Kinlan, B.P., Gaylord, B. and Gaines, S.D. (2003) Lagrangian descriptions of marine larval dispersion.
- Siegel, D.A., Mitarai, S., Costello, C.J., Gaines, S.D., Kendall, B.E., Warner, R.R. and Winters, K.B. (2008) The Stochastic nature of larval connectivity among nearshore marine populations. *PANS* **105**(26).
- Signell, R.P., Carniel, S., Chiggiato, J., Janekovic, I., Pullen, J. and Sherwood, C.R. (2008) Collaboration tools and techniques for large model datasets. *Journal of Marine Systems* **69**(1-2), 154-161.
- Smith, I. (2007) Global climate modelling within CSIRO: 1981 to 2006. *Australian Meteorological Magazine* **56**(3), 153-166.
- Spillman, C.M. and Alves, O. (2009) Dynamical seasonal prediction of summer sea surface temperatures in the Great Barrier Reef. *Coral Reefs* **28**, 197-206
- Spillman, C.M., Alves, O. and Hudson, D.A. (2012) Predicting thermal stress for coral bleaching in the Great Barrier Reef using a coupled ocean-atmosphere seasonal forecast model. *International Journal of Climatology* **33**, 1001-1014.
- Spillman, C.M., Alves, O., Hudson, D.A., Hobday, A.J. and Hartog, J.R. Using dynamical seasonal forecasts in marine management. . In 'MODSIM 2011, 19th International Congress on Modelling and Simulation. Modelling and Simulation Society of Australia and New Zealand, December 2011', 2011. (Eds. F Chan, D Marinova and RS Anderssen), pp. 2163-2169
- Spillman, C.M. and Hobday, A.J. (2014) Dynamical seasonal ocean forecasts to aid salmon farm management in a climate hotspot. *Climate Risk Management* **in press**.
- State of Queensland. 1999. Fisheries (East Coast Trawl) Management Plan 1999. Subordinate legislation of the Fisheries Act 1994, Office of the Queensland Parliamentary Council. State of Queensland, 296 pp.
https://www.legislation.qld.gov.au/LEGISLTN/REPEALED/F/FisherECTMP99_02K_031219.pdf.
- Stroud, J.R., Muller, P. and Sanso, B. (2001) Dynamic models for spatiotemporal data. *Journal of the Royal Statistical Society Series B-Statistical Methodology* **63**, 673-689.

- Tamaki, A., Mandal, S., Agata, Y., Aoki, I., Suzuki, T., Kanehara, H., Aoshima, T., Fukuda, Y., Tsukamoto, H. and Yanagi, T. (2010) Complex Vertical Migration of Larvae of the Ghost Shrimp *Nihonotrypaea harmandi* in Shelf Waters of Western Kyushu, Japan. *Estuarine, Coastal and Shelf Science*. **86**, 125-136.
- Tian, R.C., C., C., K.D.E., S., Rothschild, B., Cowles, G.W., Xu, Q., Hu, S., Harris, B.P. and M.C., M. (2009) Modeling the connectivity between sea scallop populations in the Middle Atlantic Bight and over Georges Bank. *Marine Ecology Progress Series* **380**, 147-160.
- Tobin, A., Schlaff, A., Tobin, R., Penny, A., Ayling, T., Ayling, A., Krause, B., Welch, D., Sutton, S., Sawynok, B., Marshall, N., Marshall, P. and Maynard, J. (2010) Adapting to Change: Minimising uncertainty about the effects of rapidly-changing environmental conditions on the Queensland Coral Reef Fin Fish Fishery. <http://www.frdc.com.au/documentlibrary/finalreports/2008-103-DLD.pdf>. Townsville: James Cook University, Fishing & Fisheries Research Centre.
- Tremblay, M.J. and Sinclair, M. (1992) Planktonic Sea Scallop Larvae (*Placopecten magellanicus*) in the Georges Bank Region: Broad-scale Distribution in Relation to Physical Oceanography. *Canadian Journal of Fisheries and Aquatic Sciences* **49**(8), 1597-1615.
- Treml, E.A., Halpin, P.N., Urban, D.L. and Pratson, L.F. (2008) Modeling population connectivity by ocean currents, a graph-theoretic approach for marine conservation. *Landscape Ecology* **23**, 19-36.
- Vidard, A., Balmaseda, M. and Anderson, D. (2009) Assimilation of Altimeter Data in the ECMWF Ocean Analysis System 3. *Monthly Weather Review* **137**(4), 1393-1408.
- von Storch, H. and Zwiers, F.W. (2001) 'Statistical Analysis in Climate Research.' (Cambridge University Press)
- Waller, L.A., Carlin, B.P., Xia, H. and Gelfand, A.E. (1997) Hierarchical spatio-temporal mapping of disease rates. *Journal of the American Statistical Association* **92**(438), 607-617.
- Wang, S. (2007) Analysis of early life history stages of the saucer scallop *Amusium balloti* (Bernardi, 1861) : impacts on the development of hatchery practices. The University of Queensland
- Weaver, A. and Hughes, T.M. (1992) Stability and variability of the thermohaline circulation and its link to climate. *Trends in physical oceanography* **1**, 15-70.
- Weeks, S.J., Bakun, A., Steinberg, C.R., Brinkman, R. and Hoegh-Guldberg, O. (2010) The Capricorn Eddy: a prominent driver of the ecology and future of the southern Great Barrier Reef. *Coral Reefs* **29**, 975-985.
- Weeks, S.J., Steinberg, C. and Congdon, B.C. (2013) Oceanography and seabird foraging: within-season impacts of increasing sea-surface temperature on the Great Barrier Reef. *Marine Ecology Progress Series* **490**, 247-254.
- Wijffels, S. and Meyers, G. (2004) An Intersection of Oceanic Waveguides: Variability in the Indonesian Throughflow Region. *Journal of Physical Oceanography* **34**(5), 1232-1253.
- Wikle, C.K., Berliner, L.M. and Cressie, N. (1998) Hierarchical Bayesian space-time models. *Environmental and Ecological Statistics* **5**(2), 117-154.
- Williams, M.J. and Dredge, M.C.L. (1981) Growth of the Saucer Scallop, *Amusium japonicum balloti* Habe in Central Eastern Queensland. *Aust. J. Mar. Freshwater Res.* **32**(4), 657-666.

Appendices – References

Williams, P.D. and Hastings, A. (2013) Stochastic Dispersal and Population Persistence in Marine Organisms. *The American Naturalist* **2**.

Wolff, M. (1987) Population dynamics of the Peruvian scallop *Argopecten purpuratus* during the El Nino phenomenon of 1983. *Canadian Journal of Fisheries and Aquatic Sciences* **44**(10), 1684-1691.

Wolff, M., Taylor, M., Mendo, J. and Yamashiro, C. (2007) A catch forecast model for the Peruvian scallop (*Argopecten purpuratus*) based on estimators of spawning stock and settlement rate. *Ecological Modelling* **209**(2-4), 333-341.

Worley, S.J., Woodruff, S.D., Reynolds, R.W., Lubker, S.J. and Lott, N. (2005) ICOADS release 2.1 data and products. *International Journal of Climatology* **25**(7), 823-842.

Wunsch, C., Heimbach, P., Ponte, R.M., Fukumori, I. and Members, E.-G.C. (2009) The global general circulation of the ocean estimated by the ecco-consortium. *Oceanography* **22**(2), 88-103.

Wyrski, K. (1962) Geopotential topographies and associated circulation in the western South Pacific Ocean. *Australian Journal of Marine and Freshwater Research* **13**, 89-105.

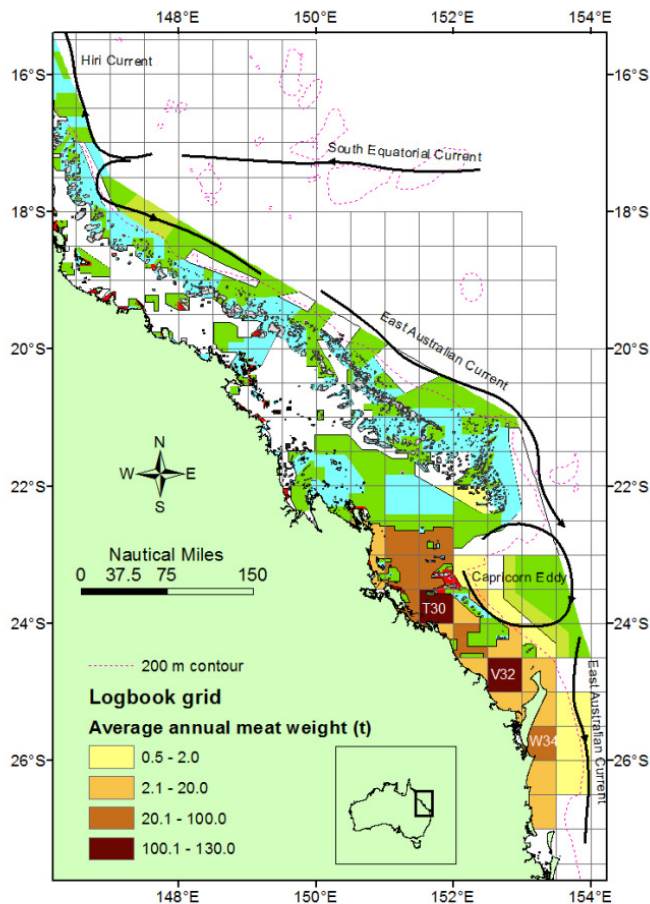
18 Appendix 4. Review of relevant literature, data and physical oceanographic features

This section of the report addresses Objective 1) *Review recent advances in the study of physical oceanographic influences on fisheries catch data, and describe the major physical oceanographic features that are likely to influence Queensland reef fish and saucer scallops.*

18.1 PHYSICAL OCEANOGRAPHIC FEATURES OF THE QUEENSLAND EAST COAST

18.1.1 Geology

The geological framework of the Queensland continental shelf was established during the Palaeozoic Era (541-252 million years ago). In southeast Queensland two sedimentary basins have been identified. The Capricorn Basin extends from approximately 21°S to 23°S and consists of more than 2,600 m of Mesozoic (252-66 million years ago) and Tertiary (65-1.8 million years ago) deposits. It lies between the Bunker and Swain 'highs' which are composed of sedimentary and metamorphic materials of greater age than the basin. The highs provide the foundations on which the Capricorn, Bunker and Swain groups of reefs have developed (Figure 18-1). The Maryborough Basin extends from 23°S to 27°S and was formed earlier than the Capricorn Basin from about 6,000 m of Palaeozoic and Mesozoic sediments. In the central Queensland region (21°S) the continental shelf extends widely from the coast for approximately 290 km, while in southern Queensland and for most of the New South Wales coast (24°S-38°S) the shelf is steep and narrow, and averages 40 km in width. The depth of the shelf edge increases southwards from about 72 m at 25°S to over 160 m 33°S. Much of the shelf is terraced at well-defined depths (Bank of New South Wales 1979).



An outstanding physical feature of the southeast Queensland coast is the large quartz sand barrier islands of North and South Stradbroke, Moreton, and Fraser; the latter being the largest in the world. During glacial and interglacial periods of the Quaternary Period the sea level rose and fell exposing large areas of the shelf that were covered in quartz sand (Hekel *et al.* 1979). The sand is thought to be largely from materials eroded by rivers in the highlands of northern New South Wales and swept northwards by long-shore currents (Maxwell 1970). Strong south-easterly winds, likely to have been associated with the glacial climatic conditions of the period, heaped the sand into large dunes which now comprise the bulk of the islands.

Figure 18-1. Distribution of the Queensland scallop fishery and the Capricorn Eddy. The blue, green and red are zones in the Great Barrier Reef Marine Park.

18.1.2 East Australian Current

Water movement on the Queensland coast is largely driven by the South Equatorial Current, which flows west across the Coral Sea. Church (1987) described the dynamics of the current immediately adjacent to the Great Barrier Reef. As it approaches Australia's continental shelf, the South Equatorial Current bifurcates between 14°S and 18°S resulting in the north-flowing Hiri Current and the south-flowing East Australian Current (EAC). The Hiri Current feeds the equatorial currents with some leakage through the Indonesian Archipelago to the Indian Ocean (Figure 18-1).

The EAC is a complex and highly energetic western boundary system and is dominated by a series of mesoscale eddies (Ridgway and Hill 2009). Flow is strongest in summer, often seen as a tongue of warm water extending as far south as Tasmania (Ridgway and Godfrey 1997). Most of the early studies on the EAC focused on the higher latitudes (i.e. > 30°S) associated with the Tasman Sea (Boland and Hamon 1970; Boland 1973; Boland and Church 1981; Nilsson and Cresswell 1981). It was not until after the 1980s that some key features of the EAC at lower latitudes were examined, in particular the southern Great Barrier Reef (Griffin and Middleton 1986; Church 1987; Griffin *et al.* 1987; Middleton *et al.* 1994).

Hamon (1965) first described the EAC as being about 150 km wide and often U-shaped, with a southward current near the shelf and a northward counter current further offshore. Boland (1973) supported the U-shape description, based on temperature-depth profiles at 33°S. Current speeds of greater than 1.0 m s⁻¹ occur near surface waters of the shelf break, while the continental slope and mid-shelf currents are generally weaker at about 0.5 m s⁻¹ (Huyer *et al.* 1988). Maximum speeds (up to 2.5 m s⁻¹) occur between 25°S and 30°S (Wyrki 1962). The current decreases to half its surface speed at a depth of 250 m. Anticyclonic eddies of approximately 250 km in diameter are shed by the current about once every 170 days near the continental shelf (Nilsson and Cresswell 1981) and move southward and away from the coast at approximately 0.05 m s⁻¹ (Hamon 1965). The eddies are important for nutrient cycling and affect gemfish and tuna populations (Ridgway and Hill 2009).

Potter (1975) studied bottom currents in southeast Queensland coastal waters using seabed drifters which were released in depths from 9-147 m. His results suggested that during autumn-winter (May-June), there was clearly a predominant northward-flowing bottom current off Caloundra. However, during the same period, there were both northward and southward flowing currents off Jumpinpin. Drifter recoveries indicated that during spring and summer there appeared to be both northward and southward flowing bottom currents at both locations. The Jumpinpin recoveries indicated some east-west movement of drifters, while the Caloundra drifters tended to move either northeasterly or southeasterly.

Harris (1993b; 1993a) obtained measures of near-bed currents, temperature and salinity on the southeast Queensland shelf by deploying self-recording current meters at depths ranging between 30 and 190 m in areas near Fraser Island and Mooloolaba. Near-bed currents were found to flow southwards at all times near Fraser Island. A maximum current speed of 1.35 m s⁻¹ was observed in 72 m while the strongest mean current of 0.33 m s⁻¹ was obtained in 33 m. Currents were weaker and less directional at the Mooloolaba stations. Currents were affected mostly by non-tidal forces and attained relatively high speeds for periods of 4-5 days, followed by periods of weaker currents at both areas. Harris suggested the periods of high speed were due to eddies being shed by the EAC. Tidal currents were of greatest importance for the inshore stations.

The EAC undergoes changes on interannual timescales, but only a very weak ENSO signal is evident in observations (Ridgway and Hill 2009). Long-term observations show that the EAC has strengthened and extended further southward over the past 60 years. The south Tasman Sea region has become both warmer and saltier, with mean trends of 2.28°C/century and 0.34 psu/century over the 1944-2002 period, which corresponds to a poleward advance of the EAC Extension of about 350 km (Ridgway and Hill 2009).

18.1.3 The Capricorn Eddy

A significant physical oceanographic feature which forms adjacent to the Queensland coast between 22°S and 24°S is the Capricorn Eddy (Figure 18-1). Properties of the eddy have been described by Church (1987), Griffin *et al.* (1987), Middleton *et al.* (1994) and Weeks *et al.* (2010; 2013). The Queensland scallop fishery is mainly located between 21°S and 26°S in depths of 20-70 m, directly west of and adjacent to the Eddy. Most of the fishery is located in the southern Great Barrier Reef (GBR) but it also extends south into Hervey Bay, near Fraser Island.

Griffin *et al.* (1987) used data from current meters, drifter studies and satellite-tracked buoys to suggest that the south-eastward flowing EAC drives the large cyclonic (clockwise) Capricorn Eddy in the lee of the Swain Reefs. Middleton *et al.* (1994) also described the slow clockwise circulation of water deeper than ~100 m over the Marion Plateau from research cruises in 1990. The region south of the Plateau is dominated by Fraser Island and its associated reef called Breaksea Spit (at the tip of Sandy Cape at 25°S) which extends from the coast to the shelf break. To the north, the continental shelf widens at about 23°S from about 80 km to more than 200 km, leaving a substantial gap in the reefs known as the Capricorn Channel. The offshore Swain and Saumarez Reefs on the eastern extent of the shelf significantly impede the strong pole-flowing EAC resulting in the clockwise eddy. Middleton *et al.* (1994) reported nutrient uplift from the upper slope to the outer shelf proper in the Capricorn Channel. Interestingly they also reported a cold nutrient-rich ‘blob’ of cold water near Double Island Point, just south of Fraser Island, which may also affect the infrequent occurrence of significant scallop catches in the area.

Weeks *et al.* (2010) used observational measures and model data to validate satellite images of the Capricorn Eddy. They showed the eddy raises cooler, nutrient-enriched oceanic subsurface water, transporting it to the reef zone and eventually into the GBR lagoon. The influence of the eddy upon the scallop fishery has received scant attention, despite its close proximity to the fishery.

18.2 EXAMPLES OF COASTAL AND OCEANOGRAPHIC INFLUENCES ON FISHERIES

Tremblay and Sinclair (1992) examined the distribution of larval sea scallop (*Placopecten magellanicus*) on the Georges Bank region, near Nova Scotia. Larval abundance peaks were associated with high sea water temperature stratification and tended to be positively related to the speed of the along-front current. Tian *et al.* (2009) used the Finite Volume Coastal Ocean Model (FVCOM) to model transport of *P. magellanicus* egg, trochophore, veliger and pediveliger stages and quantify exchange rates across fishing grounds between Nova Scotia and Massachusetts.

Mauna *et al.* (2008; 2011) examined relationships between the distribution and abundance of Patagonian scallop (*Zygochlamys patagonica*) and major current systems and Chl-a in the Argentine Sea (SW Atlantic). They found variability in adult abundance and recruits was strongly related to spatial variability of the SW Atlantic Shelf Break Front (SBF) and Chl-a.

Wolff (1987) and Wolff *et al.* (2007) examined the influence of El Niño events on the population dynamics of the Peruvian scallop *Argopecten purpuratus* in Independencia Bay, Peru (~14°S). *A. purpuratus* is a relict of tropical/subtropical fauna inhabiting the Peruvian and Chilean waters which has maintained its warm water characteristics during evolution in the cold upwelling water because of periodic warm water El Niño events. The population of Peruvian scallops greatly increases during El Niño periods. Wolff *et al.* (2007) constructed a multiple regression model to predict catch for the year after recruitment, based on catch during the spawning period and temperature, which was used as an index of larval settlement. The model explained 93% of the variation in catches. Annual landings are largely a function of spawning stock size when temperatures are low, but the importance of spawning stock size decreases as temperature increases.

The influence of coastal and oceanographic conditions on the population dynamics and fisheries for saucer scallops (*A. balloti*) and rock lobsters (*Panulirus cygnus*) in Western Australia has been

examined by Joll and Caputi (1995), Caputi *et al.* (1996; 2010; 2015) and Lenanton *et al.* (2009). Strong *La Niña* conditions (with strong Leeuwin Current flow and high SST) during the winter spawning months are always associated with poor scallop larval settlement. While the strength of the Leeuwin Current is significantly affected by El Niño Southern Oscillation (ENSO), the EAC seems much less affected.

Spatial distributions of southern bluefin tuna (SBT) along the east Australian coast have been modelled using a statistical habitat preference model, forced by ocean temperature, to assist management authorities in minimising unwanted SBT capture (Hobday *et al.* 2011). The habitat preference model was constructed based on archival satellite tag data and combined with ocean temperature information (both observed and forecast), to describe three zones of expected SBT distribution (Hobday and Hartmann 2006). The location of SBT habitat along the east coast of Australia is dominated by the EAC, with distributions further south in warmer-than-average years, when the EAC moves further south, and further north than usual in cooler years (Hobday *et al.* 2011). Based on this habitat information, three corresponding management zones are then created by fishery managers in the region. Access by fishers to these zones is regulated based on the level of observer coverage and on the amounts of SBT quota they are holding (Hobday *et al.* 2009), and enforced with observer coverage and vessel monitoring systems (Hobday *et al.* 2011).

18.2.1 Coral bleaching

Mass coral bleaching is caused primarily by anomalously warm ocean temperatures. Bleaching results when corals under stress expel their zooxanthellae, giving rise to the typical white coloration. Major bleaching events tend to occur during the summer months, with coral mortality determined by the duration and magnitude of high water temperatures. Both the severity and frequency of such events are predicted to increase under global warming (Hoegh-Guldberg 1999; Baker *et al.* 2008). The ability to forecast potential ocean conditions that could lead to coral bleaching is a great advancement in the management and conservation of such sensitive systems.

The Australian Bureau of Meteorology currently produces two operational seasonal forecast products tailored for the Great Barrier Reef (GBR) daily in real-time (http://www.bom.gov.au/oceanography/oceantemp/GBR_SST.shtml). The system used is the Predictive Ocean Atmosphere Model for Australia (POAMA) and is currently the only dynamical prediction system used for forecasting coral bleaching on a seasonal time-scale. These forecasts have been demonstrated to have useful skill up to three months into the future during the summer months, and captured both the 1998 and 2002 GBR bleaching events (Spillman and Alves 2009; Spillman *et al.* 2012).

Seasonal forecasts are a valuable tool in marine management, allowing for proactive management responses and the early implementation of preventative measures. POAMA forecasts for the GBR form an important component of the Early Warning System in the GBR Marine Park Authority Coral Bleaching Response Plan (Maynard *et al.* 2009). The Coral Bleaching Response Plan is a strategic framework comprising an early warning system and an assessment and monitoring component. The early warning system consists of three stages: climate monitoring, sea temperature monitoring and monitoring of bleaching by the general public and tourist operators. POAMA seasonal forecasts for the GBR form an important part of the first stage, providing outlooks of potential bleaching conditions for the upcoming summer (Spillman *et al.* 2011). Currently seasonal forecasts of bleaching risk are most valuable in directing resources and focusing monitoring to increase knowledge of the evolution, causes and consequences of bleaching (Spillman *et al.* 2011).

18.2.2 Oceanography and aquaculture

Atlantic salmon are grown in Tasmania in coastal sea cages for the final two years of production, where the fish are subject to the local environmental conditions (Spillman and Hobday 2014). Fish health and growth are both strongly influenced by ocean temperatures, with salmon in Tasmania grown in waters approaching their upper thermal limit in summer (Battaglene *et al.* 2008). A strong

relationship between monthly observed estuarine salmon farm temperatures and average ocean conditions around Tasmania was found for 1991-2010, indicating that despite farms generally being located within relatively sheltered coastal waters, temperatures were strongly influenced by the adjacent ocean and regional atmospheric processes. In general terms, if ocean conditions around Tasmania are warmer than normal, salmon farm temperatures are also generally warmer (Spillman and Hobday 2014). Average temperatures in this region are projected to be 2.8°C higher than the 1990–2000 average by 2050 (Hobday and Lough 2011), due in part to the strengthening of the EAC and increased southward flow (Ridgway 2009). Dealing with impacts of a warmer climate is both a current (climate variability) and a long-term challenge (climate change) for salmon farmers in this region (Hobday et al. 2008; Spillman and Hobday 2014).

18.3 OCEAN MODELLING

18.3.1 A synopsis of data, numerical, and assimilation modelling

Over the last 150 years, the oceanographic community has made increasing efforts to improve our understanding of the World Ocean, in terms of circulation, production, transformation and spread of water masses, and to identify the associated forcing mechanisms (Brasseur *et al.* 1996). As a result of the numerous surveys achieved so far, vast amounts of *in situ* data have been collected, either for regional or basin-scale studies (Bograd *et al.* 1999; Chang and Chao 2000; Ganachaud 2003; Worley *et al.* 2005; Roemmich and Gilson 2009). From the 1980s onward, satellite-borne instruments began to provide steady, massive influxes of concurrent data (McClain *et al.* 1985; Gordon 1997; Gregg and Casey 2004). One of the most traditional ways to examine these collections of observations is the production of synthetic maps of hydrological properties, depicting the “mean” climatological state of the sea (Roemmich and Sutton 1998; Ridgway *et al.* 2002). Maps of transient deviations, better known as anomalies, can be produced as well (Kaplan *et al.* 1998; Beggs *et al.* 2011).

Even before the advent of computers, the oceanographic community also began to develop a number of simple ocean circulation models (Weaver and Hughes 1992; England and Oke 2002). The first real progress towards a primitive equation ocean circulation model came with the work of Bryan and Cox (Bryan and Cox 1967; Bryan and Cox 1968), who developed a model of ocean circulation carrying variable temperature and salinity, based upon the conservation equations for mass, momentum, heat and moisture, and the equation of state (England and Oke 2002). Since the early efforts of Bryan and Cox, a great number of ocean model developments have occurred (McWilliams 1996; Griffies *et al.* 2000; Marsland *et al.* 2003; Shchepetkin and McWilliams 2005; Chassignet *et al.* 2007; Smith 2007). To a large extent, numerical models are driven by observations (in the form of climatological or anomaly fields), namely as boundary conditions. Therefore, the quality of numerical ocean model predictions depends not only on the algorithms, but also on the input data (Large *et al.* 1997; Doney *et al.* 2004).

The interplay between models and data has become more intricate with the development of data assimilation (Bennett 1992). The relative paucity of measurements, especially below the surface, and the limitations of models provided the impetus for this line of research. The outcome was a set of methods that produce estimates for the oceanic fields of temperature, salinity, pressure, and three-dimensional velocity, which are maximally consistent with observations and numerical model dynamics, allowing for errors in both (Oke *et al.* 2002; Moore *et al.* 2004; Paduan and Shulman 2004). Several groups are currently involved in real-time ocean analysis, incorporating diverse forms of data (i.e. ARGO float profiles, XBT data, sea-surface temperature, etc.) into global and regional ocean models. Global real-time analyses and forecasts are produced by the European Centre for Medium Range Forecasts (Vidard *et al.* 2009), CSIRO and the Australian Bureau of Meteorology (BOM) (Oke *et al.* 2008), the U.S. National Center for Environmental Prediction (Huang *et al.* 2008), and others. Retrospective hind-casts, also called reanalyses, are produced by several groups, including MIT-JPL (Wunsch *et al.* 2009), the University of Maryland (Carton and Giese 2008), and CSIRO-BOM (Oke *et al.* 2013).

18.3.2 Sharing data and knowledge

Numerical ocean models produce large four-dimensional datasets that range from tens of megabytes to terabytes. Often, this information is delivered to users via the World Wide Web, as graphical images or binary files. As a special class of users, scientists typically want to obtain the actual data, or at least, be able to use their own analysis and visualisation tools. They usually focus their interest on a few variables, a narrow temporal window, and a subregion of the numerical model. Hence, they need an efficient way to slice and dice the data over the web. Scientists also do not want to learn a new set of tools for each different model, and would prefer a consistent interface that can access any model output, irrespective of how the original model output was written, or what vertical or horizontal coordinate system was used (Signell *et al.* 2008).

When scientists from distinct disciplines work together on related problems, they often face what Edwards and colleagues (Edwards *et al.* 2011) aptly called ‘science friction’. This can be pictured as the time, energy and human attention needed to share data and knowledge. As science becomes more data-driven, collaborative, and interdisciplinary, demand increases for interoperability among data, tools, and services. Thus, a fundamental component for effective scientific collaboration is to save model results in a form that is machine-independent, binary (or easily translated), and self-describing. Within the Earth Sciences community, there are several formats that meet these criteria, namely NetCDF (Network Common Data Form), HDF (Hierarchical Data Format), and GRIB (Gridded Binary). Use of NetCDF, in particular, has become widespread in the oceanographic community. This format is freely available, is supported by Unidata, and has interfaces for many languages, including C, C++, FORTRAN, Java, Perl, Matlab, R, and IDL. NetCDF files can be placed in THREDDS (Thematic Real-time Environmental Distributed Data Services) catalogs, provided by THREDDS Data Servers (TDS), and accessed via the web e.g. with HTTP (Hyper Text Transfer Protocol) or OPeNDAP (Open-source Project for Network Data Access Protocol). The latter, formerly known as DODS (Distributed Ocean Data System), makes slices of data accessible to remote locations, regardless of local storage format (Signell *et al.* 2008; Cornillon *et al.* 2009).

18.3.3 Dominant patterns of ocean variability

Even after trimming numerical ocean model output into a selected spatial and temporal slice, with just a few properties, the amount of information therein might be too complex to absorb. For this reason, it might be useful to employ spatio-temporal statistics to summarise the data further, into dominant patterns of variability. Over the last decade, several books and edited volumes have contributed to the subject of spatio-temporal statistics. Von Storch and Zwiers provided a valuable primer on statistical methods for climate science (von Storch and Zwiers 2001). Other books have chapters and discussions on the subject of spatio-temporal statistical modelling (Cressie 1993; Banerjee *et al.* 2004; Schabenberger and Gotway 2004).

Complex spatio-temporal processes can often be decomposed into relatively simple conditional probability models (Brown *et al.* 1994; Handcock and Wallis 1994; Waller *et al.* 1997; Knorr-Held and Besag 1998; Wikle *et al.* 1998). Over the last 20 years, several state-space environmental models have been developed (Guttorp *et al.* 1994; Berliner *et al.* 2000; Stroud *et al.* 2001; Lemos and Sanso 2009). The latter four references, in particular, present applications in ocean modelling.

19 Appendix 5. Coastal and oceanographic influences on the Queensland (Australia) east coast saucer scallop (*Amusium balloti*) fishery

This section of the report addresses all three Objectives, but is mainly focused on scallops:

- 1) Review recent advances in the study of physical oceanographic influences on fisheries catch data, and describe the major physical oceanographic features that are likely to influence Queensland reef fish and saucer scallops.
- 2) Collate Queensland's physical oceanographic data and fisheries (i.e. reef fish and saucer scallops) data.
- 3) Develop stochastic population models for reef fish and saucer scallops, which can link physical oceanographic features (e.g. sea surface temperature anomalies) to catch rates, biological parameters (e.g. growth, reproduction, natural mortality) and ecological aspects (e.g. spatial distribution).

A. J. COURTNEY¹ AND C. M. SPILLMAN²

¹ Queensland Department of Agriculture and Fisheries, GPO Box 267, Brisbane , QLD 4001 AUSTRALIA

Email: Tony.Courtney@daf.qld.gov.au (corresponding author)

² Centre for Australian Weather and Climate Research (CAWCR), Bureau of Meteorology, GPO Box 1289, Melbourne, VIC 3001 AUSTRALIA

Email: C.Spillman@bom.gov.au

Running title: Coastal and oceanographic influences on saucer scallops

19.1 ABSTRACT

This study examined relationships between adjusted mean catch rates of saucer scallops (*Amusium balloti*) at the start of the fishing year in November in the Queensland trawl fishery and coastal and oceanographic properties (freshwater flow, water temperature, sea level, eddy kinetic energy; EKE, Chlorophyll-a; Chl-a and the Southern Oscillation Index; SOI). The largest statistically significant correlation was 0.85 between catch rates and Chl-a concentration five months prior in June. Physical oceanographic properties associated with the Capricorn Eddy area had more strong-correlations with catch rates than any other area. November catch rates decline by about 50% as eddy bottom temperature anomalies increase from -0.2 to 0.15°C three months prior. Positive surface water temperature anomalies during the scallop's winter spawning (May-July) were also associated with reduced catch rates 16-18 months later. This is very similar to the relationship between SST and recruitment of *A. balloti* in Western Australia. Management advice on the scallop stock could be improved by incorporating key relationships in the quantitative population models used to assess the stock and compare harvest strategies.

Keywords: scallop catch rate, ocean data reanalysis, BRAN, Capricorn Eddy

19.2 INTRODUCTION

Scallop fishery catch rates and landings are often characterised by large annual variation. As a result, much research has focused on how coastal and physical oceanographic processes affect scallop population dynamics. Examples include the relationship between ENSO and Peruvian scallop (*Argopecten purpuratus*) catch rates (Wolff 1987; Wolff *et al.* 2007), the influence of the Atlantic shelf break front on the distribution of Patagonian scallop (*Zygochlamys patagonia*) (Mauna *et al.* 2008; 2011) and La Niña conditions on saucer scallop (*Amusium balloti*) recruitment in Western Australia (Joll and Caputi 1995; Lenanton *et al.* 2009; Caputi *et al.* 2015).

The Queensland saucer scallop (*A. balloti*) fishery is a valuable sector within the larger Queensland east coast otter trawl fishery (QECOTF), which targets penaeid prawns, saucer scallops, scyllarid lobsters and squid (in decreasing order of catch value). Fishers are also permitted to retain incidental catches of mantis shrimp, cuttlefish, portunid crabs and threadfin bream.

Over the past two decades catch and effort in the QECOTF have declined. A significant decline followed the introduction of an effort unitisation scheme in 2000 as part of the Fisheries (East Coast Trawl) Management Plan 1999. Further reductions followed the implementation of the Great Barrier Marine Park Authority's representative areas program in 2004, which increased the area closed to fishing in the park (Fernandes *et al.* 2005; Fletcher *et al.* 2015) and bought-out commercial fishing licenses. Reduced profitability in the fishery, due to rising fuel and labour costs, combined with low or stagnant prawn prices, has also contributed to reduced effort and catches over this period. Despite these declines, the QECOTF remains Australia's largest trawl fishery, in terms of number of licensed vessels and annual fishing effort. Logbook data indicate that in 2013 301 active licensed vessels expended 33,000 boat-days of effort for a total landed catch of 7,800 t valued at approximately AUD\$93 million.

The saucer scallop fishery is mainly located between 22°S and 27°S in shelf water depths of 20-60 m. While all vessels in the QECOTF are permitted to trawl for scallops, not all do so. Annual catches have been relatively variable, peaking at 1930 t (meat weight) in 1993 and falling to a minimum of 270 t in 2011. The catch in 2013 was 420 t with a value of AUD\$6-7 million. The history of management in the scallop fishery is characterised by numerous interventions which have included three different minimum legal sizes, a daylight prohibition on trawling, and seasonal and rotational spatial closures. Other measures include a maximum net size of 109 m (this is the combined head rope and foot rope length of all nets deployed) per vessel and a minimum codend mesh size of 75 mm.

Although considerable research has been undertaken on the population dynamics of the Queensland saucer scallop fishery (Dredge 1981; Williams and Dredge 1981; 1985; Dichmont *et al.* 2000; Campbell *et al.* 2010b; 2012) the influence of coastal and physical oceanographic processes on the stock has received scant attention. This is surprising given that scallop populations are notorious for their large fluctuations in recruitment due to environmental effects. Therefore, the objective of this study is to investigate relationships between coastal and physical oceanographic conditions and the Queensland east coast saucer scallop fishery, so that variation in catch rates and landings might be better explained, predicted and managed.

19.3 METHODS

The study domain encompassed the scallop fishery, coastal catchments, and inshore and offshore waters between 22°S and 27°S (Figure 19-1). Relationships were examined between scallop catch rates and the following coastal and physical oceanographic properties; freshwater flow, sea water temperature at the surface and at various depths in the water column, sea level height, eddy kinetic energy (EKE), Chlorophyll-a (Chl-a) and the Southern Oscillation Index (SOI).

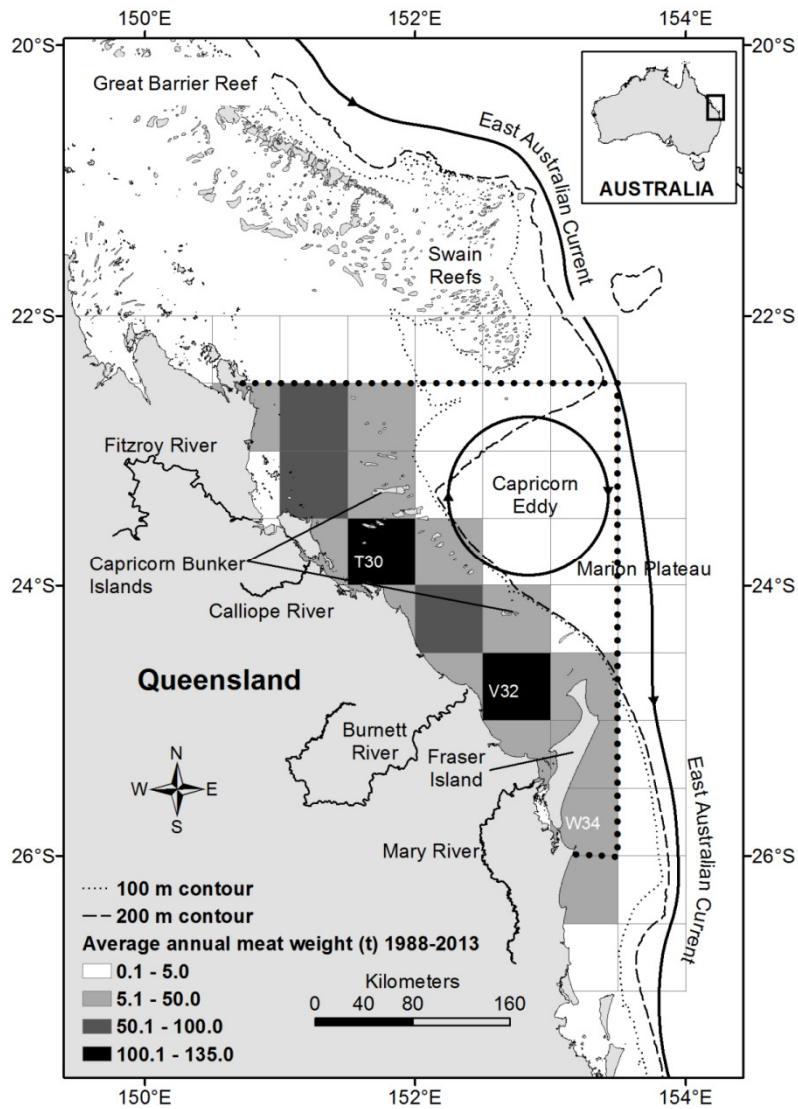


Figure 19-1. Map of the study domain showing the location of the major rivers, the distribution of saucer scallop catches, logbook grids T30 Bustard Head, V32 Hervey Bay and W34 Fraser Island, the Capricorn Eddy and the Whole fishery (thick black dots).

19.3.1 Scallop catch rates

Saucer scallop catch rate data were based on the mandatory commercial fishery logbook database program known as CFISH, which requires fishers to provide daily details of their catch and fishing effort and has been ongoing since it was implemented in January 1988.

In order to simplify the analyses, logbook catch rates from a single month (November) were used, because they can be more readily associated with a prior coastal condition or event, rather than continuous catch rates, or from an extended period of several months. November is an important month for the scallop fishery as about one-quarter of the annual catch and effort occur at this time. Furthermore, the scallop biomass is likely to be at its peak at this time, because management measures imposed from May to October are designed to minimise fishing effort during the winter spawning season (Dredge 1981) and dissuade fishers from harvesting scallops when their adductor muscle meat weight condition is low (Williams and Dredge 1981). As a result, November is generally considered to be the start of the scallop fishing year.

A. balloti reach their maximum asymptotic length (L_{∞}) of 105-111 mm shell height (SH) by about 12 months (Williams and Dredge 1981) and an estimate of their instantaneous rate of natural mortality ($M=0.025 \text{ week}^{-1}$) indicates that fewer than 10% survive beyond two years of age (Dredge 1985). Sample length frequency distributions of saucer scallops from October fishery-independent surveys (Dichmont *et al.* 2000; Courtney *et al.* 2008) show the population is composed of two distinct year classes at this time, typically with modes at about 60 and 90 mm SH. Juveniles are defined as <78 mm SH and because they are assumed to have been spawned in the winter (i.e. June to August) immediately preceding October, they are less than one year old (i.e. 0+ year class, hereafter referred to as the “0+”). Adults are defined as ≥ 78 mm SH and are more than one year old (hereafter referred to as the “1+”) and as such, are spawned during the winter of the previous year. These definitions are consistent with the growth rates and spawning patterns of *A. balloti* in Queensland (Dredge 1981; Williams and Dredge 1981; Campbell *et al.* 2010b). Because fishers are not permitted to retain scallops smaller than 90 mm SH and because they only record their retained catch, the November CFISH catch rates are largely composed of 1+ scallops.

19.3.2 SOI and freshwater flow

SOI data were obtained from the Australian Bureau of Meteorology. Freshwater influences on the scallop population dynamics were considered using Queensland Department of Natural Resources and Mines flow data for the four largest rivers in the region (Figure 19-1); Mary River (monitoring station 138014A), Burnett River (stations 136007A and 136001B), Calliope River (station 132001A) and the Fitzroy River (station 130005A). Daily flow (ML per day) data were obtained from each river from January 1986 to December 2013.

Regional oceanographic data

The region’s continental shelf and slope environment are oceanographically dynamic and governed by complex topography, tides and the East Australian Current (EAC) (Middleton *et al.* 1994). At 22°S the shelf extends widely to about 300 km from the coast, encompassing the Swain Reefs. At 25°S the shelf narrows to about 60 km and the region is dominated by Fraser Island, the world’s largest sand dune island. The extended shelf width at 22°S impedes the south-flowing EAC, creating a mesoscale cyclonic lee eddy west of the EAC, known as the Capricorn Eddy (Griffin *et al.* 1987) (Figure 19-1).

The eddy creates upwelling, bringing cool, relatively nutrient-enriched water up from the depths of the Marion Plateau (i.e. ~500-2000 m) and depositing it on the shelf in the proximity of the Capricorn Bunker Islands (Weeks *et al.* 2010; Mao and Luick 2014). As the eddy is a significant oceanographic feature of the region, occurring in close proximity to the fishing grounds, its influence on the scallop population dynamics is of particular interest.

Physical oceanographic parameters were obtained from a 19-year numerical hindcast Bluelink ReAnalysis (BRAN 3.5) dataset which is based on the Bluelink ocean model (Oke *et al.* 2013). BRAN 3.5 consists of three-dimensional fields of ocean temperature, salinity and currents, as well as two-dimensional fields of sea level height, with a horizontal resolution of approximately 10 km and a vertical resolution of 5 m in the top 200 m. The parameters were monthly mean sea level height, and water temperature and eddy kinetic energy (EKE) at the surface and at selected depths. Eddy kinetic energy was calculated as follows:

$$EKE = 0.5(u^2 + v^2)$$

where u is zonal velocity and v is meridional velocity in cm s^{-1} at each grid point.

A significant attraction of the BRAN 3.5 dataset is that it covers the period 1 January 1993 to 30 September 2012, which largely coincides with the period for which CFISH logbook data are available for the fishery.

Monthly anomalies were calculated using monthly climatologies based on the long-term average for each variable for each month over the 19-year period. Areally averaged indices were derived for five areas within the study domain; 1) the Capricorn Eddy (23.0-24.0°S, 152.0-153.4°E, based on Weeks *et al.*, (2013)), 2) three 0.5° logbook grids where major scallop catches occur T30 Bustard Head (23.5-24.0°S, 153.5-152.0°E), V32 Hervey Bay (25.0-25.5°S, 152.5-153.0°E) and W34 Fraser Island (25.5-26.0°S, 153.0-153.5°E), and 3) the Whole fishery area (22.5-26.0°S, 151.0-153.5°E) (Figure 19-1).

Monthly Chl-a data for each of the five areas were downloaded from the Australian Government Bureau of Meteorology eReefs Data Access - Thredds data server (http://ereefstds.bom.gov.au/ereefs/tds/catalogs/ereefs_data.html) for the period July 2002 to February 2015 in the form of netCDF files (King *et al.* 2014). These data were obtained by NASA's Moderate Resolution Imaging Spectroradiometer (MODIS) aboard the Aqua satellite which was launched in May 2002. As the global Ocean Colour algorithms are inaccurate in nearshore waters of the Great Barrier Reef (Qin *et al.* 2007) inversion algorithms developed by the CSIRO (Brando *et al.* 2012) were applied to the data significantly improving the estimation of Chl-a concentrations.

19.3.3 Statistical analysis

Catch rates were standardised by applying a linear mixed model with restricted maximum likelihood (REML), using the statistical software package GenStat (2011). This was undertaken to adjust for changes in fleet fishing power over the logbook's multi-decadal time series, mainly due to vessels adopting various technologies and also due to vessels of different fishing power entering and exiting the fishery. The response variable was the vessel's logarithm-transformed daily catch of scallops from 1988 to 2013. (Note that fishers report their daily unprocessed scallop catch in logbooks as 'number of baskets' and that monthly adductor muscle condition factors are used to later convert the catch to meat weight.)

Individual vessels were treated as random terms. Fixed terms were fitted for abundance (i.e. logbook grid, year, month and their two-way interactions), lunar phase, prawn catch, hours fished and vessel characteristics affecting fishing power (i.e. engine horse power, sonar, net type and size, net ground gear type, otter board type, propeller nozzle and bycatch reduction device). Any influential correlations of parameter estimates were assessed and terms were dropped from the analysis if necessary. Further details of the catch rate standardising methods can be found in O'Neill and Leigh (2007) and Campbell *et al.* (2010a). From the model, standardised mean catch rates (i.e. log baskets per boat-day) were derived for November each year from 1989 to 2013.

Relationships between coastal and oceanographic parameters and scallop catch rates were investigated using the Pearson Product-Moment Correlation Coefficient (r). Lags were applied to the parameters ranging from 0 (i.e. concurrent) to 24 months. Given that retained scallops caught in November are 15-18 months old, a maximum lag of 24 months extends back to about six months prior to their birth and was considered long enough to encompass most conditions and events affecting their abundance.

Catch rate data used in the correlations were the adjusted mean November catch rate for each year for the whole scallop fishery for the period 1988 to 2013 (i.e. 26 annual observations). The precise number of catch rate observations used in each correlation varied due to lag size and availability of the abiotic data, e.g. flow data are available from 1986-2013, while BRAN data are available from 1993-2012 and Chl-a data are limited to post-2001. Significance levels were based on Porkess (1988) where 10% is a possible correlation, 5% is a probable correlation, 1% is a very probable correlation and 0.1% almost certain correlation. It is important to note that whenever a large number of correlations are generated, about 5% can be expected to be significant simply by chance.

19.4 RESULTS

19.4.1 Scallop catch rates

The general seasonal pattern in adjusted mean monthly logbook catch rates (Figure 19-2) is characterised by a peak in late spring or early summer (November–January) followed by a decline to a minimum in winter (June–August). From November 1988 to November 2013 catch rates varied between 3.2 and 27.4 baskets per boat-day. The high catch rates from November 1992 to November 1993 resulted in an annual peak in total catch of 305,000 baskets in 1993. November catch rates fell to a minimum in 1996 and generally increased from 2002 to 2009. Gaps in the time series after 2000 reflect an annual closure of all trawl fishing in the region from 20 September to 1 November.

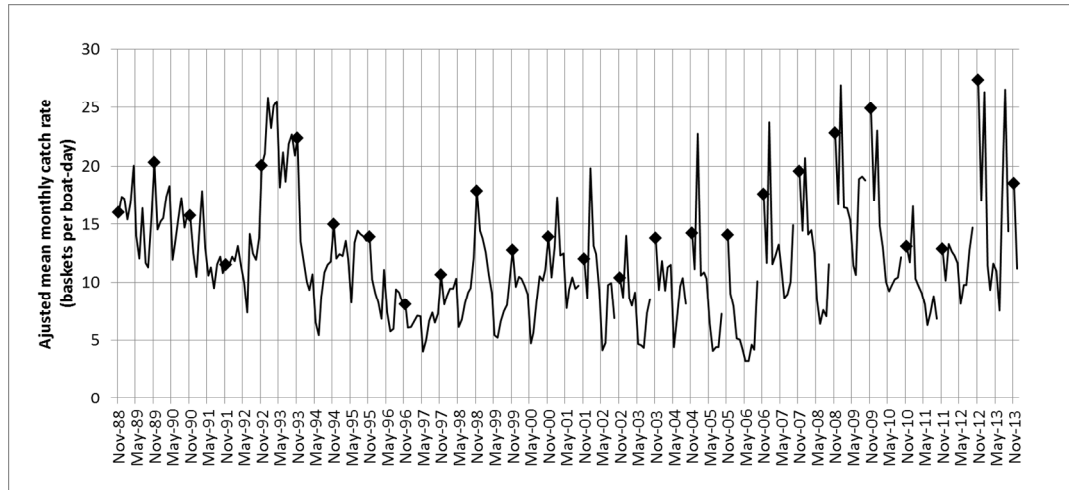


Figure 19-2. The adjusted mean monthly catch rates of scallops based on the mandatory CFISH logbook database, in baskets boat-day⁻¹. The means were derived from the REML model. November catch rates (black stars) were used in the correlation analyses.

19.4.2 Freshwater flow

Of the four river systems examined, the Fitzroy River accounts for about 69% of freshwater flowing out to sea in the region, followed by the Mary (18%) and Burnett (11%) Rivers, while the Calliope River accounts for about 2%. Flows generally peak in January or February (summer) and decline to a minimum in August (winter) (Figure 19-3). Notable flood events occurred in the Fitzroy River in January 1991 as a result of tropical cyclone (TC) Joy, and across all four river systems in December 2010 and January 2011 due to TC Yasi. Severe flooding also occurred in the more southern rivers in January 2013 due to TC Oswald. An extended period of relatively low flow rates occurred across the region from 2001 to 2009.

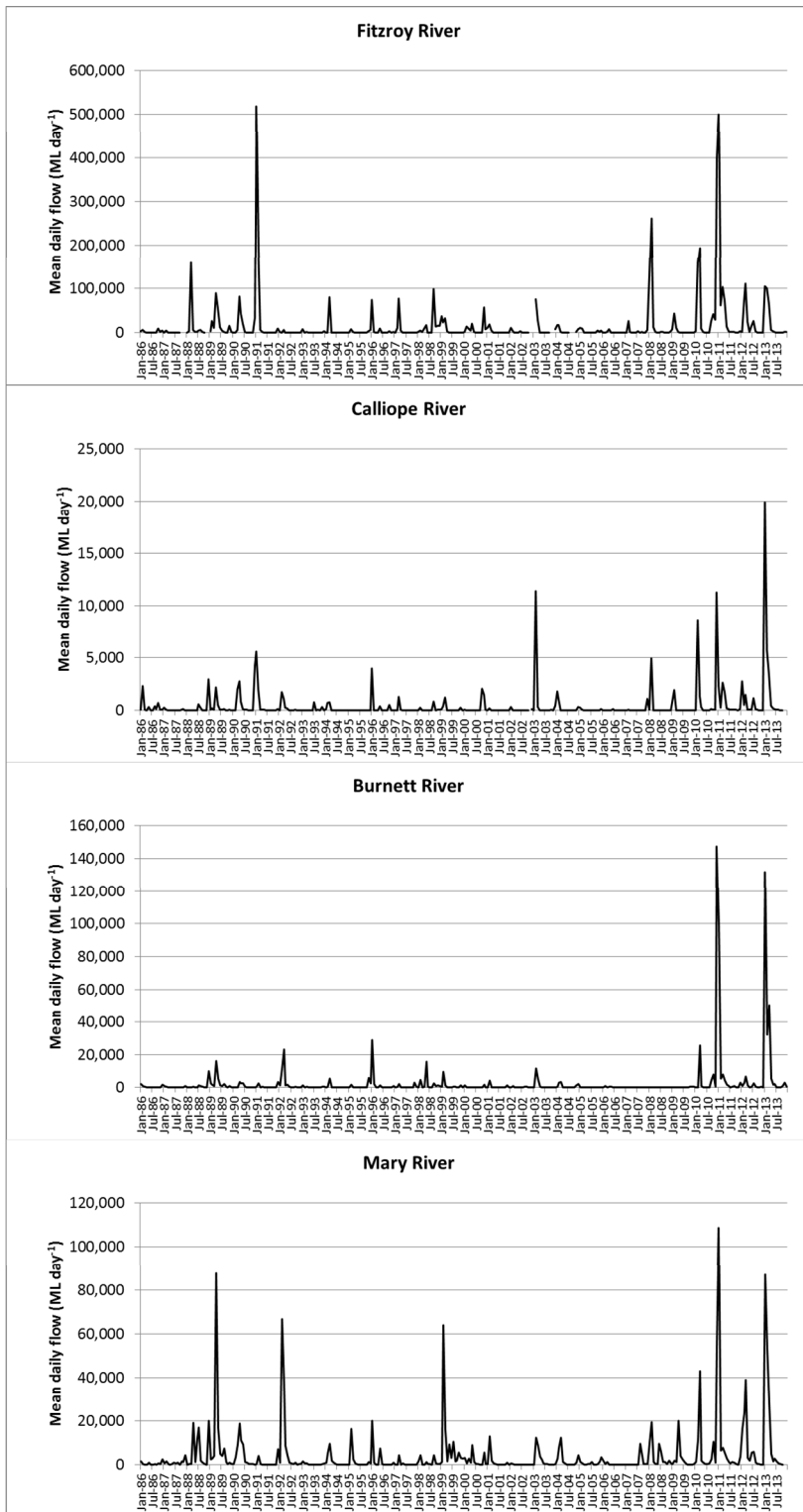


Figure 19-3. Mean daily flow in the major coastal river systems adjacent to the Queensland saucer scallop fishery from January 1986 to December 2013.

The correlations were based on monthly mean flow data from each river from November 1986 to November 2013, and adjusted mean November catch rates from 1988 to 2013. Some trends in the correlation coefficients were common across all four rivers, as well as their combined flows (Figure 19-4).

Appendices – Correlations with scallop catch rates

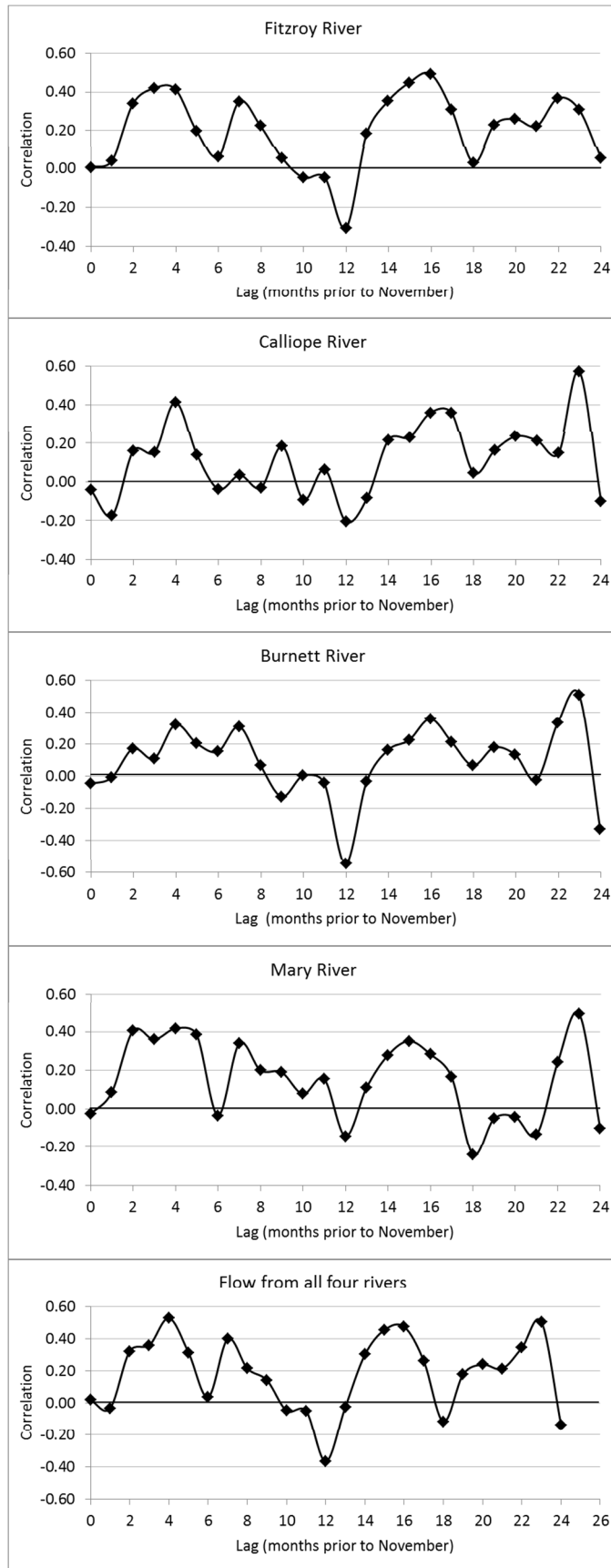


Figure 19-4. Correlations between adjusted mean catch rates of scallops in November (log number of baskets boat-day⁻¹) and freshwater flow from four adjacent coastal river systems. Logbook data are from 1988 to 2013, inclusive.

Appendices – Correlations with scallop catch rates

For example, there was no significant correlation with concurrent flow (i.e. zero lag - November catch rates correlated against November flow). At a four-month lag (i.e. July flow) correlations were positive and ranged from 0.32 (d.f.=24, $p < 0.1$ possible correlation, Burnett River) to 0.53 (d.f.=24, $p < 0.01$ almost certain correlation, combined flow). At a 12-month lag (i.e. flow in November of the previous year) correlations were negative and ranged from -0.14 (d.f.=24, $p > 0.1$ not significant n.s., Mary River) to -0.55 (d.f.=24, $p < 0.01$ almost certain correlation, Burnett River). Consistent positive correlations, ranging from 0.28 (d.f.=24, $p > 0.1$ n.s., Mary River) to 0.49 (d.f.=24, $p < 0.01$ almost certain correlation, Fitzroy River) were obtained at a 16-month lag (i.e. flow in July the previous year). Positive correlations ranging from 0.31 (d.f.=24, $p > 0.1$ n.s., Fitzroy River) to 0.57 (d.f.=24, $p < 0.01$ almost certain correlation, Calliope River) were obtained at a lag of 23 months (i.e. flow in December two years earlier). Over 70% of the correlations for flow were positive. The 0.57 correlation based on the Calliope River data was the largest absolute coefficient obtained for the flow analyses.

19.4.3 Sea water temperature

BRAN 3.5 estimates of mean monthly bottom and surface water temperatures and their anomalies, were examined for the period January 1993 to December 2011. Because of the relatively shallow depths (<40 m) at T30 Bustard Head, V32 Hervey Bay and W34 Fraser Island, the water layers were well mixed, resulting in little differences in temperature between surface and bottom layers. The general seasonal trend is a peak in mean monthly temperature of 26-27°C in February (summer) and a minimum of 19-20°C in August (winter). While surface waters at the Capricorn Eddy area and Whole fishery also followed this pattern, their bottom temperatures were much colder and less variable; mean monthly bottom temperatures varied between 4.2°C and 4.8°C, and 2.9°C and 3.4°C, at the Eddy area and Whole fishery, respectively. This is because bottom temperatures were derived from the deepest layer at each site and because the maximum depths at these sites are very deep (i.e. >1100 m).

The monthly mean surface and bottom water temperature anomalies displayed similar trends for T30 Bustard Head, V32 Hervey Bay and W34 Fraser Island (Figure 19-5). A feature of the time series common across the three logbook grid locations, as well as at the surface of the Eddy area and the Whole fishery area, is the 1.5-2.0°C rise in temperature from February to May 1998, followed by a significant negative anomaly of 1.5-2.0°C from December 1999 to February 2000. Bottom temperature anomalies at the Eddy area and Whole fishery differed markedly from the logbook grid sites and were generally negative at about -0.2°C in the early 1990s, rising to slightly positive from 2000 to 2007 and falling to negative values of -0.1°C to -0.2°C from 2008 to 2012 (Figure 19-5). Note the relatively narrow range in bottom anomalies for the Eddy area and Whole fishery.

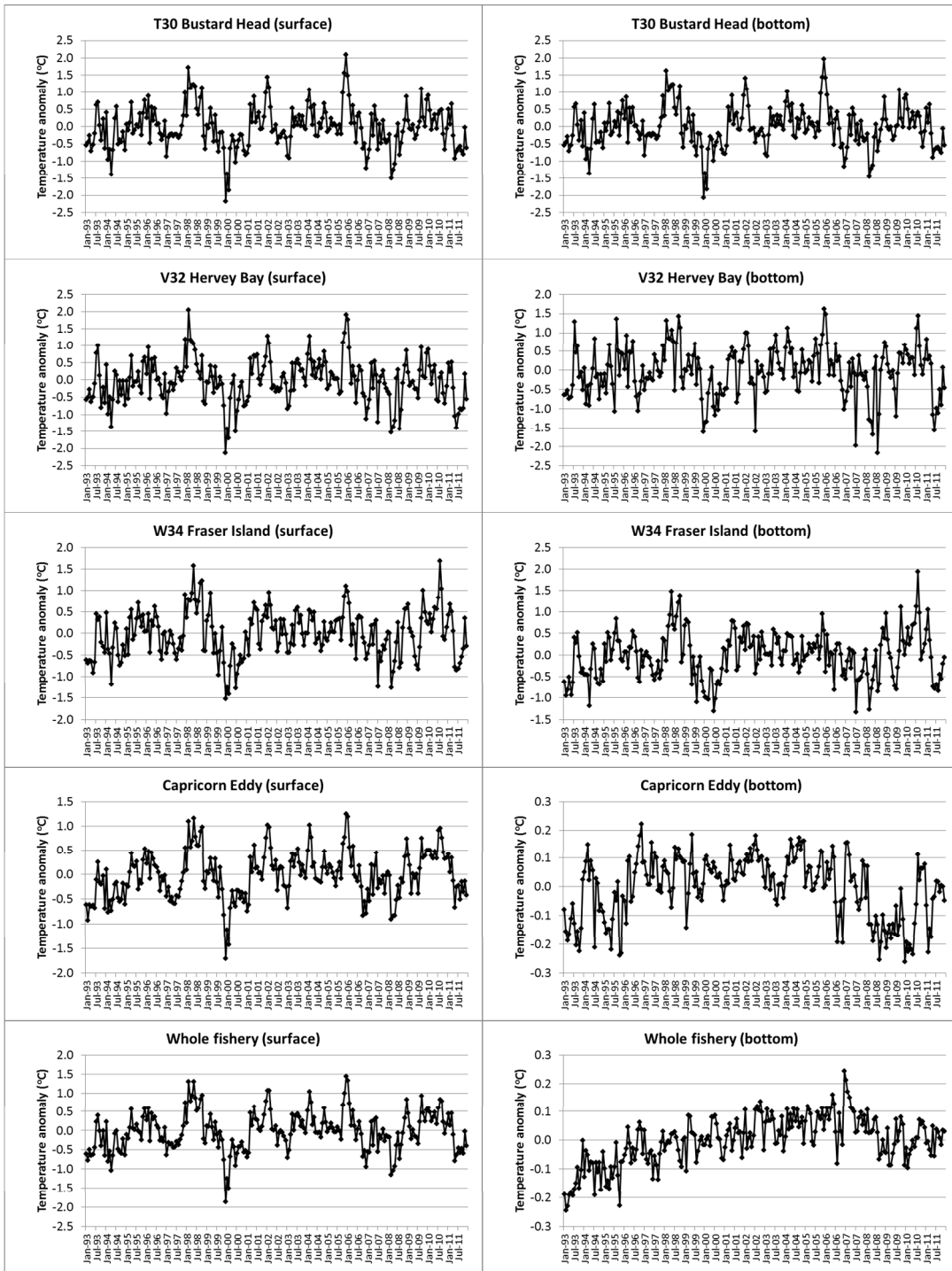


Figure 19-5. Monthly surface and bottom water temperature anomalies at T30 Bustard Head, V32 Hervey Bay, W34 Fraser Island, the Capricorn Eddy area and the Whole fishery area.

As expected, correlations between adjusted mean November catch rates and temperature anomalies (Figure 19-6) show little difference between the surface and bottom at the shallow locations T30 Bustard Head, V32 Hervey Bay and W34 Fraser Island, due to the mixing of layers. In contrast, there were marked differences between surface and bottom correlations at the Eddy area and Whole fishery area. Surface correlations were positive and ranged from 0.13 (d.f.=17, $p>0.1$ n.s., W34 Fraser Island) to 0.33 (d.f.=17, $p>0.1$ n.s. T30 Bustard Head) at a lag of two months (i.e. September temperature anomalies). Surface correlations then declined at a lag of seven months (i.e. April temperature anomalies) and ranged from -0.27 (d.f.=17, $p>0.1$ n.s., T30 Bustard Head) to -0.36 (d.f.=17, $p>0.1$ n.s.,

Appendices – Correlations with scallop catch rates

W34 Fraser Island). While none of these correlations were significant, the trends suggest that warmer surface waters in September are associated with increased catch rates two months later in November, while warmer waters in April are associated with reduced November catch rates.

At lags of 16-18 months (May-July, winter of previous year) surface correlations were consistently negative (Figure 19-6) and ranged from -0.28 (d.f.=17, $p>0.1$ n.s., V32 Hervey Bay) to -0.51 (d.f.=17, $p<0.05$ probable correlation, Capricorn Eddy area). This indicates that warmer surface water temperatures during the winter spawning period of the previous year are associated with reduced November catch rates. This relationship is similar to that obtained in the WA scallop stocks where the November survey abundance of 0+ scallops was negatively related to the SST in the previous winter when spawning takes place.

Bottom temperature anomaly correlations at the Capricorn Eddy area and Whole fishery area were negative at lags of 0-4 months (Figure 19-6) and generally increased with lag duration, peaking at 0.65 (d.f.=16, $p<0.01$ almost certain correlation) in the Whole fishery area at 23 months. The largest absolute correlation for water temperature anomalies was -0.74 (d.f.=17, $p<0.01$ almost certain correlation) for Eddy bottom temperature at a lag of three months (August). This correlation indicates that catch rates declined by about 50%, from about 22 baskets boat-day⁻¹ to 11 baskets boat-day⁻¹, for bottom temperature anomalies at the Eddy area ranging from -0.20 to 0.15°C (Figure 19-7). It is important to note that the bottom temperatures at this depth are relatively stable and hence, the range in anomalies is quite narrow.

It is noteworthy that there was a continuum of strong negative correlations at lags of 0-7 months for bottom water temperature anomalies at the Eddy area (Figure 19-6). These ranged from -0.34 to -0.74 and suggest that elevated Eddy area bottom temperature any time from April (7 month lag) to November (zero lag) is likely to be associated with reduced November catch rates. There was a similar continuum of large positive, statistically significant correlations, ranging from 0.47 to 0.65 for bottom temperature anomalies at the Whole fishery area at lags of 21 to 24 months. This indicates that warmer bottom water temperatures at the Whole fishery two years earlier are associated with elevated November catch rates.

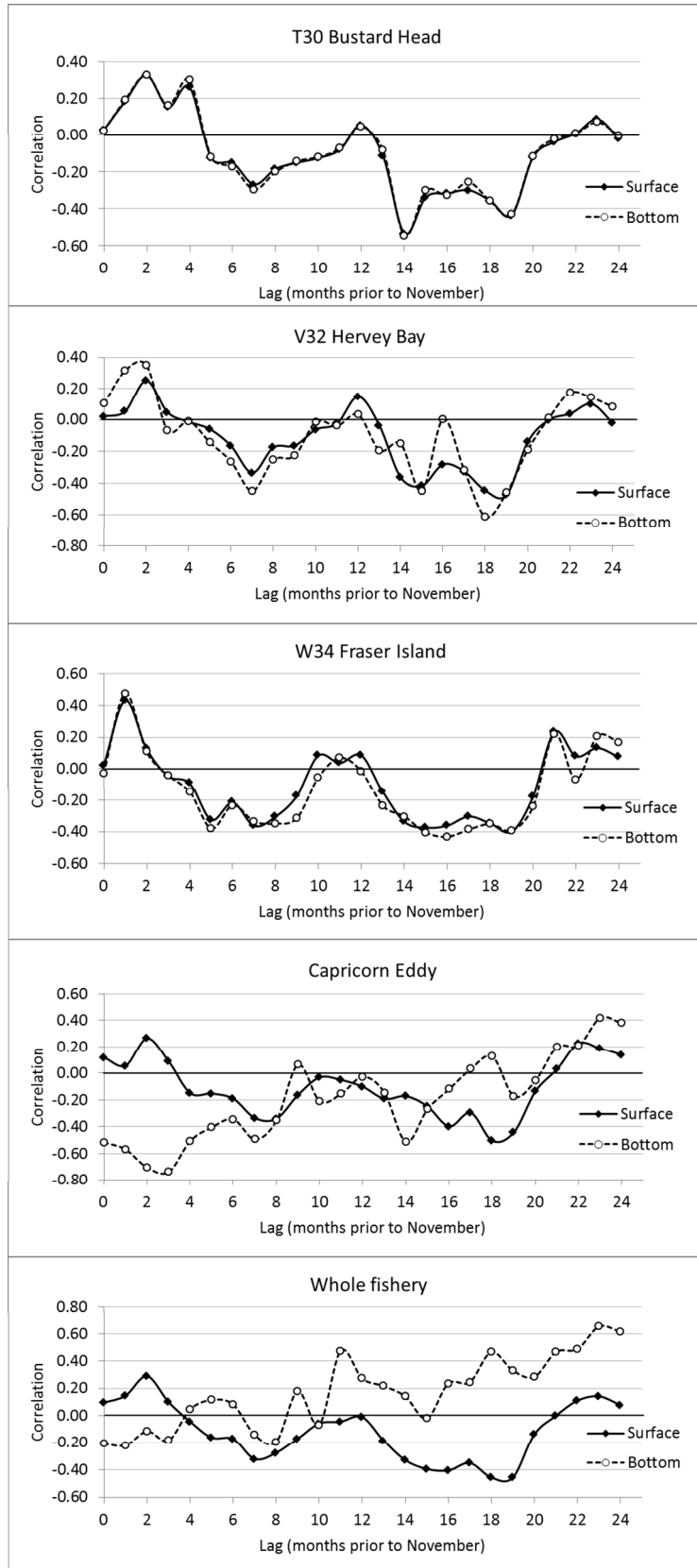


Figure 19-6. Correlations between adjusted mean catch rates of scallops in November and water temperature anomalies at five locations. The similarity between surface and bottom correlations at T30 Bustard Head, V32 Hervey Bay and W34 Fraser Island is due to the mixing of water at different depth layers in these relatively shallow coastal areas.

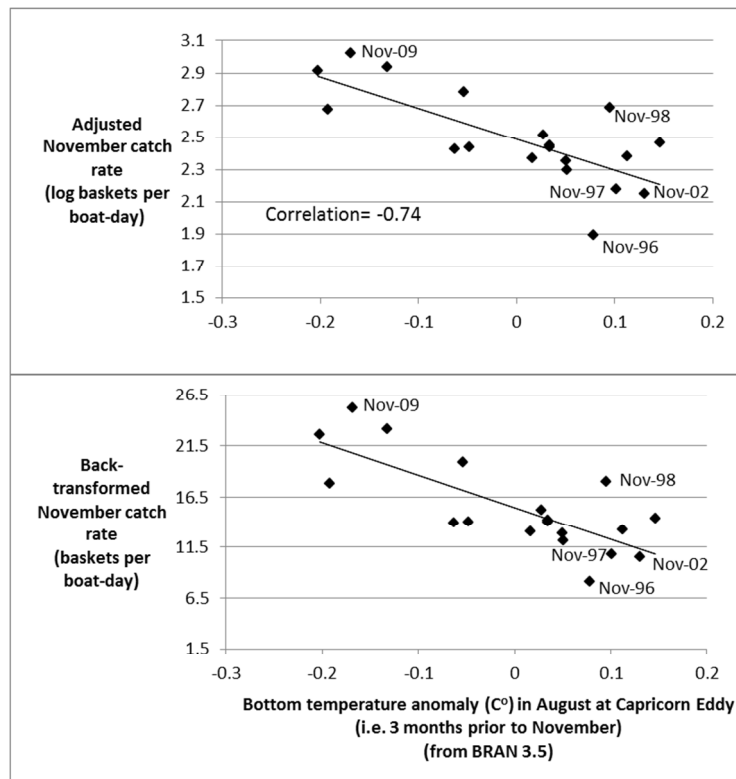


Figure 19-7. The correlation between adjusted mean catch rates of scallops in November and bottom water temperature anomalies at the Capricorn Eddy three months earlier in August (from BRAN 3.5). The upper graph shows logged catch rates from the REML while the lower graph shows the back-transformed catch rates. Straight lines are simple linear regressions of best fit. Catch rates for selected years are labelled for clarity. Note the record low 1996 catch rate.

19.4.4 Sea level

Monthly mean sea levels and their anomalies were derived from BRAN 3.5 for each of the five locations for the period January 1993 to December 2011 (Figure 19-8). Means varied between a minimum of 0.24 m at W34 Fraser Island in November 1994 to a maximum of 0.65 m at T30 Bustard Head in April 2001. The general seasonal pattern across locations was characterised by a peak in April or May, followed by a decline to a minimum in November. Sea level was consistently lower at W34 Fraser Island, by about 0.1 m, and highest at T30 Bustard Head. Sea level variation at the Eddy area was low compared to the other locations.

The overall trends in correlations between adjusted mean November catch rates and monthly sea level anomalies were similar across locations (Figure 19-9). At a lag of one month (sea level in October) correlations were positive and ranged from 0.19 (d.f.=17, $p > 0.1$ n.s., Capricorn Eddy area) to 0.52 (d.f.=17, $p < 0.05$ probable correlation, V32 Hervey Bay). At a three month lag (i.e. sea level in August) correlations were negative and ranged from -0.45 (d.f.=17, $p < 0.1$ possible correlation, T30 Bustard Head) to -0.60 (d.f.=17, $p < 0.01$ almost certain correlation, Capricorn Eddy area). Correlations changed from predominantly negative at a three month lag to predominantly positive at a lag of 24 months (i.e. November sea level two years prior). The largest absolute correlation was -0.60 at the Capricorn Eddy area at a lag of three months. Based on this correlation, November catch rates declined by about 50% as August sea level anomalies increased from about -0.07 m to 0.04 m (Figure 19-10).

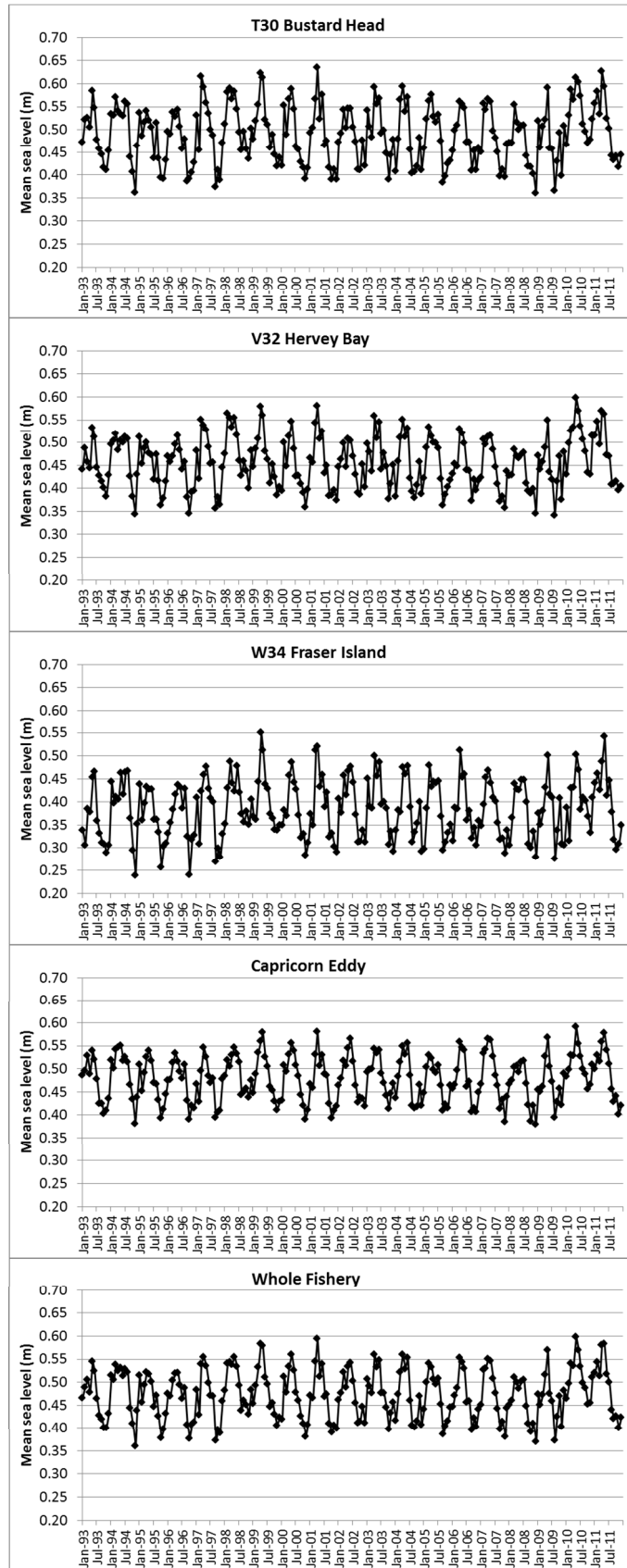


Figure 19-8. Monthly mean sea level at T30 Bustard Head, V32 Hervey Bay, W34 Fraser Island, the Capricorn Eddy area and the Whole fishery area, from BRAN 3.5.

Appendices – Correlations with scallop catch rates

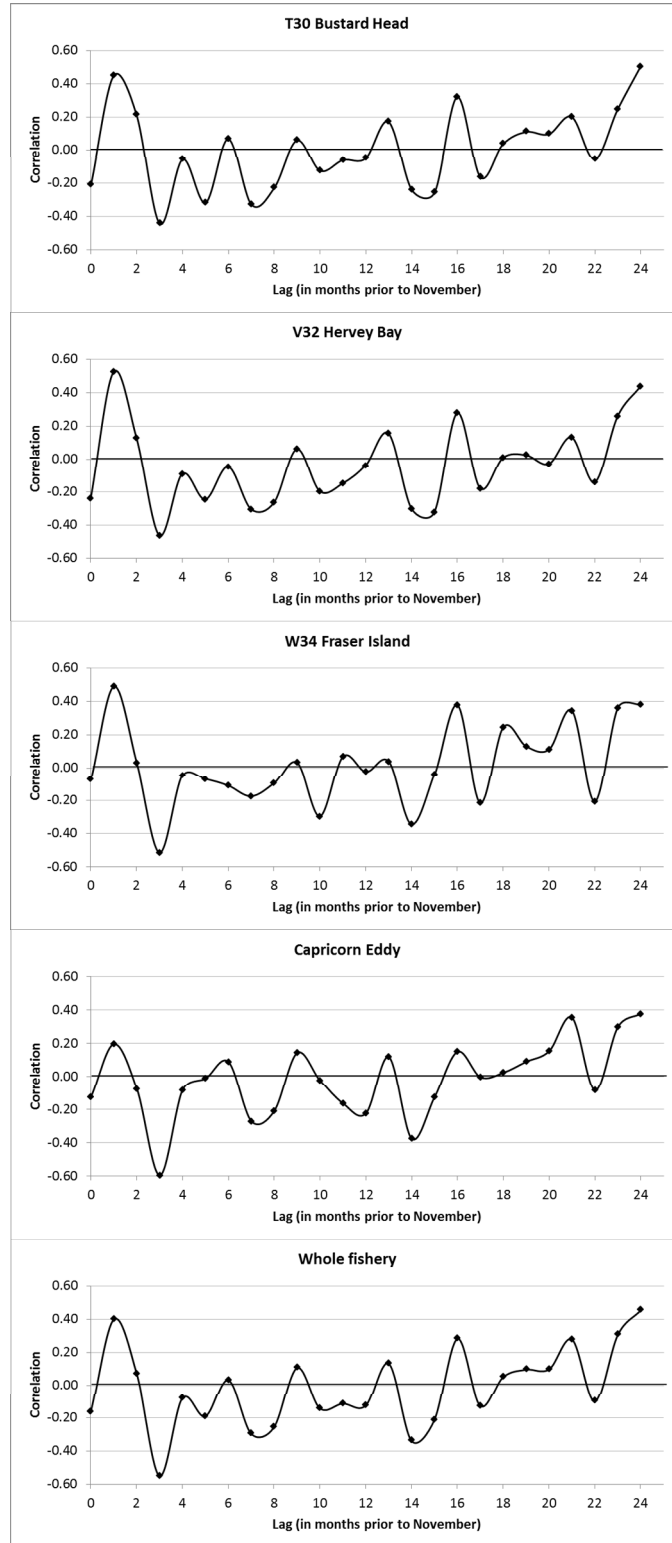


Figure 19-9. Correlations between adjusted mean catch rates of scallops in November and monthly sea level anomalies at the five locations.

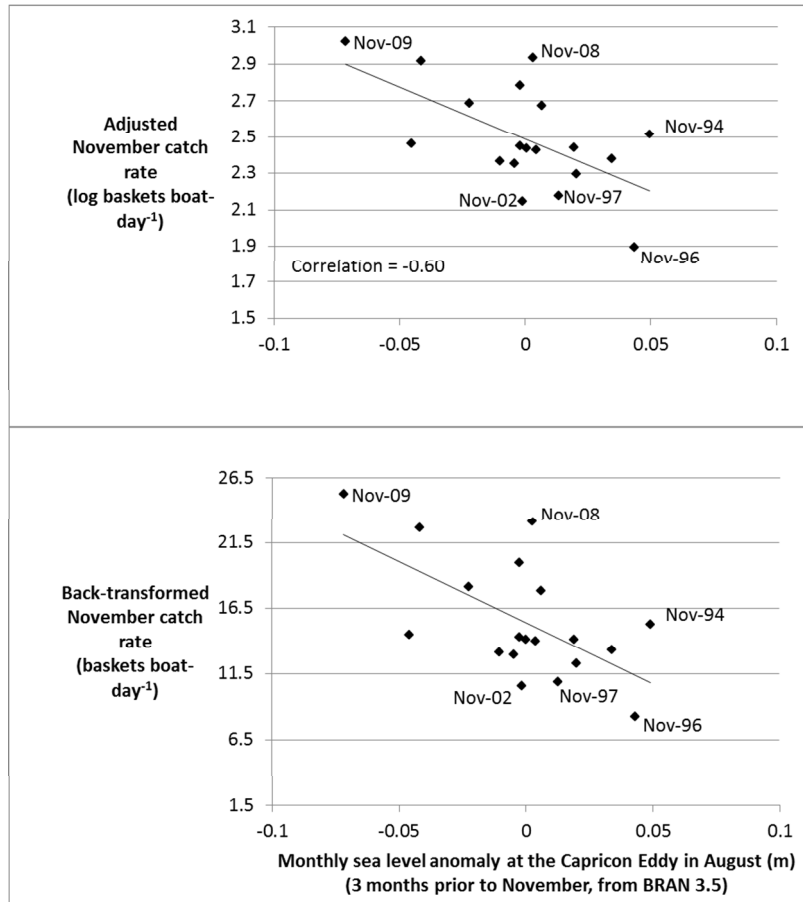


Figure 19-10. The correlation between adjusted mean catch rate of scallops in November and monthly sea level anomalies at the Capricorn Eddy area three months earlier in August (from BRAN 3.5). The upper graph shows logged catch rates from the REML while the lower graph shows the back-transformed catch rates. Straight lines are simple linear regressions of best fit. Catch rates for selected years are labelled for clarity.

19.4.5 Eddy kinetic energy

Monthly EKE was derived for each location at the surface and the bottom from January 1993 to July 2012. EKE was 2-10 times higher at the surface than at the bottom at all locations (Figure 19-11), and consistently higher at the Eddy area where a maximum of $0.152 \text{ m}^2\text{s}^{-2}$ occurred at the surface in March 1997. V32 Hervey Bay had the lowest monthly EKE, possibly due to Fraser Island buffering the Bay from offshore currents and the predominantly south-easterly winds. The seasonal pattern in EKE at both the surface and bottom was characterised by a maximum in March (autumn) and a minimum in September (spring).

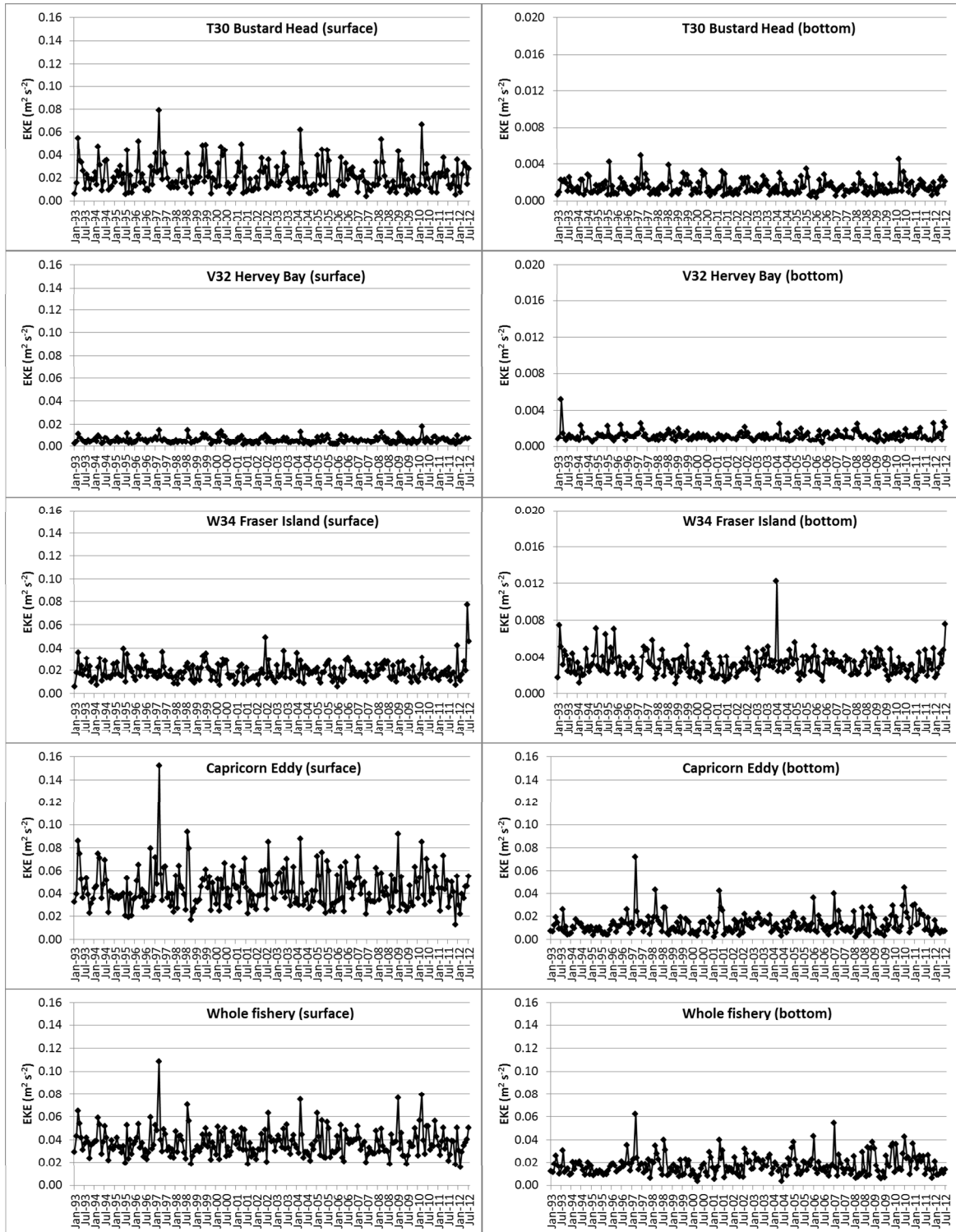


Figure 19-11. Monthly EKE at the surface and bottom at T30 Bustard Head, V32 Hervey Bay, W34 Fraser Island, the Capricorn Eddy area and the Whole fishery area, from BRAN 3.5. Note the y-axis scale is not fixed.

Correlations between adjusted mean November catch rates and lagged monthly EKE were highly variable, both within and between locations, while trends at the surface and bottom were similar (Figure 19-12). A very high proportion of correlations were less than 0.389, which is the critical Pearson product moment correlation coefficient (d.f.=17, $p < 0.1$) indicative of a possible correlation, and were therefore not significant.

Appendices – Correlations with scallop catch rates

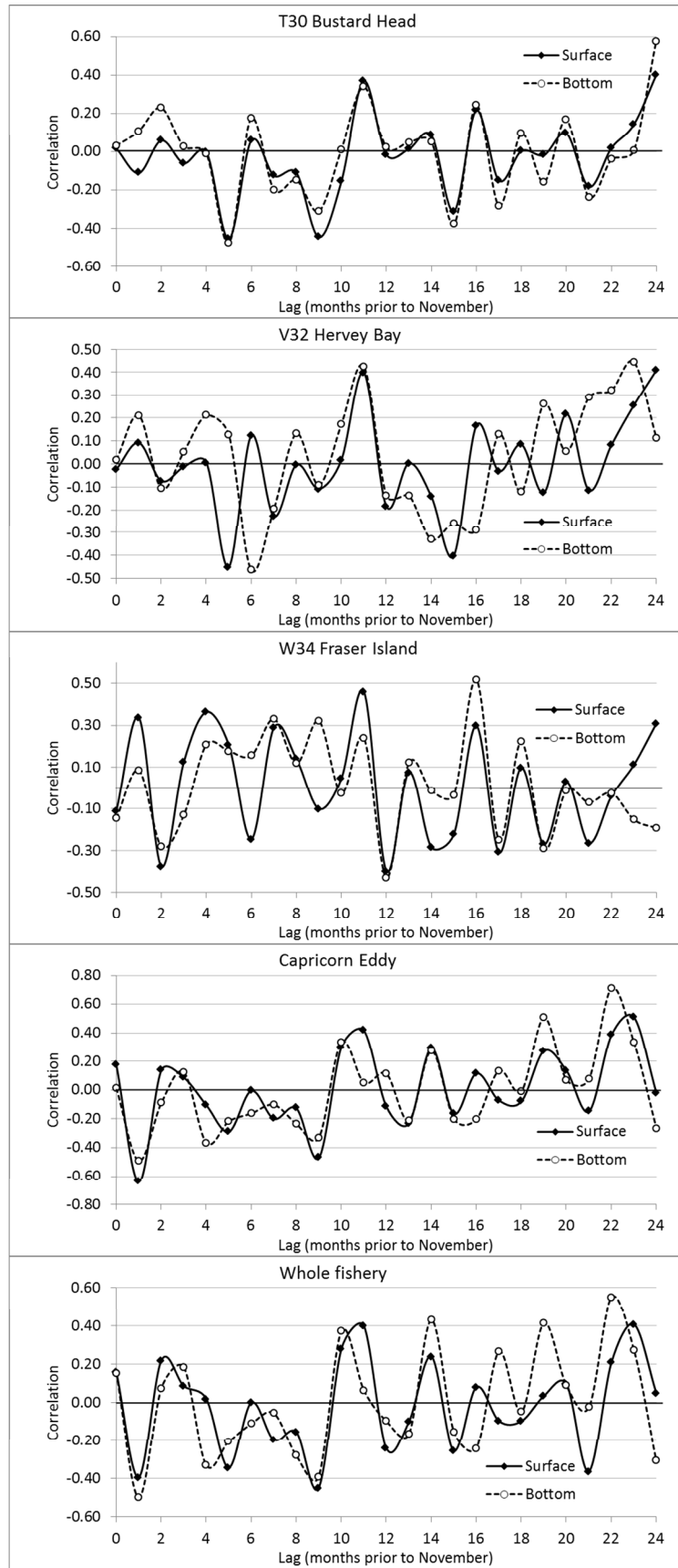


Figure 19-12. Correlations between adjusted mean catch rates of scallops in November and monthly EKE at the surface and bottom at the five locations.

Appendices – Correlations with scallop catch rates

The two largest absolute correlations were both observed at the Capricorn Eddy area; -0.64 at the surface (d.f.=17, $p < 0.01$ almost certain correlation) at a one month lag (October EKE) and 0.71 at the bottom EKE (d.f.=17, $p < 0.01$ almost certain correlation) at a lag of 22 months (January EKE two years prior) (Figure 19-12). Based on this correlation, adjusted mean November catch rates doubled from about 12 baskets boat-day⁻¹ to 24 baskets boat-day⁻¹ as bottom EKE at the Eddy area increased from 0.005 m²s⁻² to 0.04 m²s⁻² in January 22 months prior (Figure 19-13).

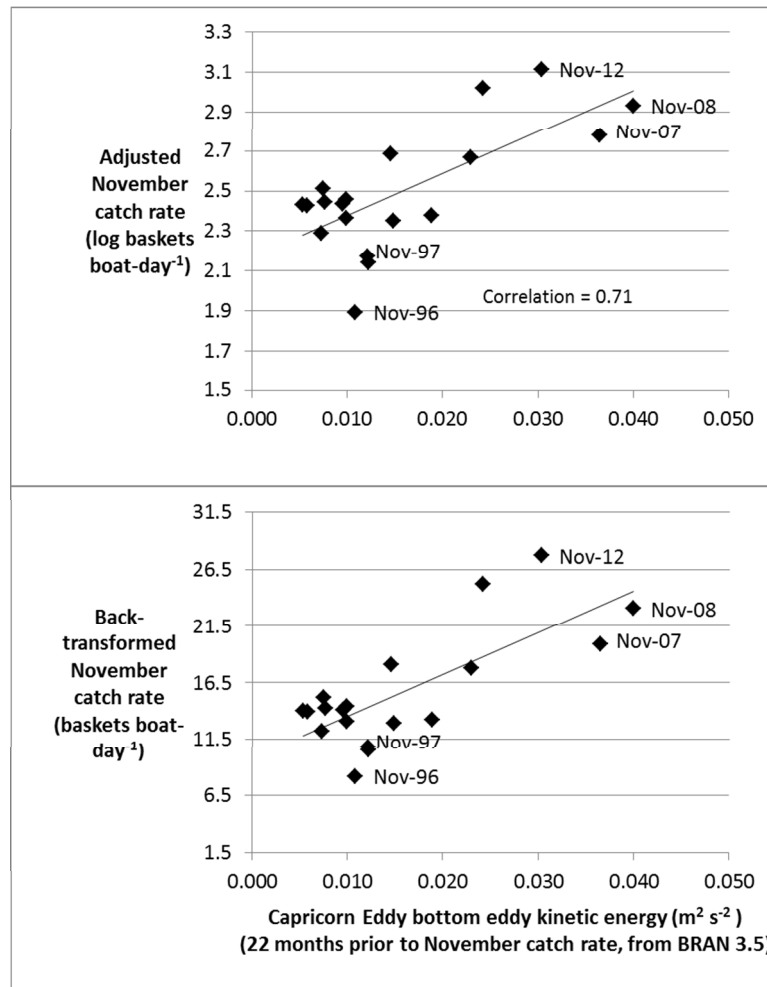


Figure 19-13. The correlation between adjusted mean catch rate of scallops in November and bottom EKE at the Capricorn Eddy area 22 months earlier in January (from BRAN 3.5). The upper graph shows logged catch rates from the REML while the lower graph shows the back-transformed catch rates. Straight lines are simple linear regressions of best fit. Catch rates for selected years are labelled for clarity.

19.4.6 Chlorophyll-a

The time series for Chl-a data is shorter than the other parameters because the MODIS Aqua satellite was only launched in May 2002, with Chl-a data available from July 2002. Trends in mean monthly Chl-a (mg m⁻³) at each of the five locations are provided in Figure 19-14 for the period July 2002 to February 2015. V32 Hervey Bay had consistently higher Chl-a concentrations compared to the other areas, while the Eddy area had the lowest. Chl-a concentration declined with distance from the coast. Monthly means were generally <1.0 mg m⁻³ at most locations, while a maximum of 5.0 mg m⁻³ occurred in V32 Hervey in February 2013. Peaks generally occurred about one month after flooding (Figure 19-3). The seasonal pattern in Chl-a concentration was also similar to that of freshwater flow,

although slightly lagging flows by about one month, peaking in February (summer) and declining to a minimum in September (spring).

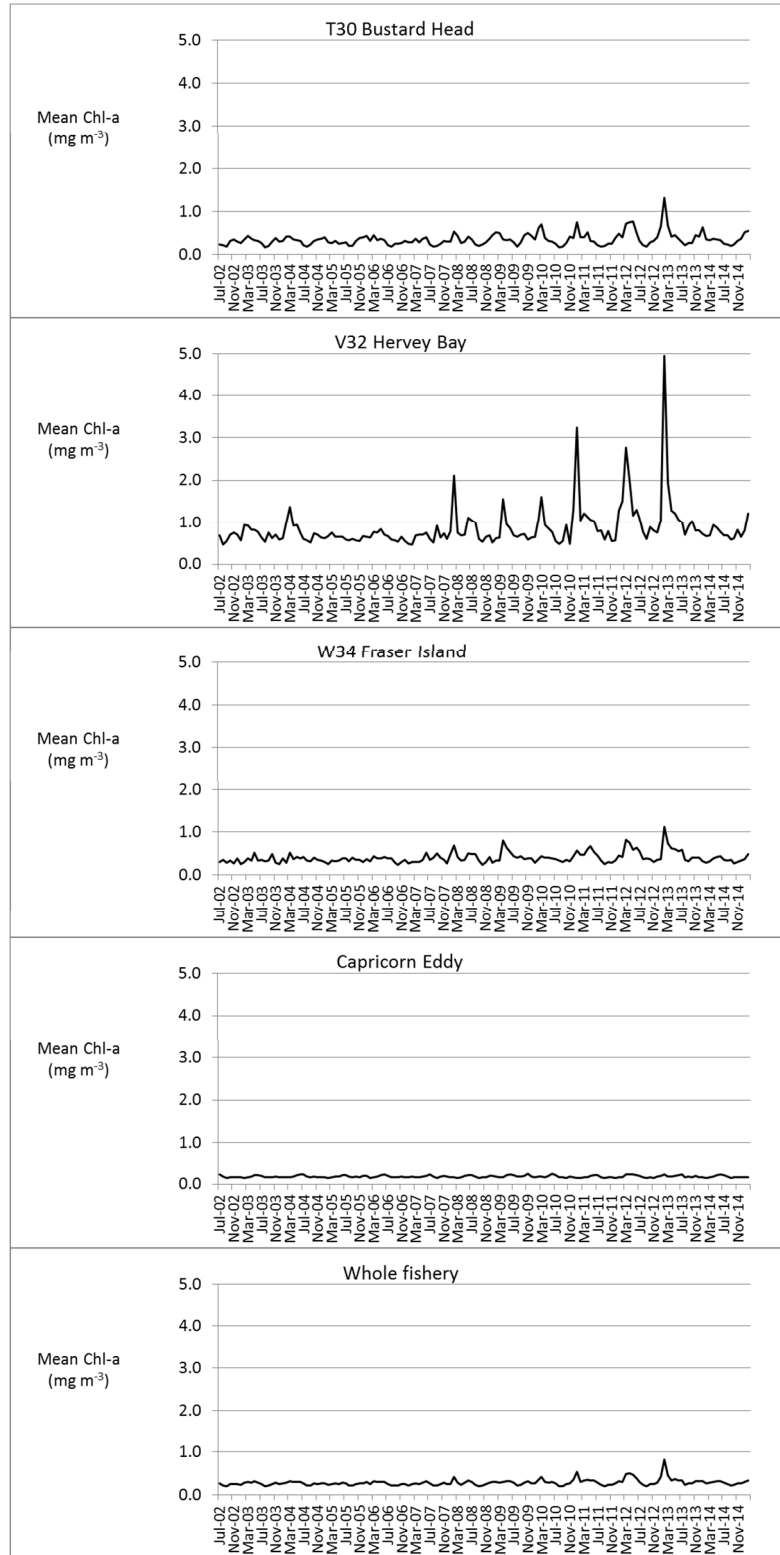
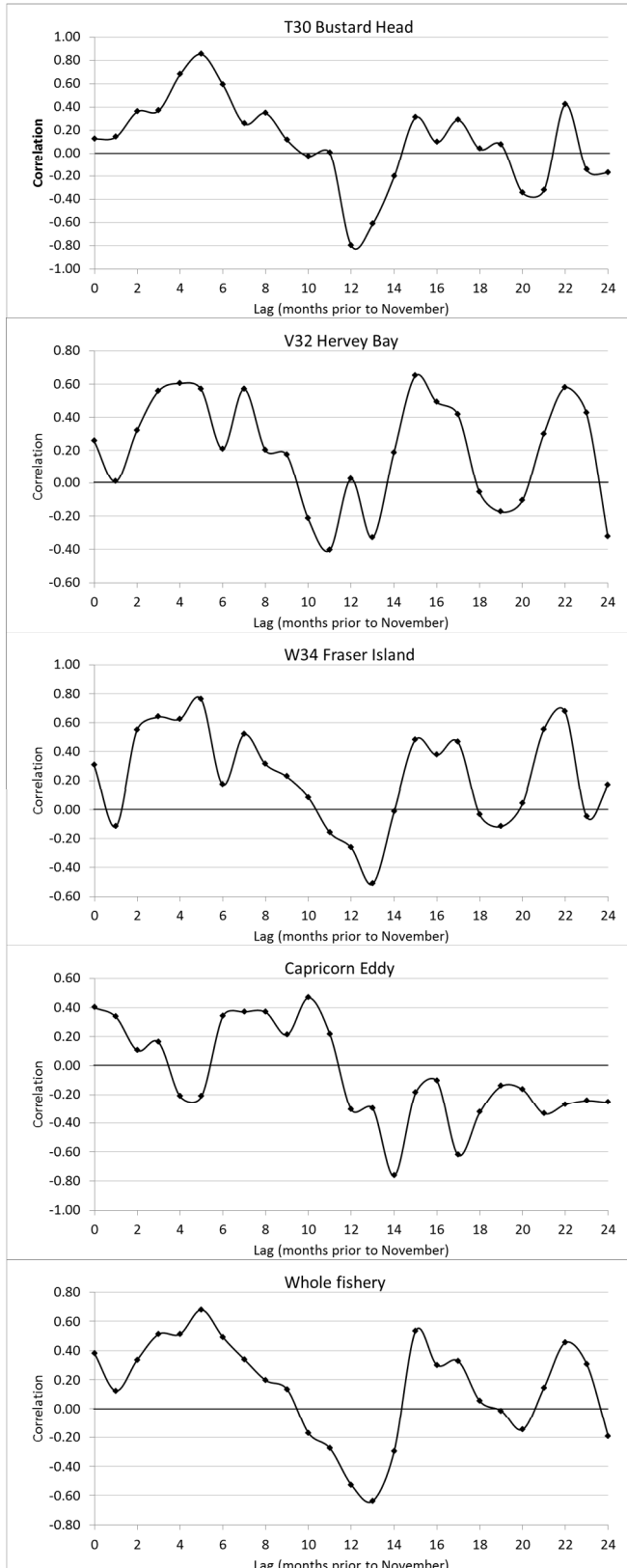


Figure 19-14. Time series of mean monthly Chl-a concentrations from T30 Bustard Head, V32 Hervey Bay, W34 Fraser Island, the Capricorn Eddy area and the Whole fishery. The data were acquired by the MODIS Aqua satellite and provided by the Australian Government Bureau of Meteorology.

Appendices – Correlations with scallop catch rates

Caution is required interpreting the correlations due to the short Chl-a time series. Correlations were based on a maximum of 12 observations (i.e. adjusted November mean catch rates from 2002 to 2013) but fell to only 10 when lags of more than 15 months were considered. The small sample size lowers the degrees of freedom and reduces the probability that the correlations are significant.



There were some marked differences in the correlation trends between the logbook grid locations (T30 Bustard Head, V32 Hervey Bay and W34 Fraser Island) and the Capricorn Eddy area (Figure 19-15). The grid correlations were all positive and ranged from 0.57 (d.f.=10, $p < 0.05$ probable correlation, V32 Hervey Bay) to 0.85 (d.f.=10, $p < 0.01$ almost certain correlation T30 Bustard Head) at lags of 4-5 months (i.e. Chl-a in June and July, winter). In contrast, the Eddy area correlations were negative at -0.21 at these lags, although not significantly (d.f.=10, $p > 0.1$ n.s.). It is noteworthy that correlations were predominately negative at lags of 12-14 months (i.e. September to November, spring the previous year) and ranged from zero (W34 Fraser Island) to -0.80 (d.f.=9, $p < 0.01$ almost certain correlation, T30 Bustard Head). A marked decline in correlations can be observed for the Whole fishery, from 0.67 (d.f.=9, $p < 0.05$ probable correlation) at a five month lag to -0.64 (d.f.=9, $p < 0.05$ probable correlation) at a 13 month lag.

Figure 19-15. Correlations between adjusted mean catch rate of scallops in November and monthly mean Chl-a concentrations from the five locations.

Appendices – Correlations with scallop catch rates

Based on the largest absolute correlation of 0.85 at T30 Bustard Head at a lag of five months, adjusted mean November catch rates approximately double from 13 baskets boat-day⁻¹ to about 27 baskets boat-day⁻¹ as Chl-a concentration increases from about 0.3 mg m⁻³ to 0.5 mg m⁻³ in June (Figure 19-16).

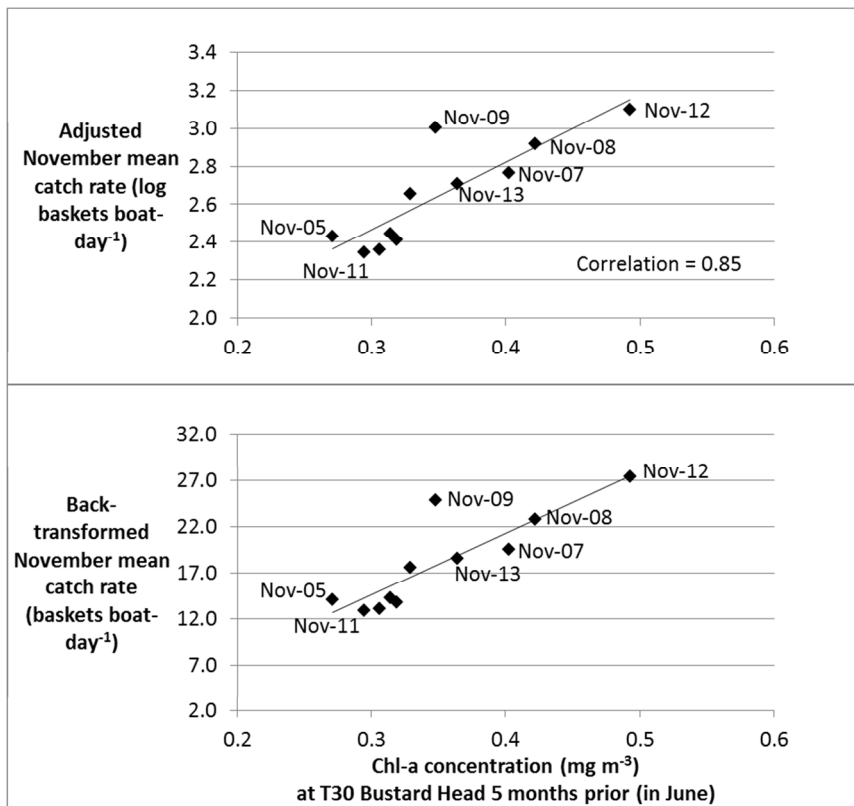


Figure 19-16. The correlation between adjusted mean catch rate of scallops in November and Chl-a concentration in T30 Bustard Head five months earlier in June. The upper graph shows logged catch rates from the REML while the lower graph shows the back-transformed catch rates. Straight lines are simple linear regressions of best fit. Catch rates for selected years are labelled for clarity. The MODIS Aqua satellite dataset for Chl-a does not extend back to 1996 when the fishery crashed.

19.4.7 SOI

A time series of the SOI from January 1987 to February 2014 is provided in Figure 19-17. A sustained positive SOI (La Niña) is associated with wetter than usual conditions in eastern and northern Australia, while a sustained negative index (El Niño) is associated with reduced rainfall. The elevated indices from April 2010 to April 2011 were associated with extreme flood events in central and southern Queensland at this time (reflected in river flow Figure 19-3), while the predominantly low indices from 2002 to 2007 were associated with severe drought. The period of low SOI from February 1997 to June 1998 is noteworthy because of the rapid decline from February to June 1998, followed by an extended period of low indices for more than one year, and then by a rapid increase from March to June 1998.

The correlations, which were based on 26 adjusted mean November catch rates (i.e. 1988-2013) and the SOI, were consistently low (Figure 19-17), with the largest absolute correlation of 0.26 at a lag of 23 months. None of the correlations between SOI and catch rates were significant (d.f.=23, p>0.1 n.s.).

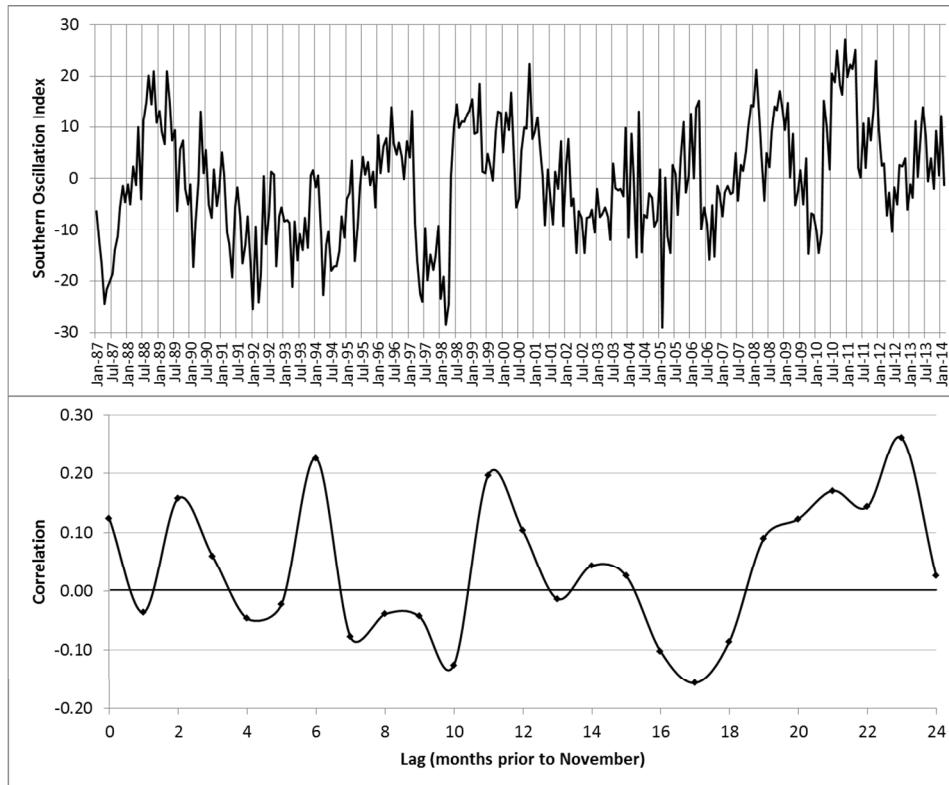


Figure 19-17. The Southern Oscillation Index (upper graph) and correlations between the SOI and adjusted mean catch rates of scallops in November (lower graph). Lags ranging from 0 (no lag) to 24 months have been applied to the SOI.

19.5 DISCUSSION

19.5.1 Suitability of BRAN

A fundamental assumption of the study is that the oceanographic parameters, water temperature, sea level and EKE derived from BRAN 3.5, accurately reflect conditions at the five locations. Chiswell and Rickard (2014) compared BRAN 3.5 estimates of current velocity and EKE against those obtained from Global Drifter Program drifters at the surface and Argo floats at 1000 m within a large domain of the Australian oceanographic region (i.e. 0°-50°S and 90°-180°E). They found that BRAN’s velocities near the surface (12.5 m) compare well with drifter velocities, except in the Antarctic Circumpolar Current (ACC) (> 45°S) where drifter velocities were higher. At approximately 1000 m the BRAN and observational velocities were similar in our study domain (i.e. 22°-27°S), but in the equatorial region BRAN velocities can be up to five times higher than Argo float observations, and weaker in the ACC.

19.5.2 Influential coastal and oceanographic properties

Of the 900 correlations examined between adjusted mean catch rates in November and the coastal and oceanographic parameters (freshwater flow, water temperature, sea level, EKE, Chl-a and SOI), the strongest correlation found was 0.85 for Chl-a at T30 Bustard Head five months prior in June (Figure 19-16). Strong positive correlations for Chl-a at a five-month lag were common across all locations, except the Eddy area (Figure 19-15) which is located further offshore and has lower Chl-a concentrations, compared to the other locations.

While no cause or effect has been demonstrated for any of the correlations, it seems reasonable to speculate that elevated Chl-a concentrations in June result in higher survival, and/or increased

catchability of 1+ scallops in November. As saucer scallops are filter feeders, increased Chl-a concentrations may result in increased food availability, increasing the survival and growth rates of the scallops. However, it is difficult to explain the negative Chl-a correlations which were common across all locations at lags of 12-14 months (Figure 19-15). These suggest that elevated Chl-a in September-November are associated with reduced catch rates in November the following year.

Correlations for freshwater flow (Figure 19-4) and Chl-a (Figure 19-15) showed similar trends. Both showed strong positive correlations at lags of 4-5 months which then declined to negative correlations at 12-14 months, although the trend for Chl-a generally lagged flows by about one month. A possible explanation for this is that flows provide nutrients to the inshore coastal habitats, including the scallop fishing grounds, which result in increased Chl-a concentrations a few weeks later. While flows and Chl-a showed similar trends, the absolute correlation values were generally larger for Chl-a.

Saucer scallops *A. balloti* have a relatively narrow temperature range which limits their distribution on Australia's continental shelf and affects their survival. Wang (2007) found the optimum water temperature for larval *A. balloti* survival was 18-20°C, and that these temperatures were similar to ambient water temperatures on the central Queensland coast in July and August during their winter spawning period. Hence, understanding sea water temperature variation may be useful for explaining variation in scallop biomass, catch rates and annual landings in the Queensland fishery.

In Shark Bay WA fishery-independent surveys of *A. balloti* have been conducted annually in November for more than 30 years and used to examine the influence of coastal and oceanic conditions on the scallop's population dynamics and fishery. WA researchers have shown that strong La Niña conditions during the scallop's winter spawning (May-August), which result in a strong south-flowing Leeuwin Current and high SST, are always associated with poor recruitment of scallops (i.e. the 0+ age class) (Joll and Caputi 1995; Lenanton *et al.* 2009; Caputi *et al.* 2015). The researchers use sea level as a proxy measure of the strength of the Leeuwin Current, which is why sea level was also examined in the present study.

Following a severe marine heat wave event on the WA coast during the austral summer of 2010-11, where SST exceeded 5°C above average (Pearce and Feng 2013), the Shark Bay scallop population collapsed to an historically low level, resulting in the fishery's closure since May 2011 (Caputi *et al.* 2015). The heat wave had wide-ranging ecological impacts on seagrass/algal habitat, coral communities, abalone (*Haliotis roei*) and blue swimmer crabs (*Portunus armatus*), and also resulted in fish kills and range extension of tropical species, but its impact on the saucer scallop population appears particularly severe and long-lasting. The heat wave event was exacerbated by water temperature being above average for the two summers following the heat wave resulting in the spawning stock being the lowest in the 30 years that surveys have been operating (Caputi *et al.* 2015).

In the present study, we examined both sea level and temperature, including bottom and surface water temperatures anomalies at five locations associated with the Queensland scallop fishery. The largest absolute correlation for temperature was -0.74 for the bottom water temperature anomaly at the Capricorn Eddy area in August, three months prior to the November catch rates (Figure 19-6). The largest absolute correlation for sea level anomalies (-0.60) also occurred at the Eddy area in August (Figure 19-9). The results show that catch rates of 1+ scallops in November decline markedly when bottom water temperature (Figure 19-7) and/or sea level (Figure 19-10) at the Eddy area are elevated in August. Importantly, there is a continuum of strongly negative correlations associated with bottom water temperature at the Eddy area at lags from 0-8 months (Figure 19-6), indicating that elevated bottom temperature at the Eddy area anytime from March to November will likely be associated with reduced November catch rates.

As the Queensland saucer scallop fishery has maintained a minimum legal size limit of at least 90 mm SH in November since the logbook program commenced in 1988, it is important to note that it is the catch rate of adults (i.e. ≥ 78 mm SH) that declines in relation to these two three-month lag correlations. We cannot infer any such similar relationship for egg production, or the abundance of larvae or

juveniles (i.e. the 0+ age class which are <78 mm SH) as these age classes are not represented in the commercial catches.

The relatively strong negative surface temperature anomaly correlations, which ranged from -0.28 to -0.51 (Figure 19-6) at lags of 16-18 months (May-July, winter of previous year), are more relevant to reproductive output and the survival of larvae and juveniles, as they reflect conditions at the time when those adult scallops making up the November catches were spawned in the winter of the previous year. These negative correlations were common across all locations.

Collectively, the analyses indicate that elevated water temperatures (i.e. positive anomalies) are associated with reduced catches of 1+ scallops in November; this is reflected in the three-month lag (August) for bottom temperature at the Capricorn Eddy area, and in the 16-18 month lags (May-July, winter of previous year) for surface temperature at all locations. While there were a few positive correlations for water temperature (Figure 19-6), there were many more negative correlations. In addition, the negative correlations were generally stronger, with larger absolute values, and were statistically significant more often than the positive correlations, which were generally weak (i.e. <0.3).

There are some similarities between WA Shark Bay and the Queensland east coast, in regards to water temperature effects on the population dynamics of *A. balloti*. The relationships between adjusted mean November catch rates and SST 16-18 months earlier (May-July previous year) are consistent with the detrimental effect of elevated SST during the winter spawning (May-August) of scallops in Shark Bay. It seems that on Australia's west and east coasts, elevated SST during the scallop's winter spawning is associated with reduced recruitment and subsequently, reduced commercial landings about 18 months later. These similarities across stocks in Australia makes this environmental correlation quite robust.

Again we speculate, that elevated August bottom temperature at the Eddy area lowers the survival and/or catchability of 1+ year old scallops three months later in November. Reduced survival could be attributed to increased predation and/or reduced food availability. Reduced catchability could result if the warmer Eddy area water alters the behaviour of the scallops. Elevated SST during the winter spawning (May-July, 16-18 month lag) may lower reproductive output and/or larval survival, resulting in reduced catch rates in November the following year. Larval survival is affected by food availability, tides, currents, predation and the time exposed to these while the larvae are passively transported in the water column. Joll and Caputi (1995) speculated that the stronger the Leeuwin Current, the more scallop larvae were flushed out of Shark Bay away from fishing grounds, lowering recruitment and commercial catches. Following the severe WA marine heat wave, Caputi *et al.* (2015) suggested the high mortality experienced by adult scallops was due to thermal stress and possibly a change in food availability.

19.5.3 Spatial comparison of coastal and oceanographic influences

In the absence of knowledge about the location of influential environmental drivers, we put forward five areas associated with the fishery; three logbook grids where significant catches of scallops are reported annually, an area representing the location of the Capricorn Eddy, and an area encompassing the Whole fishery (Figure 19-1). A total of 125 correlations were examined for each area based on their physical oceanographic properties (water temperature anomalies, sea level and EKE) derived from BRAN 3.5. Using an absolute value ≥ 0.5 as indicative of strong correlation, we found that the Eddy area had the most strong correlations (i.e. 12 correlations ≥ 0.5), followed by the Whole fishery area with five. T30 Bustard Head had four strong correlations, while V32 Hervey Bay and W34 Fraser Island each had two. This tends to support our early hypothesis that the Capricorn Eddy is likely to have a relatively strong influence on the scallop's population dynamics and fishery.

The high correlation between November catch rates and Chl-a at T30 Bustard Head five months earlier (Figure 19-16) might suggest that this area also has a relatively strong influence on the scallop population dynamics, although strong positive correlations were common at a five-month lag across all locations, except the Eddy area.

In terms of ranking parameter influence, Chl-a and water temperature anomalies had the strongest correlation with November catch rate, while no significant correlations were obtained for SOI. The lack of strong SOI correlations is surprising given the association between strong La Niña conditions and reduced scallop larval settlement in Shark Bay, WA (Caputi *et al.* 2015). This is likely attributed to the ENSO having a much stronger influence on the Leeuwin Current in WA, compared to the EAC. The effect of the SOI on scallops in WA is due to the ENSO influence on the strength of the Leeuwin Current which affects the water temperature along the coast. In comparison, the ENSO influence on the EAC is weak (Ridgway and Hill 2009). This is because the main oceanic pathway of the ENSO influence is the Indonesian region and a waveguide around western and southern Australian coastal boundaries (Wijffels and Meyers 2004).

The influence of the remaining parameters (freshwater flow, sea level and EKE) could be deemed as intermediate. The lack of strong correlations for EKE and the relatively unstable trend across lags (Figure 19-12) could be attributed to a lack of directional vectors associated with this variable. For example, equally strong south-flowing and north-flowing currents at a particular location would have resulted in the same EKE value, making interpretation of correlations difficult. Directional vectors should therefore be included in future analyses involving EKE.

19.5.4 Management implications

The Queensland saucer scallop fishery has been operating for over 40 years, with mandatory daily logbook data available since 1988. In 1996 the fishery was considered to have crashed, resulting in the lowest November catch rate on record (Figure 19-2) and considerable hardship upon fishers and processors, as well as concern by fishery managers and scientists. The analyses presented here may help explain this decline, and may have potential to forewarn stakeholders of similar future events. For example, the low catch rates of November 1996 were associated with elevated bottom temperature (Figure 19-7) and sea level (Figure 19-10) at the Capricorn Eddy area three months prior in August. Although Chl-a was associated with the strongest correlation found in the present study, we cannot comment on the significance of Chl-a in 1996 as satellite data have only been available since 2002. Nevertheless, daily Chl-a data for the region are now readily available from the Australian Government Bureau of Meteorology and could be used to explain future variation in scallop catch rates, including upcoming fishing seasons. While Chl-a data are readily available, the physical oceanographic properties (water temperature, sea level and EKE) were all derived from BRAN 3.5, which is a hindcast dataset that ended in September 2012. Hence, the availability of physical oceanographic data is generally more difficult, especially for the bottom water properties. The analyses in this study highlight the importance of updating the BRAN data in the future.

Assessment of the scallop stock and the evaluation of alternative harvest strategies have been based on quantitative modelling of the scallop population, including the effects of fishing mortality (Campbell *et al.* 2010a; 2012). As these models have not previously incorporated environmental influences, it is likely that some model outputs, including estimates of biomass, recruitment and predicted catch rates, could be improved by incorporating one or more of the high-correlation relationships. This would likely lead to more accurate estimates of key fishery management reference points, such as maximum sustainable yield (MSY), possibly reducing the risk of overfishing.

19.6 CONCLUSIONS

This study examined relationships between coastal and oceanographic properties (i.e. freshwater flow, sea water temperature anomalies, sea level, EKE, Chl-a and SOI) and adjusted mean November catch rates from the Queensland trawl fishery for saucer scallops. The minimum legal size applied to saucer scallops in Queensland means that the catch is made up largely of 1+ year old individuals. The strongest correlation found was 0.85 for Chl-a concentration five months earlier in T30 Bustard Head. Elevated bottom water temperature anomalies at the Capricorn Eddy area three months prior (in August) were associated with reduced catch rates. Elevated surface water temperature anomalies at all

locations 16-18 months earlier (May-July previous year) were associated with reduced November catch rates. Physical oceanographic properties associated with the Eddy area had more strong-correlations with scallop catch rates than any other area. The results help explain long-term variation in scallop catch rates, including what is widely regarded as recruitment failure in 1996. Inclusion of one or more specific high-correlation relationships in the quantitative population models used to assess the stock will likely improve management advice, including estimates of MSY.

19.7 ACKNOWLEDGEMENTS

This study was funded by the Australian Fisheries Research and Development Corporation (FRDC): Project 2013/020. We appreciate the assistance of Dr Andreas Schiller, Russ Fiedler and Griffith Young (CSIRO & Bureau of Meteorology, Australia) for access to and assistance with the BRAN dataset.

20 Appendix 6. Larval Advection Patterns in the Queensland Scallop Fishery

Jesse Thomas and Ricardo T. Lemos

This section of the report addresses all three Objectives, but is mainly focused on scallops:

- 1) *Review recent advances in the study of physical oceanographic influences on fisheries catch data, and describe the major physical oceanographic features that are likely to influence Queensland reef fish and saucer scallops.*
- 2) *Collate Queensland's physical oceanographic data and fisheries (i.e. reef fish and saucer scallops) data.*
- 3) *Develop stochastic population models for reef fish and saucer scallops, which can link physical oceanographic features (e.g. sea surface temperature anomalies) to catch rates, biological parameters (e.g. growth, reproduction, natural mortality) and ecological aspects (e.g. spatial distribution).*

20.1 ABSTRACT

This section of the report uses simulation to investigate temporal and spatial variability in the distribution, source and settlement of larvae in the Queensland saucer scallop fishery. The advection of 'larvae', seeded in 411 0.1 degree grid cells in the fishery during the scallop's winter spawning season, was examined for 19 consecutive years (1993-2011, inclusive). Connectivity, wastage and self-seeding within and between grid sites were examined. Larvae are generally advected northward and towards the coast. Three areas approximating the rotational scallop replenishment areas were found to experience moderately high self-seeding, which may partially explain the high productivity in these areas. Corresponding time periods from different years did not necessarily experience the same patterns of connectivity, suggesting that a traditional climatology cannot be summarised for the connective dynamics. Hence, regions identified as a source of larvae that are subsequently protected from fishing, may not act as sources in all years. Finally, the modelled distribution of simulated larvae was fitted against the observed spatial distribution of 0+ recruits from the long-term fishery-independent monitoring. Despite an extremely flexible model specification, the achieved fit did not reach an acceptable level. The difficulty in fitting suggests the stock-recruitment relationship is more complex than assumed and that the simulated advections need refinement. In particular, the incorporation of tidal vectors, which are not considered in BRAN, and vertical behaviour of larvae in the water column, may improve the model fit.

20.2 INTRODUCTION

The scallop species *Amusium balloti* forms the backbone of the Queensland Scallop industry, and responsible management of their population level is crucial to the sustainable continuation of this industry. Various population models have been employed for this species over time, with the most recent having been developed by Campbell *et al.* (2012). The primary goal of this study is to complement Campbell's model with spatial information gleaned from *A. balloti* advection patterns, which may eventually allow us to enhance stock assessment and fisheries management. In addition to this overriding goal, two research questions of particular interest will be addressed, having been identified as gaps in the literature on larval advection. First, it is common in studies of larval advection to simulate advection in accordance with ocean current data for only one or two spawning seasons, and base conclusions on those observed patterns, without questioning whether the patterns are in fact common to other seasons. It tends to be assumed that oceanic current patterns, and therefore advection patterns, are cyclical on an annual timescale, and that the same month displays roughly the same advection dynamics across years. We are in the fortunate position of having 19 years of ocean reanalysis data on our hands, and therefore in a position to investigate the validity of this assumption.

The second novel angle of research we pursue involves exploring the role of larval advection in the stock-recruitment relationship, and whether our simulations match real data. We do this by combining our simulated advection patterns with a stock-recruitment model, and fitting this model to real recruitment data. To our knowledge, such a step is without precedent, but we see it as the only way assumptions about the recruitment process made in simulation setup can be tested and refined. We take on this challenge in Chapter 4, and also attempt to assess which advection patterns are more favourable to successful recruitment than others. The study is divided into four chapters, with relevant literature reviewed in Chapter 1. Each of the three research objectives is then explored in turn in Chapter 2 Numerical Modelling, Chapter 3 Climatology Performance Assessment, and Chapter 4 Statistical Modelling of Recruitment, before a final presentation of our major results and suggestions for further research in the concluding section.

20.3 CHAPTER 1 LITERATURE REVIEW

20.3.1 Scallop Recruitment Modelling

Campbell et al. (2012) have recently provided a population model for the Queensland scallop fishery, which extends from 22.5°S to 27°S along the Australian east coast. This model utilises biological and fisheries-related parameters. While these factors are expected to have the predominant effect on the regional scallop population, a need has been recognised to refine some aspects of the stock-recruitment relationship (SRR), so that it accounts for environmental variability and spatial connectivity. The existing population model pools the spawners at various locations across the fishery into a total population, and calculates the expected larval production and spat retention from this gross population. This approach, which ignores both the spatial distribution of parental biomass, and regional connectivity, inherently assumes that larvae from each location have an equal chance of successful retention, that each location has a constant chance of being reseeded with spat in a given year, and that each of the various locations are equally and collectively responsible for seeding the entire region.

Ignoring population spatial distribution and connectivity is only reasonable if the region is well mixed. However, if consistent currents exist such that one scallop bed S_1 , upstream from another scallop bed S_2 , is primarily responsible for seeding S_2 , while the reverse is not true, then the larvae are not well mixed. Under such a situation, the spawners at S_1 could be a better predictor of the recruits of S_2 for the following season than the total spawning population of S_1 plus S_2 as applied in the current model. It is easy to imagine that such relationships may exist, and if they do, they have important fisheries management implications. Green Zones for example, are established by the GBRMPA to protect populations from fishing and preserve a breeding population to replenish the region. For example, protected marine areas with the objective of preserving a breeding population are the most effective if they are chosen on their ability to seed a very wide region. Also, if certain zones are identified to be solely self-seeding, deliberate monitoring must take place to ensure a minimum breeding population is maintained. The current study has developed an advection model to inform such management decisions.

20.3.2 Oceanography in the Queensland Fishery

To form an initial impression of the advection patterns we expect to observe, it is necessary to conduct a landscape analysis, documenting the dynamics of meso-scale oceanic features within the Queensland Fishery. Later, we will endeavour to determine to what extent each feature affects advection patterns. Beyond simply determining the exchange of larvae between sites, currents are essential for transporting nutrients, and determining temperature and sea surface height. Oceanic fronts, found at the boundary of distinct current systems, also provide localised areas of high food abundance, improving reproduction and recruitment rates (Bakun 2006). The EAC creates one such known front in the Queensland Fishery, and the Capricorn Eddy another. On an inter-annual scale, El Niño and La Niña events influence the intensity of the EAC, and dramatically affect temperature and atmospheric activity. As such, below we note the mechanics, variability, and impact of the EAC, the Capricorn Eddy, and the El Niño-Southern Oscillation (ENSO).

The EAC results from a bifurcation of the South Equatorial Current at approximately 15°S (Ridgway and Dunn 2003). From there the current flows south along the Australian coastline until 33°S where another bifurcation takes place, sending a large portion of the current east into the Tasman Sea, while the remainder continues toward to the South Pole. Traversing this landscape, the current undergoes three distinct stages (Ridgway and Dunn 2003): formation, intensification, and separation. Formation of the EAC takes place when the southern stream of the bifurcated South Equatorial Current moves onto the Australian Continental Shelf, and heads south at a depth of between 200 and 500 meters. At this point the current has been known to flow at up to 15 cm/s. Intensification of the current can be observed from approximately 22°S, where the narrowing of the shelf forces acceleration up to speeds of 91cm/s. However, at around 31°S the current dramatically loses as much as 60% of its intensity, and begins separation into distinct southern and eastern directed streams.

The strength of the EAC varies seasonally, experiencing greatest intensity during the summer months (Roughan *et al.* 2011). Inter-annual fluctuations in EAC strength have also been observed, and are correlated with anomalously high sea levels (Holbrook *et al.* 2010) conveniently enabling researchers to take sea surface height as a proxy for gauging EAC intensity. Uncovering how the EAC affects advection, Condie *et al.* (2011) and Roughan *et al.* (2011) simulated larval transport patterns around the Australian continental coast and noted that the EAC acts as a barrier to particle transport between offshore and near shore environments.

Another prominent meso-scale feature is the Capricorn Eddy. This eddy is ‘spun up’ by the EAC as its inner (coastal) edge encounters the frictional forces of the shallowing sea floor and nearby land boundary (Weeks *et al.* 2010). When the EAC is strong, this eddy is likewise intense, and its presence is most visible during the seasonal acceleration of the EAC between September and November. A typical lee eddy (Bakun 2006; Weeks *et al.* 2010), the Capricorn Eddy is responsible for upwelling a large volume of relatively dense, nutrient-rich water into the Queensland Fishery, improving spawning conditions and larval food availability (Weeks *et al.* 2010). Weeks *et al.* (2013) proposed that the Capricorn Eddy has a significant effect on the distribution of fish, observing that increases in eddy intensity have a negative impact on seabird foraging success. It was proposed that the ‘spinning up’ of the eddy causes stratification in the water column, with each stratum having a distinct temperature and current profile, and that fish preferred the cooler, nutrient-rich lower stratum, below seabird diving range. If current stratification does indeed occur, it implies that larvae can be advected in at least two distinct patterns depending on the stratum they reside in (Kangas *et al.* 2012), and thus Capricorn Eddy intensity may dramatically impact the distribution of the scallop population. Eddy flow fields have also been noted to sweep particles into packets, improving recruitment probability where suitable habitat is present (Siegel *et al.* 2008).

Finally, the El Niño Southern Oscillation (ENSO), regarded as the most significant driver of inter-annual variability in the Pacific Ocean, was first observed in Peru as a warm southward current occurring around Christmas. Every few years, the El Niño current would be exceptionally strong, warm, and extend much further south than usual. It was not until the 1960s that it was empirically shown that this fluctuation was part of a larger-scale phenomenon involving changes in sea surface temperature and atmospheric pressure across the tropical Pacific Ocean (Philander 1989). This phenomenon was dubbed the El Niño Southern Oscillation, and has three phases on an inter-annual time scale: the neutral years, the El Niño years and the La Niña years. The El Niño phase is associated with warmer sea surface temperatures in the eastern and central Pacific, weak trade winds, and small differences in atmospheric pressure across the tropical Pacific. The La Niña is El Niño’s exact meteorological opposite, but lasts longer on average (Ray and Giese 2012). The third state of the ENSO is the baseline state.

Consecutive El Niños and consecutive La Niñas have been observed over the years, and it is evident that the ENSO does not cycle through these three states sequentially. Predicting ENSO events far in advance is a difficult task, but since the extremely severe El Niño of 1982-83, continuous monitoring has been in place, allowing advance warning by detecting ENSO events in formation, and following their propagation from east to west across the Pacific (Philander 1989). The effect of ENSO on weather patterns in Australia is well known and widely felt. Australia’s three wettest years since 1900 were 1974, 2010 and 2011, which were all La Niña years. These years were also cold years, with 2011 being the coldest year in a decade.

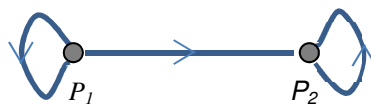
The impact is not constrained to the Australian Pacific coast either, with the Murray-Darling Basin experiencing its wettest calendar year on record in 2010, and Western Australia experiencing its wettest year on record in 2011 (Bureau of Meteorology 2012). Conversely, during El Niño events, rainfall is known to dramatically decrease in central and west Australia. Sea surface temperature has a significant effect on the WA fishery for *A. balloti*; however, warmer SSTs are typically experienced in WA during La Niña events, which are associated with a strong Leeuwin Current. ENSO events are also correlated with changes in sea surface height (Holbrook *et al.* 2010) suggesting a correlation between ENSO events and inter-annual EAC fluctuation.

20.3.3 Larval Transport

The current benchmark study of scallop fisheries in Australia is by Kangas *et al.* (2012), who investigated the scallop fishery in Shark Bay, WA. To uncover advection patterns in the region, the researchers chose two years for study, 2007 and 2009, which were high and low recruitment years respectively. Using the 3D General Estuarine Model (GETM) they randomly seeded the entire region on a bi-weekly basis throughout the entire WA spawning season, April-July. GETM only incorporates current data, and does not include tides. However, this was concluded to be a positive feature as it allowed researchers to see overall dominant patterns more clearly. Behaviourally, the particles were considered to be passive drifters, as larval swimming speed was considered negligible in the face of the speed of the currents in the region. A random walk component was added to this passive advection to account for chaotic localised influences and induce a wider spread in larvae over time. Settlement time was taken to be two weeks. In terms of vertical migration through the water column, Kangas *et al.* (2012) noted that unfortunately little is known about *A. balloti*'s vertical distribution during their pre-settlement life. As such, they simulated two distinct advection patterns, one based in the surface current stratum, and the other in the bottom stratum.

While neither scenario was thought to be completely correct, the researchers believed that these two distinct advection patterns constitute the extremes of possible advection. After each two-week simulation, the particles that ended up in the main scallop beds were traced back to their point of origin, allowing Kangas *et al.* to unveil all possible locations from which the main scallop beds were being seeded. They also explored what percentage of larvae stayed in the scallop bed from whence it was spawned, resulting in self-seeding. Finally, they explored which zones send larvae out of Shark Bay, resulting in loss from the fishery.

Other studies of larval advection in Australia and globally contain several useful ideas which could extend and simplify the Kangas *et al.* (2012) study. First among these is the application of a fisheries-wide graph theoretic analysis to capture all patterns of connectivity simultaneously. Consider that scallop populations within the region of interest can be viewed as vertices of a directed graph, with advection paths constituting edges between these vertices. This is illustrated in the simple two-population graph below, where population one (P_1), sends particles to population two (P_2), and also self-seeds. P_2 self-seeds, but does not send larvae to P_1 .



Stated formerly (Kolman and Hill 2004), a directed graph, or digraph, is a finite set of points P_1, P_2, \dots, P_n , called vertices or nodes, together with a finite set of directed edges, each of which joins an ordered pair of vertices. Once we have a digraph G , with n vertices, we can define an $n \times n$ adjacency matrix $A(G)$, whose i, j^{th} element is 1 if there is a directed edge from P_i to P_j and 0 otherwise. A connectivity matrix is a form of adjacency matrix where the non-zero entries can be counts of particles from P_i to P_j , or the percentage of the particles from P_i that ended up in P_j .

The tools of graph theory can be extremely useful in gaining an understanding of things like the relatedness of populations, as was the interest of Trembl *et al.* (2008) for example. For populations to share genes they need not exchange larvae every spawning period. Nor do the two populations need to exchange larvae directly, as they could also exchange genetic information through an intermediate population, which receives larvae from an initial population in one spawning season, and seeds the second population with second generation larvae in the next season. Adjacency matrices are well equipped to reveal such higher-order patterns through the following theorem (Kolman and Hill 2004).

Theorem 1: Let $A(G)$ be the adjacency matrix of a digraph G and let the r^{th} power of $A(G)$ be B_r :

$$[A(G)]^r = B_r = [b_{ij}^{(r)}]$$

Then the i, j^{th} element in B_r , $b_{ij}^{(r)}$, is the number of ways in which P_i has access to P_j .

Thus, for example, to find populations that are related by a maximum of a three-stage connection, we simply take $[A(G)]^3$, and any non-zero element represents a related population. Generalising this further, we can determine if all populations in the digraph share genetic information by investigating if it is strongly connected. Such was the problem that Kininmonth *et al.* (2010) sought to explore. They were interested in the connectedness of the coral reefs within the Great Barrier Reef, and in particular, if it, or any parts of it are self-sustaining independent ‘small worlds’. A small world can be defined as a pattern of connectivity such that it is possible for every region in the small world to exchange particles with every other, perhaps over several seasons.

Theorem 2: A Digraph is said to be strongly connected if for every two distinct vertices P_i and P_j there is a path from P_i to P_j and a path from P_j to P_i . In practice, a digraph with n vertices is determined to be strongly connected if its adjacency matrix $A(G)$ has the property that

$$[A(G)] + [A(G)]^2 + \dots + [A(G)]^{n-1} = E$$

has no zero entries.

Another dynamic easily revealed by connectivity matrices is well-mixed patches of population in the region – where larval exchange takes place in a reciprocal manner between all points in all spawning seasons. Such a dynamic is analogous to a clique in a digraph, which is a subset of the vertices S such that (Kolman and Hill 2004): a) S contains three or more vertices; b) If P_i and P_j are in S , then there is a directed edge from P_i to P_j and a directed edge from P_j to P_i ; and c) there is no larger subset T of the vertices that satisfies property (b) and contains S . In practice, the procedure for determining if there is a clique in a digraph (a small world in a region) is as follows (Kolman and Hill 2004).

Algorithm 1: To determine if a digraph G contains a clique,

Compute $A = [a_{ij}]$, the adjacency matrix of the digraph, and from this find the symmetric matrix $S = [s_{ij}]$, where

$$s_{ij} = s_{ji} = 1 \text{ if } a_{ij} = a_{ji} = 1 \text{ or zero otherwise}$$

Compute $S^3 = [s_{ij}^{(3)}]$.

P_i belongs to a clique if and only if $s_{ii}^{(3)}$ is positive.

Note that this procedure does not recognise well-mixed subregions involving just two sites, but these are to be given by the elements of the symmetric matrix $S = [s_{ij}]$ that are not in a clique. Thus, after forming a connectivity matrix, simple linear algebra is all that is required to reveal well-mixed subregions. Given the utility of connectivity matrices for revealing advection patterns, we will apply them in the present study also.

Several studies also differed from Kangas *et al.* (2012) in the way they elected to treat behavioural aspects of the larvae. The key behavioural factors that are particularly pertinent to modelling connectivity are whether larvae are simulated with or without random walk, whether or not they migrate vertically and how, and when they settle as recruits. Siegel *et al.* (2003), Treml *et al.* (2008), Kininmonth *et al.* (2010) and Condie *et al.* (2011), do not utilise random walk, instead modelling their larvae as purely passive. While all of these studies relate to very large scale regional connectivity, such as between island groups in the south-east Pacific, across the Great Barrier Reef, or within the Gulf of Mexico, there also exist examples of passive particle modelling applied to smaller scales.

Siegel *et al.* (2008) utilised passive particles to model advection along the southern California Coast, and Lacroix (2013) used them to model transport of flatfish in the English Channel and North Sea.

Other authors (Roughan *et al.* 2011; Kangas *et al.* 2012) do apply a random walk technique to their advected particles, in order to capture the effect of localised weather conditions, and induce wider spread. These studies considered very short time ranges of only one or two seasons, however, perhaps making this step more necessary as not all extreme values are expected to be observed in such a small time span. Applying random walk produces a range of advection paths more likely to contain the naturally occurring range than a purely deterministic approach, simply by merit of the fact that the range is wider. This method generally results in connective strength figures which are up to 40% less strong than their passive advection counterparts (Siegel *et al.* 2008). This is not necessarily bad, however, and Williams and Hastings (2013) present an interesting virtual experiment explaining why. Consider two sites, whose larvae, under a deterministic simulation are seen to neither remain in the site, nor seed the other site. Rather, they are lost to some other neighbourhood in the fishery. Under such conditions these two sites are in constant decline. Yet, with no change to the current data, when a random walk component is included in the simulated advection, it was shown that it is possible for the two sites to exchange some larvae, and that this exchange, though small, was sufficient to sustain both populations over time. The implication is that while connective strength may be lower across the region, the number of connections that exist may be greater, helping to explain sustained populations and wide exchange of genetic information.

There are also varied perspectives regarding whether periodic vertical migration through the water column ought to be considered in simulations. Vertical migration only affects larval advection if the current vectors differ at various depths and, as already noted, this may occur in the Queensland scallop fishery in the late spring and early summer months due to the Capricorn Eddy. However, the extent and pronouncement of this effect is unknown. It is also reasonable to expect the presence of near-shore stratification during the incoming and outgoing tides, but with little known about the vertical migration behaviours of *Amusium balloti*, most authors tend to simply model larval advection as if larvae remain in one homogeneous layer the entire time (Treml *et al.* 2008; Kininmonth *et al.* 2010; Condie *et al.* 2011). Kangas *et al.* (2012), however, showed that stratification of the water column, with differing currents dominating different layers, can have a significant impact on the advection pattern. Upon simulating advection in two distinct strata separately and noting the significant differences, they proposed that actual advection was probably somewhere in between. Yet this proposition does not account for the possibility of larvae migrating deliberately between the flow fields and biasing their transport in a particular direction, achieving advection paths outside the bounds of either simulation - something prawn larvae are well known to do (Tamaki *et al.* 2010). Results obtained from simulating various current strata must be discussed in this context.

The timing of larval settlement has also been treated differently by different authors. Settlement takes place near the end of the competency stage, when larvae actively seek an appropriate habitat, and in the case of scallops, descend to the sea floor as spat. This happens two to four weeks after spawning (Dredge 1981; Julie Robins, unpublished), and Siegel *et al.* (2003) have noted that varying the timing of this settlement in simulations has significant impacts on the level of connectivity that results. It is most common to use a set time instant for settlement somewhere in the middle of the expected settlement range. However, Roughan *et al.* (2011) recorded not only the final location at the end of the simulation, but all sites the larvae passed through over the expected settlement timeframe, thus capturing a range of possible connections.

Finally, a critical assumption made by the Kangas *et al.* (2012) study in Shark Bay, WA, is that advection patterns remain stable over time. Only under that assumption is it justifiable to infer a general advection pattern from information extracted based on only two years of simulations. If connectivity is unstable, however, and a connection is extremely strong in some periods and extremely weak in others, then it is possible to imagine periods where the population of the source site does not serve to adequately re-seed the receiving site. In light of this, the utility of protecting a source site for

the purpose of maintaining the receiver site may be severely limited unless it is also shown that the connection is stable over time.

20.4 CHAPTER 2 NUMERICAL MODELLING

20.4.1 Introduction

Having reviewed the state of the art in larval transport simulation, the present chapter implements a set of simulations for *A. balloti* in the Queensland Fishery in order to uncover spatial information useful in enhancing stock assessment and management practices. In doing so we make the following simulation setup decisions which we believe reflect best practice or better, and are most appropriate given what is known about the meso-scale features of the Queensland Fishery. First, rather than simulating larvae as purely passive or as having a random walk, we will do both, and compare the results in Chapter 4 Statistical Modelling of Recruitment. Second, the potential for current stratification to exist is explored through simulation in Simulation 1, and subsequent simulations adopt the approach of Kangas *et al.* (2012) by simulating an appropriate set of layers separately. Finally, settlement timing is taken to be three weeks, but we also record the location of the larvae at other time intervals, giving us the option to explore these at a later date.

20.4.2 Materials and resources

This study will utilise data from BRAN3.5 to capture regional currents and the advection of simulated larvae. The Bluelink Re-Analysis (BRAN) assimilates data from the Bluelink Ocean Data Assimilation System (BODAS) with the Ocean Forecasting Australia Model (OFAM), and can thus be thought of as interpolating data between disparate measured data points with a global oceanographic model to provide current estimates in unobserved areas. The data set runs from 1993 to 2011. BRAN3.5 has significantly improved eddy resolution capability over its predecessors, and greater accuracy across key variables such as sea surface temperature and salinity (Oke *et al.* 2013). According to Oke *et al.* (2013), BRAN3.5 is able to predict sea level to within 7.7 ± 0.5 cm, upper ocean temperature to within $0.68 \pm 0.08^\circ\text{C}$, upper ocean salinity to within 0.16 ± 0.02 psu, and near-surface velocity to within 20.2 cm/s. While it is noted that BRAN3 does produce abnormally salty and warm predictions between 500 m and 1000 m depth, this shortcoming will not affect our study as the Capricorn Bunker region does not contain such depths.

The BRAN3.5 data of regional currents was fed into a simulation program called GNOME, which was developed by the National Oceanic and Atmospheric Administration (USA) for simulating oil spills ('GNOME User's Manual', 2002). This program was chosen for its convenient ability to run large repeated simulations without manual intervention, and also for the ease with which a random walk component to particle trajectory could be added and manipulated. Its main shortcoming though, is that being designed for oil spill modelling, it is only capable of simulating on a two dimensional plane. This problem is easily circumvented by taking depth layers of the BRAN3.5 data separately and simulating advection at those depths one at a time. Another simulation program, called Connie2, which was developed by the Commonwealth Scientific and Industrial Research Organisation (CSIRO), was also considered. The current implementation of Connie2 requires each simulation to be set up manually, and as we intended to simulate a new spawning for every week in each spawning season across 19 years, this posed a serious limitation. Connie also does not allow the user to implement their own current data set, and instead only gives the option of BRAN2, or two other local data sets, neither of which cover the date range of interest. Thus, it was decided that GNOME running BRAN3.5 data provided the best simulation option. Connie's advantage, though, is its ability to simulate various depths without the need to upload different current data sets for each simulation, as GNOME does require. We utilise this feature in our first simulation to get an impression for the level of stratification in the Queensland Scallop fishery.

20.4.2.1 Simulation 1

Stratification is the phenomenon where ocean properties such as temperature, salinity, or currents rapidly change with depth. If current stratification takes place then it is an essential consideration in the simulation of advection, as larvae sitting in different layers of the water column could experience quite different advection patterns. One potential driver of stratification in the Queensland Fishery is the Capricorn Eddy, which begins to spin up in intensity as the summer months approach. However, the extent of any stratification that this may cause is not well known. Further, other unknown sources of stratification may exist. It is therefore well worth developing an initial impression of the stratification that may exist in the Queensland Fishery. Our goal in the present simulation is to glean sufficient information to be able to make an informed choice regarding whether or not we need to simulate for multiple strata in the water column, and if we do, what depth layers we should select to capture each stratum separately.

20.4.2.2 Setup

Using a freely available tool from the Commonwealth Scientific and Industrial Research Organisation (CSIRO), called Connie2, larval advection patterns were generated for five different depths across seven locations for the first week of November 2008. Connie2 utilises a hydrodynamic model for the Queensland Scallop Fishery called SHOC, which unfortunately has a limited time span. We were only able to simulate the one spawning event as the majority of the scallop spawning season is outside the date range of SHOC, but it has a good resolution of 4 km, and covers the region from Moreton Bay to mainland Papua New Guinea. Offshore boundary conditions are provided by BRAN2. In running the advection simulation, Connie2 automatically seeds 25 particles per grid cell per day for each specified source grid cell over three weeks.

20.4.2.3 Results

Figures showing simulation output are presented below (Figure 20-1). The resulting plots clearly reveal that across all seven locations, the advection pattern shifts from tending toward the coast, to tending either away from the coast, or northward, suggesting that stratification within the water column indeed occurs. Differences are particularly pronounced between the surface layers, and the layers below 13 m. This confirms the need, as in the Kangas *et al.* (2012) study, to conduct simulations for various depths across all 19 years.

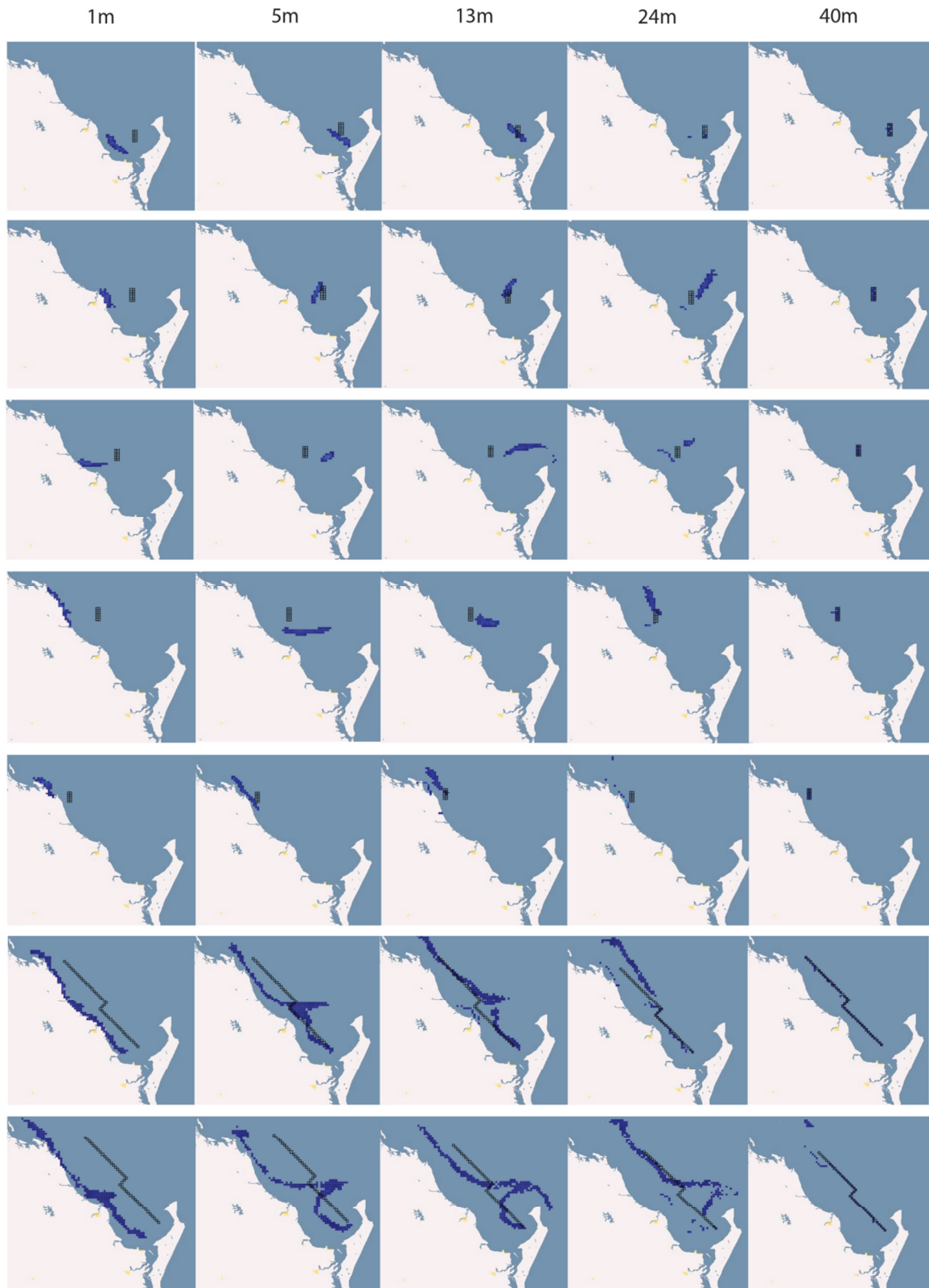


Figure 20-1. Each row of images in the figure represents a different spawning location, which is indicated by the black grid. Each column corresponds to a different depth; 1 m, 5 m, 13 m, 24 m and 40 m respectively. The blue grid indicates the location of larvae after advection.

20.4.2.4 Simulation 2

20.4.2.5 Setup

In order to uncover the patterns of scallop larval dispersion off the Queensland East Coast (QEC), we generated a 19-cell grid of 0.5° resolution, as in Campbell *et al.* (2012), covering the QEC from 22.5° S to 27° S. These large grid cells were then each subdivided into 25 smaller cells (0.1° resolution), and those not in the ocean excluded, leaving a total of 411 cells. Utilising current velocity data for this region from the BRAN 3.5 global ocean model, we were able to simulate the advection of virtual larvae for 19 spawning seasons, from 1993 to 2011. Grid cells were seeded with larvae at random, at a rate of nine tracers per week. Tracer trajectories were simulated for three weeks corresponding to scallop planktonic larval duration (Julie Robins, unpublished). This was done for twenty-four weeks, from June till October each year, corresponding to the Queensland scallop spawning season (Julie Robins, unpublished). Seeding was performed at midnight of the first day of each week. The final locations of all particles were recorded for subsequent analysis. In total, we modelled the fate of $9_{\text{Larvae}} \times 411_{\text{Cells}} = 3699$ tracer larvae seeded per week across the QEC, over a total of $19_{\text{years}} \times 24_{\text{weeks}} = 456$ weeks. This was done for the surface depth layer of 1-5 metres, and also for the 15 m depth layer, in accordance with where the Connie simulation suggested distinct current strata may exist. For both depths, both a purely deterministic simulation and a simulation with a random walk were performed. The random walk component was implemented such that at each time step, the tracers receive an impulse in a random direction at up to 5% of the magnitude of the local instantaneous current velocity.

From each weekly simulation of larval dispersion, a connectivity matrix was formed, recording the number of larvae from each origin cell that ended up in each destination cell, or was lost off the grid. An average connectivity matrix was then calculated by taking the element-wise average across all connectivity matrices recorded, allowing us to explore which zones lose the most larvae to the ocean, which cells have had the widest seeding range, which cells self-seed, and, for the regions with the highest fishing effort (Figure 20-2), where do their source larvae come from, and where do they send their larvae to. A matrix of element-wise variance over time was also calculated to capture variability in the dynamics of each site.

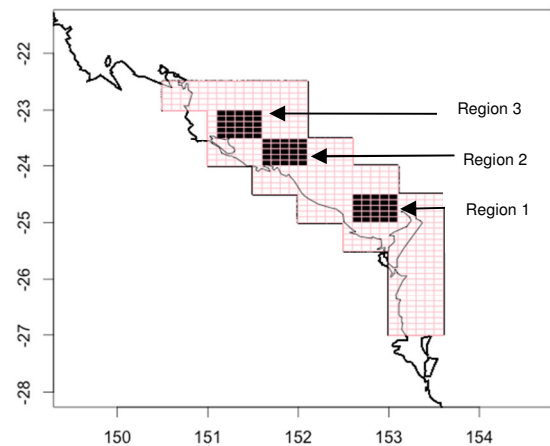


Figure 20-2. The three regions of highest fishing effort, from Campbell *et al.* (2012).

20.4.3 Results and discussion

At the level of a global average, the surface and depth layers did not produce widely different results, and so only the surface layer plots are presented in the discussion that follows. The issue of which kind of connectivity best captures the most likely advection path of the larvae is explored in depth in Chapter 4 Statistical Modelling of Recruitment. Figure 20-3a below plots the mean connectedness of each cell, where connectedness is defined simply as the number of other cells a particular cell has sent larvae to over the 19 years. Figure 20-3b plots the variance in the connectedness of each site. It is clear from the plots that the mean and the variance in connectedness are strongly correlated. This implies that the mean connectivity alone is an inadequate predictor of the connections a particular site will make in a particular spawning.

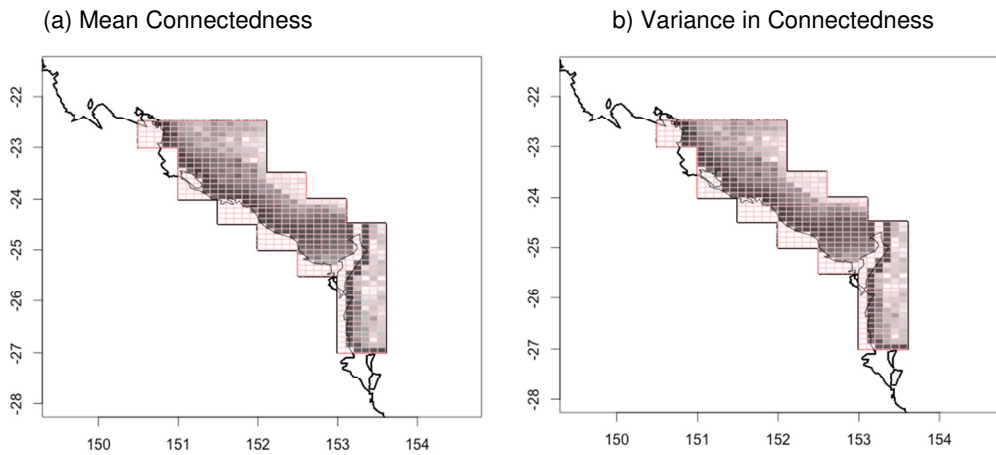


Figure 20-3. a) Mean number of connections made by each cell, and b) the variance in connectedness, for the Queensland scallop fishery. Zero is represented by white, and black represents 339 connections.

Next, in Figure 20-4 we considered which sites waste the most larvae, losing them to the open ocean. Given the dominant current in the region is northward and coastward, it is unsurprising that cells near the top end of the region experience the highest wastage. It is clear from the variance plot that the wastage dynamic is as variable as it is pronounced, however, and in a given season it is quite possible for these cells to experience either a completely wasted spawning, or a spawning with adequate retention.

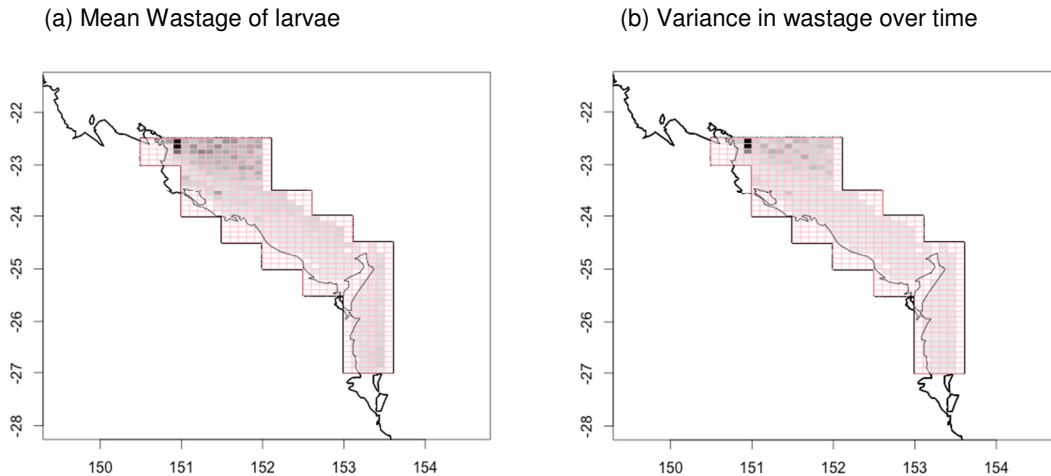


Figure 20-4. a) Mean number of larvae wasted by each cell, and b) the variance in wastage, for the Queensland scallop fishery. No wastage is represented by white, and black represents 339 connections.

The level of self-seeding by sites was also considered, as measured by the total number of larvae that settle in their initial spawning location. Significantly, High Fishing Effort Regions 1, 2 and 3 experience high levels of self-seeding, as indicated in Figure 20-5a, and a low variance over time in this pattern (Figure 20-5b). It should be noted here that the coastal region’s apparent high self-seeding is accentuated by the design of Simulation 2. When GNOME advects particles to the coast they ‘stick’ there artificially as if they settled. Some may indeed settle there in reality, but a significant portion could also become beached and die, or be flushed back out to sea.

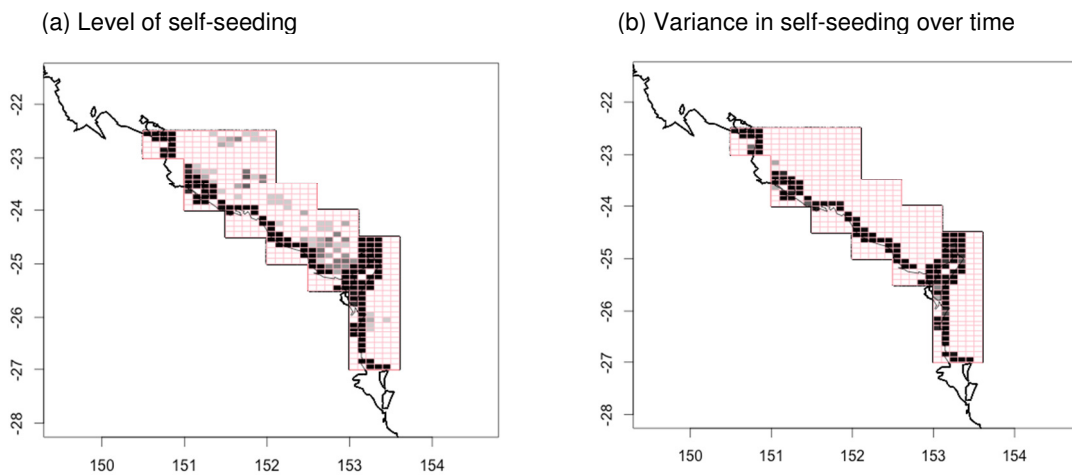


Figure 20-5. a) The level of self-seeding on a relative scale, and b) variance in that self-seeding behaviour.

Turning our attention specifically to the three regions of high fishing effort indicated in Figure 20-2, we are interested in 1) uncovering the sites whose larvae are responsible for seeding these three regions, and 2) finding out where larvae from the three regions end up. Figure 20-6 below shows where the larvae that settle in Region 1 come from using a binary scale (a) and a relative grey-scale (b). Region 1 is the region of highest fishing effort in the fishery. It is quite apparent that self-seeding is very important for this region’s maintenance. Moreover, we already know from Figure 20-5 that self-seeding here is relatively stable over time.

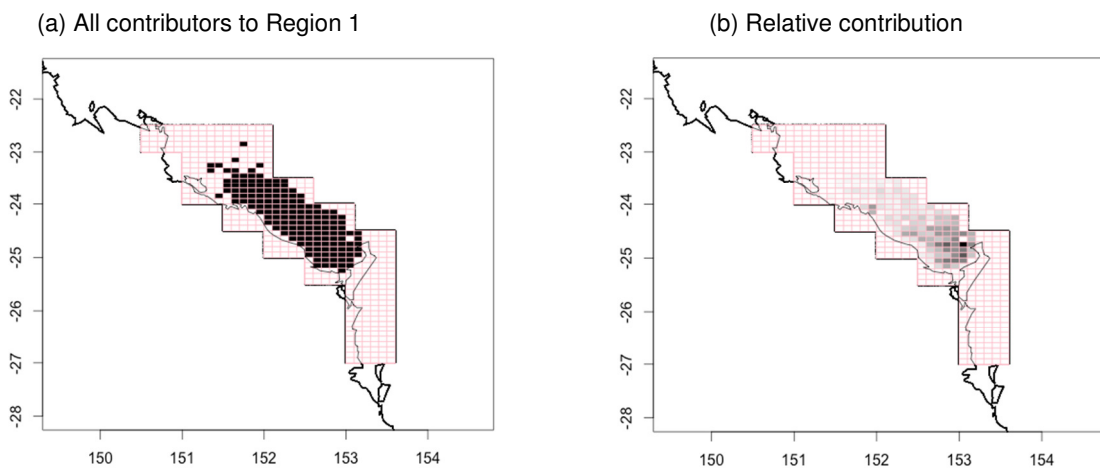
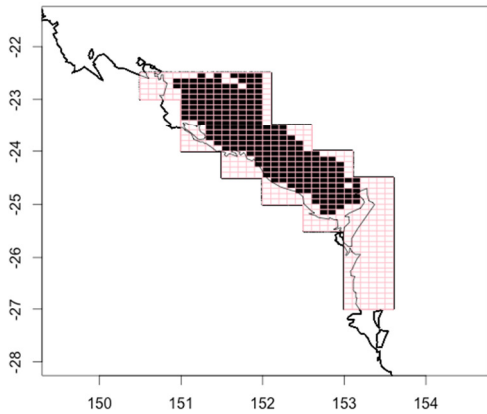


Figure 20-6. a) All potential source cells for Region 1, and b) the relative contribution by these source cells to Region 1.

Next we considered Regions 2 and 3. Figure 20-7a and Figure 20-8a display all sites that contribute to Regions 2 and 3 respectively, while Figure 20-7b and Figure 20-8b show the relative contribution of those sites. It is clear that almost any site north of Fraser Island can contribute to Regions 2 and 3 in a given spawning season. However, the dominant sources are clustered in a horizontal band that begins in each region, and stretches eastward.

(a) All contributors to Region 2



(b) Relative contribution

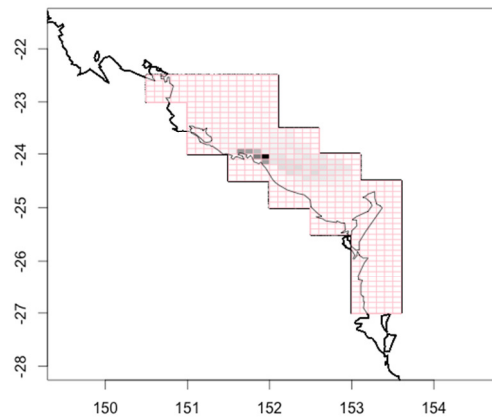
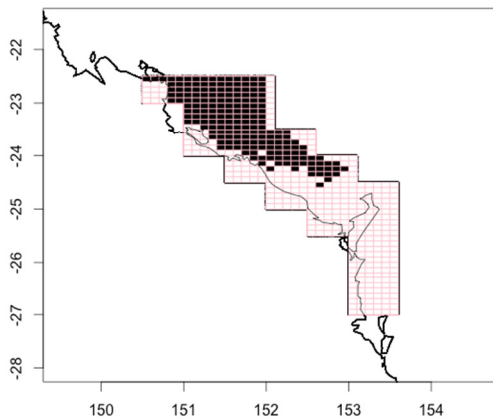


Figure 20-7. a) All potential source cells for Region 2, and b) the relative contribution by these source cells to Region 2.

(a) All contributors to Region 3



(b) Relative contribution

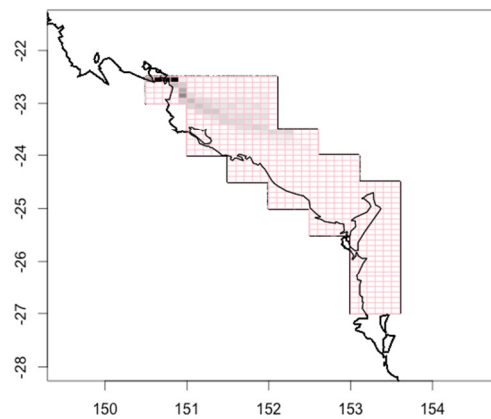


Figure 20-8. a) All potential source cells for Region 3, and b) the relative contribution by these source cells to Region 3.

In the final step of the analysis we also investigated the destination of larvae spawned from each of the three regions of high fishing effort. Results from Region 1 are plotted below (Figure 20-9). It is not surprising that the destination cells differ from the source cells, but it does come as a surprise that Region 1 appears to send the majority of its larvae to the coast, potentially resulting in beaching of the larvae and subsequent loss. This indicates that the self-seeding dynamic driving the productivity of this region is in fact not very common. Instead it is more common for larvae to be swept coastward in a given spawning event. Results for Regions 2 and 3 reflected a similar pattern, but for these regions, the larvae were not swept coastward, but out of the fishery to the north.

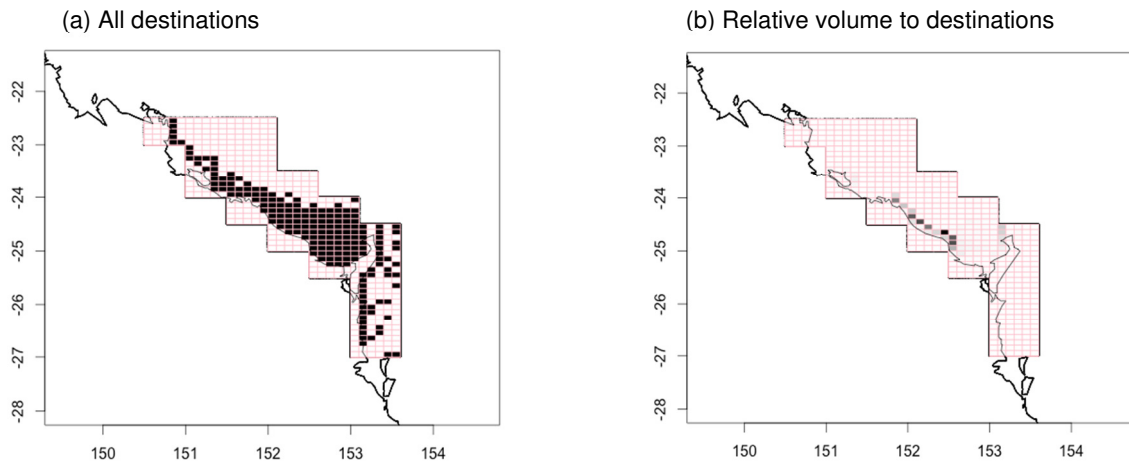


Figure 20-9. a) All potential destination cells for larvae from Region 3, and b) the proportion of larvae from Region 1 that end up in each cell. It is quite clear that the majority of larvae are washed against the coast.

20.4.4 Conclusion

A number of interesting dynamics of the Queensland Scallop Fishery's connectivity have been explored, including site connectedness, site wastage, and site self-seeding. The sources of larvae responsible for seeding the main fishing areas, and destinations of larvae from those same regions were also explored. Connectedness was measured as the number of other sites a given site has sent larvae to at any point over the 19 seasons from 1993 till 2011. It is clear from the plots that connectedness is strongest close to the coast within Hervey Bay. Significantly, however, connectedness was very variable over time, and no region could be identified which seeds many other regions with any reliable consistency.

Wastage of larvae from each cell was defined to be the number of larvae that exited the fishery within the three-week advection period. Given the dominant regional current is northward, the result found is somewhat intuitive; with the cells to the north of the grid being most likely to have their larvae lost across the northern border. The variance plots show that these cells are not guaranteed to lose larvae, however, as high variability indicates that it is possible for these cells to have a good spawning sometimes, and we thus cannot ignore their potential influence on the productivity of the fishery.

Next, self-seeding throughout the region was analysed and some very interesting results were observed. The three regions of highest fishing effort in the Queensland fishery were found to experience moderately high self-seeding, and the variance plots indicated that this pattern was consistent. We do not see this as a coincidence and instead propose that it is likely self-seeding is a driver of the high productivity of these regions. Notably, there is also a region south of Fraser Island that experiences high self-seeding with low variance. This region is not regarded as a high fishing effort region, but is known to fishers as a place to find scallops when they are experiencing unusually low catch rates elsewhere.

Focus was then directed specifically to the dynamics of the three regions of highest fishing effort. It was found that each is potentially seeded by a very wide area, but a significantly smaller number of cells are responsible for the majority of seeding. This subset of contribution regions is typically within, or adjacent to the high fishing effort region itself, reinforcing our conclusion that self-seeding plays an important role in the productivity of these regions. When we looked at where larvae spawned in these three regions, however, it was found that Region 1 sends a very large proportion of its larvae

directly to the coast, potentially resulting in the beaching and loss of those larvae. Regions 2 and 3 are also highly likely to lose the majority of larvae due to the dominant northward current carrying them off the grid. This indicates that while key to productivity, self-seeding in these regions does not occur in the majority of spawning events, but is rather the result of a less-frequent current pattern. When this pattern may occur is explored in Chapter 4.

Overall, this simulation has shown that the dynamics of regional connectivity are highly variable over time. The implication of this is that a single average connectivity matrix cannot provide a sufficient description of all connectivity patterns. This is a significant finding, as the literature to date has tended to rely on average connectivity to describe regional dispersion patterns. Crucially, we also found that self-seeding seems to be important to sustaining the scallop population in the regions of highest fishing effort. This has implications for the management of these regions as it suggests that rotational closure of portions of these regions is more likely to successfully sustain the scallop population than protecting a single sub-region whose larvae are expected to seed the rest of the region.

20.5 CHAPTER 3 CLIMATOLOGY PERFORMANCE ASSESSMENT

20.5.1 Introduction

In the previous chapter we explored some of the key aspects of connectivity in the Queensland Fishery, and observed that they vary considerably over time. It was clear that a single grand average of connectivity by itself did not tell the whole story due to hidden variance that was not constant across the fishery. However, the question of over what time period this variation takes place was not addressed. Indeed, it may well still be possible to form more descriptive summaries over some shorter timescale in which variance is low. If changes in dynamics take place from month to month, and this cycle is repeated from year to year, then it may well be possible to generalise the results of one or two seasons, as other authors have done. It is the goal of this chapter to explore whether such a cyclical pattern exists, and if so, over what time interval.

It is common practice in oceanography to form monthly climatologies (i.e. long-term monthly means) as variables are expected to be consistent across this time frame. These climatologies then form reference points going forward, allowing forecasters to form expectations about the future, and measure deviation from that expectation. For example, it is such a climatology of temperature across the Pacific Ocean that allows the detection of an El Niño formation – anomalously high sea temperatures in the South American Pacific. Climatologies can also allow predictions to be made without the need to re-measure, or measure as extensively, the variable of interest. This would mean a huge cost saving when talking about a variable such as regional advection patterns, which, as we have seen, require the running of a deterministic oceanographic current model, interpolation of those results with buoy and drifter data, and subsequent simulation of larval dispersion.

The key assumption behind the practice of using climatologies is that the variable concerned varies little within the climatological time interval – a month say – and that the variable behaves similarly in the same month from year to year. If this is the case, then a climatology can be formed with minimal information lost. However, if the variable varies more rapidly, a climatology over a shorter time period may be necessary. Further, if the time period is not self-similar from year to year, then a climatology misses a significant amount of information and is inappropriate as a reference point. We are interested to know if it is justifiable to form climatologies of connectivity for the Queensland Fishery, and if so, over what climatological time interval. Such a question has not previously been asked of marine connectivity to our knowledge.

20.5.2 Methods

Our data for connectivity is a set of $19_{\text{years}} \times 24_{\text{weeks}} = 465$ connectivity matrices. Each matrix has 411 rows corresponding to the 411 cells in the fishery grid, and 412 columns corresponding to possible destinations, where the additional destination cell corresponds to ‘off the grid’. Little guidance was found in the literature for analysing the variation within a given month, nor for comparing the similarity of a month in one year to the same month in another year when the data points are a set of 411×412 connectivity matrices. While of course various norms such as the Frobenius norm exist, and we considered techniques such as principle components analysis, none of these options were satisfactory in terms of having an interpretable physical meaning relating to connectivity pattern. Thus, we have developed the algorithm below, which is designed to test the below hypothesis:

H_0 : *There is no less variability in the connectivity experienced by corresponding weeks/months across years than what we expect between a random assortment of weeks/months.*

H_1 : *There is less variability in the connectivity experienced by corresponding weeks/months.*

More specifically, to analyse the connectivity patterns occurring in week one of the spawning season, we take the element-wise variance of all connectivity matrices corresponding to the first week of each spawning season in our data set. If the patterns are similar, then the values observed in the variance matrix should in general be lower than in a variance matrix resulting from a randomly selected set of 20 weeks. If this is found not to be the case, then we have no evidence that the first week has similar

connectivity across years. These concepts form the basis of our test statistic and the criterion to reject/not reject the null hypothesis.

The same idea is generalised to time intervals longer than a week by first taking the element-wise average of weeks in that interval, and then taking the variance across years for that interval. So for the first month of the spawning seasons say, we would take the average across the first four weeks of the season in each year, and then compute the variance matrix for those averages. Again, if the same month is similar across years, then we expect the values in the variance matrix to be lower in general than the variance matrix that results from a random assortment of months from across the years. If this is found not to be the case, then we have no evidence that months are similar across years, and we should be hesitant to extrapolate conclusions relating to connectivity beyond the simulated timeframe.

Clearly, to execute this analysis, we must also define precisely what we mean by ‘lower in general’ than the variance expected from a random assortment of connectivity matrices, and as such we define a relevant threshold as in the following paragraph. Finding the variance matrix for many random assortments of connectivity matrices yields a set of variance matrices. We can then treat the elements of these variance matrices collectively as a sample of variances that occur between cells across years.

We define the threshold to be the 0.25 quantile of this data, and then go back through our set of variance matrices, counting the number of elements in each one that fall below this threshold. The more elements below the threshold in a given variance matrix, the more similar the set of matrices are from which it was formed. These counts across the set of variance matrices yield a sample of counts against which we can now benchmark our climatologies. We then look at the connectivity matrices corresponding to the first week of each year say, take the element-wise variance between them, and count the number of cells below the threshold. If this number is large and sits well above average in our distribution of counts, we have reason to believe the matrices are more similar than a random assortment. If the count is around the average or below, then we have no reason to believe the connectivity matrices are more similar than a random assortment. The assessment is described precisely in full in the following algorithm.

Algorithm for Climatology Performance Assessment:

For a climatological time interval of x weeks with $x \in \{1, 2, 4, 10\}$ corresponding to weekly, fortnightly, monthly, and seasonal climatologies, test the performance of an x -week climatology in the following way:

Select a year and a week at random from the selection of 20 weeks in each of 19 years.

Compute an average using this week, and the $x - 1$ weeks following it.

Repeat steps 1 and 2 until you have 20 such x -week averages.

Calculate the element-wise variance among these 20 connectivity matrices.

Repeat steps one to four 1000 times, recording all mean and variance matrices.

Treating the entries of the 1000 variance matrices as a sample data set, identify a variance threshold by finding the 0.25 quantile of the sample.

Count the number of entries in each of the 1000 variance matrices that fall below this threshold. Record these counts and plot them as a histogram. You now have an empirical distribution function whose mean can serve as a benchmark for the level of variance you expect a climatology to beat.

Form x -week climatologies, and calculate the variance matrix for each.

Count the number of entries in the variance matrices of the climatologies that fall below the threshold. If the count is not significantly greater than the expectation under a random assortment, then there is no support for using that climatology.

20.5.3 Results

This algorithm was applied to test the merits of 1-week, 2-week, monthly (4-week), and seasonal (10-week) climatologies. Here we discuss the results of the monthly and bi-weekly timescales, whose results are indicative of the performance of the other time scales also. Figure 20-10 shows the results of analysing the monthly climatology.

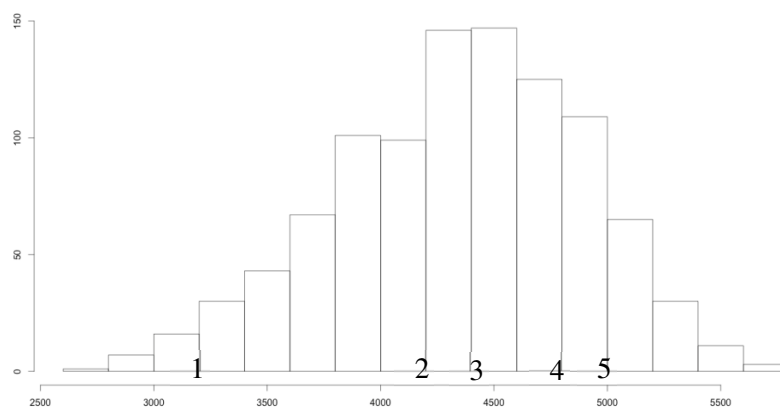


Figure 20-10. Histogram of the number of cells below the threshold in each of the 1000 average connectivity matrices. The numbers 1 through 5 represent where the counts for the variance matrix of each month June through October sit in the histogram.

Months are indicated with the labels 1-5 and correspond to June through October. Their location on the histogram indicates the value of their respective counts. Not a single one scores highly. This

indicates the similarity between each month connective pattern across years is low and we therefore find no support for relying on monthly climatologies. It is interesting though that the latter months appear to achieve higher counts than earlier months, suggesting that later months are less variable across years than earlier months. The process was then repeated for fortnightly climatologies. As before, the histogram, and where each fortnightly climatology’s count sits within it, is recorded below (Figure 20-11).

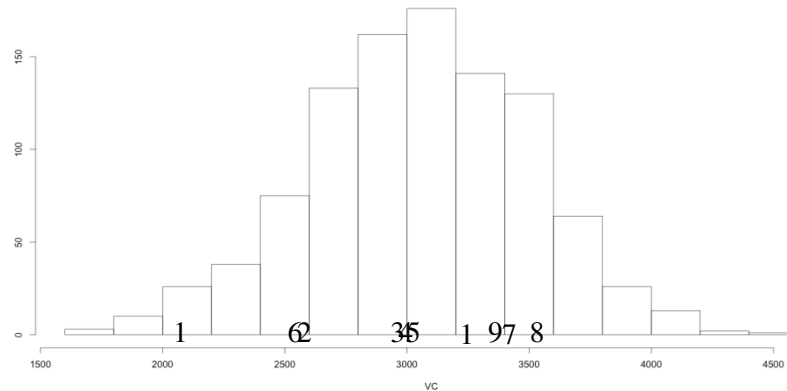


Figure 20-11. Histogram of the number of cells below the threshold in each of the 1000 average connectivity matrices. The numbers 1 through 5 represent where the counts for the variance matrix of each month June through October sit in the histogram.

The results again suggest that the connectivity patterns observed in the same period across years are no more similar than the connectivity patterns observed in a random collection of time periods – giving the use of a climatology no credibility. We also observe yet again that the stability of connectivity increases toward the latter part of the year in general. These results are indicative of what we observed when analysing other climatological time intervals too, and no climatology over any interval was identified that scored particularly well for similarity across years.

20.5.4 Conclusions

The level of similarity in connectivity between corresponding weeks, fortnights, months and seasons was gauged relative to the similarity expected from a random assortment equivalent time intervals across the 20 years. Unfortunately, the analysis suggests that corresponding time periods do not necessarily experience the same connective patterns at all from year to year. As such, a traditional climatology cannot be formed to summarise connective dynamics adequately. This finding has implications for all studies involving simulated marine currents as it does not support the assumption that observations made in one or two simulations may be generalised across time. Specifically, to use the Kangas *et al.* (2012) study as an example, the sources, sinks, and areas of high wastage identified in the two spawning seasons simulated may not be constant across years and management initiatives based on these conclusions may have limited effectiveness. Thus, regions identified as source regions and subsequently protected may not in fact act as sources at all in certain years, and thus seeding of the wider fishery by these regions in those years may fail.

The findings of this chapter do not affect the reliability of our own results in Chapter 2 Numerical Modelling, however, as all connective dynamics were considered in the context of their variance across time. For example, it is still valid to conclude that certain regions are more likely to experience self-seeding at *some time* during the spawning season than others, even though currents favourable to self-seeding cannot be expected to occur regularly in a particular week or month of the season. The implication of this is that while periodic closures of the three regions of highest fishing effort are still the best strategy for maintaining stock in those regions, the optimal timing of these closures each year is difficult to determine.

20.6 CHAPTER 4 STATISTICAL MODELLING OF RECRUITMENT

20.6.1 Introduction

A critical step in any study of natural phenomena must be to relate the simulated results back to observed data – marrying simulation and reality. Taking such a step is imperative in confirming the reasonableness of any assumptions made, and in our case, refining beliefs about the stock-recruitment relationship in the Queensland scallop fishery. As such, in this chapter, we wish to fit a statistical model involving our simulated results to actual recruitment data. It is hoped that this will reveal how realistic the assumptions made in our advection simulation are, and which time periods or connectivity patterns are most important to recruitment. Surprisingly, to our knowledge, no previous study of larval advection has undertaken these key steps in the analysis. Instead, it is assumed in the literature that advection is largely dictated by currents, and the considerable scope for scallop behaviours to confound this deterministic view by migrating deliberately, is ignored. Further, the favourability of certain time periods for spawning has been assessed considering biological parameters such as temperature, light level, sea surface height, and availability of nutrient (Williams and Dredge 1981), but has not been considered in the context of a supportive pattern of currents.

The simple model that is assumed in the literature (Siegel *et al.* 2003) takes the population of scallops at time $i + 1$, Y_{i+1} , as a function of the parent population that spawning season, Y_i , multiplied by some scale factor m , and rearranged spatially according to the currents, as captured in a connectivity matrix X_i . It is also generally assumed that the connectivity matrix X_i is not highly variable over time and so a climatology of connectivity X based on only a few simulations can be used. Our earlier results in Chapter 3 suggest that this assumption is not reasonable, but we will also test it here again by comparing the fit between predictions and actual recruitment achieved by a model using climatological connectivity, and a model that uses connectivity simulated for the relevant year only - instantaneous connectivity. We also have the opportunity to ascertain whether surface currents or 15-metre currents achieve a better fit to the data, and which of deterministic and stochastic advection is a closer reflection of reality. Potentially, the relative goodness of fit achieved by the model as it uses each of the different types of connectivity mentioned will be able to shed light on probable larval behaviour including where in the water column they reside, and the extent to which they are truly passive or not. However, it is also quite possible that the stock-recruitment relationship is more complex than is assumed, and that none of our models will fit particularly well in the absence of additional factors.

20.6.2 Methods

A model will be fitted to the data using 16 different types of connectivity. From the simulations, we have four types of connectivity: 1) Surface currents with deterministic advection; 2) Surface currents with stochastic advection; 3) 15-m currents with deterministic advection; and 4) 15-m currents with stochastic advection. For each of these categories of connectivity we will take both the instantaneous connectivity, and the climatological connectivity. Further, we also wish to test whether the granularity of the timescale matters to the fit, and so will not only use the weekly connectivity matrices from our simulations, but will also compute monthly averages. This yields 16 types of connectivity to be fitted in a model. These are summarised in Table 20-1.

Table 20-1. Types of connectivity.

Type	Instantaneous/Climatological	Timescale	Depth	Advection
1	Climatological	Monthly	Surface	Deterministic
2	Climatological	Monthly	Surface	Stochastic
3	Climatological	Monthly	15m	Deterministic
4	Climatological	Monthly	15m	Stochastic
5	Climatological	Weekly	Surface	Deterministic
6	Climatological	Weekly	Surface	Stochastic
7	Climatological	Weekly	15m	Deterministic
8	Climatological	Weekly	15m	Stochastic
9	Instantaneous	Weekly	Surface	Deterministic
10	Instantaneous	Weekly	Surface	Stochastic
11	Instantaneous	Weekly	15m	Deterministic
12	Instantaneous	Weekly	15m	Stochastic
13	Instantaneous	Monthly	Surface	Deterministic
14	Instantaneous	Monthly	Surface	Stochastic
15	Instantaneous	Monthly	15m	Deterministic
16	Instantaneous	Monthly	15m	Stochastic

A spatially explicit, but temporally constant estimate of scallop parental abundance in the Queensland fishery is provided by Campbell *et al.* (2012), and we also have recruitment data for the years 1997 – 2006 from the long-term monitoring surveys provided by the Department of Agriculture and Fisheries’ Long-Term Monitoring Program (LTMP). Within this data set, the first five years have the most comprehensive coverage of the fishery. With these data in hand, we can specify a simple Bayesian Hierarchical Model that treats recruitment as a function of parental abundance and connectivity. Connectivity is not constant over the spawning season and so is captured not in one matrix, but in a set of j connectivity matrices each pertaining to a specific week or month of the spawning season. Each of these matrices X_j is weighted by a scalar w_j , where the w_j individually represent the relative importance of that week or month’s currents to recruitment, and collectively constitute the scale factor between parents and recruits described earlier as m . Note that these w_j are assumed to be equal across years in this model, implying that the same time periods are consistently either important or unimportant to spawning each year. This may well not be reasonable given our earlier results suggesting the variability in connectivity between the same time period in different years is no lower than random, but we see this as an opportunity to ensure our earlier results are corroborated. The model is specified as a Bayesian Hierarchical Model below.

Model 1:

$$\begin{aligned}
 w_j &\sim \text{gamma}(1,1) \\
 \tau &\sim \text{gamma}(1,1) \\
 Z_i &= \sum_{j=1}^N w_j X_{ij} Y \\
 Y_{i+1} &\sim \text{gamma}(Z_i, \tau)
 \end{aligned}$$

Where:

w_j is the set of j weights for each of the j connectivity matrices.

τ is the rate parameter of the gamma distributed random variable Y_{i+1} .

Z_i is the shape parameter of Y_{i+1} as predicted by the parental abundance and weighted connectivity in year i .

Y_{i+1} denotes the distribution of recruitment in year $i + 1$, where each random variable corresponds to a different spatial cell in the fishery. According to our model it follows the gamma distribution with mean $E(Y_{i+1}) = \frac{Z_i}{\tau}$ and $Var(Y_{i+1}) = \frac{Z_i}{\tau^2}$.

The quantities \mathbf{Y} , \mathbf{X}_{ij} , and \mathbf{Y}_{i+1} are given by the parental abundance estimates, simulated connectivity matrices, and LTMP-Survey data respectively. With that information we wish to estimate the values of w_j , $0 \leq j \leq N$, and τ using Markov Chain Monte Carlo (MCMC) techniques. The gamma distribution was chosen as the first distribution to fit for each Y_{i+1} primarily because it is a distribution for positive variables. Obviously, negative abundance in a given region is impossible in reality so it makes sense to have a distribution limited from below by zero. Also, the gamma distribution has a heavy right tail above the mean, accommodating a slowly decreasing probability that the observed value is above the expected value – a feature that also seemed reasonable since one-off population spikes in a given region of the fishery are plausible under favourable advection, a short-term fishing closure, or other such factors. The prior for τ was also chosen to be gamma because, by definition, the rate parameter of a gamma distribution is positive. Lastly, for the weights, weighting a connectivity with a negative weight does not make physical sense, so this variable also had to be positive, and further, the heavy right tail of the gamma distribution accommodates well the expectation that some connectivity matrices can be more important than others.

The MCMC runs for parameter estimation were conducted using an R package called R2OpenBUGS (available on CRAN), BUGS being an acronym for Bayesian Analysis Using Gibbs Sampling. This name is somewhat deceptive as the simulator is actually an expert system that does not only apply the Gibbs sampler. Instead, depending on the complexity of the joint posterior distribution it must sample from, R2OpenBUGS may elect to sample the distribution via its set of conditional probability density functions (pdfs) using Gibbs Sampling, or may apply the Metropolis-Hastings Algorithm to sample it directly using a Markov Chain whose limiting distribution is the joint posterior distribution. Gibbs Sampling and the Metropolis Hastings Algorithm are summarised below.

Gibbs Sampler (Kroese and Chan 2012): Suppose we have a set of random variables $\mathbf{X} = (X_1, X_2, \dots, X_n)$ with a joint probability density function (pdf) $f(\mathbf{x})$. Sampling directly from $f(\mathbf{x})$ may be difficult, but it may be possible to sample from the conditional pdfs instead. Then, starting from some initial state \mathbf{X}_0 , repeat the following steps from $t = 1$ to n .

Given current state $\mathbf{X}_t = \mathbf{x}$, generate a $\mathbf{Y} = (Y_1, Y_2, \dots, Y_n)$ as below.
 Draw $Y_1 \sim f_1(y_1 | x_2, \dots, x_n)$.
 Draw $Y_i \sim f_i(y_i | Y_1, \dots, Y_{i-1}, x_{i+1}, \dots, x_n)$.
 Draw $Y_n \sim f_n(y_n | Y_1, \dots, Y_{n-1})$.
 Set $\mathbf{X}_{t+1} = \mathbf{Y}$

Note that the Gibbs sampler can take many iterations before the samples being drawn are indeed from the posterior distribution. The period this takes is known as the *burn in*. R2OpenBUGS applies a burn in period of $\frac{1}{2}t$, where t is the desired number of iterations specified by the user.

Metropolis Hastings Algorithm (Kroese & Chan 2014): Suppose we have a set of random variables $\mathbf{X} = (X_1, X_2, \dots, X_n)$ with a joint probability density function (pdf) $f(\mathbf{x})$. If it is possible to construct a Markov Chain whose limiting distribution is $f(\mathbf{x})$, then we may apply the Metropolis Hastings Algorithm to obtain samples. First, specify a transition density $q(\cdot | \mathbf{x})$ known to cover the domain and range of your target pdf $f(\mathbf{x})$. Then draw a proposal state Y from $q(\cdot | \mathbf{x})$, which is accepted or rejected based on the value of a probability function $\alpha(x, Y)$. More precisely, given a transition density $q(\mathbf{y} | \mathbf{x})$, and an initial state \mathbf{X}_0 , repeat the following from $t = 1$ to N .

Generate $\mathbf{Y} \sim q(\mathbf{y} | \mathbf{X}_t)$.
 Generate $U \sim U(0,1)$ and set $X_{i+1} = \begin{cases} Y, & \text{if } U \leq \alpha(X_t, Y) \\ X_t & \text{Otherwise} \end{cases}$,
 where $\alpha(X_t, Y) = \min\left(\frac{f(\mathbf{y})q(\mathbf{x} | \mathbf{y})}{f(\mathbf{x})q(\mathbf{y} | \mathbf{x})}, 1\right)$

For Model 1, Gibbs Sampling will draw a specified number of dependent samples from the conditional distributions

$$f(\mathbf{w}|\tau, \mathbf{Y}_{i+1})$$

and

$$f(\tau|\mathbf{w}, \mathbf{Y}_{i+1})$$

These samples are drawn iteratively, with each iteration using the sampled variable values from the previous iteration, and the LTMP data, to draw the next sample of the random variable. In this way, the sample values for τ and \mathbf{w} converge, after a burn in period, to a limiting distribution which reflects the true posterior distribution of the random variables. With these draws from the posterior distribution we can determine the expectation of each random variable; this expected value is the parameter estimate we will use in our posterior predictions.

Once the parameters have been estimated for several models, each using a different set of connectivity matrices, we compare the models based on the Deviance Information Criterion (DIC). The DIC is a measure of how much information is lost when a given model is used in place of the real data, and is calculated as the expected deviance of the model, plus a penalty for the complexity of the model, which is a function of the number of parameters (Gelman *et al.* 2013):

$$DIC = \bar{D} + p_D$$

where

$$\begin{aligned} \bar{D} &= E[D(\theta)] \\ p_D &= \frac{1}{2} var[D(\theta)] \end{aligned}$$

\bar{D} is the expectation of the deviance calculated across the MCMC run, and is a measure of how well the model fits the data. The higher it is the worse the fit. p_D is the penalty for model complexity, defined here by Gelman *et al.* (2013) as half the variance of the deviance across the MCMC run. A smaller DIC represents a better description of reality and based on comparing the DICs, a model can be chosen which will then be tested further for fit to the data.

We assess fit to data in two ways. First, for each spatial cell where we have LTMP data, we can calculate the probability of making a prediction less than or equal to the LTMP observation for that cell using the shape and rate parameters of the gamma distribution provided by the MCMC. If the probability is very low it is likely that in that cell our model over predicts. Conversely, if the probability is very high, then it is likely we are under predicting recruitment for that cell. As such, mid-range probabilities are good. Second, we can use these probabilities to implement a technique for analysing the residuals called Randomized Quantile Residuals (Dunn and Smyth 1996). As our predictions follow the gamma distribution, the discrepancies between our predictions and the observations should be gamma distributed. The method proposed by Dunn & Smyth ensures that if this is indeed the case, then the transformed residuals will be normally distributed and we can then simply analyse a quantile-quantile plot to verify whether this is the case. Taking the probabilities we have already calculated, we use the inverse CDF of the standard normal distribution to determine residual values under the standard normal distribution, and then plot them on a quantile-quantile plot. If they are normally distributed, they will closely follow a line of intercept 0 and slope 1, and this will imply that the original observations are gamma distributed as expected. If there is deviation from normality, then the model has either missed an important factor in the stock-recruitment relationship, or the inputs, such as the parental abundance estimates, or the connective patterns, are not reflective of reality.

20.6.3 Results for Model 1

Model 1 was fitted to recruitment data for the years 1997, 1998, and 2000, which are known to be El Niño, La Niña, and neutral years respectively. A plot of the DICs is presented in Figure 20-12, where the models are plotted from left to right in the same order they appear in Table 20-1. Disappointingly, no clear pattern among the DICs is evident. If 15 m depth currents fitted the data better than surface data for instance, then we would see every second pair of points achieve a lower DIC than the pair preceding them. Alternatively, if stochastic simulations consistently outperformed their deterministic counterparts, we would see every second point scoring a lower DIC than every first point. This is not the case and so no such conclusions can yet be reached.

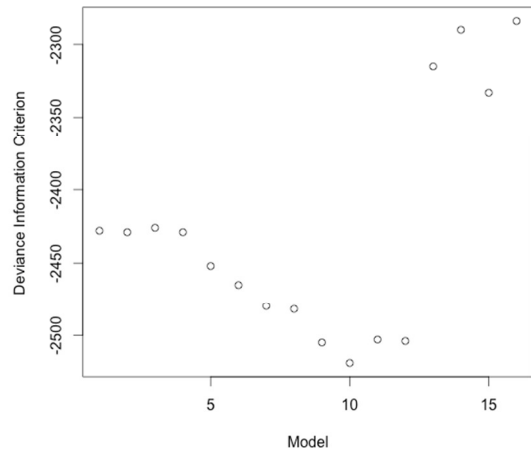


Figure 20-12. The DIC achieved by Model 1 fitted to each type of connectivity. They are plotted from left to right in the same order they appear in Table 20-1.

Figure 20-13 presents the density plots from Model 1 under type 8 connectivity. Inspecting this plot, we see that in several of the density plots, the three chains deployed in the MCMC run have not converged. This phenomenon persisted even when we ran the MCMC for up to 20,000 iterations. When bad mixing persists independent of the number of iterations it may imply that the model inadequately characterises the variability in the data. Interestingly, bad mixing was only observed for the instantaneous models while the climatological models mixed successfully, begging the question, is the fit achieved by the climatological models any good? As such, we analyse the fit of Model 1 using type 2 connectivity, and the Model 1 using type 8 connectivity below. These are the best performing models in their respective time granularities.

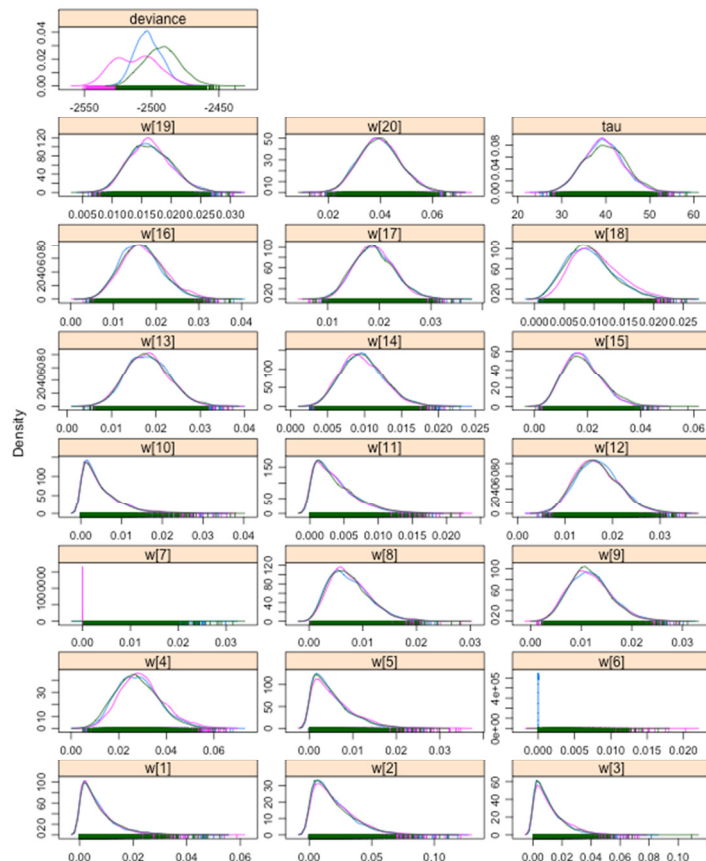


Figure 20-13. Density plots for the weights and deviance fitted using Model 1 using type 8 connectivity. It is clear for w[6], w[7], that the chains did not mix and convergence failed.

20.6.3.1 Model 1 Using Type 2 Connectivity

Figure 20-14 shows the posterior estimates for the weights. The black, red and green lines represent the lower, mean and upper bound of a 95% credibility interval for the weights respectively. Interestingly, it ranks the connectivity patterns that occur in September and October as the most important to recruitment. This is not what we expected. Considering that the LTMP survey data were collected in October, and that it is not likely that the larvae spawned in September or October would be large enough to be catchable at the time of the survey, this is a further sign the model is not operating as hoped.

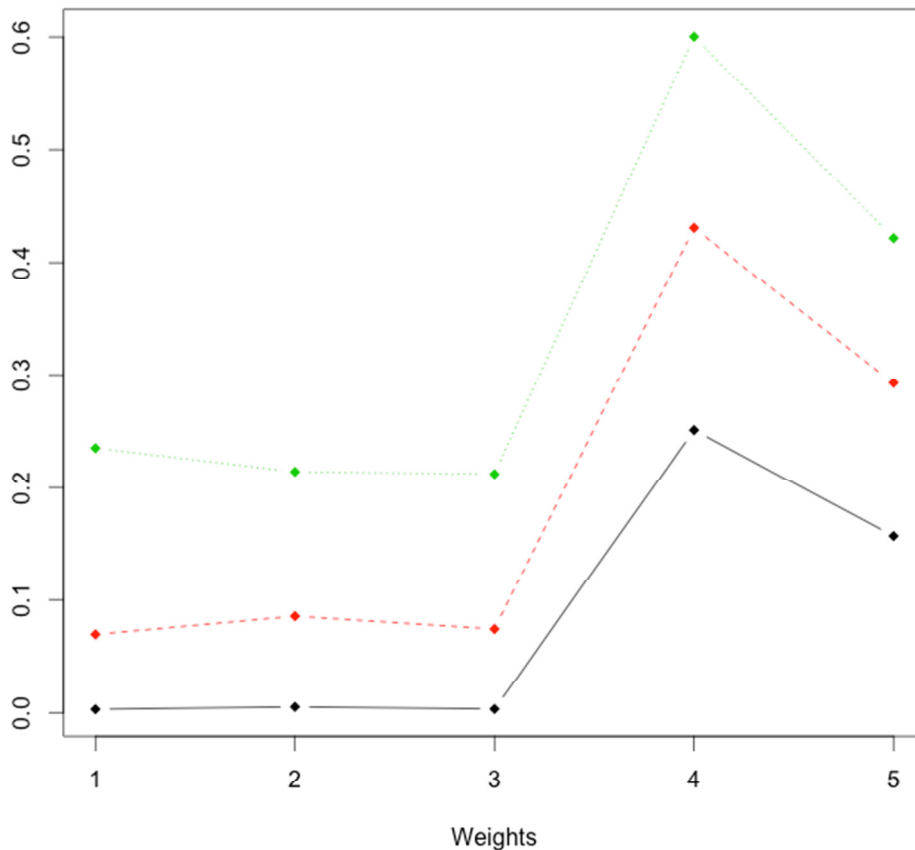


Figure 20-14. Estimates for the weights. The x axis numbers the weights from 1-5 corresponding to the months June through October. The y axis displays the estimated scalar quantity assigned to each weight. It is clear that the latter months have been weighted highly compared to the preceding three.

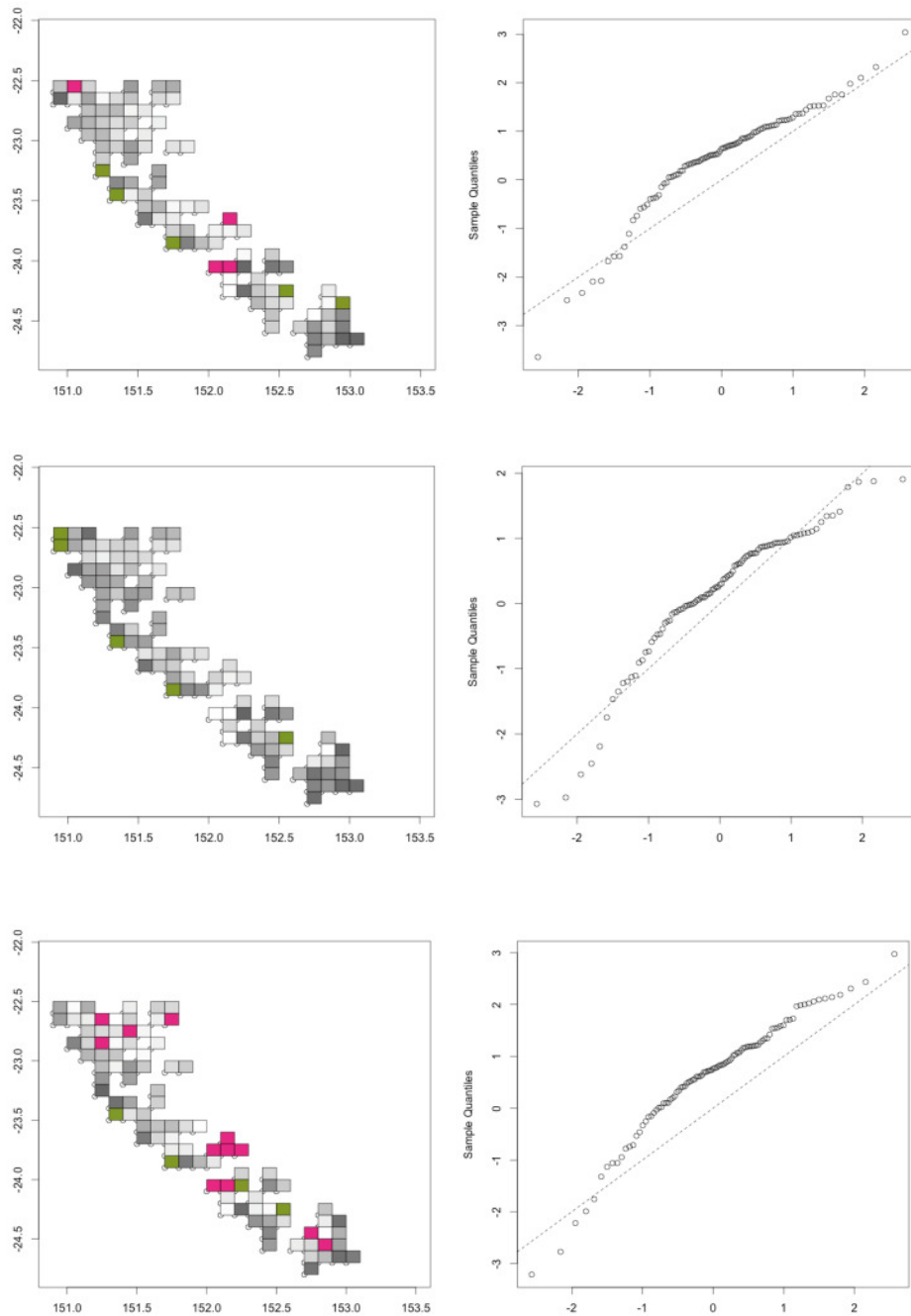


Figure 20-15. Fit plots and quantile-quantile plots. Each row of plots corresponds to a different year fitted, and rows 1-3 are the years 1997, 1998 and 2000 respectively. The fit plots on the left indicate the probability of making a prediction less than or equal to the LTMP observation. Green indicates that the probability of making a prediction less than the LTMP observation is greater than 97.5%, while red indicates the probability is less than 2.5%. Thus they represent cells where we are under predicting, and over predicting respectively.

Given we are only working with 100 grid cells in each year, as this is the extent of the LTMP-survey data, we only expect around five green or red values. However, apart from 1998, we have more anomalous predictions than we should if the model were reasonable. The plots on the left are quantile-quantile plots of the transformed residuals. It is clear to see that the residuals are not normal in any of the plots. Removal of extreme values was attempted, but this improved the lines only marginally. It is the quantile-quantile plots that resulted from the trimmed data that are presented here.

20.6.3.2 Model Using type 8 Connectivity

Figure 20-16 presents the weights as estimated by the MCMC run. This time there are two peaks, one near the beginning of the spawning season, and one four weeks from the end. Though this is more reasonable than the monthly weights structure, it is still not entirely what we expected as the late season peak is still a little close to the late October LTMP-survey date to be realistic.

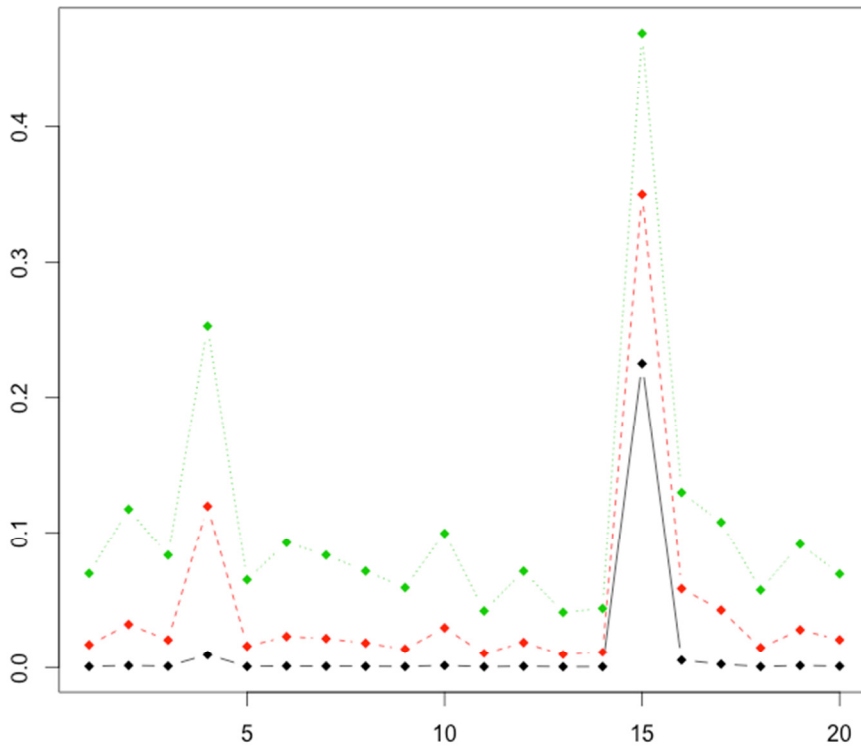


Figure 20-16. The estimates for the weights. The x axis numbers the weights from 1-20 corresponding weeks 1-20 of the spawning season. The y axis displays the estimated scalar quantity assigned to each weight. It is clear that the latter months have been weighted highly compared to the preceding three.

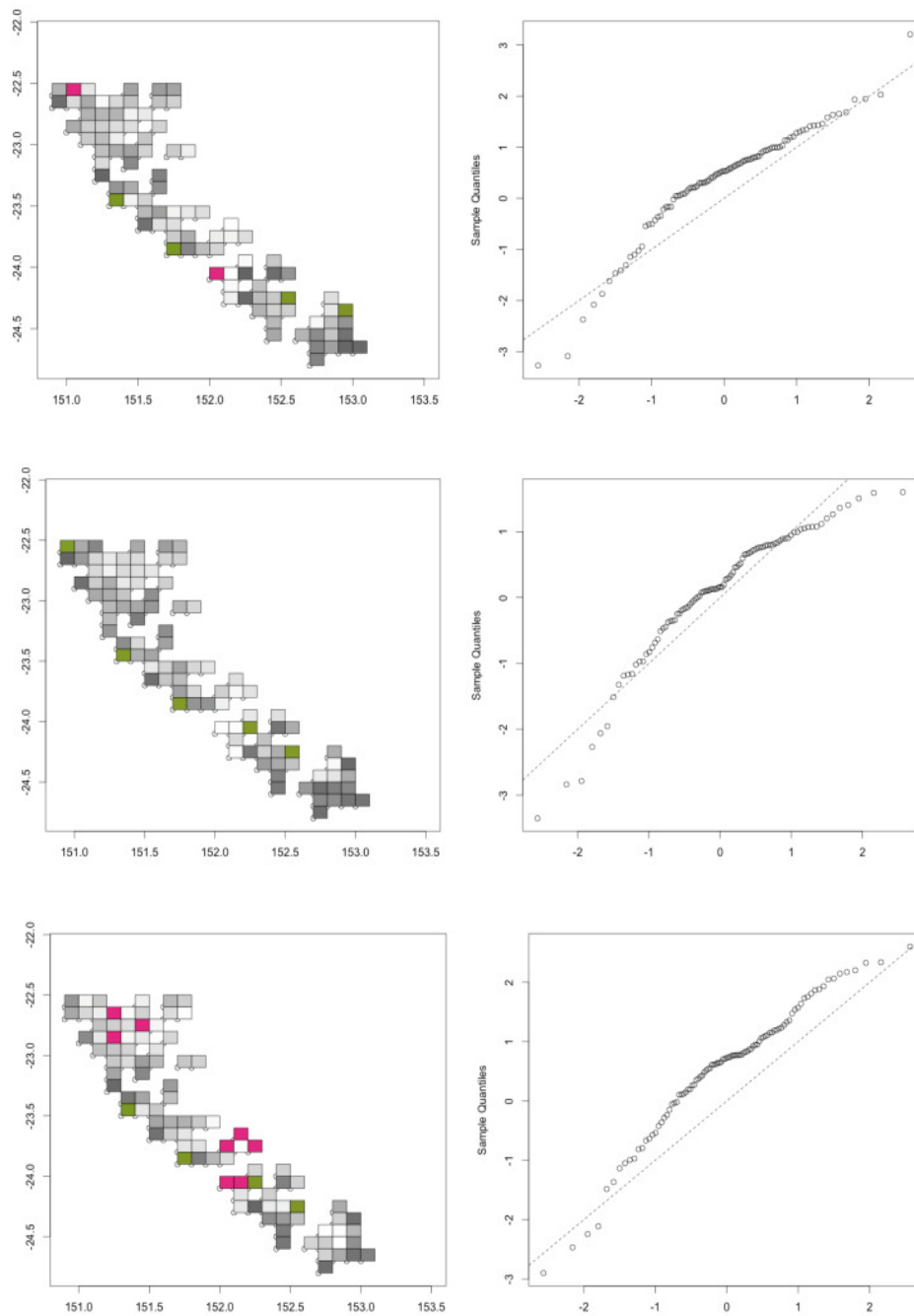


Figure 20-17. Fit plots and quantile-quantile plots. Each row of plots corresponds to a different year fitted, and rows 1-3 are the years 1997, 1998 and 2000 respectively. The fit plots on the left side of the figure indicate the probability of making a prediction less than or equal to the LTMP observation. Green indicates that the probability of making a prediction less than the LTMP observation is greater than 97.5%, while red indicates the probability is less than 2.5%. Thus they represent cells where we are under predicting, and over predicting respectively.

In addition, in Figure 20-17 we still have more green and red cells than we ought to for the year 2000. 1997 is predicted much more closely under this weekly model than the previous monthly model however, and 1998 performs roughly the same as before.

The quantile-quantile plots are marginally better under this model with 1997 and 1998 almost following the ideal line if not for their skewed tails at each ends. These skewed ends remain even after the trimming of the maximum and minimum observations, so the issue is more complex than one or two anomalous outliers leveraging the model. Something fundamentally different seems to occur in the group of cells whose observations cause these tails. Given the lack of mixing under Model 1, and the poor fit to data of the models that did mix, it was clear we needed to specify a more flexible model.

20.6.3.3 Additional Methods

In Model 2, the first modification is the addition of an annual intercept parameter I_i . This parameter serves to capture a baseline level recruitment that may take place across the fishery independent of the currents. Our rationale behind adding such a parameter came from the fact that in several of the instances where observations exceeded our predictions under the Model 1, the model had predicted near zero recruitment due to currents. Potentially larvae have more control over their trajectory than we currently assume, and deliberately recruit to the region from whence they were spawned in certain circumstances. Next, we also allowed each year's recruitment to have a different level of variation by estimating a new τ for each year. The weights also were given the freedom to vary from year to year, and finally, the distribution of Y_{i+1} was changed to a generalised gamma distribution with a third parameter β . The new model is as below, and the rationale behind the switch to the generalised gamma distribution is explained subsequently.

Model 2:

$$\begin{aligned}
 I_i &\sim \text{gamma}(1,1) \\
 w_{ji} &\sim \text{gamma}(1,1) \\
 \tau_i &\sim \text{gamma}(1,1) \\
 \beta_i &\sim \text{gamma}(1,1) \\
 Z_i &= I_i + \sum_{j=1}^N w_{ji} X_{ij} Y \\
 Y_{i+1} &\sim G\text{gamma}(Z_i, \tau, \beta)
 \end{aligned}$$

Where:

I_i is the intercept parameter, serving as a baseline level of recruitment across the fishery in a given year.

w_{ji} is the set of j weights for each of the j connectivity matrices.

τ_i is the rate parameter of the gamma distributed random variable Y_{i+1} .

β_i is the second shape parameter of the Generalised Gamma distribution.

Z_i is the shape parameter of Y_{i+1} as predicted by the parental abundance and weighted connectivity in year i .

Y_{i+1} denotes the distribution of recruitment in year $i + 1$, where each random variable in the vector corresponds to a different spatial cell in the fishery. According to our model it follows the Generalised Gamma Distribution with mean $E(Y_{i+1})$ being the predicted recruitment and $Var(Y_{i+1})$ the variance in recruitment.

The pdf of the Generalised Gamma Distribution is implemented in R2OpenBUGS as

$$f(x|a, b, c) = \frac{c}{\Gamma(a)} b^{ca} x^{ca-1} e^{-(bx)^c}$$

Where Γ is the gamma function. The expectation of the Generalised Gamma Distribution (Khodabin & Ahmadabadi, 2010) is given by

$$E(X) = \frac{\Gamma(a + 1)}{b\Gamma(a)}$$

The power of using the Generalised Gamma Distribution is that depending on its parameters, it can take the form of several sub-families, essentially giving the model complete flexibility even so far as deciding which positive distribution is most appropriate for the data. When $c = 1$ the Generalised Gamma Distribution takes the shape of the Gamma Distribution. This obviously implies that it can also take the form of the Exponential (when $a = 1$) and Chi-Squared Distributions (when $a = \frac{n}{2}, b = \frac{1}{2}$, where $n = 1, 2, 3 \dots$), which are subfamilies of the gamma. The Weibull distribution is another sub-family of the Generalised Gamma Distribution, as is the Rayleigh Distribution, the Maxwell-Boltzman Distribution, and the Half Normal Distribution – the distribution of the absolute value of a normal random variable. All these distributions are limited from below by zero, and thus the Generalised Gamma is a very broad choice for modelling physical phenomena. Once the model is fitted, the parameter values of the Generalised Gamma Distribution may be used to identify the best sub-family to fit the data to a third, more restrictive model. Parameters were estimated as before using MCMC with the same 16 different connectivity models all refitted under the new model specification.

20.6.4 Results for Model 2

A plot of the DICs for Model 2 using each type of connectivity is shown in Figure 20-18. Being in a range of -2260 to -2200, the DICs achieved by this model are higher, and therefore worse than Model 1. At first this may seem strange, as greater flexibility should lead to better fit, and therefore less information lost about the data under the specified model. However, DIC penalises a model for complexity, and this new model is certainly more complex than Model 1, so the result is not surprising. This reasoning is also behind why under this model, the weekly connectivity models score so much worse than the monthly – they have 60 weight parameters as opposed to 15. What we are

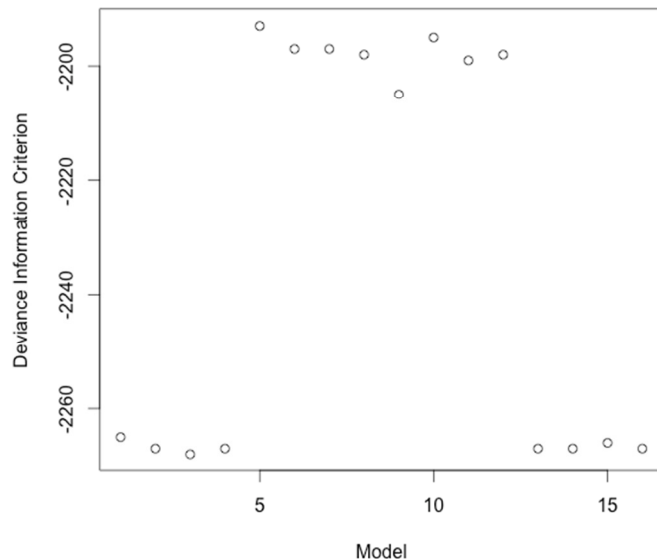


Figure 20-18. The DIC achieved by Model 1 fitted to each type of connectivity. They are plotted from left to right in the same order they appear in Table 1.

more interested in is the quality of fit achieved by the models, and the parameters of the Generalised Gamma that were estimated, which might allow us to develop a third, simpler model with a new distribution from among the sub families of the Generalised Gamma to fit the data. The fit of the best models across both the climatological and instantaneous models for each time granularity is described below.

20.6.4.1 Model 2 Using Type 3 Connectivity

Figure 20-19 shows the weights estimated by the MCMC run. The green, red and black lines are respectively the upper bound, mean and lower bound of a 95% Bayesian credibility interval for the weight estimates. The first 5 weights correspond to the first year, the second 5 to the second, and so on. It is clear from this plot that the connective patterns experienced near the beginning of the spawning season are the most important to October recruitment as recorded in the LTMP data. This is more realistic than the statements being made under Model 1. As in Model 1, this climatological

model mixed well. Interestingly, the fit for the parameter β suggests its value is close to 1 and that the generalised gamma distribution is thus taking a gamma-like shape after all, as opposed to any of its other sub-families. It is also interesting to note that the intercept parameter estimates were almost identical from year to year, implying that a similar base level of recruitment unexplained by the currents takes place each year. Further, τ is similar each year, suggesting it did not need to be allowed to vary from one year to the next. Figure 20-20 shows the fit plots and quantile-quantile plots for the three years fitted, and indicates how well the model fits the data. It is clear that there are less extreme values here than under the Model 1 but the quantile-quantile plots show fit is still poor, with residuals deviating systematically away from the normal line.

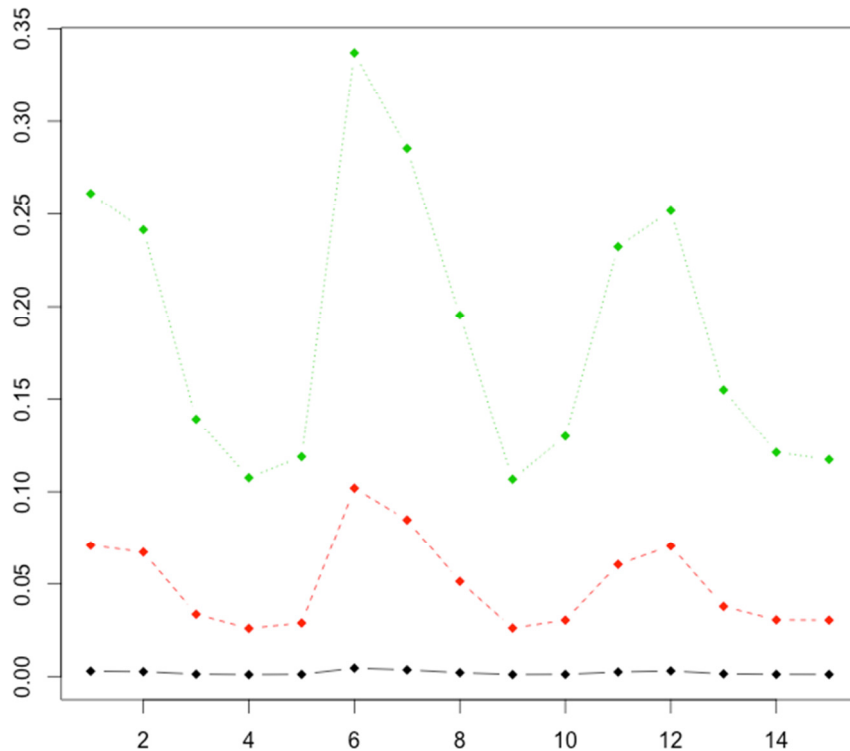


Figure 20-19. The estimates for the weights. The x axis numbers the weights from 1-15 corresponding to the months June through October for the years 1997, 1998 and 2000. The y axis displays the estimated scalar quantity assigned to each weight. It is clear that the latter months have been weighted highly compared to the preceding three.

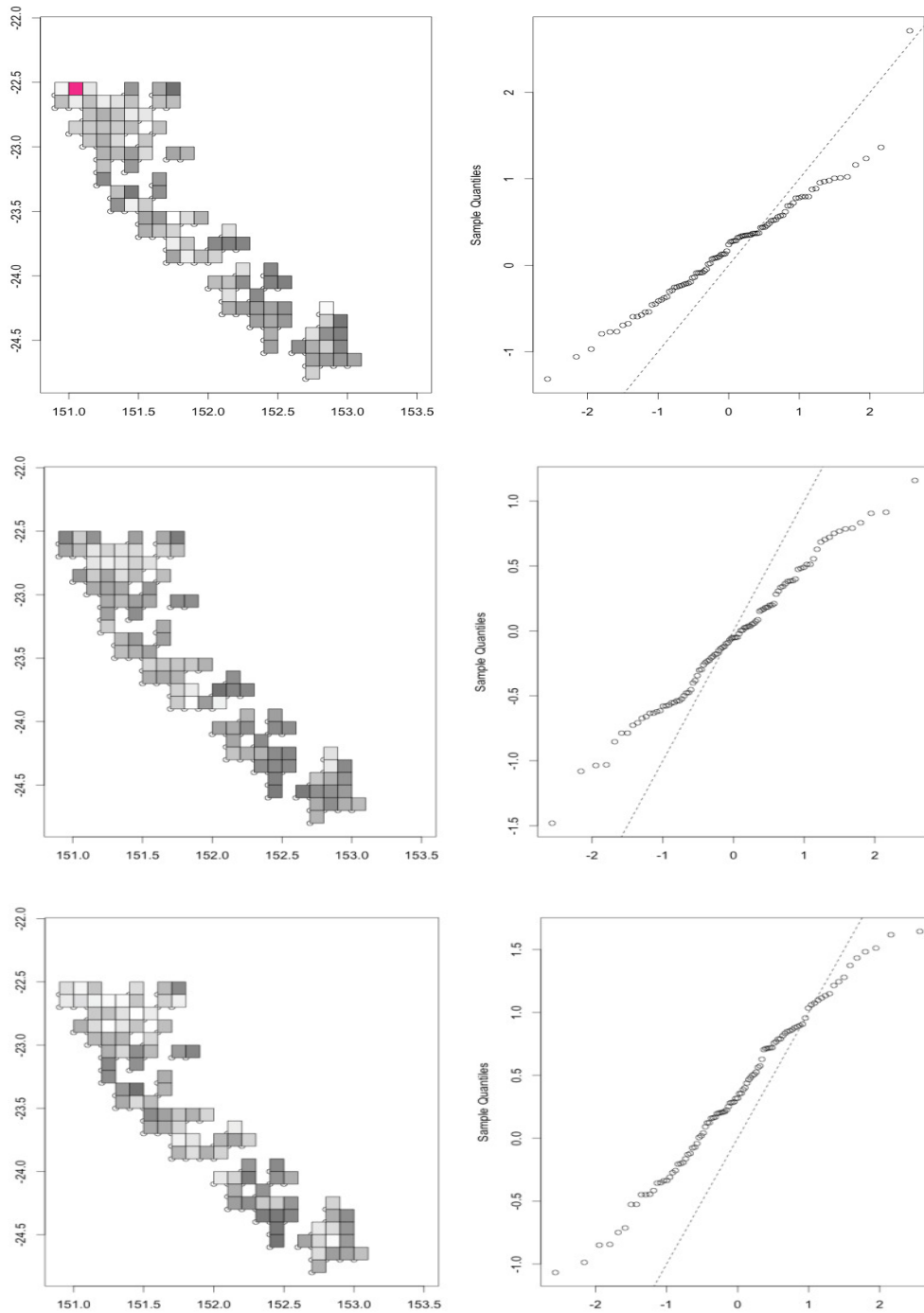


Figure 20-20. Fit plots and quantile-quantile plots. Each row of plots corresponds to a different year fitted, and rows 1-3 are the years 1997, 1998 and 2000 respectively. The fit plots on the left size of the figure indicate the probability of making a prediction less than or equal to the LTMP observation. Green indicates that the probability of making a prediction less than the LTMP observation is greater than 97.5%, while red indicates the probability is less than 2.5%. Thus they represent cells where we are under predicting, and over predicting respectively.

20.6.4.2 Model 2 Using Type 8 Connectivity

In Figure 20-21 the same pattern as already observed in the monthly model above is repeated – Connectivity at the beginning of the spawning is a predictor of recruitment in October.

This model mixed well and the density plots revealed that the mean of β for each year is close to 1, again suggesting that the Gamma distribution is the most appropriate sub family of the Generalised Gamma to use in modelling recruitment. The intercepts and τ 's are in the same range as the Monthly Climatological model suggested, once more implying we did not need to let them vary from year to year.

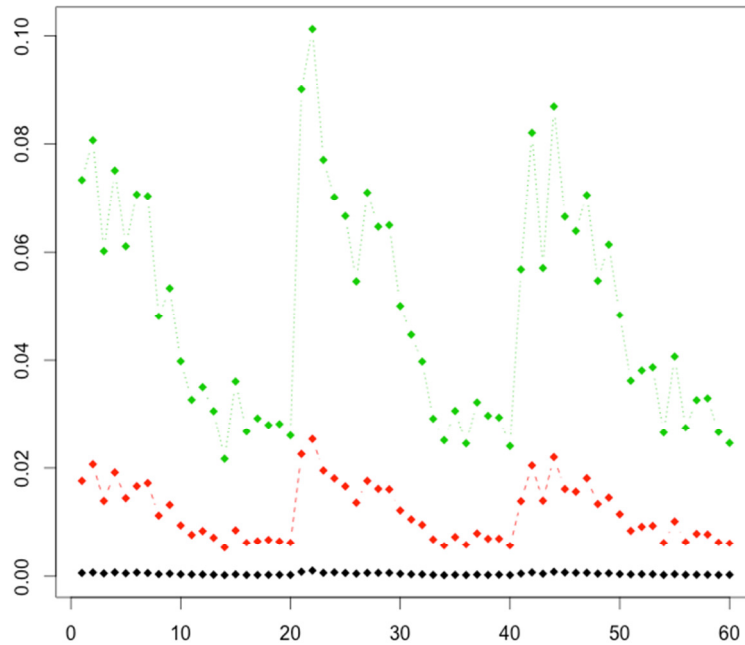


Figure 20-21. The estimates for the weights. The x axis numbers the weights from 1-60 corresponding to weeks 1-20 of the spawning season for the years 1997, 1998 and 2000. The y axis displays the estimated scalar quantity assigned to each weight. It is clear that the latter months have been weighted highly compared to the preceding three.

Figure 20-22 shows the fit and quantile-quantile plots for each year. The number of extreme values in the fit plots are within the bounds of what you would expect across 100 grid cells. The quantile-quantile plots here follow the normal line far more closely than the monthly climatology model, with the residuals for the year 2000 following the line clearly. The fit is certainly an improvement, but not as close as one might hope with skewed upper tails in 1997 and 1998 persisting.

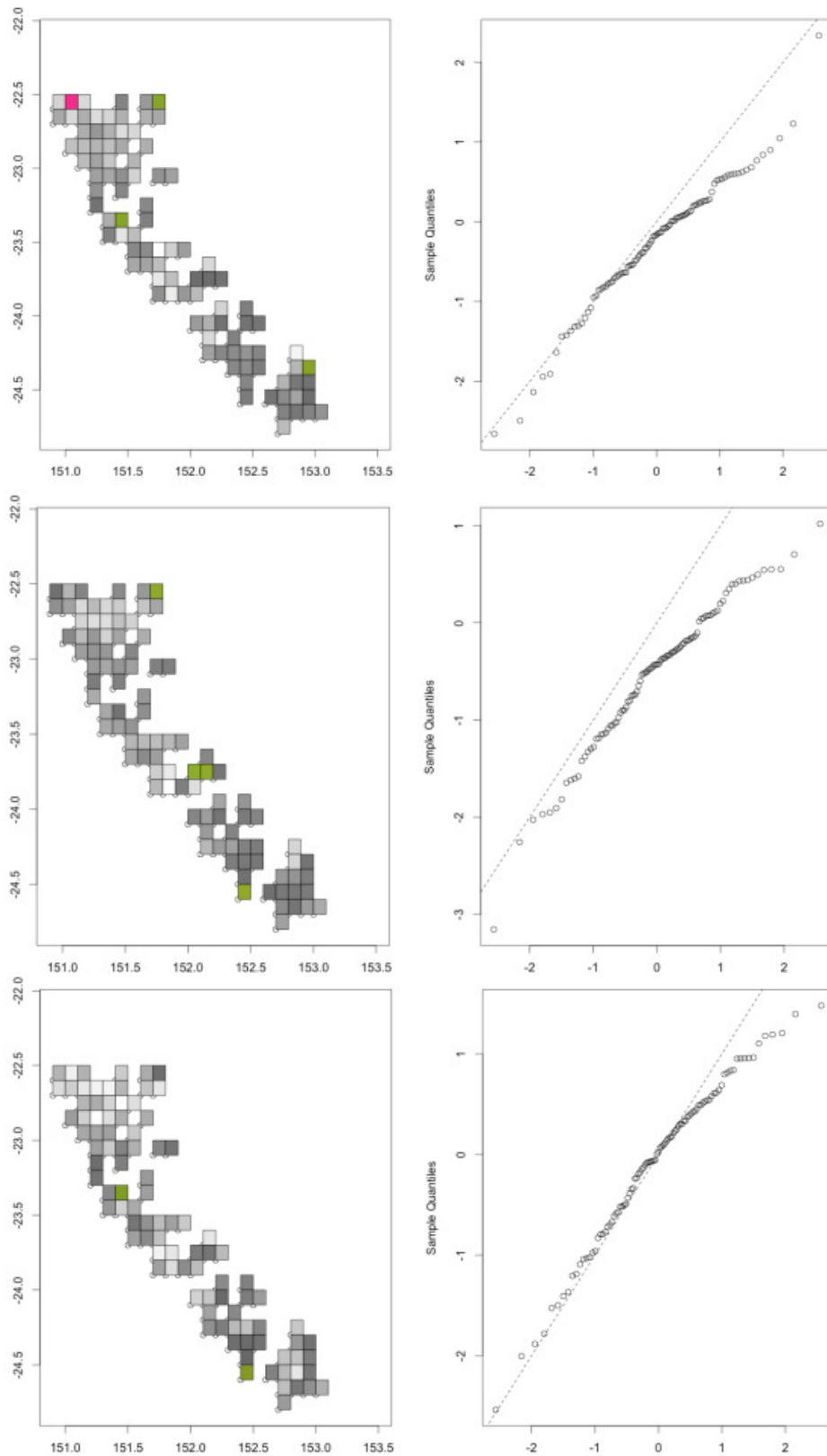


Figure 20-22. Fit plots and quantile-quantile plots. Each row of plots corresponds to a different year fitted, and rows 1-3 are the years 1997, 1998 and 2000 respectively. The fit plots on the left side of the figure indicate the probability of making a prediction less than or equal to the LTMP observation. Green indicates that the probability of making a prediction less than the LTMP observation is greater than 97.5%, while red indicates the probability is less than 2.5%. Thus they represent cells where we are under predicting, and over predicting respectively.

20.6.4.3 Model 2 Using Type 9 Connectivity

Figure 20-23 presents the weights estimated under the weekly non-climatological surface deterministic simulation. The weights given to the first few weeks of 1997 are completely dominant that year, and their magnitudes dominate the entire plot. The 1998 weights show two distinct moments of importance near the beginning and middle of the year, and in 2000, it is again the first few weeks that are dominant.

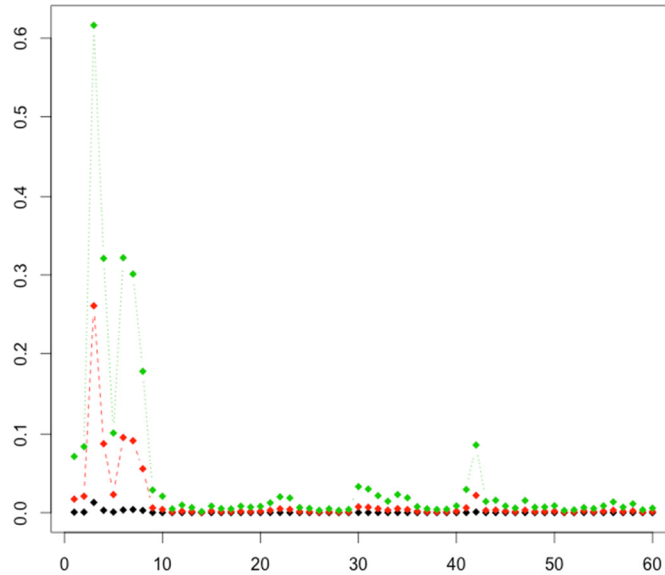


Figure 20-23. The estimates for the weights. The x axis numbers the weights from 1-60 corresponding to weeks 1-20 of the spawning season for the years 1997, 1998 and 2000. The y axis displays the estimated scalar quantity assigned to each weight. It is clear that the latter months have been weighted highly compared to the preceding three.

Figure 20-24 shows the density plots of all model parameters except the weights. Previously, this non-climatological model refused to mix even after many iterations, but, as hoped, all parameters mix well under Model 2. Once again, the expectation of β is close to one implying the gamma is the most appropriate choice of subfamily.

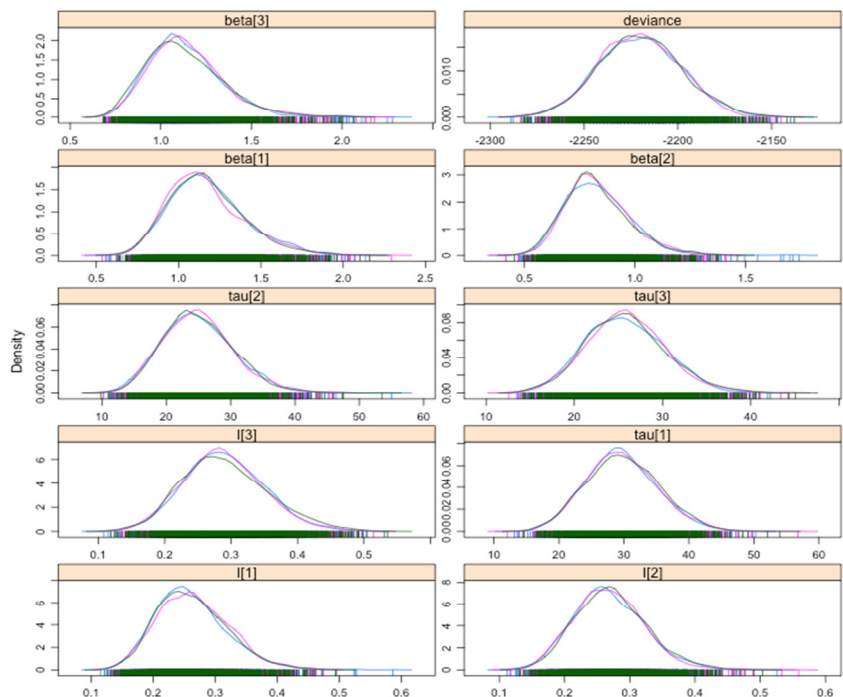


Figure 20-24. Density plots for parameters fitted for Model 2 using type 9 connectivity (excluding the 60 weights).

Figure 20-25 shows the fit and quantile-quantile plots for 1997, 1998 and 2000. Again, the number of extreme values observed are within the bounds of acceptable. The residual plots follow the normal line marginally more closely than the weekly climatological model and the quantiles for the year 2000 in particular are very well behaved, but several distinct outliers still exist in 1997 and 1998.

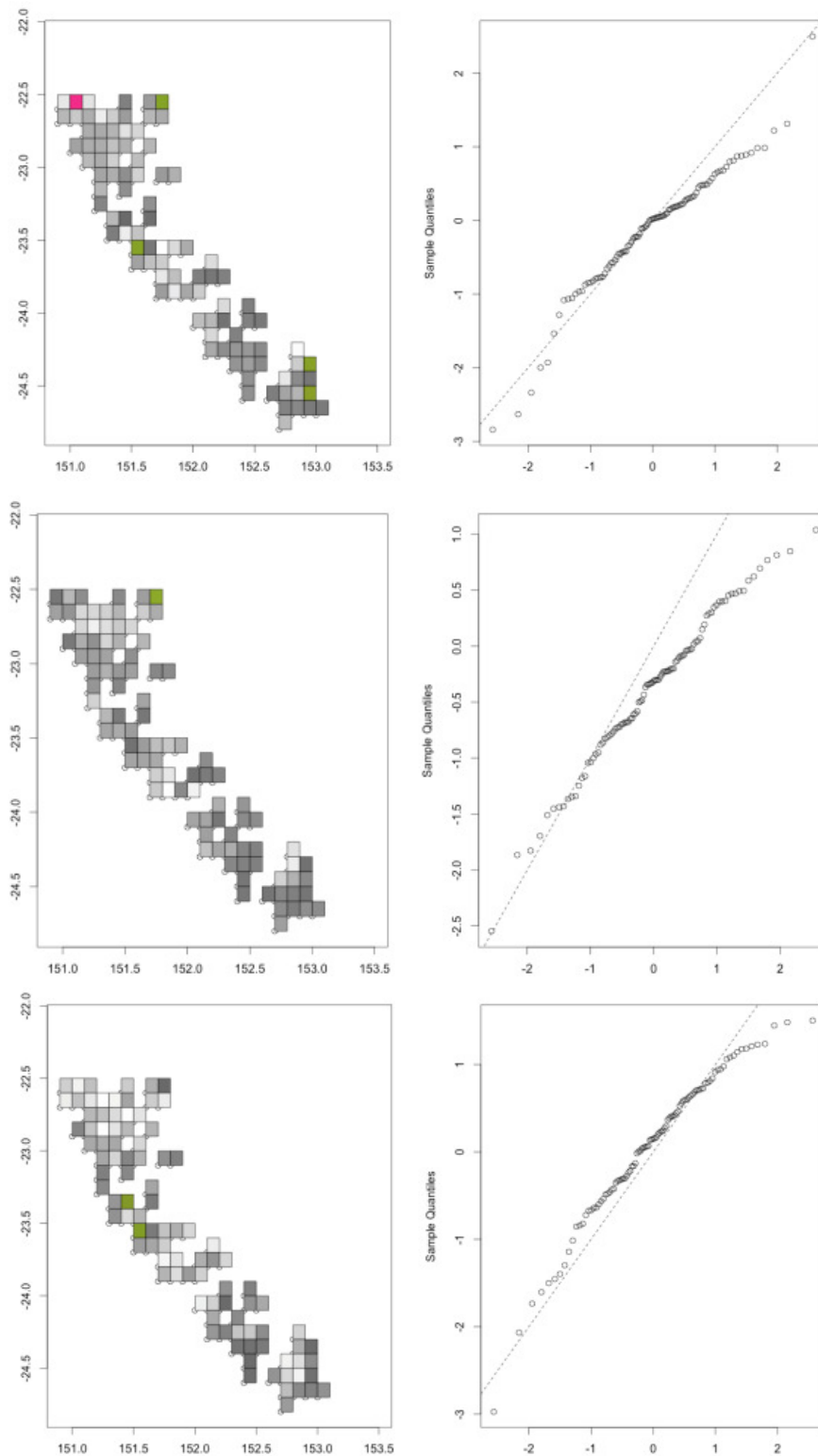


Figure 20-25. Fit plots and quantile-quantile plots. Each row of plots corresponds to a different year fitted, and rows 1-3 are the years 1997, 1998 and 2000 respectively. The fit plots on the left size of the figure indicate the probability of making a prediction less than or equal to the LTMP observation. Green indicates that the probability of making a prediction less than the LTMP observation is greater than 97.5%, while red indicates the probability is less than 2.5%. Thus they represent cells where we are under predicting, and over predicting respectively.

20.6.4.4 Model 2 Using Type 14 Connectivity

Figure 20-26 presents the estimates of the weights, and it appears the first month has been weighted as the most important each year. Apart from the first month, the weights given to the remaining months are not dramatically different. The density plots showed that that this model mixed well, unlike under Model 1.

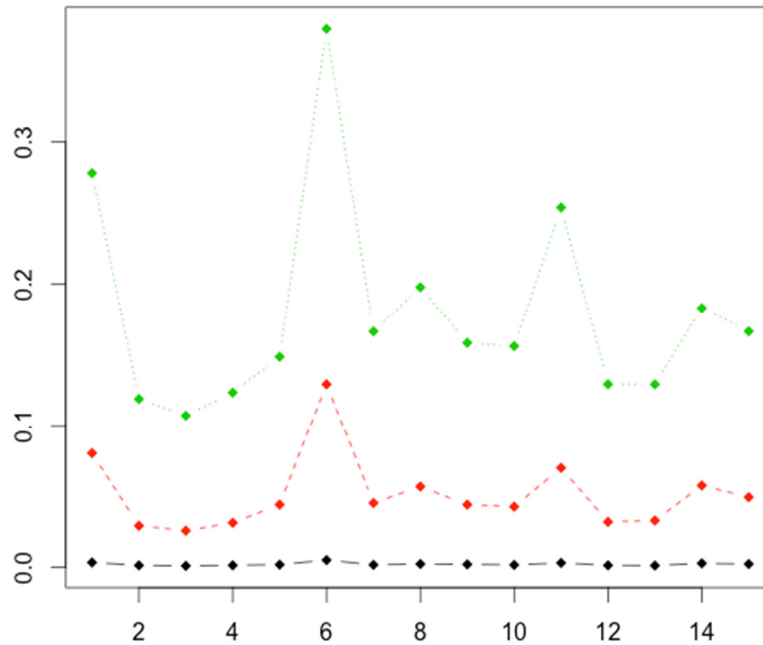


Figure 20-26. The estimates for the weights. The x axis numbers the weights from 1-15 corresponding to June through October for the years 1997, 1998 and 2000. The y axis displays the estimated scalar quantity assigned to each weight. It is clear that the latter months have been weighted highly compared to the preceding three.

Figure 20-27 shows fit plots and quantile-quantile plots for the model fit to 1997, 1998, and 2000. While the number of extreme values observed is low, the residuals certainly do not follow the normal line as well as in the weekly instantaneous model.

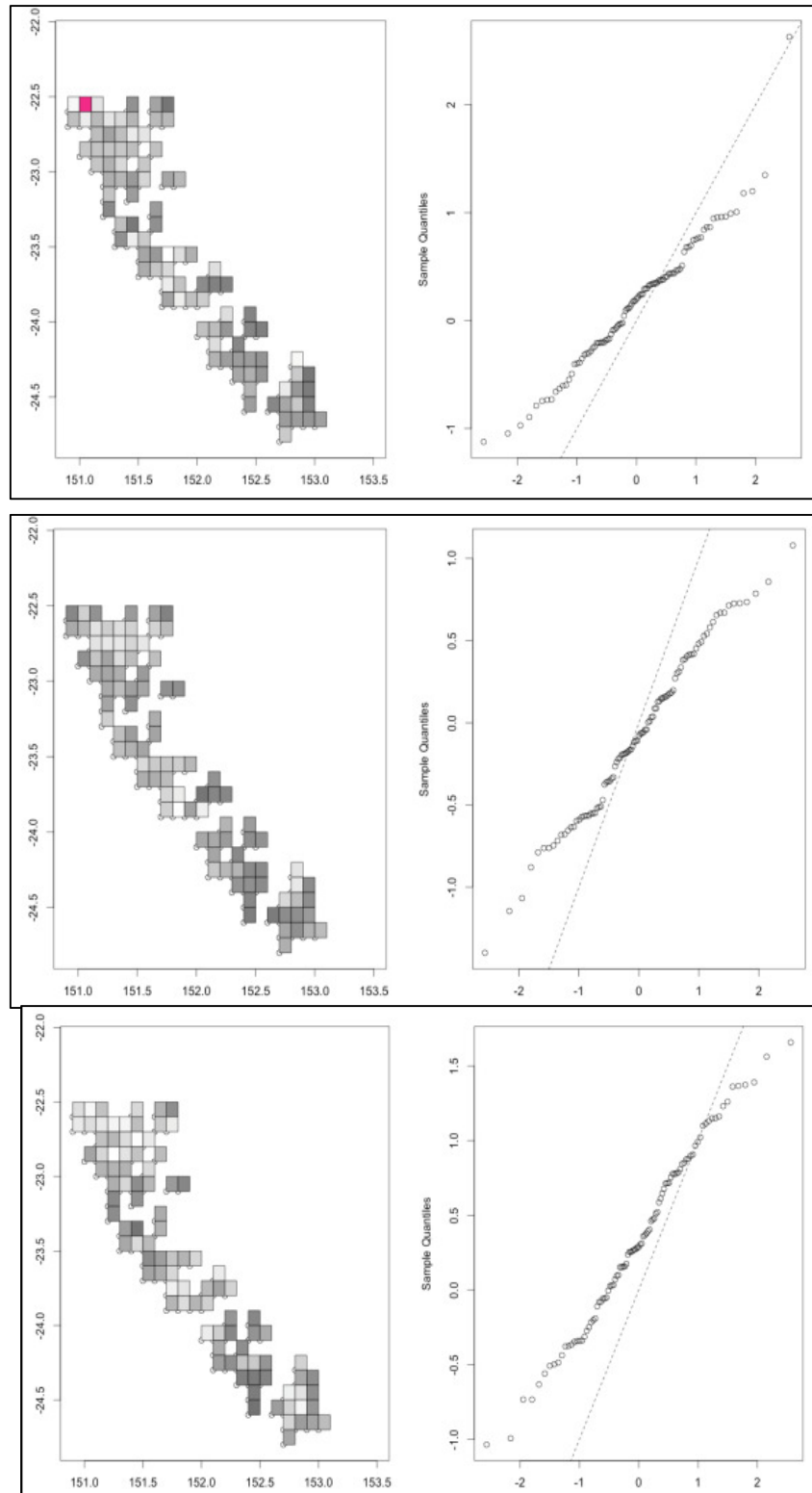


Figure 20-27. Fit plots and quantile-quantile plots. Each row of plots corresponds to a different year fitted, and rows 1-3 are the years 1997, 1998 and 2000 respectively. The fit plots on the left size of the figure indicate the probability of making a prediction less than or equal to the LTMP observation. Green indicates that the probability of making a prediction less than the LTMP observation is greater than 97.5%, while red indicates the probability is less than 2.5%. Thus they represent cells where we are under predicting, and over predicting respectively.

20.6.5 Conclusion

All models mixed well under the Model 2 specification. The intercept and τ were free to vary from year to year, but estimates suggest this was not necessary, as their values remained relatively constant. Unfortunately however, the quantile-quantile plots remain skewed to varying degrees, indicating the fit of the model still requires improvement. Parameter estimates for the generalised gamma distribution across all models fitted indicate that the gamma distribution is the most appropriate subfamily to fit the data. Considering this was the distribution we tried up front in Model 1, which did not achieve good fit at all, it is clear that improvements must come from somewhere other than changing the prior distributions in our model. The current model either ignores a key factor influencing recruitment, or is suffering from inputs that do not reflect reality. As such, below we review the two best fitting models found, their implications and how they might be improved through further research, and we subsequently discuss how the inputs to the models can be improved to hopefully further improve agreement between our predictions and reality.

Looking across the four connectivity models analysed under Model 2 it is clear that the two best fitting results, as far as the residuals are concerned, were obtained using type 8 connectivity and type 9 connectivity. Of the two, the Model 2 with type 9 connectivity has the better DIC and so is the preferred model overall. However, having to use an instantaneous connectivity means prediction is a very difficult task. Beside the need to simulate advection every year in order to predict the next, the weights applied to each connectivity matrix are different from year to year, and cannot be estimated in advance without greater knowledge of the causal mechanism that drives some weeks to have favourable advection patterns, and others not. In this vein, a closer analysis is necessary in order to determine whether there is anything in common between the weeks that are ranked as important in the three years fitted. Perhaps some kind of weather or oceanographic event, arriving at different times each year, triggers these favourable patterns. This is an area for further research.

Another feature worth discussing is the difference between the weight estimates in 1997 compared to other years. The first half of the season in 1997 is extremely important to recruitment that year, while the remainder of the year is almost inconsequential, and these early 1997 weights dwarf the highest weightings from other years. This is potentially due to the fact that late 1997 was the strongest El Niño period on record in Australia (Bureau of Meteorology, 2012). El Niño's may bring warm water to the Queensland Coast, and it is known that scallops prefer cooler waters for breeding (Julie Robins, unpublished), so it is quite possible that the arrival of the El Niño brought an early end to spawning that year, explaining why recruitment is primarily determined by advection patterns that took place early in the year.

As we consider the credibility intervals for the weight estimates, it must be noted that the lower bound of virtually all estimates is zero. In other words, it is still possible that recruitment is independent of advection pattern. This is highly unlikely however, as larvae have a very weak swimming ability compared to the velocity of currents. More likely, this is a further symptom of the model not doing a good job capturing the dynamics of the data, and it specifically points to the connectivity matrices as part of the problem. Raising further suspicion, the right tails in 1997 and 1998 are skewed below the normal line as in all other models, indicating that the predictions generated by the model for those cells are above the LTMP observations. Given the flexibility built into the model having used a Generalised Gamma distribution, and allowing the weights, intercept, and shape parameters to all vary from year to year, there is little more that can be done to accommodate these points. Instead, a closer look at the connectivity matrices and other inputs of the model is necessary.

In forming the connectivity matrices in the current setup, simulated advection includes no behavioural aspects of the larvae. This choice was made because information on the behaviour of *A. balloti* larvae is largely unavailable. However, deliberate vertical migration has been observed in other larval species where larvae move up and down depending on the light level, and to ride certain current streams to maximise transport in a particular direction (Tamaki *et al.* 2010). Both vertical and lateral migration

have also been observed in response to food sources such as algae in some species (Tamaki *et al.* 2010). Any such deliberate behaviour could have a significant impact on the final recruitment pattern.

Further, the current data from BRAN 3.5 does not include tidal information. On a large scale and over longer periods it is generally assumed in the literature that dominant currents will drive advection overall, with tides just creating periodic noise (Kangas *et al.* 2012). This may not necessarily hold true for the Queensland Fishery, however, as it is a relatively shallow fishery with an average depth of just 31 metres. The greater tidal fluctuations experienced in shallow regions may well induce a greater level of mixing and wider dispersion of larvae in the fishery overall, as well as accentuating differences between surface and current strata. In addition, simulations suggest that one of the more dominant advection patterns is for the larvae to be swept northward and coastward. This pattern may be disrupted as tides are likely to have a periodic flushing effect operating against the coastward current. It should also be noted that the region is well populated with coral reefs, which would certainly funnel tidal streams between them creating local periodic fast-moving water jets. The combination of these tidal effects may have a dramatic effect on the actual advection that takes place.

Finally, it needs to be recognised that the estimates of parental population density we are applying from Campbell *et al.* (2012) do not vary with time. The estimates are based on an analysis of fishery logbook data and the LTMP data, and are an average across the years for which data were available. How these densities change annually has not been explored, but it is clear that ignoring annual variation will always be a simplification, and as a result the predictions for some years based on these estimates will always be further from reality than other years. In utilising these estimates we also took the parental population densities from a coarse grid provided by Campbell *et al.* (2012) and transferred those estimates to our finer grid assuming that this density was constant across the larger cells in Campbell's coarse grid. The extent to which this assumption deviates from reality is difficult to determine, but Campbell *et al.* do distinguish between total area and effective fishable area when discussing the grid cells, and these numbers are never equal.

20.7 FINAL SUMMARY

The initial objective of this research was to investigate advection patterns of *A. balloti* in the Queensland Fishery. This was done in Chapter 2 Numerical Modelling, where simulations of advection were conducted. A key point of innovation in our approach to the simulations was the inclusion of an analysis of the variability of connectivity. Other studies typically have not had sufficient data to conduct such an analysis. The presentation of larval loss, region connectedness, and self-seeding in the context of their variability has led us to two important findings. The first is that connectivity dynamics are, in general, very variable, and as such, any expectation formed based solely on *average* behaviour, without considering its *consistency*, is likely to be quite wrong in many spawning events, so caution should be exercised. The second major finding was that self-seeding seems to be a key driver of the productivity of the three regions of highest fishing effort. This being the case, it was recommended that the most effective way to ensure sustained breeding stock is the implementation of a rotational closure scheme, as opposed to expecting any one protected region to reliably seed the wider region.

In Chapter 3 Climatology Performance Assessment we considered whether larval advection patterns in a given month or week were similar across years, implying an annual cycle, or not. It is typically assumed in the literature that advection is indeed annually cyclical, and as such, that it is justifiable to extrapolate patterns observed in one or two years, to all years. This was found not to be the case. Instead, it was found that overall, the same weeks or months across years exhibit advection patterns as different as any other random set of weeks or months might. For fisheries researchers this means that it is not justifiable to assume years are similar, and that similar advection patterns will be observed at similar times of the season each year.

Chapter 4 Statistical Modelling of Recruitment addressed the final objective – fitting a stock-recruitment model incorporating connectivity pattern to a real data set. The typical assumption made in the literature is that a certain multiple of the parent population is spawned as larvae, which are then redistributed according to the dominant currents, and settle as recruits between two and four weeks later. Despite an extremely flexible model specification, which allowed for a baseline level of recruitment independent of the advection pattern and all parameters to be estimated uniquely for each year, the fit to data achieved by the model did not reach an acceptable level. The difficulty in fitting a model suggests to us that the stock-recruitment relationship is more complex than assumed, and that our simulated advections need refinement. In particular, the BRAN 3.5 data set does not include tidal information, potentially rendering it unrealistic in a shallow fishery like the Queensland Fishery. Additionally, behavioural parameters of the larvae such as vertical migration habits are largely unknown and were therefore not considered in our simulation. Research into such behavioural aspects of the larvae is necessary to further refine the advection simulation and hopefully achieve better fits. Lastly, our model utilised an estimate of abundance that was not time varying, which is clearly unrealistic. Although the intercept term in the model attempted to compensate for this, more accurate, temporally and spatially explicit parental abundance estimates are likely to improve the model's ability to achieve a good fit also.

In summary, there is considerable scope to improve the fit of the model through improved data inputs and further research into *A. balloti* larval behaviours. Beside this, three major findings have been reached; that variability in advection dynamics cannot be ignored, that advection pattern is not cyclical on an annual scale, and that self-seeding is an important driver of productivity in the Queensland Fishery with significant implications for management.

21 Appendix 7. Impacts of low-pressure systems on the Great Barrier Reef: Confirmation of a causal mechanism using catch rates of the coral trout fishery

George M. Leigh

This section of the report addresses all three Objectives and is focused on coral-reef fish:

- 1) *Review recent advances in the study of physical oceanographic influences on fisheries catch data, and describe the major physical oceanographic features that are likely to influence Queensland reef fish and saucer scallops.* Current knowledge of the effect of tropical cyclones on coral-reef fish is described.
- 2) *Collate Queensland's physical oceanographic data and fisheries (i.e. reef fish and saucer scallops) data.* Data on fishery catch rates, tropical cyclones and measured wave heights along the Queensland east coast are collated, along with available information on other weather systems such as Tropical Lows, East Coast Lows and high pressure cells over New Zealand and inland Australia.
- 3) *Develop stochastic population models for reef fish and saucer scallops, which can link physical oceanographic features (e.g. sea surface temperature anomalies) to catch rates, biological parameters (e.g. growth, reproduction, natural mortality) and ecological aspects (e.g. spatial distribution).* Fishery catch rates are standardised for the effect of weather systems in order to produce time series that are believed to more accurately reflect the underlying abundance of coral trout. It is shown that, with current levels of information and oceanographic modelling, the standardisation has to be subjective because the effect of a weather system on catch rates depends critically on the weather system's exact position and size. Availability of physical wave-height measurements, however, makes the standardisation more objective.

21.1 ABSTRACT

This chapter describes tropical cyclones and other weather systems that affect the Great Barrier Reef (GBR) line fishery. It describes a previously published causal mechanism by which some cyclones but not others generate large waves on the GBR, presents wave-height data from both a numerical oceanographic model and direct physical measurements, and finally presents a method of standardising coral trout catch rates for the effect of weather systems. The causal mechanism for large waves involves inshore fetches running southeast to northwest parallel to the coastline, over which strong winds can build large waves. Use of inshore fetches by cyclones overcomes the natural protection afforded by the GBR's outer barrier reefs which efficiently dissipate waves that come from the ocean. No known oceanographic model accurately accounts for either this dissipation or the inshore fetch mechanism; therefore the wave heights predicted from the oceanographic model show only a moderate correlation with coral trout catch rates. Direct measurements of wave height are collated from the Queensland Government's beach monitoring program, data from which date back to 1975, making it a very valuable information source. These measurements help to identify which weather systems are important to the fishery: many of these are in fact not tropical cyclones but systems such as tropical lows, east coast lows, Tasman Sea highs and, occasionally, central Australian highs. Weather systems identified as important are put into a generalised linear model for coral trout catch rates: this model allows each weather event to cause a fall in catch rates over about six months, followed by a recovery over about another six months (months 7–12) back to the rate that prevailed prior to the weather event. Durations for the fall and especially the recovery can be substantially greater than six months for exceptionally powerful cyclones. Notably, after the GBR was struck by three very severe cyclones in successive years (Hamish in 2009, Ului in 2010 and Yasi in 2011), it appears to have taken until 2013 for coral trout catch rates to recover. The end result of the standardisation is a time series of catch rates that we believe is a much more accurate reflection of coral trout abundance than has been available to date.

21.2 INTRODUCTION

Tropical cyclones are known to have a large effect on line fishers' catch rates of the important predator fish common coral trout (*Plectropomus leopardus*) on coral reefs of the Great Barrier Reef (Leigh *et al.* 2014). Catch rates fall immediately after a major tropical cyclone, and remain low for up to several years afterwards. Underwater visual surveys undertaken by divers indicate that the abundance of coral trout is not greatly affected by cyclones: a cyclone appears not to kill large numbers of fish outright, but rather to change their behaviour and make them unwilling to take bait.

Although falls in catch rates following tropical cyclones are obvious in fishery data, correlation with quantitative measurements of cyclones has to date defied analysis. Some cyclones that would be expected to have a major effect on the fishery have no discernible effect, while others expected to be minor have extremely large impacts. Leigh *et al.* (2014) analysed wind energy of cyclones at the fishing location, as a possible explanatory variable for mixing of water from different depths in the sea. They found a statistically significant effect, but the catch rates adjusted for the effect of cyclones remained very close to the unadjusted ones. Therefore the results were not useful as a means of predicting what the catch rates would have been in the absence of cyclones.

This project considered various measurements of tropical cyclones. It initially intended to use the cyclone-induced sea surface temperature (SST) cooling anomaly as a measure of the intensity and impact of tropical cyclones. SST is typically measured by weather satellites and abundant data were available.

The use of SST was made more attractive by the presence of a correlation between SST and seabird prey availability (Peck *et al.* 2004; Erwin and Congdon 2007; Weeks *et al.* 2013), and the ability to make forecasts of SST anomalies months in advance (Spillman and Alves 2009; Hobday *et al.* 2011). For tropical cyclones, however, there is no evidence that the magnitude of the SST cooling anomaly can be predicted more than a day or two in advance. Individual tropical cyclones are not amenable to long-term forecasting.

Oceanographic specialists on and outside the project's steering committee recommended the use of more direct measures of the physical effects of tropical cyclones, such as those used for modelling storm surges (see, e.g., Burston *et al.* 2013). We note that when assessing effects of cyclones on prawn stocks in Western Australia, fishery scientists there use rainfall as an index of seasonal cyclone activity (Nick Caputi, WA Department of Fisheries, personal communication).

Available possible explanations for the depressed catch rates of coral trout that result from a tropical cyclone infer direct physical damage to coral reefs and consequent breakdown of ecosystem processes. We are aware of two potential explanations, neither of which has been experimentally verified:

- Forage fish that form the major prey for coral trout may no longer be able to shelter from predators and hence may become easy prey, removing any need for predators to supplement their diet by taking bait.
- Damaged coral may emit different chemosensory cues to those of healthy coral, which may act as a signal for widespread slowing down of metabolisms across the coral-reef ecosystem (suggested by Mr Chris Neill, reef line fisher and member of the project's steering committee).

We expected such explanations to be closely correlated to the height of swells generated by tropical cyclones. Importantly, wave height increases with the fetch length over which cyclonic winds blow, which is an important factor not taken into account by Leigh *et al.* (2014).

To this end, we acquired oceanographic data on wave heights generated by tropical cyclones (Marjietta L. Puotinen, 2014, unpublished data). The model that generated these data had been used by the Great Barrier Reef Marine Park Authority (GBRMPA) to provide broad warning signals after a tropical cyclone as to the parts of the Great Barrier Reef that might be affected by the cyclone. This article in part presents the correlation of these data with catch rates of coral trout.

The analysis uses the Reef Bioregions defined by expert committees assembled by GBRMPA; these are illustrated in Figure 21-1. Some of the Bioregions were divided into two or more parts from north to south, called Sub-bioregions, as in Leigh *et al.* (2014). The Subregions on which these divisions were based are shown in Figure 21-2.

The project then took a turn that was unexpected at the outset: it focussed on a hitherto overlooked mechanism which not only explained the impact of tropical cyclones on the coral trout fishery, but also explained why some very powerful cyclones had no discernible effect and why correlations based on meteorological data offshore of the Great Barrier Reef were so poor. The evidence for this mechanism became, in the end, a major output of the reef-fish related part of the project.

The project also found that some of the biggest impacts of weather systems on the fishery stemmed not from tropical cyclones but from low-pressure cells that did not meet the criteria for tropical cyclones and hence were not recorded in the commonly-used cyclone databases.

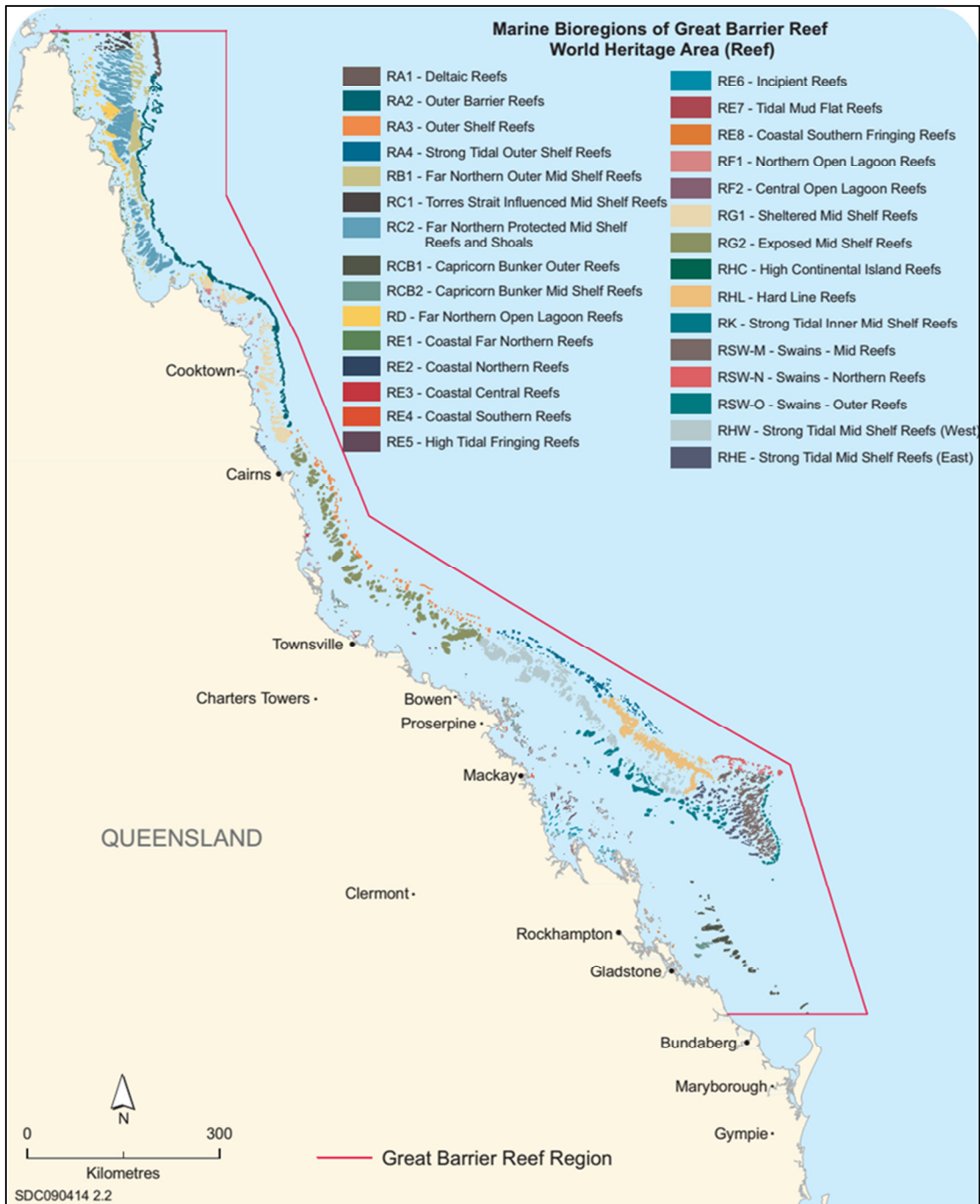


Figure 21-1. Reef Bioregions defined by GBRMPA expert committees as part of the preparation for the Representative Areas Program implemented in 2004. Source: GBRMPA (2009).

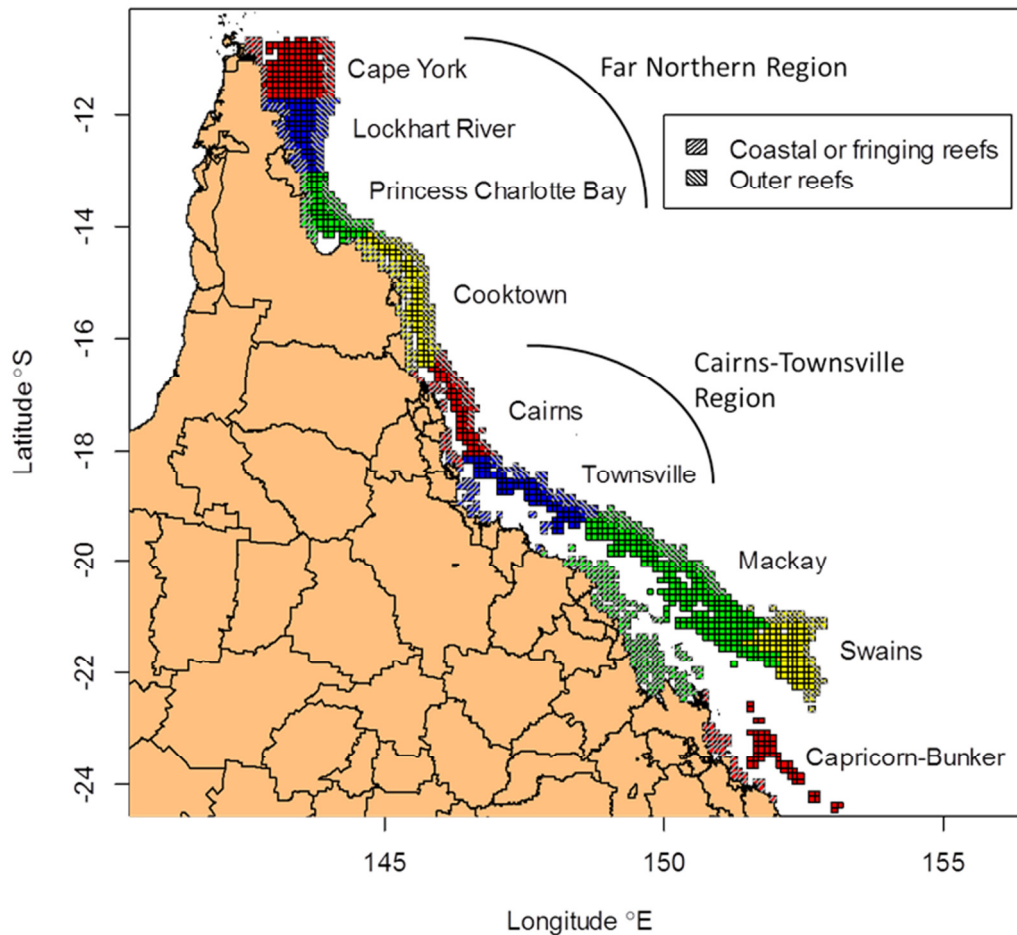


Figure 21-2. Map showing the Regions and Subregions of the GBR used by Leigh *et al.* (2014), which were used to divide the northern Reef Bioregions from Figure 21-1 into Sub-bioregions. Regions are based on the Reef Bioregions, and two of the northern Regions are split into Subregions by latitude to account for increases in fishing intensity from north to south: the Far Northern Region is divided into three Subregions, and the Cairns–Townsville Region is divided into two Subregions. The small squares on the map are six-nautical-mile fishery logbook grid squares. Colours are chosen only to distinguish the Regions and Subregions, and have no other meaning. Source: Leigh *et al.* (2014).

21.3 OBSERVATIONS FROM PREVIOUS ANALYSIS

It was already known which tropical cyclones were the most important to the Great Barrier Reef (GBR) fishery between the mid-1990s and 2013 (Leigh *et al.* 2014, p. 71, Fig. 22). Both statistical catch-rate analysis and comments from commercial fishers indicated that cyclones Justin (1997), Hamish (2009) and Yasi (2011) had the biggest effects. The major problem was to explain why these cyclones had such big impacts on the fishery but other equally powerful cyclones had very little impact.

Although the sample of highly influential cyclones consists of only three members, they were very different in character, making the sample informative:

- Justin was very large and long-lived, but not of exceptional strength, especially when it was near the GBR, and spent most of its life at least 340 km to the northeast of the GBR
- Hamish was small but extremely powerful and long-lived, and moved parallel to and close to the GBR
- Yasi was extremely large and also extremely powerful, but spent only a short time on or near the GBR.

In general there is an inverse correlation between the size of a cyclone and the strength of its winds: small cyclones usually produce stronger winds than large ones (Callaghan 2011b). Yasi was an exception to this rule, being both large and powerful. From these three cyclones, we were able to infer the following conclusions about cyclones that have major effects on the coral trout fishery:

- Great strength is not necessary.
- Long times spent on or near the GBR appear to produce larger effects.
- Long times are not necessary if the cyclone is extremely large and powerful.
- Cyclones spending time northeast of the GBR have the biggest effects on it.
- The effect of a major cyclone is very wide-ranging, covering most of the central and southern parts of the GBR.

We note that Yasi formed over the Pacific Ocean about 2300 km to the east, three days before it hit the GBR. It could have had time to generate big seas even while it was a long way from the GBR.

Because the cyclones kept moving throughout their lives, it was impossible to distinguish whether the time effect was due to time spent over a particular location or simply to the large area affected as the cyclone moved.

A new analysis of the data used by Leigh *et al.* (2014) (section 21.4.2 below) showed that the effect of cyclones on fishery catch rates drops off markedly north of Townsville. In the Cairns locality there is an effect substantially less than that in Townsville, but north of Cairns there were no noticeable effects of cyclones on coral trout catch rates.

A list of significant tropical cyclones to hit the GBR since the commercial logbook system began is provided for reference in Table 21-1. Many of these cyclones, although powerful, had no discernible effect on the fishery.

Appendices – Cyclone influences on reef fish

Table 21-1. Cyclones with winds of gale force (17 ms^{-1}) or above to affect the GBR since 1988. Location is roughly classified as North (Cape York to Cairns Subregions), Central (Townsville Subregion and Whitsunday Islands) or South (Mackay Region south of the Whitsundays, to Swains or Capricorn–Bunker); P_{\min} = minimum central pressure (hPa); V_{\max} = maximum wind speed (ms^{-1}). Note that P_{\min} and V_{\max} are taken over the life of a cyclone, including times when it is not impacting the Great Barrier Reef. Cyclones with high numbers of four-metre wave locations in Table 21-2 below are listed in boldface. Source: Leigh et al. (2014), original data from Australian Bureau of Meteorology (BoM) and Joint Typhoon Warning Center (JTWC) Best Tracks databases.

Name	Dates	Location	P_{\min}	V_{\max}
Charlie	21–29 Feb 1988	Central	972	21
Aivu	01–04 Apr 1989	Central	935	62
Meena	05–10 May 1989	North	990	26
Felicity	15–18 Dec 1989	North	975	31
Hilda	04–08 Mar 1990	South	970	31
Ivor	16–22 Mar 1990	North	965	39
Joy	19–26 Dec 1990	Central	940	46
Kelvin	25 Feb – 5 Mar 1991	North	980	28
#18	20 Feb 1992	South	NA	18
Betsy	06–15 Jan 1992	South	949	49
Mark	08–10 Jan 1992	North	980	28
Fran	06–17 Mar 1992	South	898	72
Nina	23 Dec 1992 – 04 Jan 1993	North	960	39
Oliver	04–12 Feb 1993	South	950	59
Roger	12–22 Mar 1993	South	980	28
Rewa	28 Dec 1993 – 21 Jan 1994	South	920	64
Celeste	26–29 Jan 1996	Central	965	33
Dennis	13–17 Feb 1996	North	990	23
Ethel	08–13 Mar 1996	North	980	23
Gillian	10–12 Feb 1997	Central	995	23
Ita	24 Feb 1997	Central	994	18
Justin	06–25 Mar 1997	Central	974	55
Katrina	02–24 Jan 1998	North	940	46
Nathan	21–30 Mar 1998	North	990	33
Rona	10–12 Feb 1999	North	970	28
Steve	26 Feb – 01 Mar 2000	North	975	23
Tessi	01–02 Apr 2000	Central	980	26
Vaughan	03–06 Apr 2000	North	975	26
Abigail	24–27 Feb 2001	North	970	33
Fritz	10–12 Feb 2004	North	985	25
Grace	21–22 Mar 2004	South	997	18
Ingrid	06–12 Mar 2005	North	910	67
Kate	22–23 Feb 2006	North	985	26
Larry	18–20 Mar 2006	North	937	59
Monica	17–24 Apr 2006	North	916	80
Guba	13–19 Nov 2007	North	967	39
Ellie	31 Jan – 01 Feb 2009	North	996	18
Hamish	05–11 Mar 2009	South	922	69
Olga	22–30 Jan 2010	North	989	23
Ului	11–21 Mar 2010	Central	918	72
Tasha	24–25 Dec 2010	North	993	21
Anthony	23–30 Jan 2011	Central	989	28
Yasi	30 Jan – 03 Feb 2011	Central	922	69
Oswald	17–28 Jan 2013	North	988	18
Tim	13–19 Mar 2013	South	984	26
Zane	29 Apr – 01 May 2013	North	983	31
Dylan	30 Jan 2014	Central	975	28
Edna	31 Jan – 05 Feb 2014	South	992	21
Ita	01–14 Apr 2014	North	930	59

21.4 THE CAUSAL MECHANISM

21.4.1 Description

A mechanism that explains the above observations is provided by Callaghan (2011a) in connection with Cyclone Justin. We are not aware of any other published source that mentions it:

“Large waves are rarely observed along the tropical east coast waters of Queensland due to the protection by the Great Barrier Reef and the limited lengths of open water. During 9 March 1997 and 10 March 1997 some very large wave heights were reported between Rockhampton and Townsville. ...

“There is a large opening (Capricorn Channel) in the southeastern end of the reef through which wave energy can pass. The wind observations [of Cyclone Justin] show a large area of gales of relatively constant direction extending from around Hayman Island to the Capricorn Channel, a distance of some 500 km. Gales blowing over a body of deep open deep water 500 km long for 18 hours can generate waves up to 6 metres in height. The wind field was similar at 1100 UTC 8 March 1997 and at 2300 UTC 9 March 1997 so that constant gales were blowing over the one body of water for more than 36 hours. The wind direction was orientated along the longest fetch of water inside the reef. This explains the occurrence of these waves which would even be considered large in the open ocean.

“North of the Whitsunday Island Group the coastline changes orientation such that the large southeasterly swell remained offshore moving parallel to the coast. This resulted in lower height readings at coastal wave recording stations. Significant wave heights [average height of the highest one-third of waves in a record] reached only 1.5 metres at Abbot Point (near Bowen) and 1.4 metres at Townsville during this period [as opposed to 3.09 m at Emu Park, 3.10 m at Hay Point, 4.81 m at Mackay Offshore and 3.85 m at Lindeman Island].”

Considering the fishery, we note that, although the wave heights may be lower at the inshore stations at Townsville and Bowen, the waves generated along the southeast to northwest inshore fetch of the GBR will make a direct hit on the prime fishing grounds on the GBR between Bowen and Townsville (the southern half of Bioregion RG2 in Figure 21-1).

21.4.2 Explanation

The explanation for the major effect of some cyclones and the complete lack of effect of other powerful cyclones is therefore as follows:

- The GBR is very well adapted to dissipate large swells coming from offshore, and generally does not suffer significant damage from such swells.
- In special circumstances, cyclones generate large southeasterly swells *along the inshore fetch* of the GBR between Rockhampton and Townsville. The mid-shelf reefs of the GBR, where the fishery is primarily situated, are extensively damaged by these swells.
- The nature of this mechanism, which consumes the entire fetch from Yeppoon to Townsville, means that the affected area of the GBR is very large.
- The fetch takes a slight left-hand bend heading from Bowen to Townsville (see Figure 21-1). The swell is directed straight at the fishing grounds in this locality, and has a big effect there, in addition to its effects further south.
- The fetch then takes quite a sharp right-hand bend heading to Cairns, and also becomes much narrower. Wave generation inshore of the GBR is much less effective north of Townsville, and cyclones have no significant effect on the fishery in the northern part of the GBR.

21.4.3 Predictions

Following the scientific method, whereby a theory should include predictions that can be checked, on the basis of the above explanation we expect the following:

- The magnitude of a cyclone’s impact on the fishery is essentially a random event, sensitive to the exact position and size of a cyclone, and is impossible to predict before the cyclone strikes. A small fraction of cyclones will have major impacts on the GBR. Most cyclones will have only minor effects, even though they may appear very similar to the important cyclones.
- Immediately after the event, the effect that a cyclone will have on the fishery can be fairly accurately predicted from the wave heights recorded inshore of the GBR, such as the recording stations maintained by the Queensland Government at various locations between Cairns and Brisbane and used by Callaghan (2011a). Analysis of a cyclone’s generation of swells offshore of the GBR is usually not necessary.

21.5 ANALYSIS OF WAVE HEIGHT DATA FROM AN OCEANOGRAPHIC MODEL

21.5.1 Methods

Data on wave heights (Puotinen, 2014, unpublished data) induced by tropical cyclones came from an oceanographic model. Such models are quite complex and involve various types of approximations, which differ between models. The important aspect to note, however, is that the model was not fetch-limited: it assumed that the length of fetch in the ocean over which waves could be generated was always adequate, and hence that wave heights were limited only by wind speed and the length of time of exposure to cyclonic winds. It is unclear to what extent an oceanographic model could consider the capability of coral reefs to dissipate waves, because reef tops are positioned at approximately sea level and the only mapping data available, even for the intensively-mapped GBR, provide outlines of “dry reef” which projects above sea level, and “wet reef” which is permanently submerged down to a depth of roughly 15 metres. No comprehensive data set exists to provide reef depth as a function of location.

The wave-height data set covered a fine (about two-nautical-mile) grid of locations, and comprised the estimated number of hours over which waves of a certain height were present at each location. The data covered the period from February 1985 to April 2014.

The tropical cyclone data consisted of two data files for each calendar month: one for a sea state of waves two metres or more in height, and one for a state of waves four metres or more. The sea state measurement was the “significant wave height”, commonly denoted H_{sig} , which was the average height of the highest one-third of waves; the technical definition of the height of an individual wave is that it is measured from peak to trough between successive zero up-crossings. The maximum wave height, commonly denoted H_{max} , is usually about two and a half times H_{sig} . Usually only one significant cyclone affected the GBR in any calendar month, but occasionally there were two in one month: notably, Tropical Cyclone Anthony in January 2011 was followed almost immediately by Severe Tropical Cyclone Yasi.

Firstly it had to be decided which cyclone measurements to use. Any of six obvious measures could turn out to be the most suitable, all of which were physically sensible. These were two-metre and four-metre versions of

- Maximum number of hours for which any location was subject to waves of the specified height
- Total hours of waves of the specified height, summed over all locations
- Number of locations over which waves of the specified height were present, irrespective of the number of hours.

The observations from section 21.3 above were used to inform the selection of which measurements to use for analysis.

The selected cyclones’ measures were then condensed down to the six-nautical-mile grid cells used in the fishery for catch reporting, and plotted against standardised fishery catch rates. In order to

concentrate on locations that were actually part of the fishery, each grid cell was weighted by the total logbook harvest that had been taken in it. Separate totals were used for the period January 1988 to June 2004 and the period July 2004 onwards, in order to account for the Representative Area Protection (RAP) program implemented by GBRMPA in July 2004. The RAP greatly increased the amount of area of the Great Barrier Reef that was closed to fishing.

For the catch-rate standardisation, we repeated the analysis of Leigh *et al.* (2014) with updated fishery logbook data to provide standardised catch-rate time series to the end of 2014, and to derive such a time series for each Sub-bioregion. The previous catch rate series ranged from mid-1991 to the end of 2013. The commercial catch logbook system began in January 1988, but in the early years most fishing locations were recorded only to 30-nautical-mile resolution, which was judged by Leigh *et al.* (2014) to be insufficient for statistical catch-rate analysis in a complex coral-reef system. Substantial numbers of records at six-nautical-mile resolution were available from mid-1991 onwards.

21.5.2 Results

21.5.2.1 Selection of cyclone measures

Cyclone data from 2013 and 2014 were particularly valuable in informing the selection of cyclone measures. In the two-metre wave data, Cyclone Oswald in January 2013 had by far the largest value both of total hours of two-metre waves summed over all locations and of total number of locations affected, and it had the third greatest value of maximum number of hours in any location (see Table 21-2). Judging from logbook catch rates, Cyclone Oswald had very little effect on availability of coral trout to fishers. Also Cyclone Yasi, which was known to have had a major effect on the fishery, scored low on two-metre wave measurements. Therefore data on two-metre waves appeared not to be beneficial in analysis of the effects of tropical cyclones on the fishery.

In the four-metre wave data, Cyclone Oswald did not register at all, which is in accord with observations of catch rates. In the maximum number of hours of four-metre waves at any location, Hamish ranked only tenth and Yasi 17th: hence this measurement does not appear to be useful. In total number of hours over all locations, Yasi ranked only 13th. In number of locations affected for one hour or more, Yasi ranked sixth and Justin seventh. This measurement appeared to be the most useful. In view of the above results, we decided to concentrate on analysis based on the presence or absence of four-metre waves, to downplay the two-metre wave data and to ignore the measurements that involved the length of time over which waves were present. The presence–absence measure of four-metre waves is also in accord with the hypothesis that it is physical damage to coral reefs that affects catch rates of coral trout. Coral reefs have evolved to withstand strong movements of water, and to damage them wave action must exceed a high threshold. If the threshold is exceeded, we would expect the damage to occur quickly and not increase greatly if the wave action is sustained at the same level for a few days.

From the immense size and power of Cyclone Yasi, we expect that it would have generated waves much larger than four metres, which would cause much more damage than waves of barely four metres. Therefore the effect of Cyclone Yasi may be underestimated.

21.5.2.2 Correlation with fishery catch rates

Monthly time series of standardised fishery catch rates are plotted for the Sub-bioregions with substantial amounts of fishing activity in Figure 21-3. The standardisation fitted a separate parameter for each primary fishing vessel, and parameters for the number of fishing dories and number of crew employed. The standardised catch rates are scaled to roughly average to 1 within each Sub-bioregion. The correlations between cyclone events and standardised catch rates can be seen to be poor in most cases. Many cyclones registered high in modelled wave-height but appeared to have no effect on the fishery, while a few cyclones had obvious big effects extending to Sub-bioregions in which their modelled wave-heights did not register. Hence we did not consider it worthwhile to undertake any further quantitative statistical analysis. The following features are notable, however:

Table 21-2. Some tropical cyclones to hit the GBR between 1985 and 2014, with their measurements based on wave-height. The month is that in which the cyclone formed, not necessarily when its impact was greatest. Measurements listed are the maximum number of hours of large enough waves at any location, total number of hours summed over all locations (k = 1000), and number of locations subject to large enough waves for one hour or more. Numbers in parentheses are ranks in the collection of all cyclones to hit the GBR in the period, and are shown when one or more cyclones not listed in the table have a higher rank.

Name	Month	2m wave-height measurements			4m wave-height measurements		
		Max. hours	Tot. hours	No. locs	Max. hours	Tot. hours	No. locs
Joy	Dec 1990	83	225k	7172	74	165k	6200
Fran	Mar 1992	67	202k	7551	58	138k	6402
Rewa	Dec 1993	42 (6)	144k	8445	33 (5)	79k	6751
Justin	Mar 1997	48	121k	9068	40	62k	4019
Hamish	Mar 2009	30 (12)	240k	14266	20 (10)	139k	11492
Yasi	Jan 2011	15 (20)	62k (11)	6066	9 (17)	24k (13)	4414
Oswald	Jan 2013	52	569k	23280	0	0	0
Dylan	Jan 2014	34 (10)	178k	10258	NA	NA	986 (22)
Ita	Apr 2014	35 (9)	168k	15788	26 (8)	72k	4845

- Correlations are exceptionally poor in the northern GBR. Cyclones very rarely affect catch rates there.
- Cyclone Hamish (March 2009), however, appears to have a consistent effect in the northern Sub-bioregions, even though the wave-height data do not show even two-metre waves there. This may be a genuine effect caused by the combination of Hamish’s power and proximity to the GBR, but it is also possible that it is induced by fishers moving from the southern to the northern GBR because they were unable to catch fish in the south. The far northern GBR requires specialised fishing skills, which these fishers may not have possessed.
- Cyclones Hamish and Yasi (January 2011) both have big effects from Cairns south, including in Sub-bioregions where the wave-height data for Yasi did not show even two-metre waves.
- Cyclone Ita (April 2014) also appears to have a big effect from Townsville south, and possibly also in the Cairns Subregion.
- Cyclone Justin (March 1997) has a big effect from Mackay south, but is not so clear in the Cairns and Townsville Subregions.
- The Swains Region is noticeably affected by cyclones but less than the Townsville Subregion and the Mackay Region.
- Cyclone Rewa (December 1993) appears to have an effect in the Swains Region.
- No cyclones other than Rewa, Justin, Hamish, Yasi and Ita showed consistent effects on catch rates.
- The catch rate time series showed substantial rises and falls that could not be associated with any cyclones.

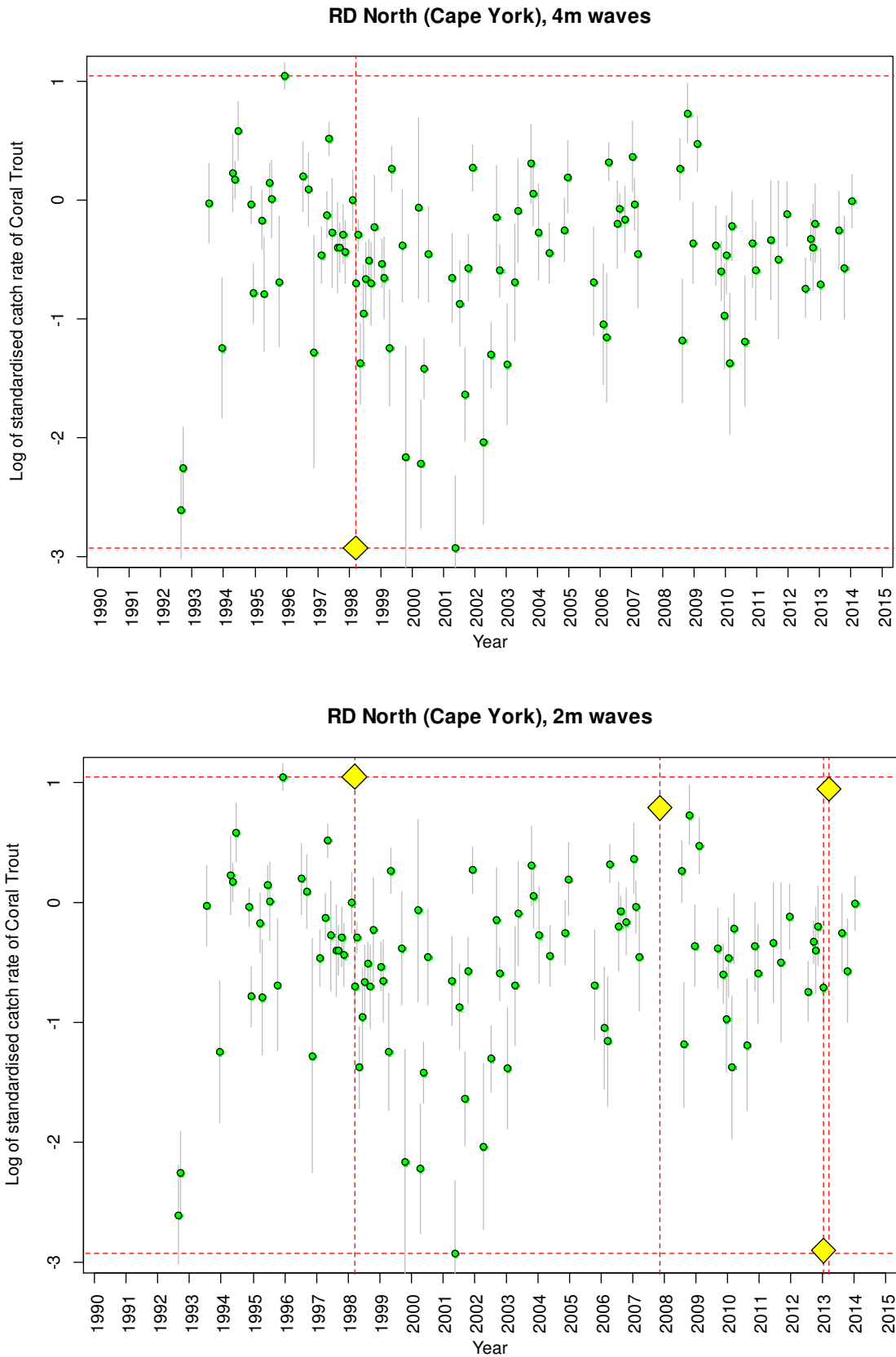


Figure 21-3. Monthly time series (green dots) of standardised catch rates of coral trout in the commercial fishery on the GBR, for each Sub-bioregion. The grey bars show standard errors. The yellow diamonds show the proportions of Sub-bioregion area affected by 4 m or 2 m waves: the lower horizontal red dotted line represents zero area, and the upper one represents 100% of the Sub-bioregion area. (Continued next 19 pages)

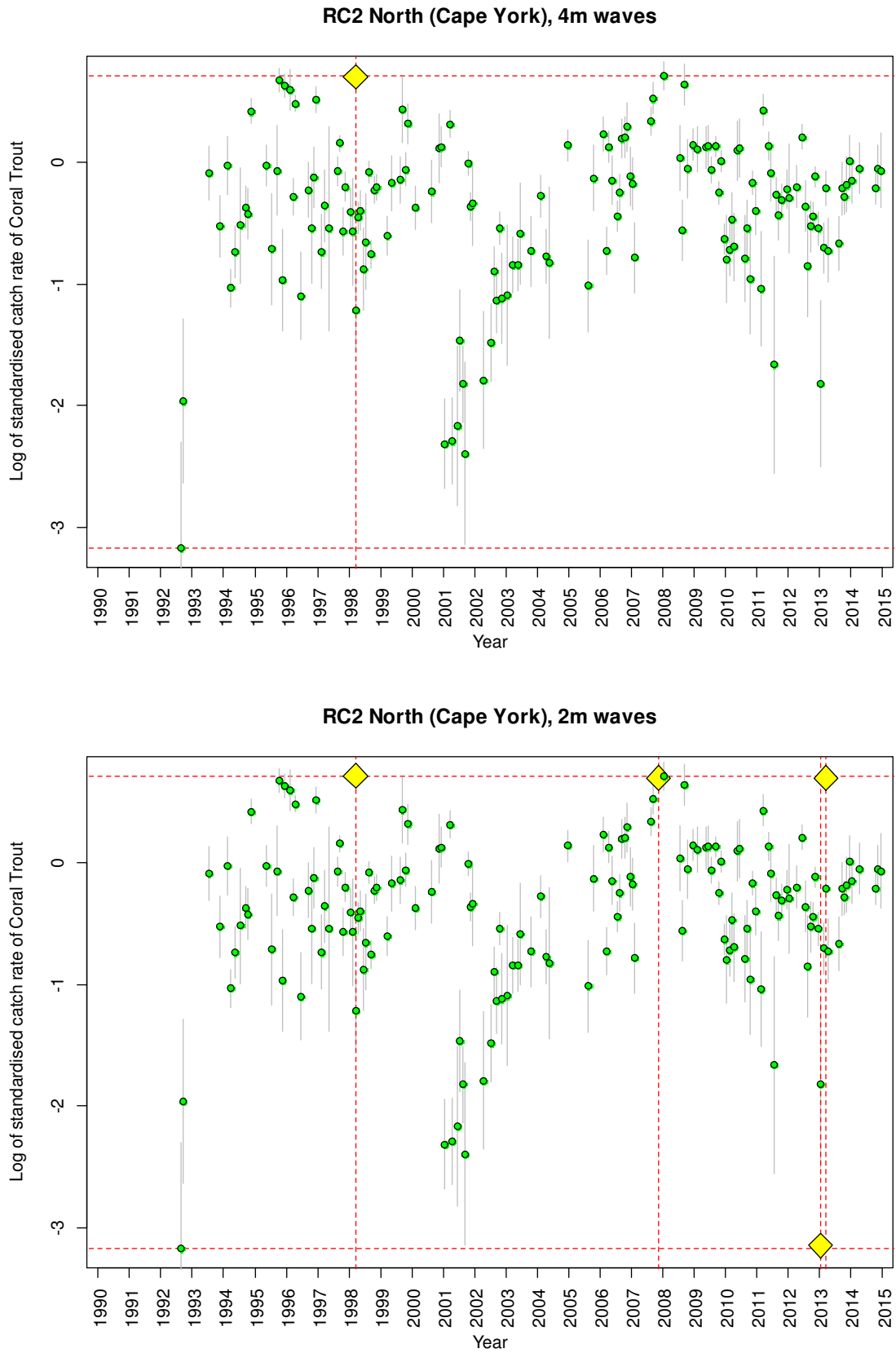


Figure 21-3, continued from previous page and on next 18 pages.

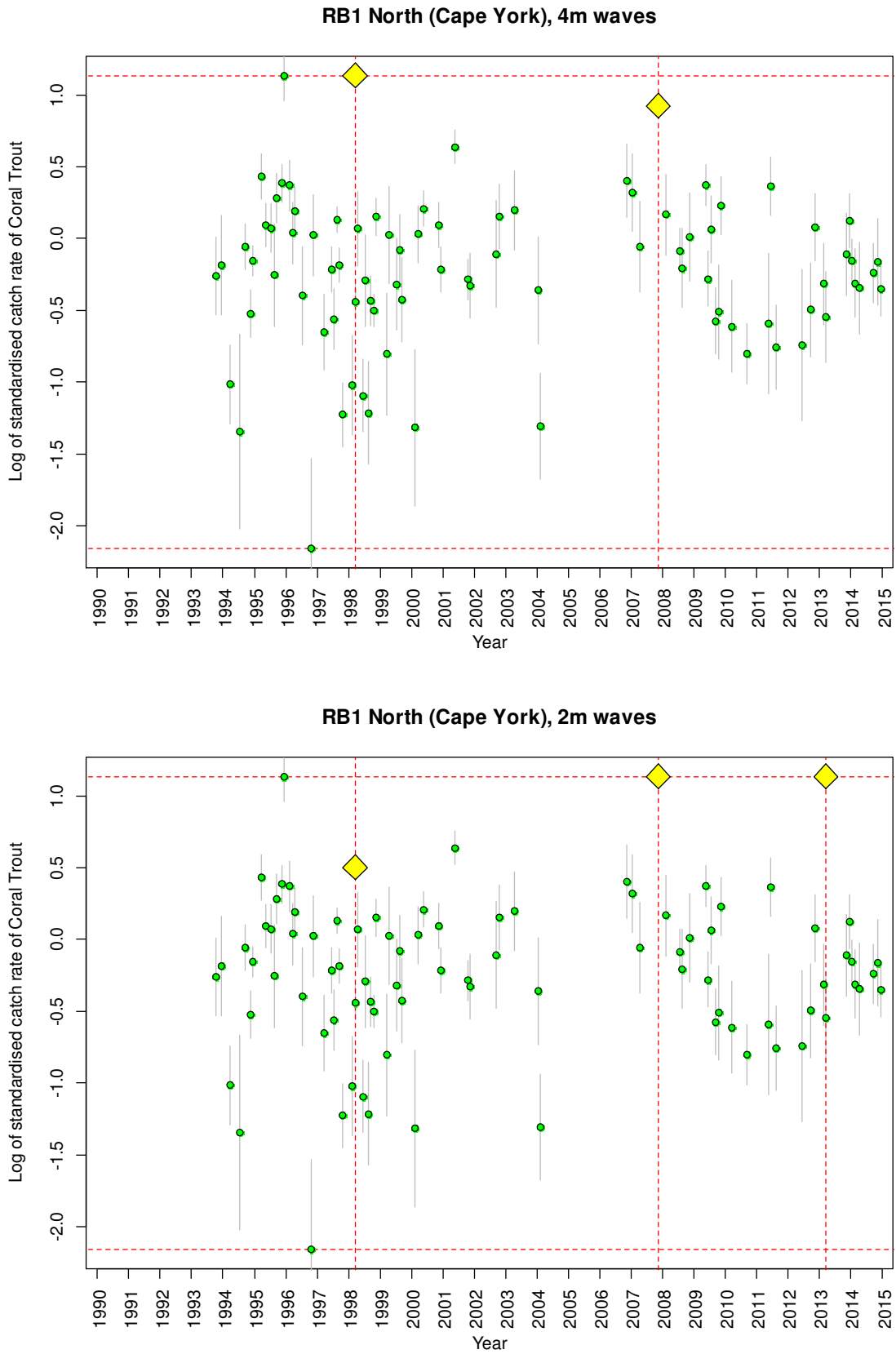


Figure 21-3, continued from previous 2 and on next 17 pages.

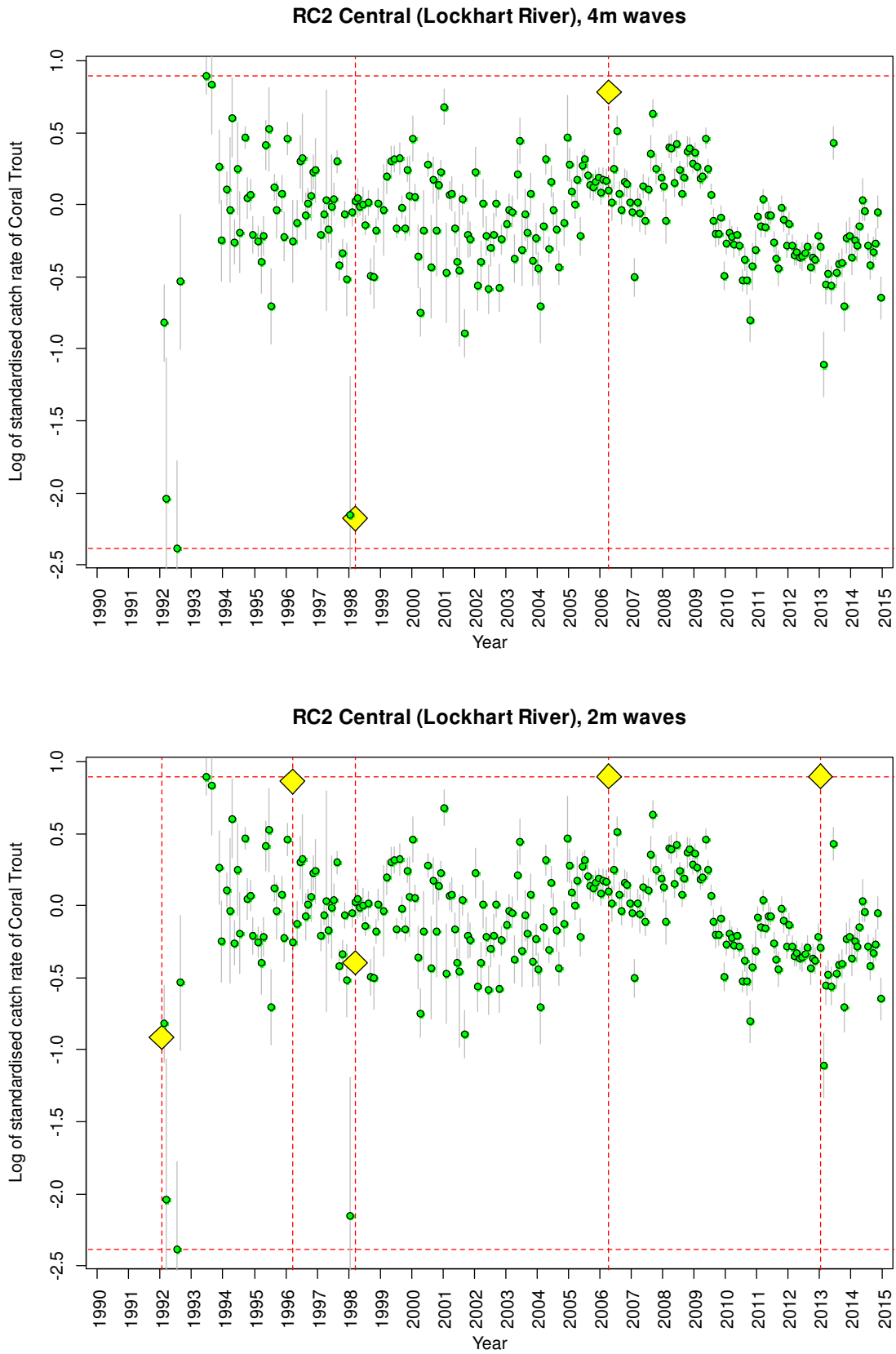


Figure 21-3, continued from previous 3 and on next 16 pages.

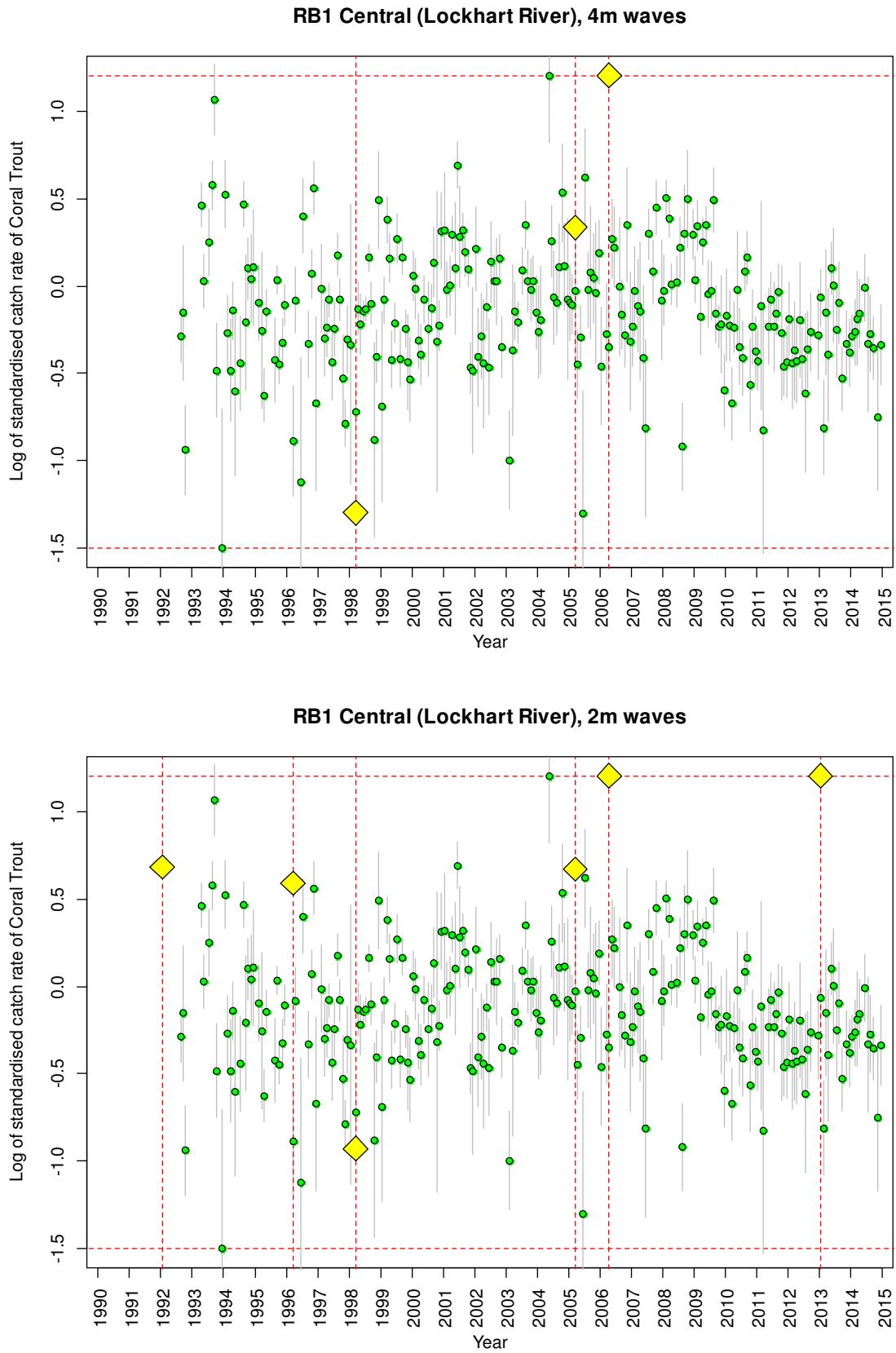


Figure 21-3, continued from previous 4 and on next 15 pages.

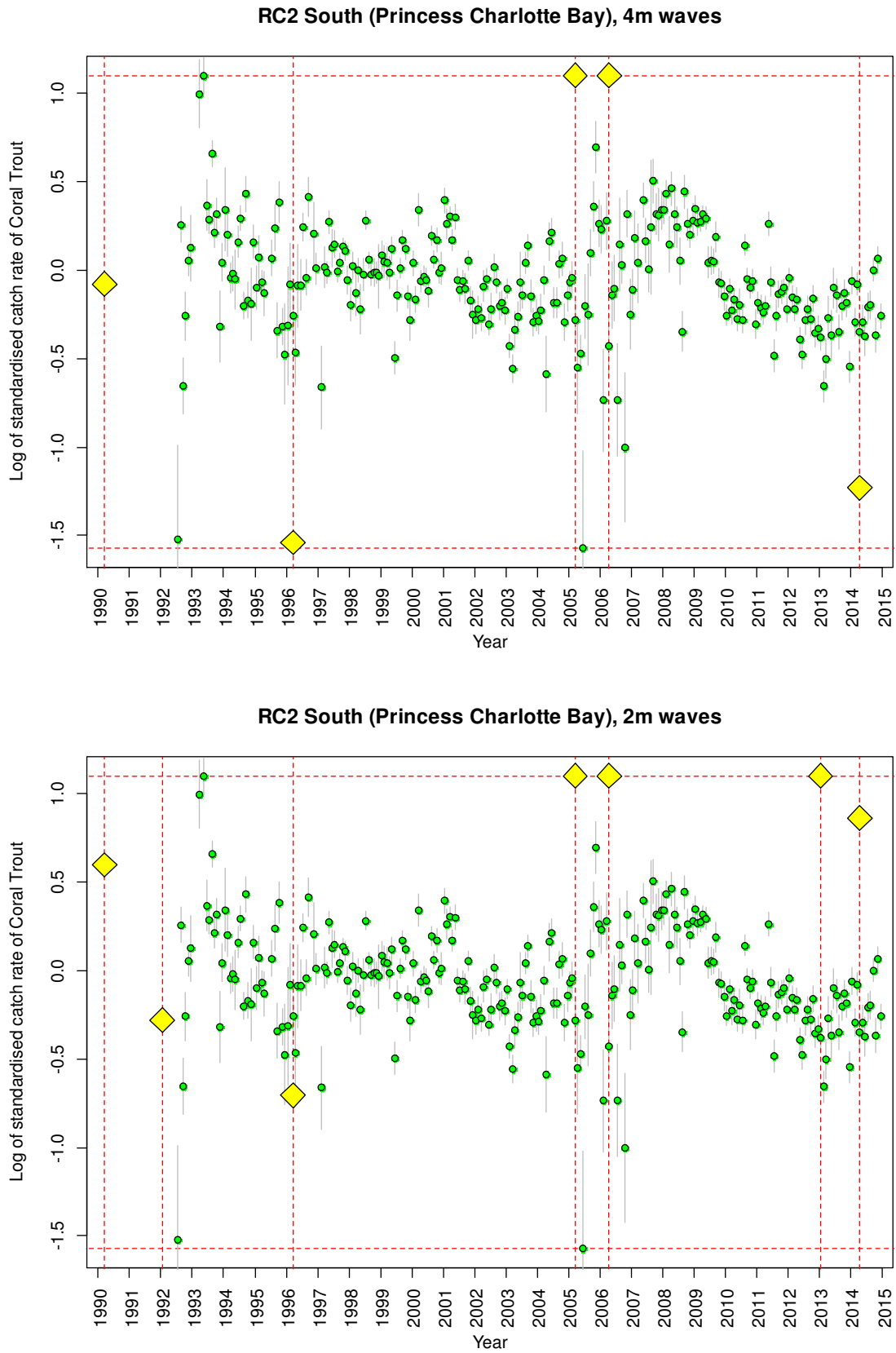


Figure 21-3, continued from previous 5 and on next 14 pages.

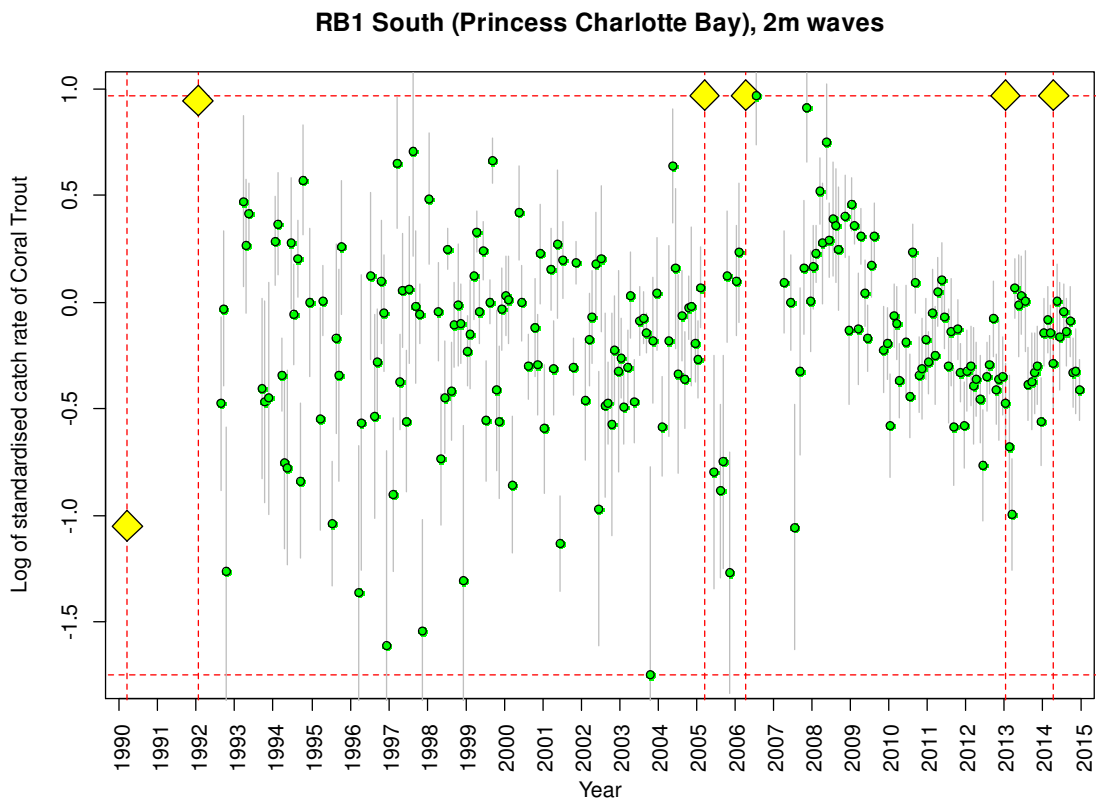
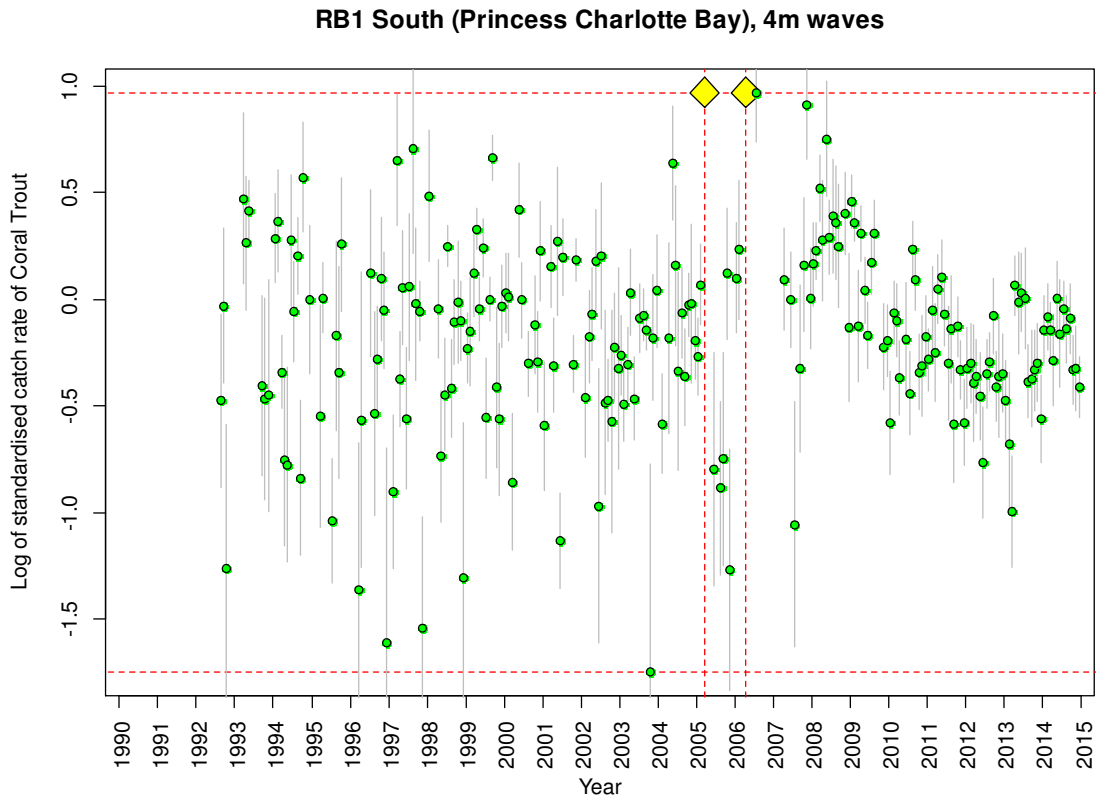


Figure 21-3, continued from previous 6 and on next 13 pages.

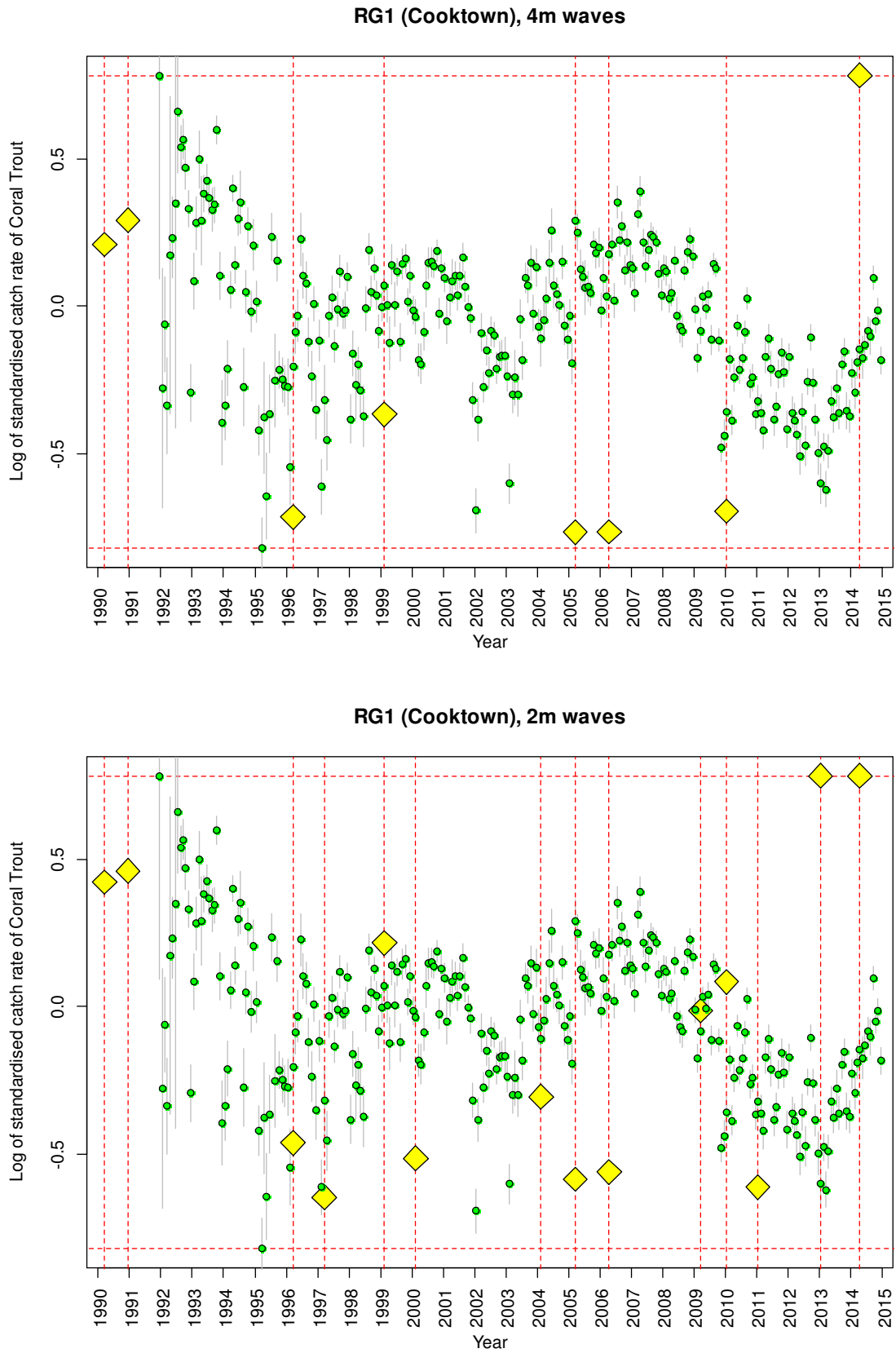


Figure 21-3, continued from previous 7 and on next 12 pages.

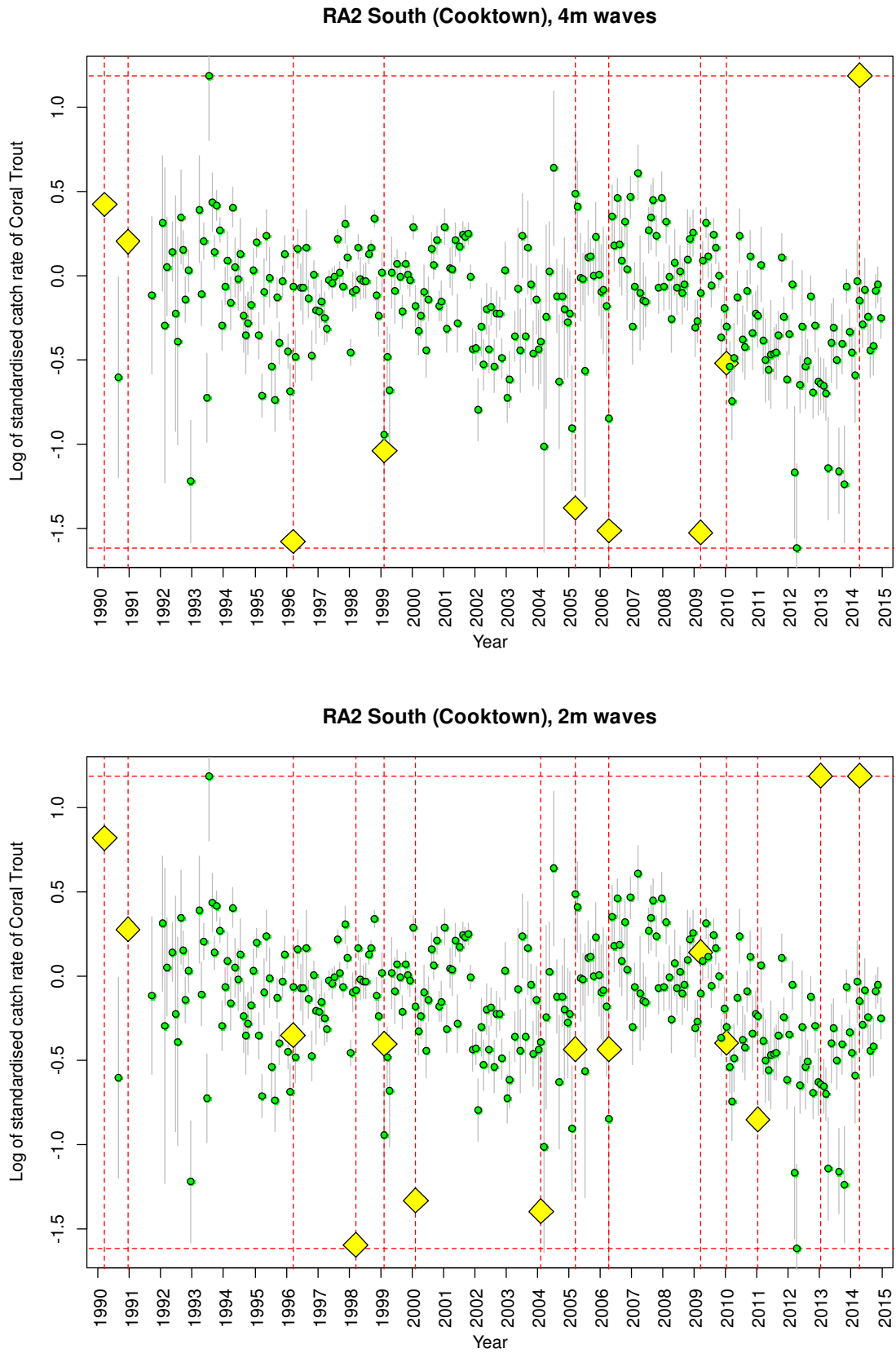


Figure 21-3, continued from previous 8 and on next 11 pages.

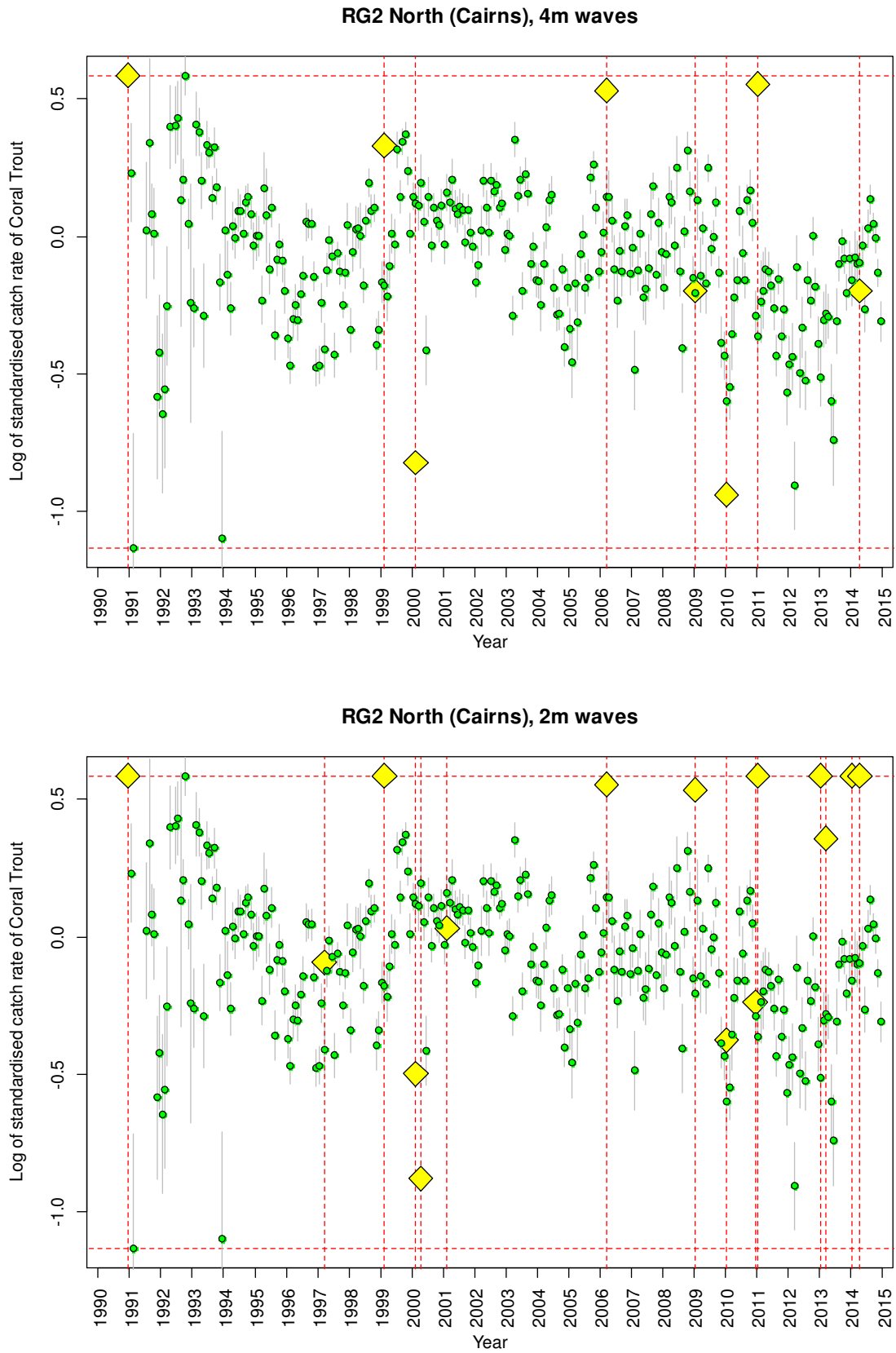


Figure 21-3, continued from previous 9 and on next 10 pages.

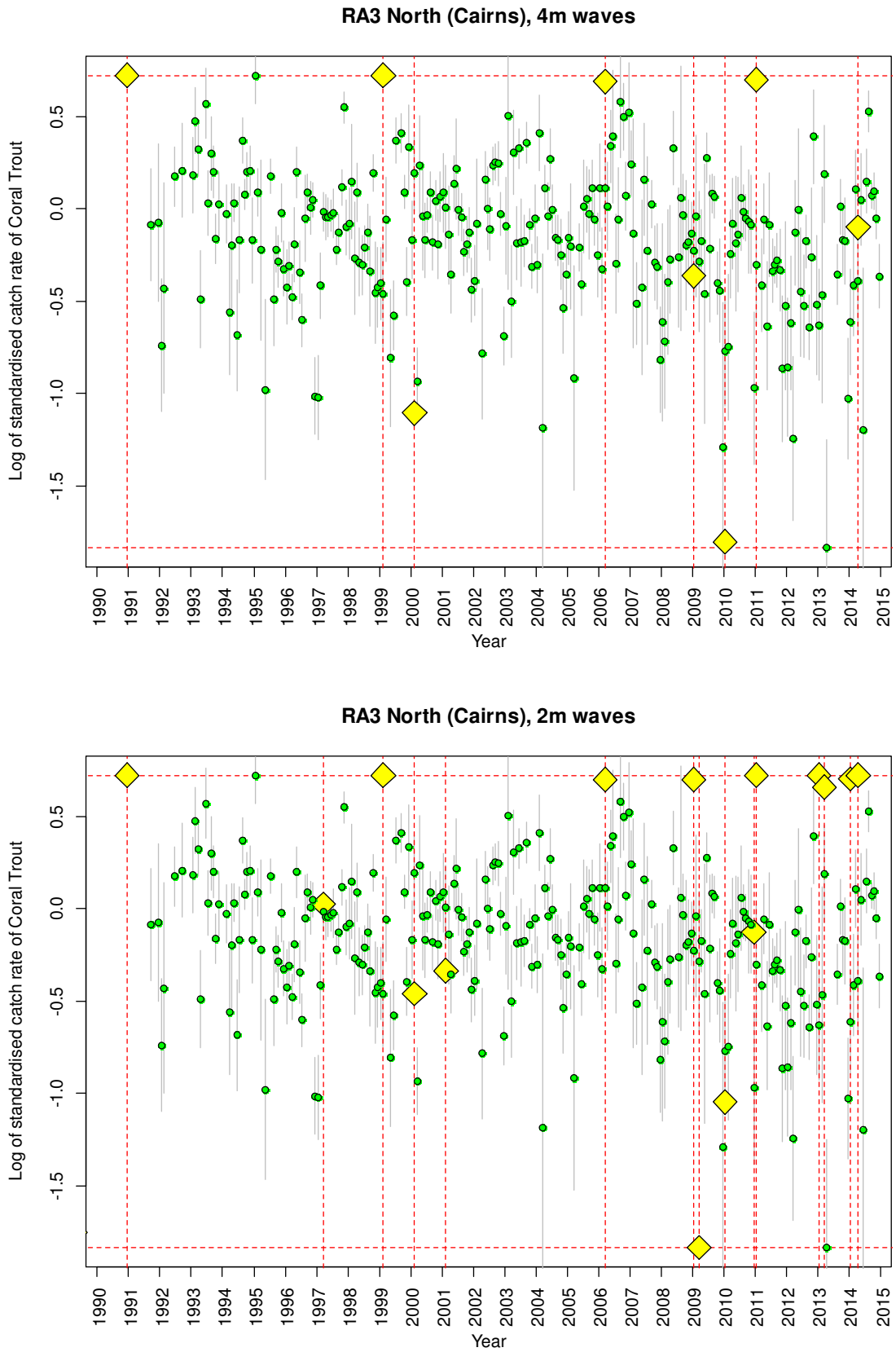


Figure 21-3, continued from previous 10 and on next 9 pages.

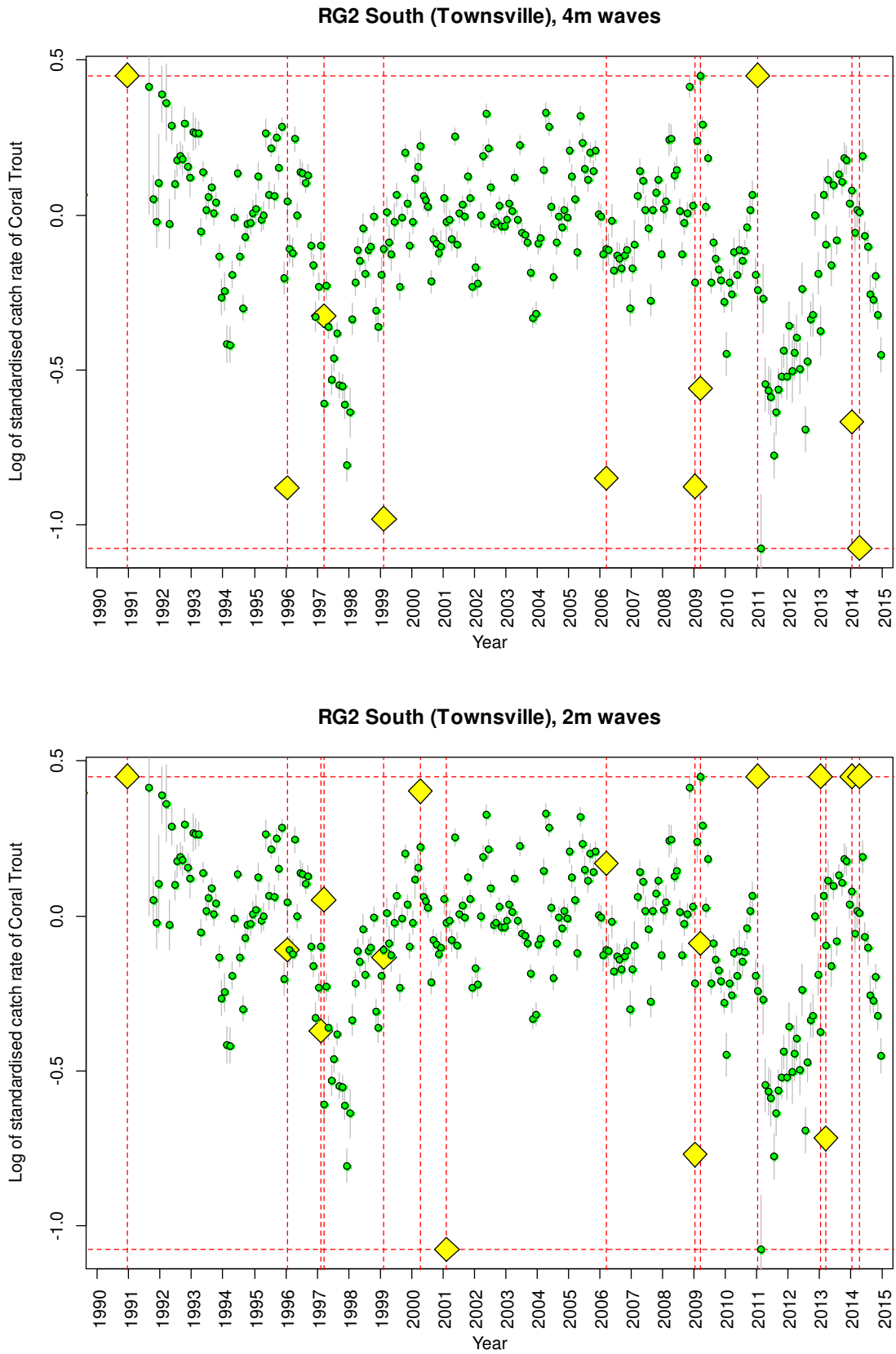


Figure 21-3, continued from previous 11 and on next 8 pages.

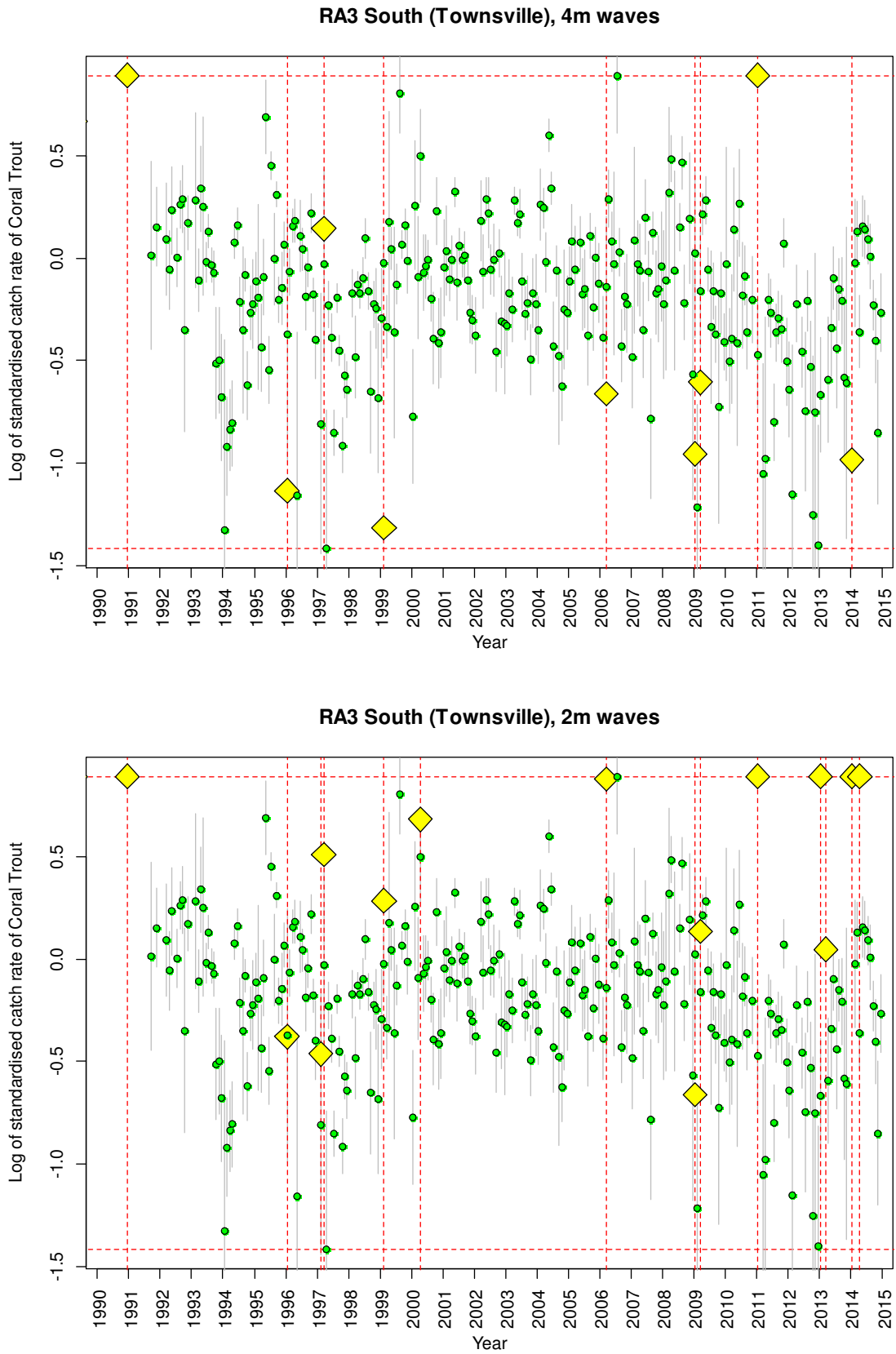


Figure 21-3, continued from previous 12 and on next 7 pages.

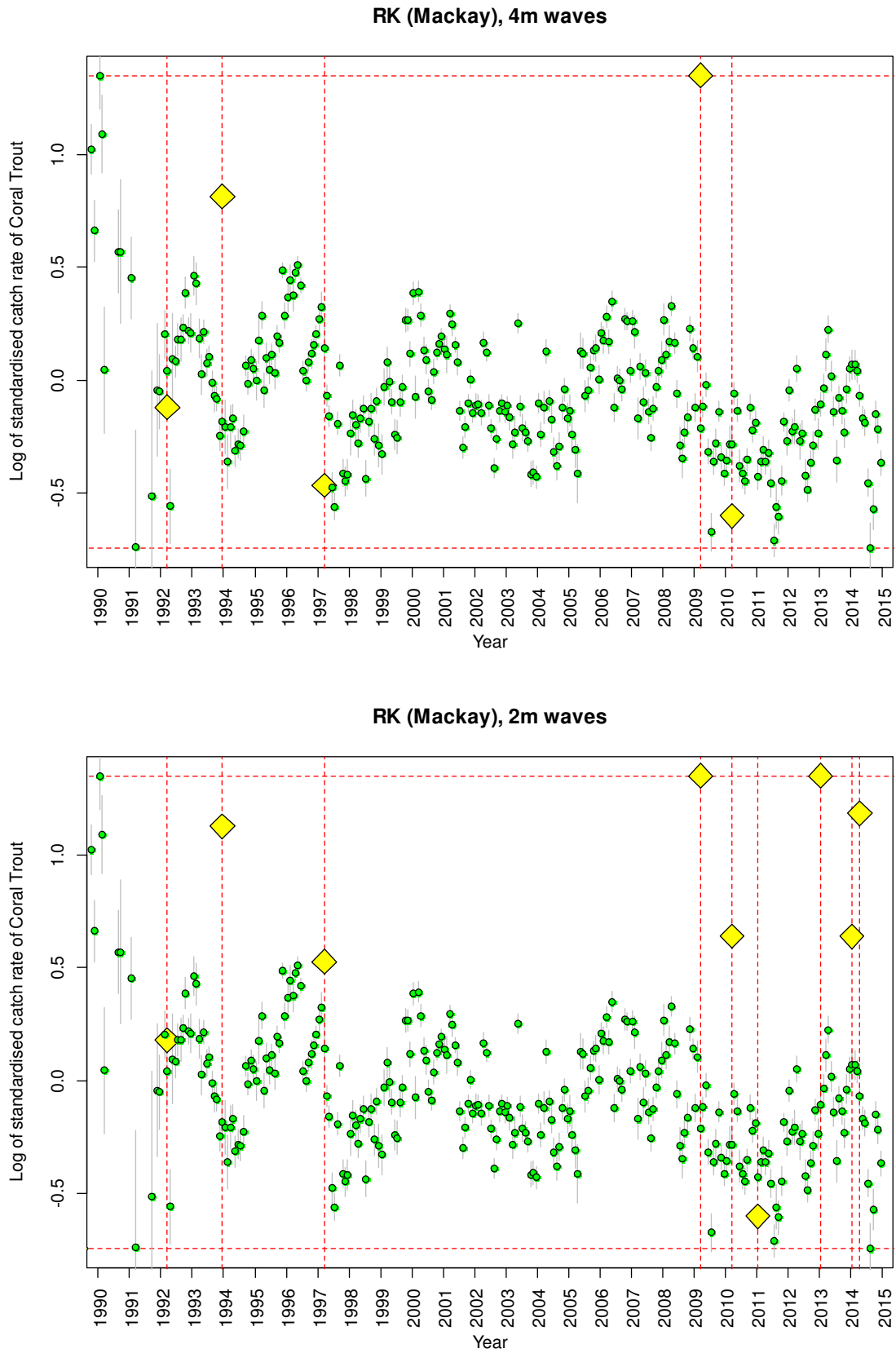


Figure 21-3, continued from previous 13 and on next 6 pages.

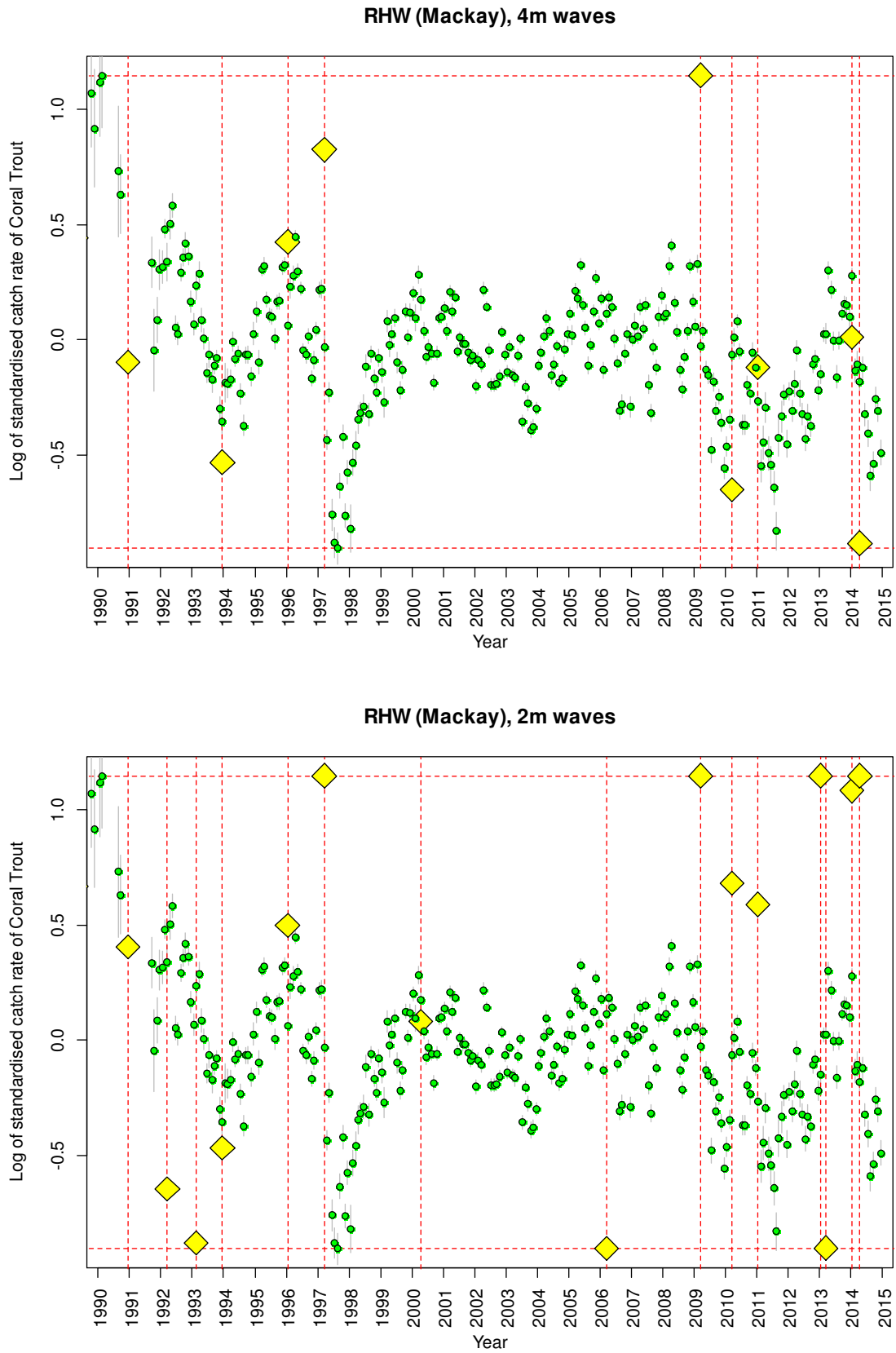


Figure 21-3, continued from previous 14 and on next 5 pages.

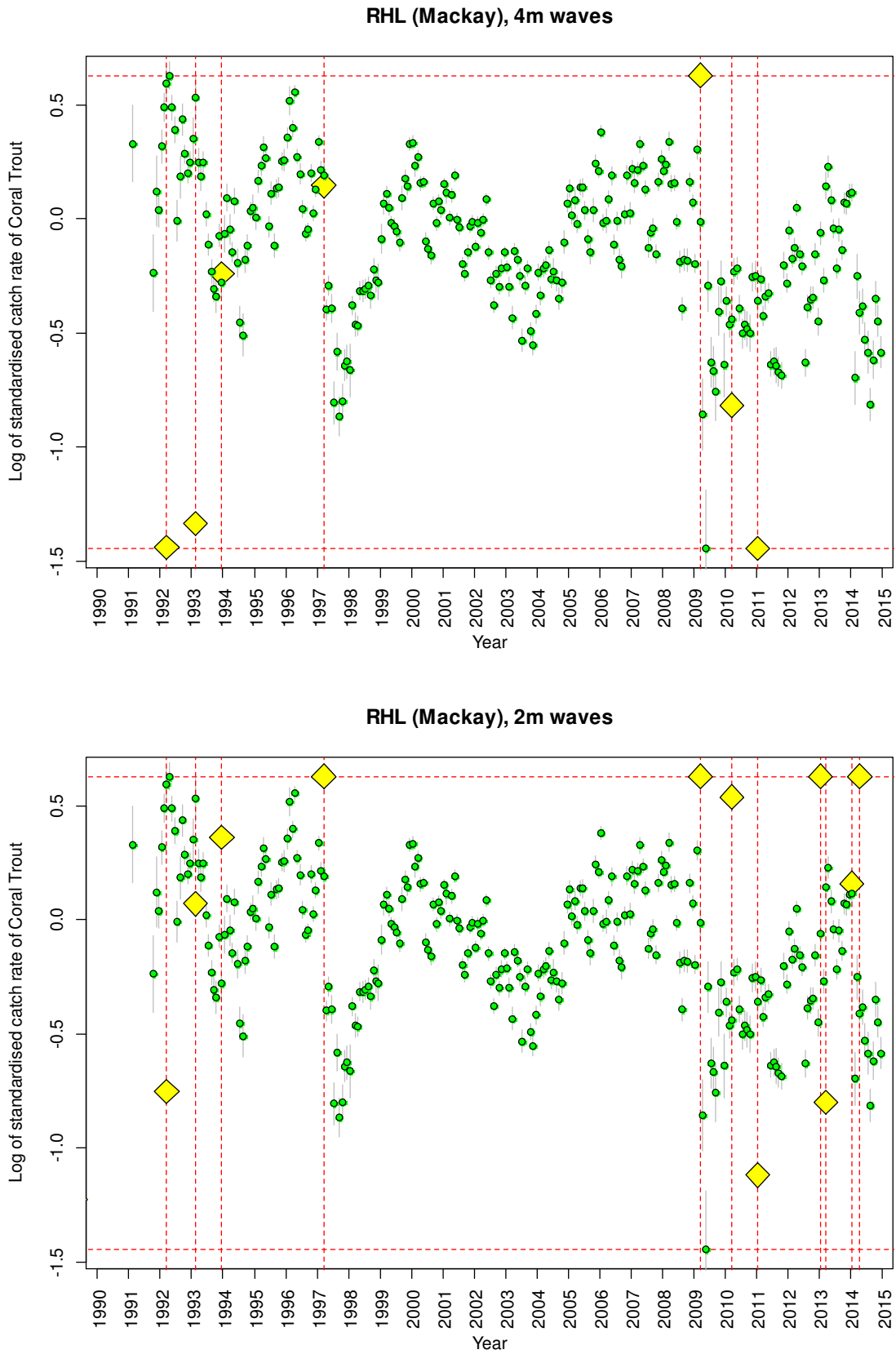


Figure 21-3, continued from previous 15 and on next 4 pages.

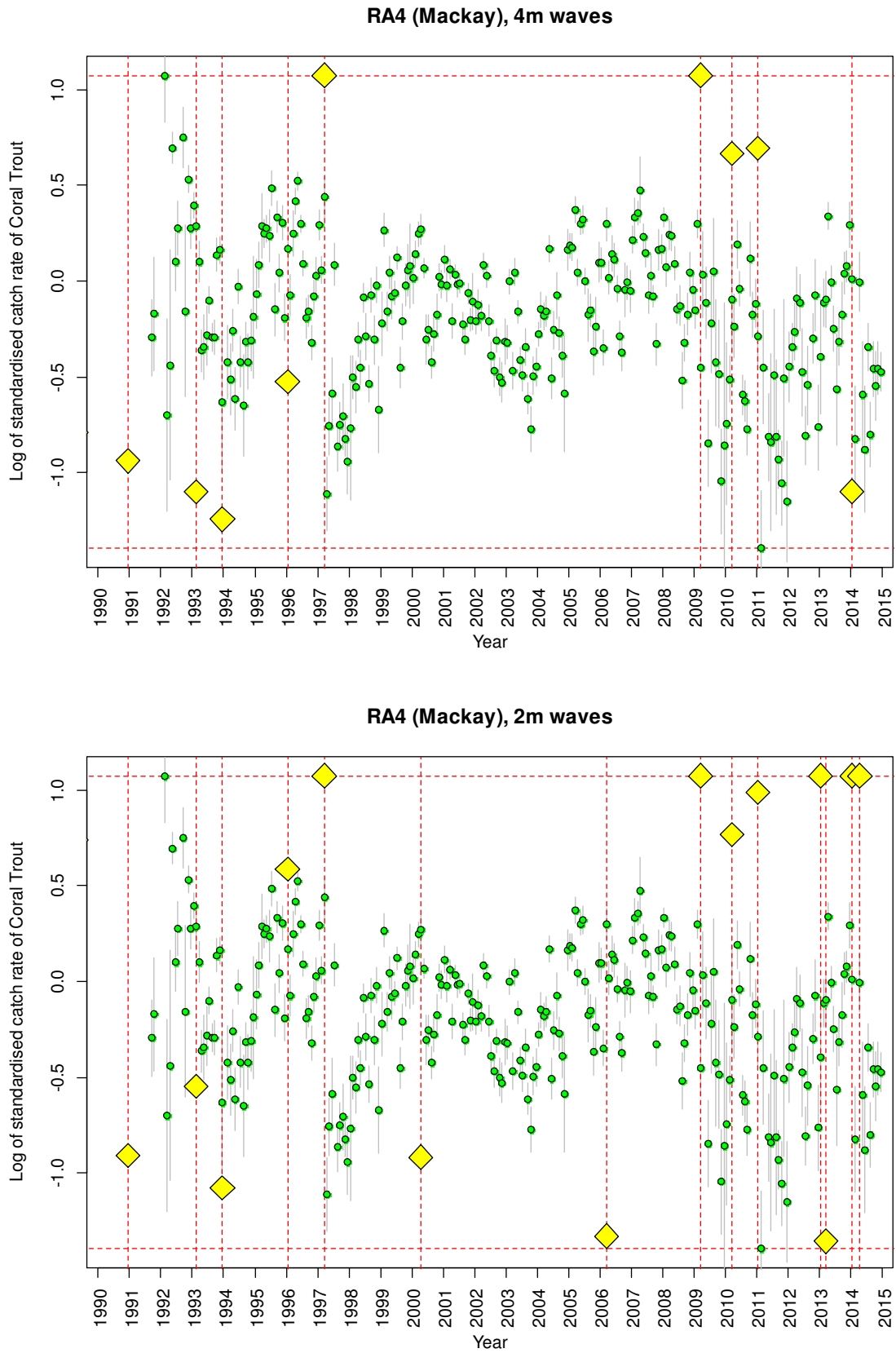


Figure 21-3, continued from previous 16 and on next 3 pages.

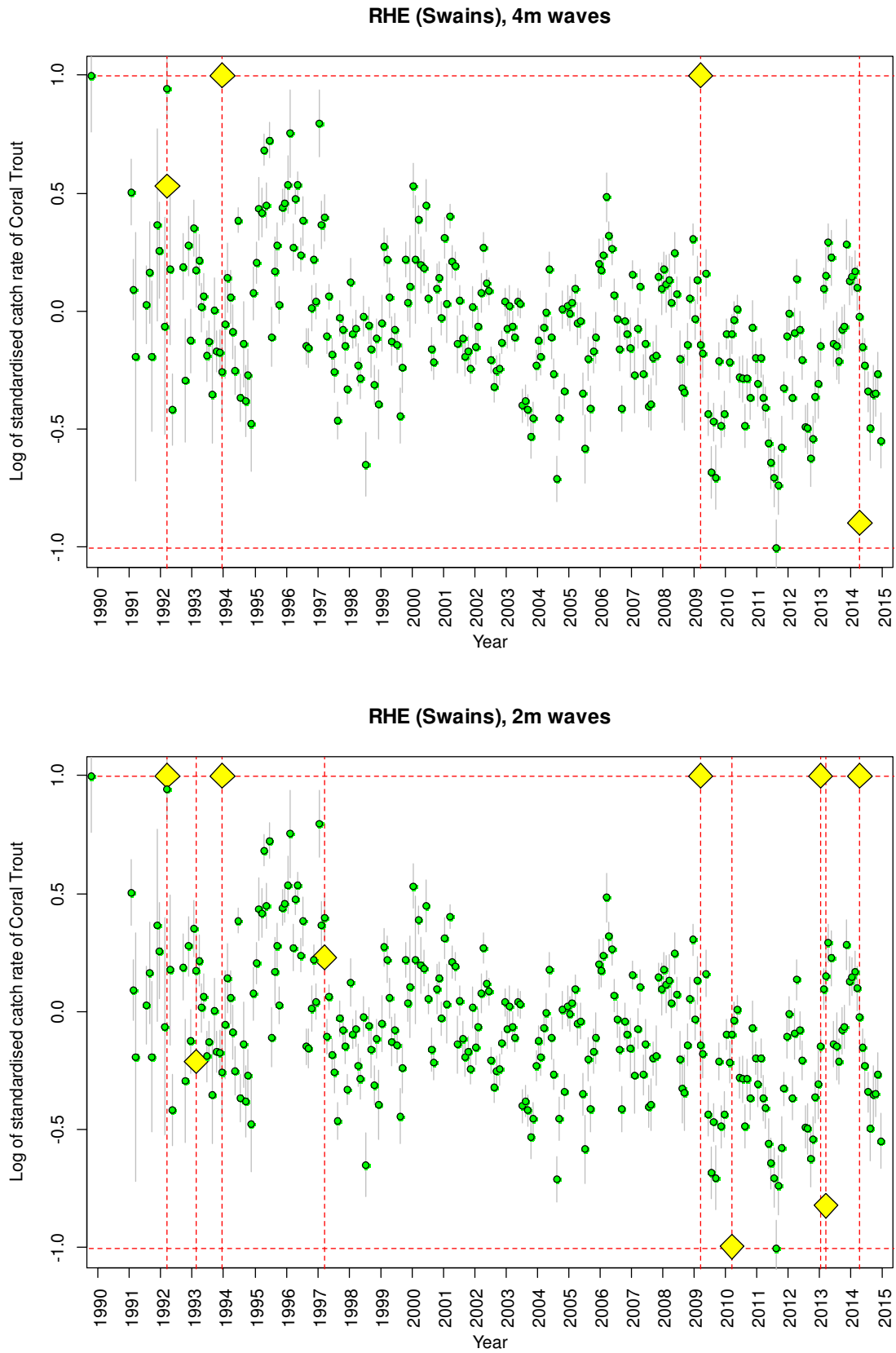


Figure 21-3, continued from previous 17 and on next 2 pages.

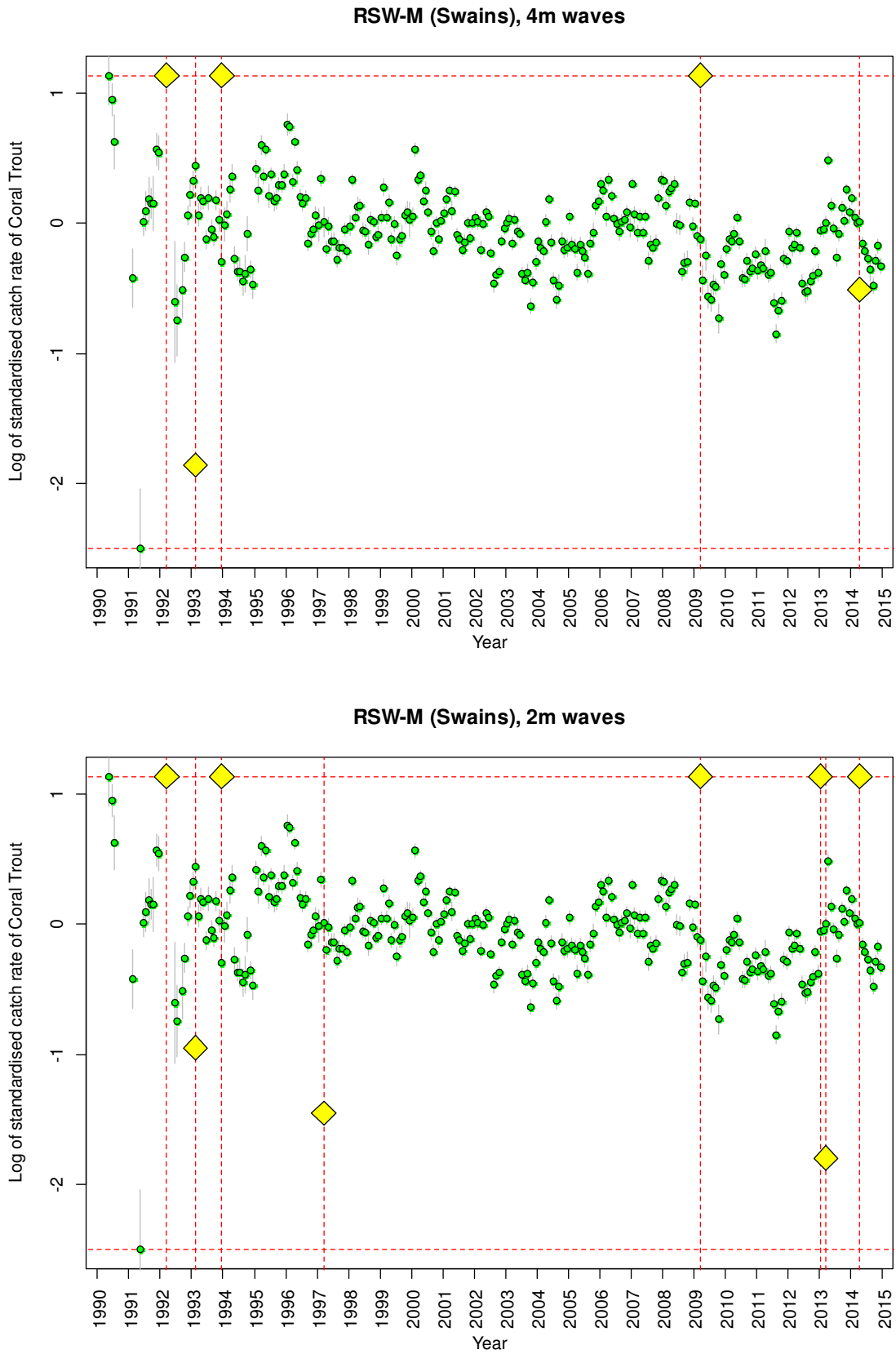


Figure 21-3, continued from previous 18 pages and on next page.

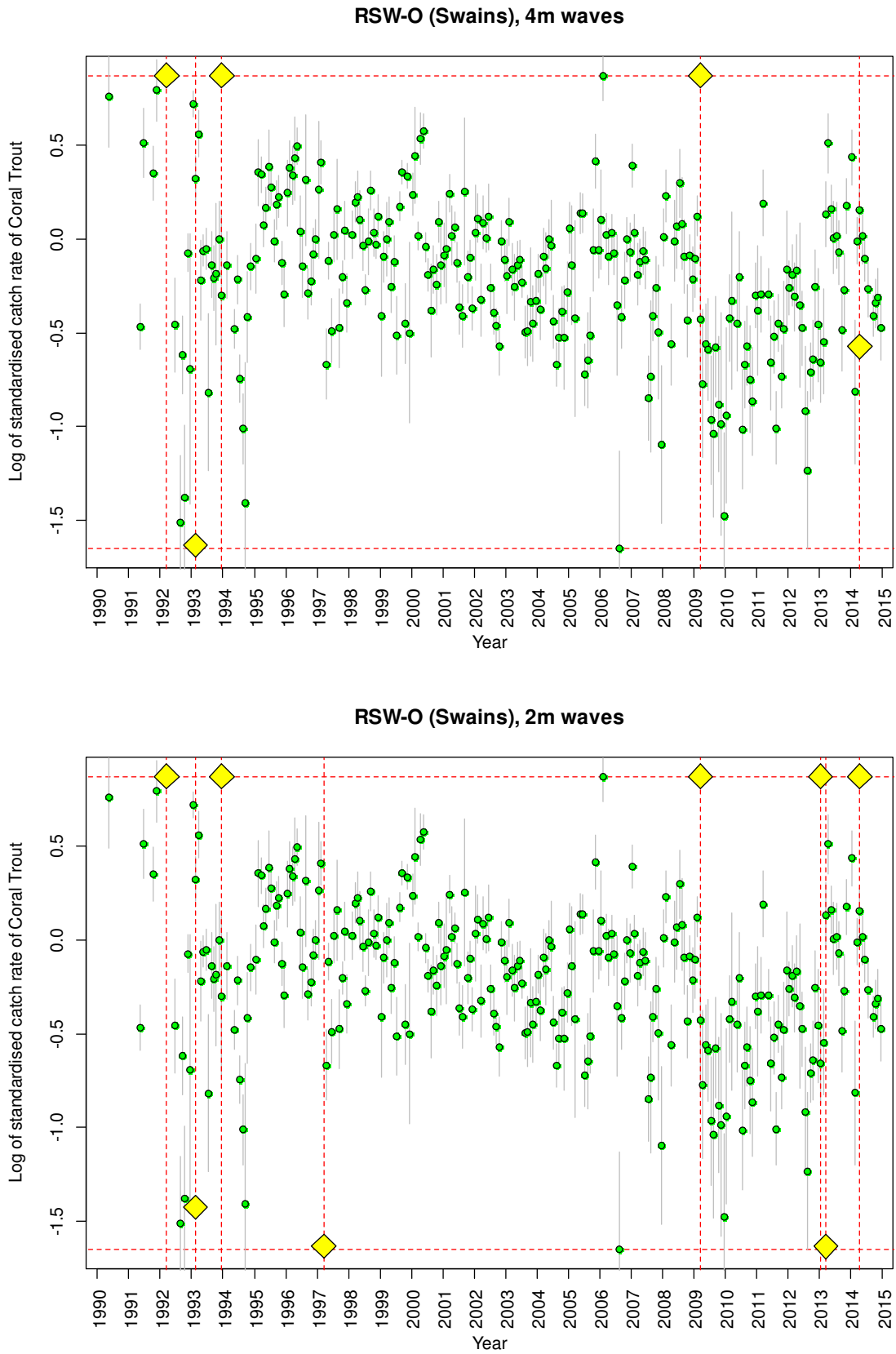


Figure 21-3, continued from previous 19 pages.

21.6 DIRECT MEASUREMENTS OF WAVE HEIGHT

Direct measurements of wave height were collated from the Queensland Government’s monitoring program (<http://www.qld.gov.au/environment/coasts-waterways/beach/monitoring>). Nine stations had long time series of measurements: from north to south, these were Cairns, Townsville, Abbot Point, Mackay, Hay Point, Emu Park, Gladstone, Brisbane and Gold Coast. The earliest measurements began in 1975, but some stations did not begin recording until much later and there were also some gaps in the data records. Together, however, the different stations provide a long and continuous time series of wave heights near the Queensland east coast.

The stations at Mackay and Brisbane were located well offshore, but the other stations were close inshore. The Brisbane and Gold Coast stations, although well south of the GBR, were included in order to capture swells from offshore cyclones that might not have produced large waves at the close-inshore coastal monitoring stations in GBR latitudes, but still may have affected the GBR.

A major advantage of the wave-height data was that the exact date on which large waves were generated could be correlated to the weather system that caused them, thus providing certainty of cause and effect.

Wave heights recorded for variance low-pressure systems are listed in Table 21-3.

Table 21-3. Highest recorded significant wave heights (H_{sig}) for low-pressure systems that affected the GBR. The list includes all tropical cyclones of Australian Tropical Cyclone Category (“Cat”) 3 or above, and all other low pressure systems that produced large wave heights and for which records were available. Locations are (left to right) Cairns, Townsville, Abbot Point, Mackay, Hay Point, Emu Park, Gladstone, Brisbane and Gold Coast. Non-cyclonic weather system abbreviations are East Coast Low (ECL, single centre formed outside the tropics), East Coast Hybrid Low (ECHL, multiple centres formed outside the tropics), Tropical Hybrid Low (THL, multiple centres formed in the tropics), Tropical Low (TL, single centre formed in the tropics). Sources: Queensland Government wave station data, cyclones records from the Australian Bureau of Meteorology (BoM); cyclone track summaries from www.australiasevereweather.com; case studies from www.hardenup.org (a project of Green Cross Australia); other reports where available, including many by J. Callaghan (BoM, retired).

Date	Cat	Name	Cai	Tow	Abb	Mac	Hay	Emu	Gla	Bri	Gol
19/01/1976	3	David				2.90					
29/02/1976	4	Colin									
27/04/1976	3	Watorea		1.46							
31/01/1977	1	Keith	1.91	1.89							
01/02/1978	0	THL				2.66	2.59				
03/01/1979	1	Peter	1.80	2.36							
12/01/1979	1	Gordon				3.56	2.23			2.71	
01/03/1979	4	Kerry		2.76	2.22	4.02	2.15			2.93	
25/02/1980	3	Simon								3.20	
27/02/1981	2	Freda				2.73	2.07			2.44	
06/04/1982	4	Bernie				2.21				2.99	
26/02/1983	4	Elinor									
16/01/1984	3	Grace									
18/01/1985	4	Odette								2.96	
31/01/1986	3	Winifred		2.50							
01/03/1988	2	Charlie			3.14	2.52					
11/04/1988	0	ECL								4.10	4.82
05/06/1988	0	THL								4.48	4.45
04/04/1989	4	Aivu			3.79	3.51					
25/04/1989	0	TL								6.11	5.60
16/12/1989	1	Felicity			2.21	3.34				2.48	
09/03/1990	3	Hilda								3.27	2.73
23/03/1990	3	Ivor	1.92	1.78							
23/12/1990	4	Joy	2.24	2.96	3.43	3.88					

Date	Cat	Name	Cai	Tow	Abb	Mac	Hay	Emu	Gla	Bri	Gol
13/01/1992	4	Betsy								4.89	2.89
17/03/1992	4	Fran				2.56				5.08	3.42
07/02/1993	4	Oliver		1.79		2.41				3.94	2.48
17/03/1993	2	Roger				2.74	1.88			7.36	5.73
19/01/1994	5	Rewa				2.87	1.53			3.23	2.63
19/01/1976	3	David				2.90					
03/03/1994	5	Theodore								4.61	2.78
06/03/1995	3	Violet								4.54	3.23
20/04/1995	4	Agnes									
08/01/1996	4	Barry		2.13							
27/01/1996	3	Celeste			2.77						
24/02/1997	1	Ita		2.02	2.67						
09/03/1997	2	Justin			1.57	4.68	3.10	3.09		4.25	2.76
24/03/1997	1	Justin		3.58	2.54						
17/01/1998	4	Katrina									
11/02/1999	3	Rona	2.49	2.63	1.74	2.99	2.28	2.41		3.28	3.60
27/02/2000	2	Steve	2.77	2.00	1.61	2.85	1.97	2.40			2.26
02/04/2000	2	Tessi			2.44	2.30	1.72	1.76			
02/05/2000	0	TL	1.60		1.68	3.13	2.42	3.01		4.79	3.95
03/03/2003	2	Erica				3.25	2.23	2.71		3.28	
05/03/2004	0	ECHL	1.26	1.99		3.29	2.34	2.89		6.98	5.89
24/03/2004	2	Grace	1.58	2.15		2.67	1.82	2.35		4.82	4.18
10/03/2005	4	Ingrid	1.34	1.92							
20/03/2006	4	Larry	1.37	2.91		3.22	2.04	2.40			
25/03/2006	4	Wati								4.76	3.07
19/04/2006	3	Monica	1.53	1.87							
31/01/2009	1	Ellie		2.08		3.47	2.27	2.49			
08/03/2009	5	Hamish	1.31	1.48		3.41	2.24	3.01		4.70	3.27
20/03/2010	4	Ului				5.67	3.34	3.05	2.32		
25/12/2010	1	Tasha		1.99							
16/01/2011	4	Zelia								4.88	3.27
30/01/2011	1	Anthony				2.79	2.28	2.25	1.84	3.69	2.16
03/02/2011	5	Yasi	2.39	5.46		2.35	2.25	1.62	1.27		
30/12/2012	5	Freda									
27/01/2013	0	Oswald	2.32	2.75		3.06	2.38	3.90	3.15	7.11	6.27
05/03/2013	1	Sandra				2.71	2.18	2.40	1.97	3.63	2.46
01/05/2013	3	Zane		1.59							
03/02/2011	5	Yasi	2.39	5.46		2.35	2.25	1.62	1.27		
30/01/2014	2	Dylan		1.91		5.02		3.46	2.78		
05/02/2014	1	Edna		1.95		3.24				4.82	
09/03/2014	1	Hadi				3.20		2.49			
12/04/2014	5	Ita	3.43	3.60		3.23		2.90	1.97	3.62	

21.7 SUBJECTIVE STANDARDISATION OF CATCH RATES FOR WEATHER SYSTEMS

21.7.1 Methods

In view of the specific causal mechanism for large waves on the Great Barrier Reef (see section 21.4) and the difficulty of accurately estimating wave heights from a numerical oceanographic model (see section 21.5), standardisation of catch rates for weather systems had to be subjective.

For each major Sub-bioregion in the coral trout fishery, weather systems that appeared to have substantial effects on coral trout catch rates were chosen from the list in Table 21-3. To reduce the

subjectivity involved, all the chosen weather systems had to produce large recorded wave heights at one or more of the wave-height recording stations in Table 21-3.

Each weather system was assumed to produce a linear fall in the log of the coral trout catch rate over a period of roughly six months following the occurrence of a weather system (months 1–6), and then a linear recovery over a similar or somewhat longer period (months 7–12 or more) to the catch-rate level that prevailed prior to the weather system. These linear effects were fitted by a Poisson generalised linear model (GLM) in which the response variable was the harvest weight and the explanatory variables were the special effects of weather systems and the standardised fishing effort from a previous GLM analysis of catch rates that did not take account of weather systems.

The result of the analysis was, for each major Sub-bioregion, a time series of estimates of what the standardised catch rate would have been if the weather systems had not occurred.

21.7.2 Results

Four major Sub-bioregions were chosen for this analysis: RG2 South (Townsville Subregion), RK (Mackay), RHW (Mackay) and RSW-M (Swains). These Sub-bioregions had enough fishery data to have relatively small standard errors on the monthly catch rates (see Figure 21-3).

The final standardised catch rates are plotted in Figure 21-4 (bold black lines). They are often substantially higher than the time series that do not include the effects of weather systems (red lines in Figure 21-4).

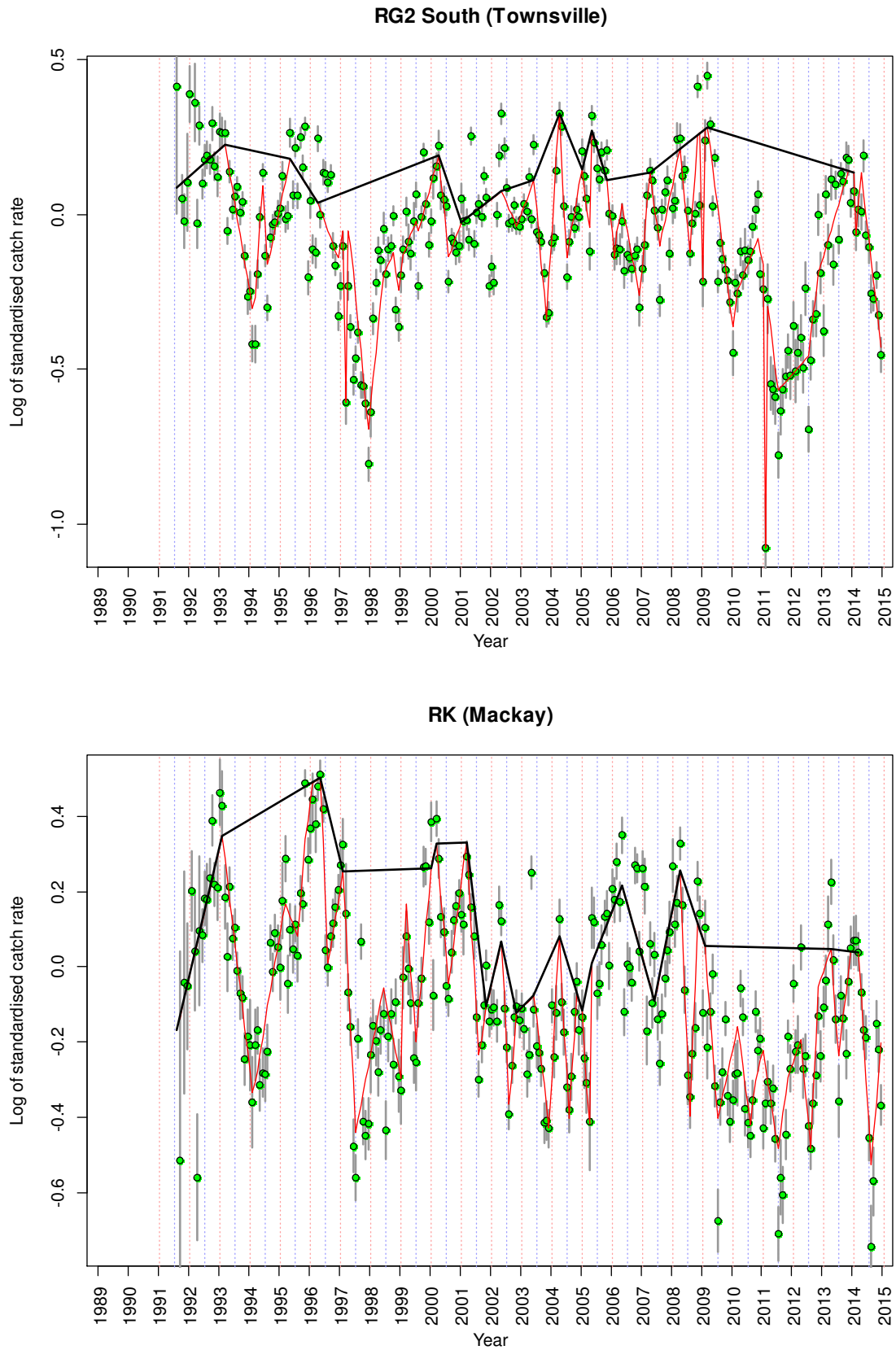


Figure 21-4. Subjective standardised catch rates (bold black lines) of coral trout to account for effects of weather systems in the major Sub-bioregions of the reef line fishery. Catch rates that don't account for weather systems are also shown (red lines). The green dots are the same as in Figure 21-3 and are monthly standardised catch rates from a model that does not include any effects of weather systems. (Continued next page)

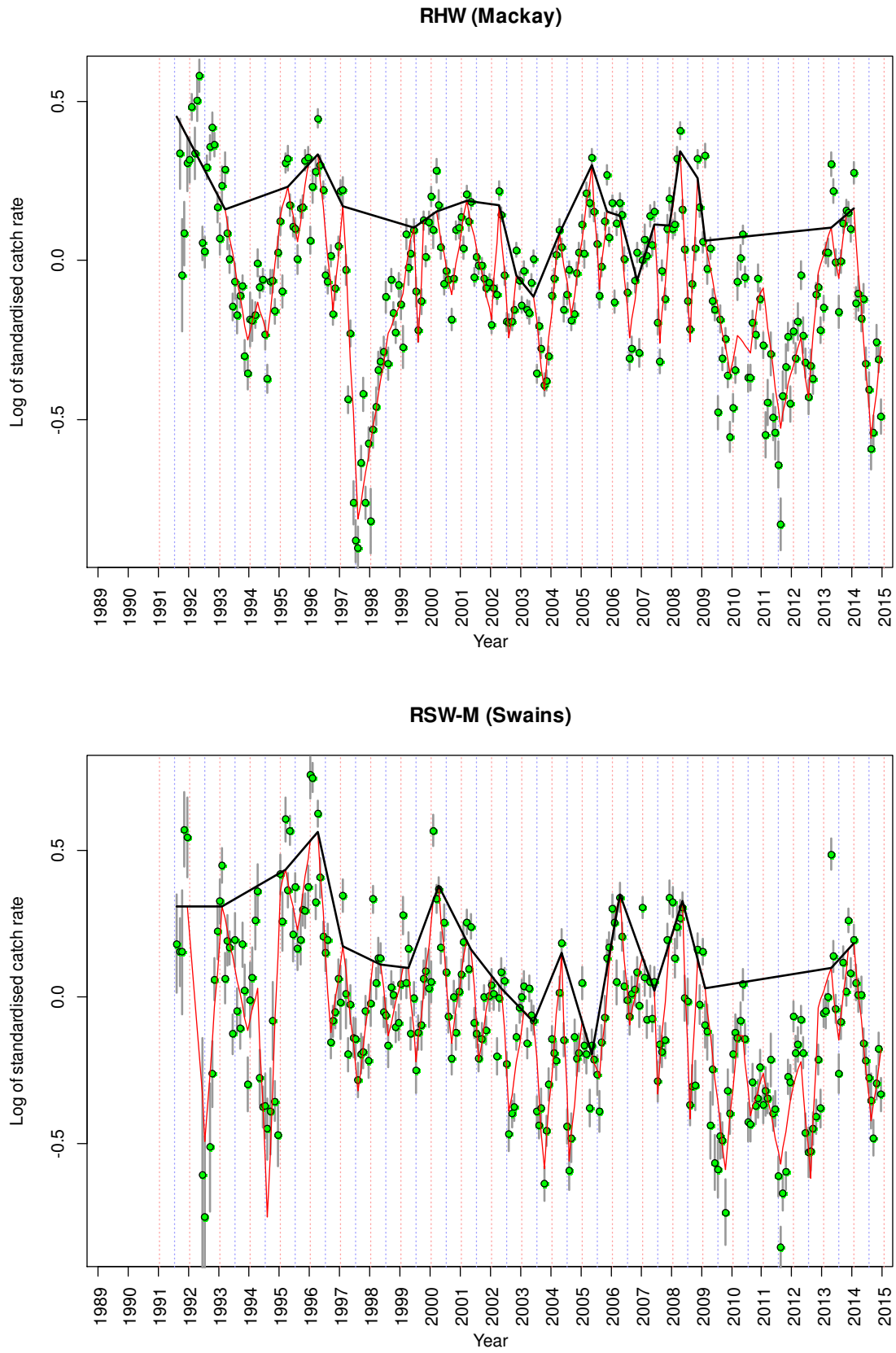


Figure 21-4 (continued).

21.8 DISCUSSION AND RECOMMENDATIONS

The subjective standardisation of coral trout catch rates for weather systems was necessitated by the poor correlation between the best available cyclone data and coral trout catch rates. It was, however, rendered more objective by choosing only weather systems that produced large recorded waves on the Queensland east coast (see Table 21-3). The goal of a fully objective standardisation for weather systems may be met in future by an advanced oceanographic model that takes account of the inshore fetch parallel to the coastline; to our knowledge such a model does not yet exist.

The existing oceanographic model has, however, been beneficial in indicating that it is the presence or absence of exposure to particular wave heights that is important, and that the duration of such exposure is much less important. This corroborates the hypothesis that it is physical damage to coral reefs that affects fishery catch rates.

The time series of fishery catch rates support the theory from section 21.4 that the major impacts of cyclones to the GBR come from the few cyclones that are able to use the waters inshore of the GBR as a fetch and generate large southeasterly swells behind the outer barrier of the GBR. The correlations of catch rates with the wave-height model using offshore fetch are poor, as were the correlations of Leigh *et al.* (2014) using cyclone wind energy. The inshore-fetch mechanism is the only available hypothesis that can explain the observations.

Apart from explaining why only a few cyclones have significant effects on the GBR fishery, while many powerful cyclones do not, the inshore-fetch mechanism also explains:

- why the effects of the important cyclones cover such huge areas of the GBR which cannot be explained by other means, and
- why cyclones have little if any effect north of Cairns.

The potential big effect of Cyclone Ita (April 2014) is a new result from this project. Previously it was known that coral trout catch rates fell in 2014, resulting in a decrease in quota allocations in 2015, but even the fishers as far as we know did not suggest that Cyclone Ita was responsible.

It is also notable that some major effects on fishery catch rates come from systems that do not meet the criteria for tropical cyclones. Records of these systems are much more difficult to find.

This project has taken substantial steps towards finding a useful correlation between cyclone measurements and coral trout catch rates. The cyclone measurements that are needed appear to be easy to collect and already are being collected as part of Queensland's beach protection program. Models based on offshore fetch and northeasterly swells are not likely to be useful because the outer reefs of the GBR are very well adapted to dissipating swells from offshore of the GBR.

Models based on the sea surface temperature effects of cyclones, the original aim of this project, will be even less useful.

We put forward the following recommendations:

- Inshore wave height measurements should be recognised for their critical importance in gauging the effects of tropical cyclones on the GBR.
- New oceanographic models for the GBR should be developed which take account of the prime importance of the inshore-fetch mechanism in generating damaging swells.
- Historical inshore wave height measurements should be collated and used in new fishery catch rate standardisations that can properly take account of the effects of tropical cyclones.

New catch rate standardisations should prove very valuable in fishery management as they may finally separate the effects of tropical cyclones from the effects of fishing, which to date has been impossible to do. The process of setting quota in the fishery could then be based on the effects of fishing alone and made largely independent of cyclones.

22 Appendix 8. Local averaging optimisation and sea surface temperatures

James Thompson & Ricardo Lemos

22.1 ABSTRACT

This report aims to investigate sea surface temperatures using local averaging optimisation. A previous paper on local averaging optimisation, McNames [4], was reviewed and the method improved upon. Analysis of sea surface temperatures is an important consideration for climate change as well as fishing and agriculture industries. The results obtained suggest sea surface temperatures have consistently increased but care needs to be taken in recognising the effects of other phenomena such as the ENSO cycle. The model implemented works for both non-chaotic and chaotic isochronic time series and therefore, this model can be used to model various other types of data.

Keywords: Time series analysis, local averaging models, sea surface temperatures

22.2 INTRODUCTION

Important to understanding climate change and its effects on natural phenomena, such as coral reefs, is forecasting models for sea surface temperatures and other oceanographic data (e.g. salinity). BRAN (Bluelink Reanalysis) [3], provided by the CSIRO, has begun to collect and model oceanographic data across the globe. Using this current dataset, future sea surface temperatures can be predicted using time series analysis. The results gained from this sort of analysis are key to understanding the magnitude of climate change as well as better preparing for the effects of climate change, in particular its effects on coral reef ecosystems.

A time series is a data set generated over time [1]. When the time between measurements is equal, analysis on the time series, or time series analysis, becomes much simpler. An example of time series analysis, is forecasting future values [1]. This paper uses local models to predict the future values of the sea surface temperature time series, downloaded from BRAN [3].

Local models use only a portion of the time series to predict future values [4]. Many methods exist to determine which portion of points are used for this prediction. This paper uses local averaging models (equation 1) to forecast the future sea surface temperatures, in a similar way to McNames [4]. It is expected that using this forecasting model will only provide accurate forecasts for a small number of steps ahead. However, using McNames's [4] method, the accuracy of the local model should be optimised.

22.3 METHODS

McNames [4] uses a generalised cyclic coordinate method to optimise model parameters for chaotic time series prediction. To create the forecasting function (1), iterative prediction and local averaging models, based on Takens' theorem [6], are used. McNames [4] justifies the use of the biweight function (equation 2) as the weighting function with the weighted Euclidean distance (equation 3) as the distance measure between input vectors. The generalised cyclic coordinate method [4] then minimises the multi-step cross-validation error (equation 4) to jointly optimise the number of neighbours (k), through an exhaustive search (up to k_{max}), and the metric weights, through a gradient-based optimisation algorithm using an initial lambda (λ_i). Previous local averaging models optimised the selection of the embedding dimension [2], instead of model parameters. McNames's approach [4] effectively optimises the embedding dimension (n_d), if appropriate, by setting some of the metric weights to zero during the optimisation process. As such, this approach outperforms previous local averaging models.

When calculating the multi-step cross-validation error (MSCVE) (equation 4), the forecasting function (equation 5) in McNames’s [4] method utilises all available data points except the omitted value $c(i) + j + 1$. However, when using the function to predict future data points, only previous data points can be used in forecasting. This is an issue as the forecasting function used to calculate the MSCVE does not match the forecasting function used for data prediction. To improve McNames’s [4] method, this paper uses an adjusted forecasting function (equation 6), alleviating this issue.

$$\hat{y}_{t+1} = \hat{g}(x_t) = \frac{\sum_{i=nd}^{nt-1} w_i^2 * y_{i+1}}{\sum_{i=nd}^{nt} w_i^2} \quad (1)$$

$$w_i^2 = \begin{cases} (1 - (\frac{d_i^2}{d_{k+1}^2}))^2 & d_i^2 \leq d_{k+1}^2 \\ 0 & otherwise. \end{cases} \quad (2)$$

$$d_i^2(x_t, x_i) = \sum_{j=1}^{nd} \lambda_j^2 (x_{t,j} - x_{i,j})^2 \quad (3)$$

$$\bar{C} = \frac{1}{n_c n_s} \sum_{i=1}^{n_c} \sum_{j=1}^{n_s} (y_{c(i)+j+1} - \hat{g}^-(x_{c(i)+j}))^2 \quad (4)$$

$$\hat{g}^-(x_t) = \frac{\sum_{i=nd, i \neq t}^{nt-1} w_i^2 * y_{i+1}}{\sum_{i=nd, i \neq t}^{nt-1} w_i^2} \quad (5)$$

$$\hat{g}^-(x_t) = \frac{\sum_{i=nd}^{t-1} w_i^2 * y_{i+1}}{\sum_{i=nd}^{t-1} w_i^2} \quad (6)$$

22.4 RESULTS

Figure 22-1 compares the forecasting results (red), calculated using local models, to actual data (blue), taken from BRAN [3]. The forecast results do not align perfectly but do, however, follow a similar shape to the actual data. This is important as forecasting the shape of the curve correctly allows for more accurate long-range forecasts, especially important in climate change analysis.

Comparing Figure 22-1, Figure 22-2 and Figure 22-3 suggests that one of the largest contributors to forecasting inaccuracy and imprecision is the data set length used for forecasting. Figure 22-3 (data set length = 1000 time steps) and Figure 22-1 (data set length = 719 time steps) represent a more accurate forecasting model compared to Figure 22-2 (data set length = 66 time steps) with the forecast values (red dots) aligning closely with the shape of the curve depicted by the original data (blue dots). The accuracy of the model does, however, decrease over time as the values forecast further in time use the values forecast previously, exponentially increasing the possible errors. This result suggests that in order to accurately model sea surface temperatures and other data sets using BRAN datasets [3], a larger amount of data must be downloaded and used to forecast future values. This is because local models rely on past data containing similar portions of data to the last “nd” (embedding dimension) points and the smaller the data set, the less similar portions are available.

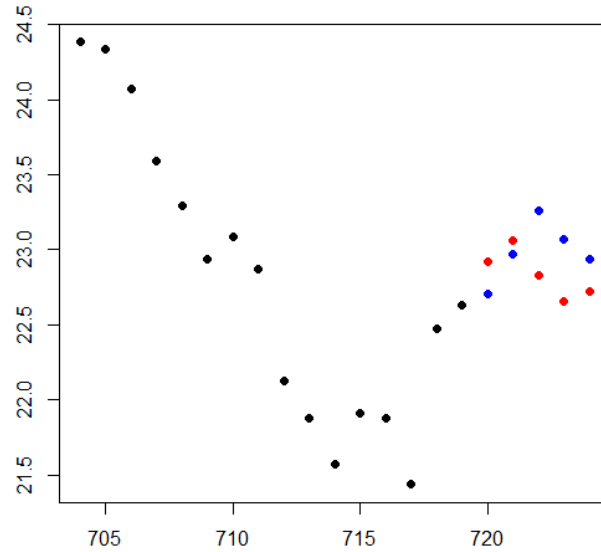


Figure 22-1. Sea surface temperatures (°C) varying with time (weeks after the 07/06/2006) taken from a depth of 15 m at a latitude and longitude of -22.95 and 155.95 respectively were used to forecast the next 5 temperatures (through to the 25/10/2006). The black points represent the original data used in the forecasting function, the red points the forecast values for the next 5 time steps and corresponding original data values are in blue. The optimum forecasting parameters were determined to be $k_{opt} = 9$ and $\lambda_{opt} = (0.896281607, 0.317031591, 0.088095156, -0.010149950, -0.017388793, -0.008844277, -0.009258766, -0.006303262, -0.006683757, -0.003470069, -0.009484341, -0.010851779, -0.008957675, -0.013793656, -0.015319032)$ using the input values; $n_d = 15, n_c = 5, n_s = 5, k_{max} = 10, \lambda_i = (2e^{-x}, 2e^{-2x}, \dots, 2e^{-x*n_d})$.

Comparing Figure 22-1 and Figure 22-3 directly suggests the time series which has been mathematically constructed, the Lorenz time series (Figure 22-3), is much more accurately modelled than the data set taken from the environment, the sea surface temperatures (Figure 22-1). This comparison suggests real data, not mathematically constructed data, will be less accurately modelled using local averaging optimisation.

The data depicted in Figure 22-4 shows a slight increase in consistent, warmer sea surface temperature patterns over the last 16 years. This suggests climate change is affecting these sea surface temperatures. This could be related to where the sea surface temperatures were taken, latitude and longitude of -22.95 and 155.95 respectively, corresponding to the Coral Sea between the Australian coast and New Caledonia. To test the effects of location, other data sets (different latitude and longitude) should be investigated in future studies.

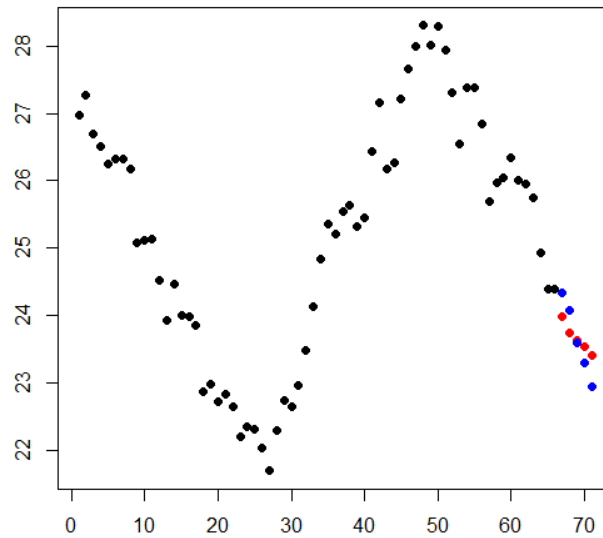


Figure 22-2. Sea surface temperatures ($^{\circ}\text{C}$) varying with time (weeks after the 02/03/2005) taken from a depth of 15 m at a latitude and longitude of -22.95 and 155.95 respectively were used to forecast the next 5 temperatures (through to the 05/07/2006). The black points represent the original data used in the forecasting function, the red points the forecast values for the next 5 time steps and corresponding original data values are in blue. The optimum forecasting parameters were determined to be $k_{opt} = 10$ and $\lambda_{opt}=(0.78096113, 0.21079572, -0.08029546, -0.15665996, -0.15551428, -0.13221321, -0.11339021, -0.10469518, -0.10193321, -0.10076513, -0.10014239, -0.09989629, -0.09983056, -0.09979750, -0.099781140)$ using the input values; $n_d = 15, n_c = 8, n_s = 5, k_{max} = 10, \lambda_i = (2e^{-x}, 2e^{-2x}, \dots, 2e^{-x*n_d})$.

Table 22-1. ENSO cycle timeline from 1991 to 2006 including strength of ENSO [5].

	Weak	Moderate	Strong
El Nino	2004/05, 2006/07	1991/92, 1994/95, 2002/03	1997/98
La Nina	1995/96, 2000/01, 2005/06	1998/99	1999/2000

The Coral Sea is greatly affected by the ENSO cycle (La Niña and El Niño) which causes warmer waters to shift between the Eastern and Western Pacific. As such, the ENSO cycle may have affected the sea surface temperatures, like climate change, on a much smaller scale.

Table 22-1 details the years and intensities of the ENSO cycle. Using these data and the results in Figure 22-4, it can be seen that the ENSO cycle does affect the sea surface temperatures. For example, the 6th peak (1997/98), a strong El Niño year has much higher sea surface temperatures than the 8th peak (1999/2000), a strong El Niño year. As such, the ENSO cycle may be affecting the observed climate change effect.

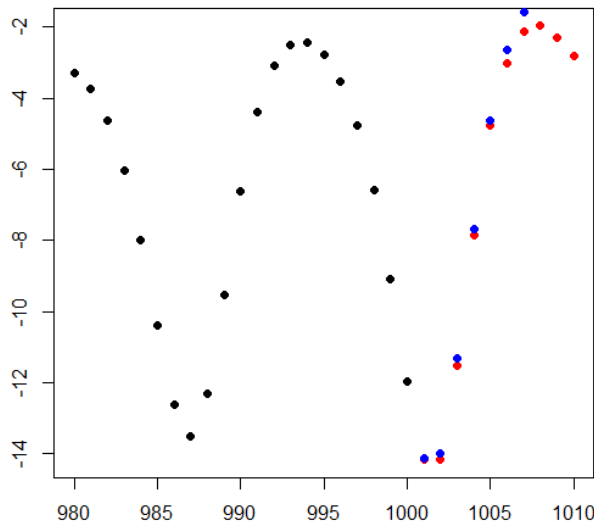


Figure 22-3. Lorenz time series from $t = 800$ to $t = 1010$. The black dots represent the data used to forecast the future values (red), which have been overlaid with the original data (blue). The forecast values were obtained using $n_d = 20, n_c = 10, n_s = 10, k_{max} = 15, \lambda_{opt} = (2e^{-x}, 2e^{-2x}, \dots, 2e^{-x*n_d})$ and $k_{opt} = 4$.

22.5 CONCLUSION

This local averaging optimisation model, similar to most time series prediction models, is limited to isochronic data sets. The BRAN [3] data were available as weekly data and therefore, this model appropriately models these data. However, the greatest strength of this local averaging model is its ability to model all isochronic data sets, either chaotic or non-chaotic. Sea surface temperatures (Figure 22-2) may appear seasonal and therefore, periodic, but the Lorenz time series (Figure 22-3) is chaotic. As such, the results show the ability of this model to forecast both chaotic and non-chaotic data sets.

Future studies should focus on using this model for various other data sets and compare the results obtained with that of other numerical models. With sufficient testing, this model may be able to be used to forecast further into the future and therefore, be used to predict the effects of phenomena such as the ENSO cycle and climate change.

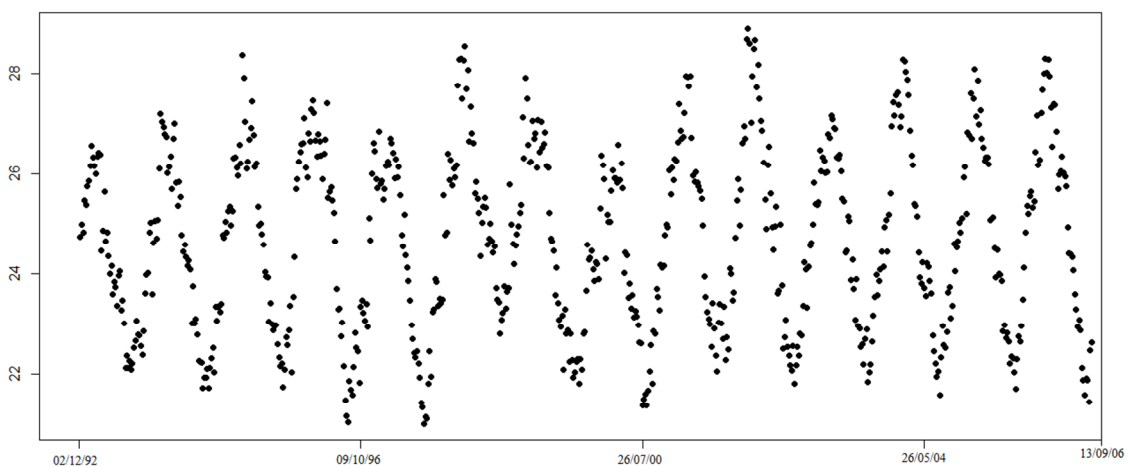


Figure 22-4. Sea surface temperatures ($^{\circ}\text{C}$) varying with time (weeks from 02/12/1992 to 13/09/2006) taken from a depth of 15 m at a latitude and longitude of -22.95 and 155.95 respectively.

22.6 REFERENCES

- [1]Box, G, Jenkins, G & Reinsel, G 2008, *Time Series Analysis*, John Wiley & Sons, New Jersey.
- [2]Cao, L 1997, 'Practical Method for Determining the Minimum Embedding Dimension of a Scalar Time Series', *Physica D*, vol. 110, pp.43-50.
- [3]CSIRO 2014, *Bluelink: Scientific and Technical Information*, accessed 1 August 2014, <<http://wp.csiro.au/bluelink/global/bran/>>.
- [4]McNames, J 2002, 'Local Averaging Optimization for Chaotic Times Series Prediction', *Neurocomputing*, vol. 48, no. 1-4, pp. 279-297.
- [5]Null, J 2014, *El Nino and La Nina Years and Intensities*, Golden Gate Weather Services, accessed 5 August 2014, <<http://ggweather.com/enso/oni.htm>>.
- [6]Takens, F 1981, 'Detecting Strange Attractors in Turbulence', *Springer Lecture Notes in Mathematics*, vol.898, pp. 366-381.

Department of Agriculture and Fisheries

13 25 23

www.daf.qld.gov.au